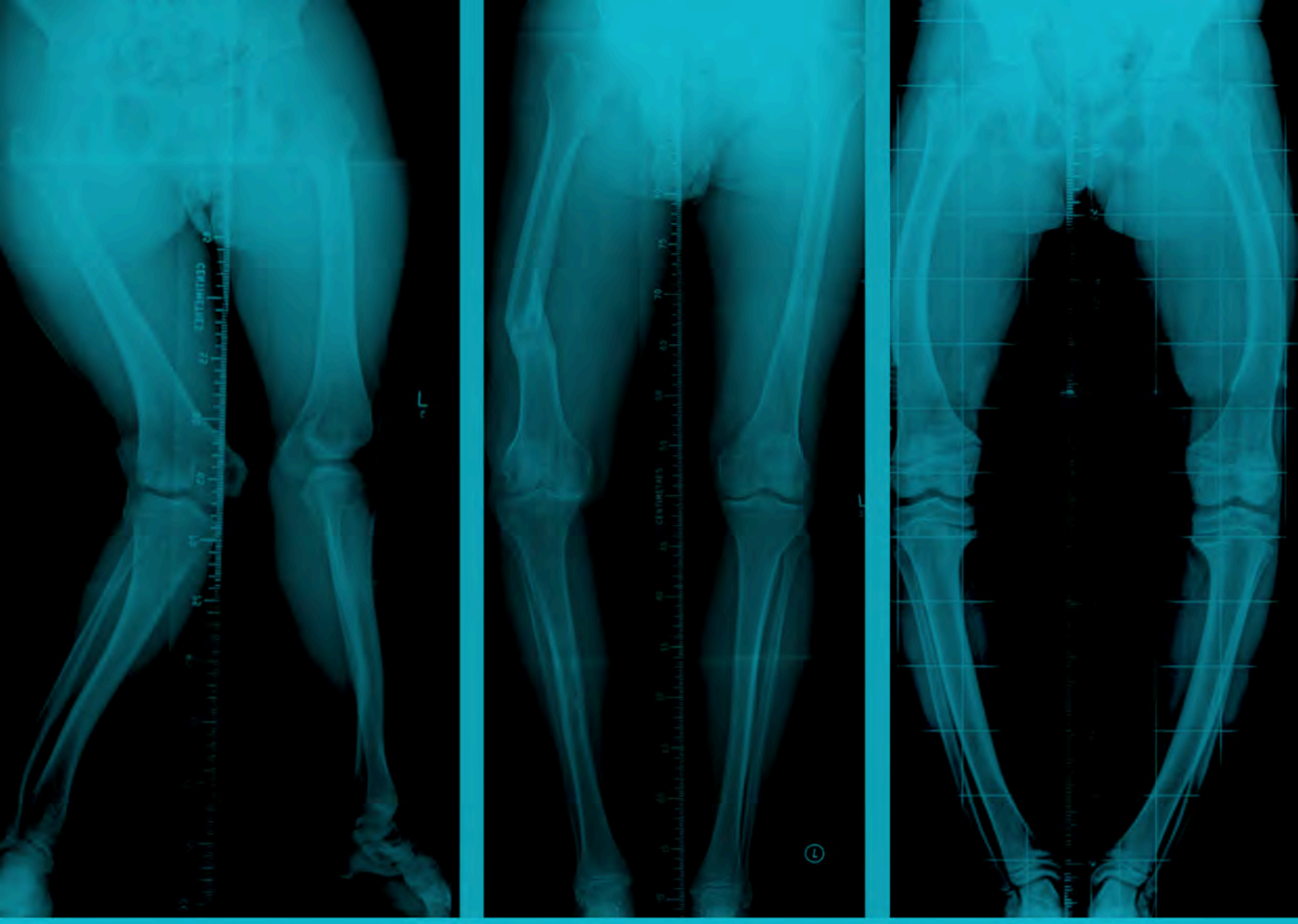

Fundamentals of Lower-Limb Deformity Analysis

Editor

Fergal Monsell

Associate Editors

Hemant Sharma

Gavin de Kiewiet

Fundamentals of Lower-Limb Deformity Analysis

Fundamentals of Lower-Limb Deformity Analysis

Editor

Fergal Monsell
Bristol, UK

Associate Editors

Hemant Sharma
Hull, UK

Gavin de Kiewiet
Sunderland, UK

NAUGHTON PUBLISHING

DEFORMITY CORRECTION

First published 2022

Published by NPM Publishing Ltd, Greystones, Tarporley Road, Whitchurch, Shropshire SY13 1R, UK

British Library Cataloguing in Publication Data
A catalogue record for this book is available from the British Library
eBook only ISBN 978-1-7395873-0-7

Project Management: NPM Ltd
Edited by Becky Freeman
Proofread by Susan Smyth
Index by Jill Dormon
Designed and typeset by Evolution, Kent, UK

Cover design by Evolution, Kent, UK

Contents

Contributors

Simon Britten
Leeds, UK

Peter Calder
London, UK

Milind Chaudhary
Akola, India

Alexander Cherkashin
Dallas, USA

Mick Dennison
Sheffield, UK

James Fernandes
Sheffield, UK

Nikolaos Giotakis
Liverpool, UK

David Goodier
London, UK

Reggie Hamdy
Montreal, Canada

Paul Harwood
Leeds, UK

Gamal Hosny
Cairo, Egypt

Bilal Jamal
Glasgow, UK

Gavin de Kiewiet
Sunderland, UK

Om Lahoti
London, UK

Fergal Monsell
Bristol, UK

Elizabeth Moulder
Hull, UK

Ross Muir
Hull, UK

Badri Narayan
Liverpool, UK

David Rowland
Glasgow, UK

Simon Royston
Sheffield, UK

Hemant Sharma
Hull, UK

Preface

Understanding the clinical and radiographic personality of lower-limb deformity is fundamental to management planning. The purpose of this book is to provide the interested but inexperienced clinician with an overview of the principles required for evaluation of these deformities.

This book is not intended to be an exhaustive work and the reader is directed to standard texts on this subject for more detailed instruction. It contains information that is necessary for the development of a sophisticated approach to analysis and uses simple geometry and trigonometry to describe a deformed bone in three-dimensional space using a two-dimensional radiographic image. It is therefore appropriate to acknowledge the giants on whose shoulders we stand, in particular Euclid, Pythagoras, Descartes and Röntgen.

All contributing authors are previous or current instructors on the UK Limb Deformity Course (https://www.deformitycorrection.co.uk). They are recognised experts in medical education and thought leaders in orthopaedic surgery and all have extensive experience in planning and surgical reconstruction of complex limb deformity.

Finally, this book should be regarded as a living document and the decision to circulate electronically and without charge is intended to ensure wider distribution and drive content modification for future editions.

Please acknowledge possession by formally downloading a .pdf version from: https://www.deformitycorrection.co.uk

Fergal Monsell
The Grand Academy
Lagado
2022

Acknowledgements

Our thanks to all current and past faculty members of the UK deformity course and the administrative team that supports this event.

We are also grateful to Nora Naughton, Becky Freeman, Amy Naughton and their colleagues for project management, editorial assistance, and processing and production of this title.

CHAPTER

1

Clinical evaluation in the context of limb deformity

Badri Narayan and James Fernandes

Introduction

Human evolution has resulted in complex upper limb function that allows accurate positioning of the hand and lower limb development that is adapted for efficient bipedal gait. The ability to walk upright is not unique to humans but other primates are capable of covering only short distances because of energy inefficiency associated with their skeletal structure and gait pattern.

The morphology of the human lower limb is consistent and appreciating the normal geometry and individual variation is a fundamental requirement for deformity planning. This allows identification and description of abnormality that follows injury or is a component of a developmental irregularity.

The purpose of this book is to provide an algorithm that simplifies the evaluation of the clinical and radiological components of an individual deformity. This will involve a description of clinical assessment, radiological evaluation and geometry of the normal limb. This is expanded with a detailed description of geometric evaluation of deformity in the frontal, lateral, axial and oblique planes. The femur, tibia and foot have individual clinical and radiological characteristics and are considered separately.

The management of skeletal deformity relies on a detailed history and comprehensive clinical assessment, with radiological imaging adding important information to the management strategy. This chapter provides an overview of the history that is relevant to skeletal deformity and outlines clinical assessment of these patients. There are important differences between the assessment of a patient with a congenital abnormality and the approach to a limb that had normal function prior to a traumatic event. There are also important differences in the evaluation of the skeletal and soft-tissue components of a limb, and the nuances associated with e ach will be explored.

History

The consequences of deformity on current and future function and the effect on lifestyle choices are fundamentally important and direct the evaluation of adult and paediatric patients. The presence of deformity does not mandate treatment and the functional limitations must be quantified from an employment, educational, social and recreational perspective.

Patients will have preconceptions about their circumstances and management options and it is crucial to understand their expectations, in addition to outlining the short- and medium-term goals in language that they can easily understand. This requires sensitive but detailed interrogation about barriers to employment and education, the effects of lifestyle modification and the implications of deformity on sporting and leisure activities. Pain, abnormalities in the pattern of walking and concerns about appearance are among the commonly reported symptoms in patients with lower-limb deformity. Recognising the pattern of evolution of symptoms and appreciating the predicted natural history are also essential, and failure to understand these components may lead to an unsuccessful outcome.

Pain may be located at the site of deformity but will often affect adjacent joints and the spine and determining the triggers, pattern and the effect on function will influence management decisions. The type and pattern of analgesic use must be documented, as non-steroidal anti-inflammatory drugs (NSAIDs) and bisphosphonates affect bone healing after fracture or osteotomy. Polypharmacy is increasingly prevalent and it is crucial to liaise with primary care to obtain detailed information on current and previous prescription medication. The wider implications of intrusive pain, including long-term use of opioids, will also inform the discussion.

Secondary effects on adjacent joint function may present greater difficulty than the primary deformity and this should be discussed in detail. The aesthetic consequences may be concealed by a self-conscious patient and it is an error to underestimate the contribution of appearance to the overall symptomatic profile.

The nature of previous treatment, whether supportive or operative, must be detailed during the initial consultation. Patients with complex deformity will often have undergone a series of procedures and a surgical timeline should be constructed. It is particularly important to understand the patient's perception of the effect of each surgical event, whether positive and negative, as this will influence future treatment options. A history of infection may not always be obvious and focused questions on wound healing, antibiotic prescription, sinus formation and unexpected pain may indicate previous deep infection and mandates a structured diagnostic work-up.

The influence of co-morbidities on surgical outcome is well known; some, including obesity, are readily apparent during the clinical examination, but others, including hypertension, diabetes mellitus and nutritional deprivation, are equally relevant and must be sought. Modifiable risk factors such as smoking, alcohol and recreational drug use will also have a negative effect on outcome, and patients contemplating surgical intervention can be referred for counselling and support. The effect of smoking is particularly important due to the effect on bone healing.

Deformity correction is often gradual, with treatment lasting up to 18 months. A complete social history including domestic support must be obtained and mechanisms for complex after-treatment proactively organised. Surgical reconstruction may necessitate prolonged periods of absence from, and require a graduated return to, previous employment or education. This may necessitate temporary or permanent alterations to the classroom or workplace and a potential patient and their employer must be fully informed before agreeing to treatment.

Congenital or developmental deformity

The availability of ultrasound scanning in a health provider and commercial setting has increased the incidence of pre-natal diagnosis of congenital limb abnormalities. This produces an unexpected dimension to antenatal care and requires the input of an orthopaedic surgeon at an unusually early stage. The majority of abnormalities are sporadic, but it is important to determine or exclude a family history. This is particularly relevant to pre-axial limb deformity; a significant proportion of tibial and radial dysplasias are inherited (Figure 1.1a,b).

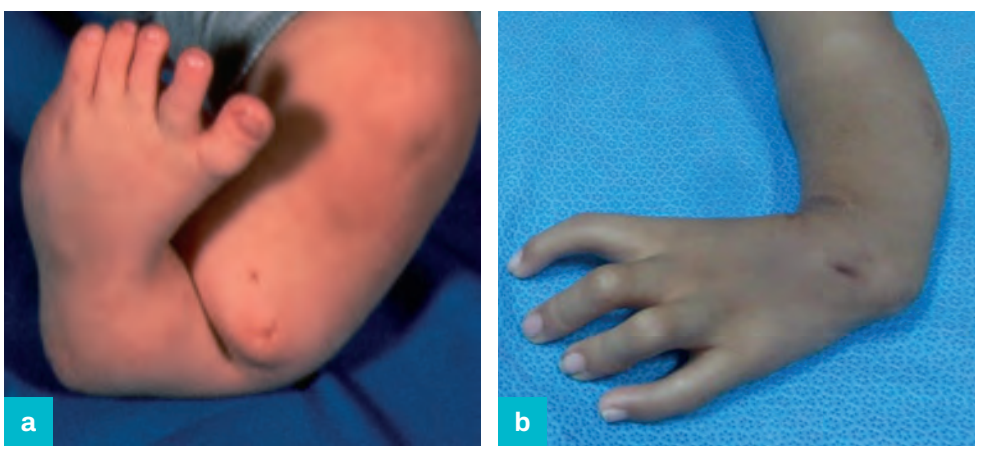

Figure 1.1
(a) Tibial dysplasia;
(b) radial dysplasia.

Important events during pregnancy include maternal illness, particularly gestational diabetes, hypertension and intra-uterine infection. Exposure to alcohol, prescription and recreational drugs should also be discussed.

The perinatal history is not usually contributory but it is important to discriminate between deformities that are present at birth and those subsequently identified. Subtle deformity often eludes detection in the immediate post-natal period and mild–moderate limb shortening may not become visible until the child pulls to stand.

A developmental history should record the timing of major motor milestones including head control, pulling to stand, walking, running and jumping. These are often normal or near normal in early childhood and intellectual and social development is expected to be normal in patients with congenital limb deficiency.

The pattern of evolution should be documented to determine whether the abnormality is increasing in proportion to overall growth, increasing at an accelerated rate or improving with growth. The majority of congenital limb reduction deformities increase in proportion to overall growth and the percentage reduction at birth will be identical to the maturity discrepancy.

Functional consequences should be discussed and are suggested by the walking pattern of pre-school-aged children, restrictions in play in early school years and sport in older children and adolescents. Compensatory strategies are common, generally involving flexion of the long leg knee and plantar flexion of the short leg ankle, which can produce a normal or near-normal pattern of walking up to mid childhood. Other important considerations include the effect on shoe size and the use of orthotics including a shoe lift and prosthetics in more substantial deformity.

Figure 1.2
Neonatal sepsis with proximal femoral growth arrest.

Abnormalities may follow a specific trigger, and a history of trauma and periods of reluctance to bear weight, even if seemingly trivial, should be recorded. Infection, particularly neonatal sepsis requiring supportive therapy, is a common cause of growth arrest and, as the effects may not be apparent for years, the causal relationship may not be appreciated by parents and this information not volunteered (Figure 1.2).

The current symptomatic profile, functional difficulties and effect on education and social development should also be discussed and documented.

Post-traumatic deformity

The extent of a skeletal and soft-tissue injury and the complications associated with management contribute to morbidity following significant lower-limb trauma.

Extant documentation from the point of retrieval, initial operative assessment, subsequent management and clinical progress informs decisions on limb reconstruction. Additional information, including the mechanism of injury, fracture configuration and extent of soft-tissue involvement, are also contained in the contemporaneous medical records and radiology. Details of primary and subsequent surgical procedures and events in the recovery period including wound breakdown, infection and antibiotic prescription should also be available to assist with sensible decision making. The specification of implants, equipment required for their removal and the vascular anatomy associated with free tissue transfer must also be available in advance of surgical reconstruction.

The functional consequences should be understood and are defined in an adult by the effect on employment, recreation, activities of daily living and additional care requirements, which may be formal or informal. Compensatory strategies are also common but less effective in the adult and elderly population, due to the loss of flexibility associated with the process of ageing. The psychological consequences of major trauma should not be underestimated and the effect on mood, outlook and chemical dependence should be discussed.

General examination

Examination is not deformity-specific, particularly if the diagnosis is unclear, and this is particularly important in the paediatric patient. There tends to be a different emphasis following limb trauma in the adult patient, in whom the rest of the skeleton is expected to the normal. Cardiovascular and pulmonary assessments are important in this group if a series of procedures involving general anaesthesia is anticipated.

Initial visual appraisal is required for gestalt diagnosis of skeletal dysplasia, metabolic and syndromic association. Cutaneous examination is important to identify vascular malformations and conditions associated with mosaic overgrowth including neurofibromatosis and fibrous dysplasia. Assessment of the face, eyes and hands assists in the diagnosis of specific skeletal dysplasias including osteogenesis imperfecta and achondroplasia.

Gait assessment

It is beyond the scope of this chapter to provide a detailed account of the methods of acquisition and interpretation of data on complex gait patterns. This description will concentrate on the essential components that are relevant to limb deformity. The gait pattern should be formally assessed by repeated observation of the patient walking for a distance that is sufficient to establish a consistent pattern. This may be difficult in children due to compliance, in adults due to pain and in the elderly due to fatigability. This also tends to be limited in a clinic room and evaluation in a corridor has many advantages. Video assessment is a useful adjunct and this can be prepared by the patient or carer in a familiar environment.

The walking pattern should be assessed with and without aids and adaptations including footwear. A head to floor evaluation of each segment in the frontal, lateral and axial planes is a requirement. This panoramic view is necessary to assess rotation from the front, fixed hip, knee and ankle flexion from the side and scoliosis, pelvic tilt and hindfoot position from the back.

It is important to make general observations to discriminate between gait abnormalities that are due to pain (antalgic), skeletal geometry (short leg or hiking), joint instability (varus/valgus thrust, Trendelenburg), contracture (fixed hip adduction/abduction, stiff knee) or a combination.

Initial contact in normal walking is with the heel; contact with the toe, forefoot or medial/lateral border indicates a pathological pattern. A high-stepping gait pattern may be due to common fibular nerve injury as a consequence of the initial traumatic event or subsequent treatment. Foot progression is either symmetrical normal, symmetrical abnormal or asymmetrical, and an abnormal pattern of knee and hip movement, particularly in the lateral plane, is a common compensatory strategy. The upper-limb pattern and position of the trunk and head should also be observed to complete the examination.

Instrumented gait analysis can be used in complex cases, with markers that can be tracked and mapped in three-dimensional space. Evaluation of kinematics, kinetics and simultaneous multi-level assessment requires instrumented motion tracking and multi-disciplinary team support and is generally reserved for complex cases.

Extremity evaluation

Measurement of arm span, and standing and sitting height are necessary to determine body proportion (Figure 1.3–1.5) and serial measurements are required to estimate height at maturity.

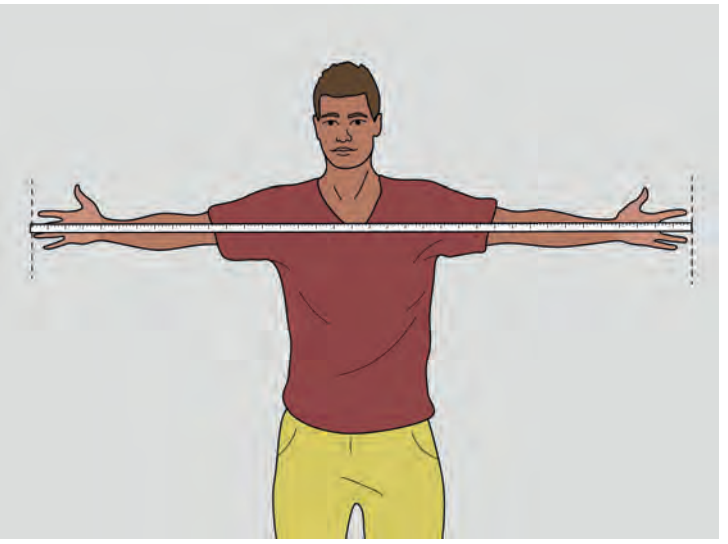

Figure 1.3
Measurement of arm span.

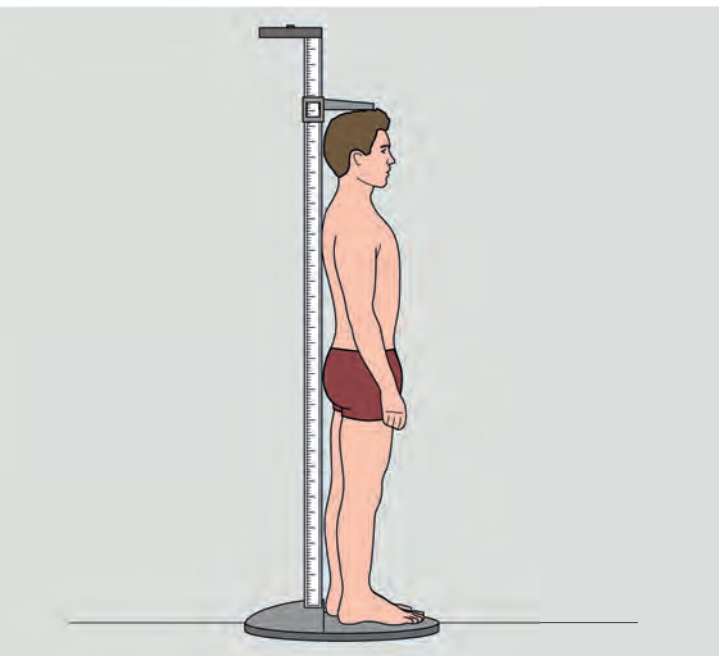

Figure 1.4
Measurement of standing height.

Figure 1.5
Measurement of sitting height.

This is important in informing decisions for limb equalisation, which may involve shortening, lengthening or a combination of the two.

Comprehensive evaluation involves inspection of orthotics, prosthetics and footwear including differential wear and a global visual assessment, including spinal balance, pelvic obliquity and compensatory strategies for limb shortening.

Graduated blocks should be available to level the pelvis and evaluate the contribution of limb-length inequality to spinal asymmetry. Scoliosis associated with limb-length discrepancy is usually corrected when the pelvis is levelled (Figure 1.6).

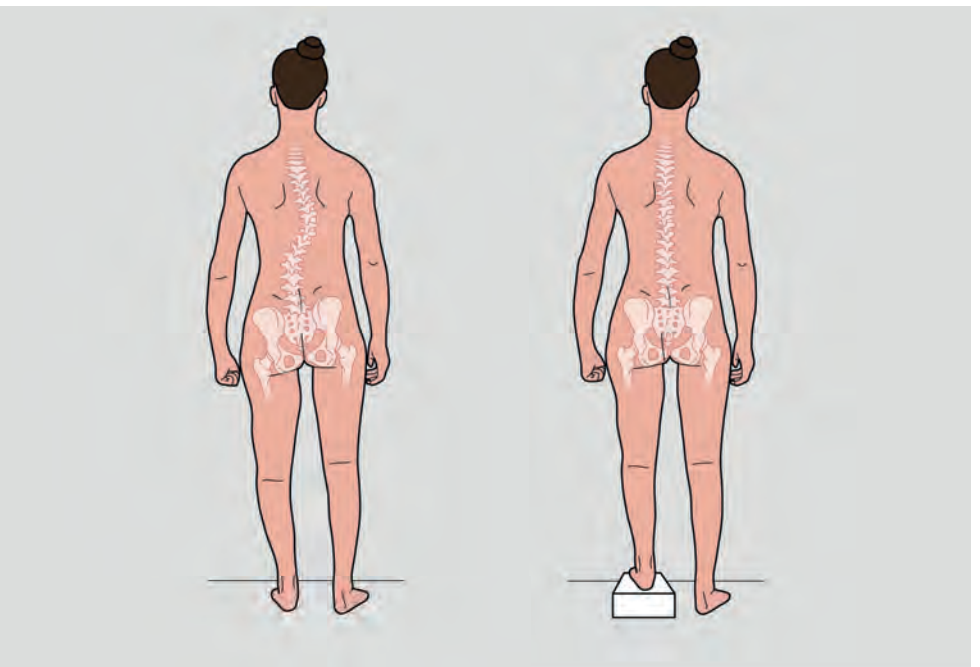

Figure 1.6
Elimination of scoliosis due to limb-length discrepancy with blocks.

This is also assessed in the seated patient, and elimination of a spinal deformity on forward bending indicates a flexible spine (Figure 1.7).

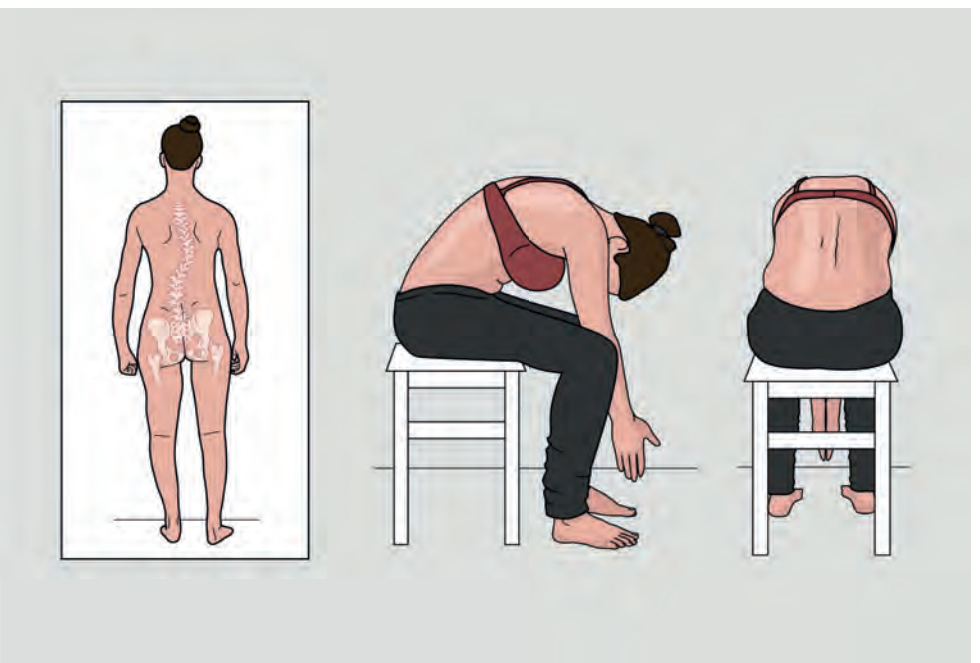

Figure 1.7
Elimination of scoliosis due to limb length discrepancy with forward bending.

Evaluation includes single-leg stance to assess abductor function (Figure 1.8), measurement of popliteal angle to assess hamstring length (Figure 1.9), and ankle range with the knee flexed and extended, to assess gastrocsoleus length (Figure 1.10).

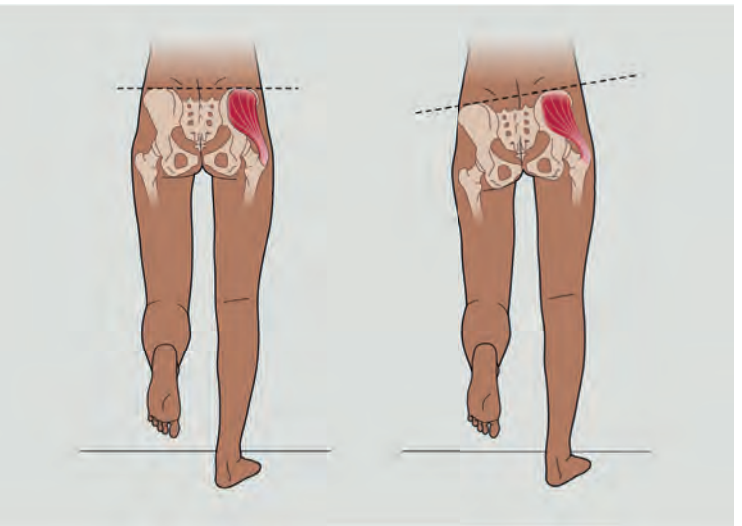

Figure 1.8
Assessment of abductor function.

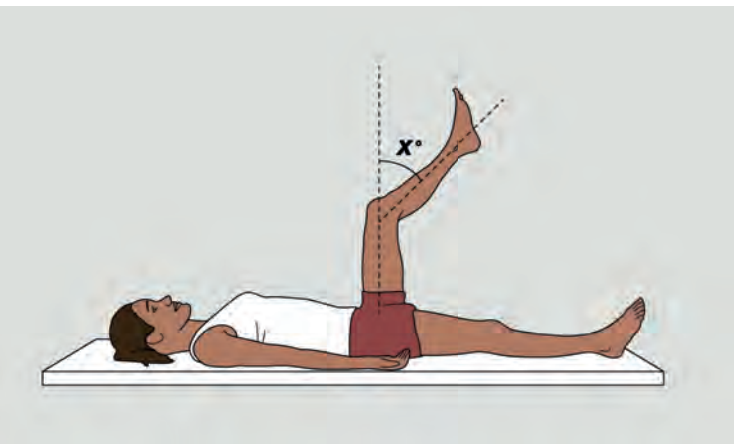

Figure 1.9
Assessment of popliteal angle.

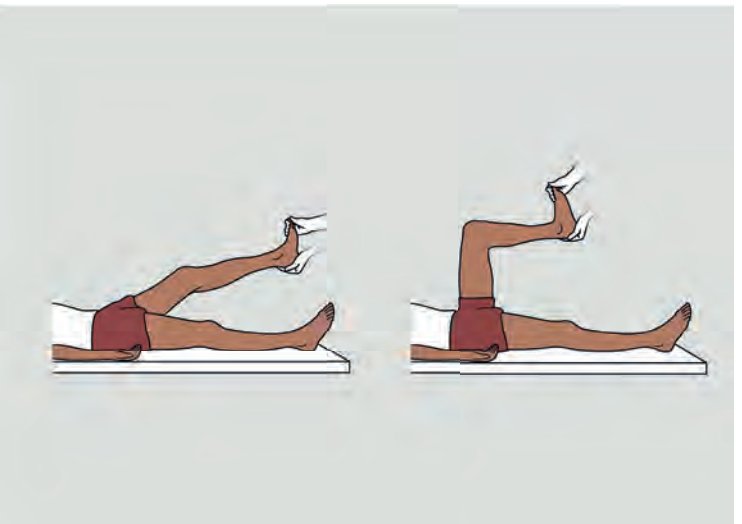

Figure 1.10
Assessment of gastrocsoleus length.

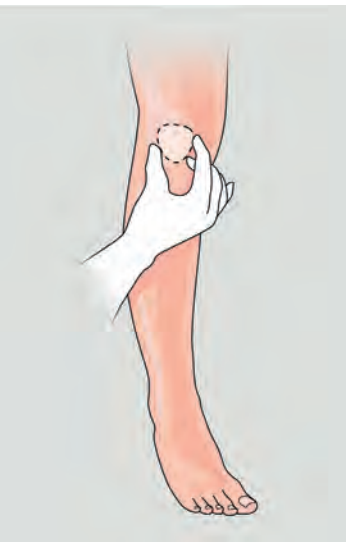

Figure 1.11
Identification of patellar position to determine limb rotation.

Coronal assessment is assisted by marking the patellar position to orientate the rotational position of the limb (Figure 1.11) and this also assists in positioning for radiological evaluation.

The structure of the foot is determined by considering the mutual positions of the hind-, mid- and forefoot with the patient standing and recumbent.

Torsional profile

The terms version, torsion and rotation are used interchangeably to describe angulation in the axial plane. This chapter will refer to normal geometry as version, angular deformity as torsion and joint movement as rotation. The evaluation of torsional alignment is a clinical exercise, with sophisticated radiological imaging used as an adjunct in selected cases. Referencing should be consistent and usually involves a description of relationship of the distal segment to the proximal segment.

The position of the foot and patella are part of the evaluation of the walking patient and while in-toeing or out-toeing will identify the overall position of the limb, this does not localise the abnormal segment. The most efficient method of assessment is with the patient prone and the contribution to the overall profile determined at each anatomical level. The hip is in a functional position of neutral extension in the prone patient and the range of hip rotation is assessed using the leg as a lever and the axis of the tibia as a point of reference (Figure 1.12).

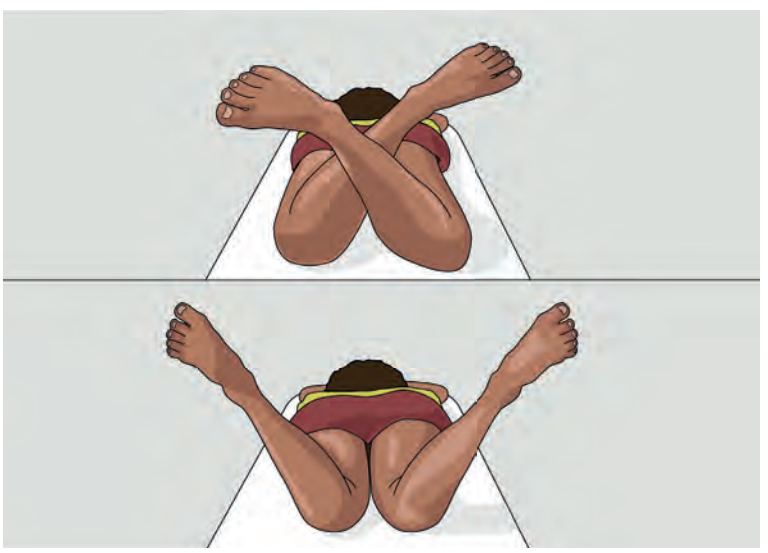

Figure 1.12
Prone assessment of hip rotation.

An asymmetrical range about a neutral point is a function of proximal femoral version and alters with age in the growing child. The population mean (normal) for femoral anteversion is 40° at birth, 20° by the age of 9 and 12–16° at 16 years. Assessment is also performed with the patient in the supine position with the hip flexed to 90° (Figure 1.13).

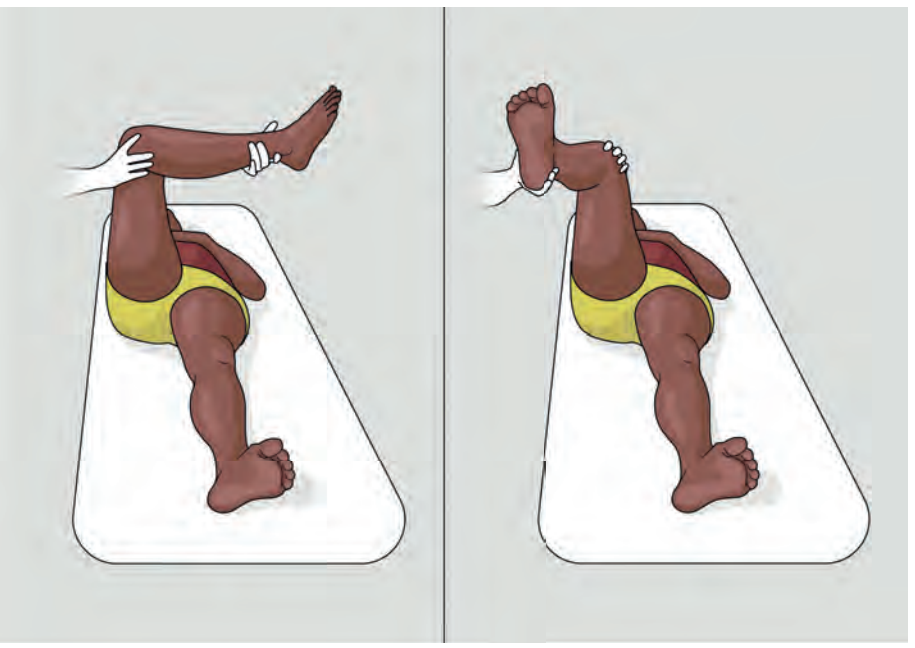

Figure 1.13
Supine assessment of hip rotation.

Differences between the arc of rotation with the hip in neutral (prone) and 90° flexion (supine) suggest loss of sphericity of the femoral head.

The thigh–foot angle is measured at the intersection between the long axis of the femur and a line bisecting the foot in its resting position (Figure 1.14). This describes the tibial contribution to the overall torsional profile with a population normal mean of 10–15° external rotation.

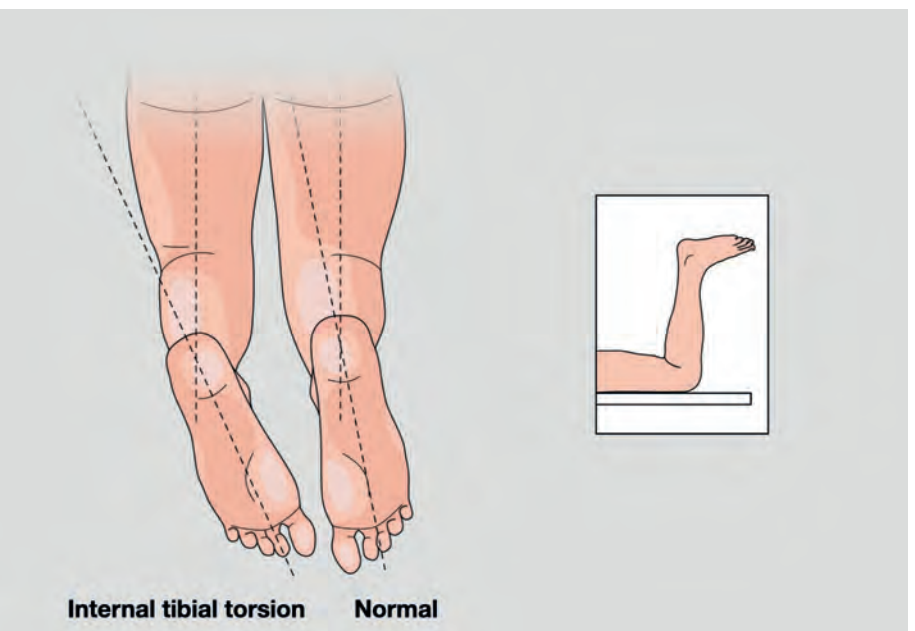

Figure 1.14
Thigh–foot angle.

The transmalleolar axis can be assessed with the patient prone or seated with a population normal mean of 20° external rotation (Figure 1.15).

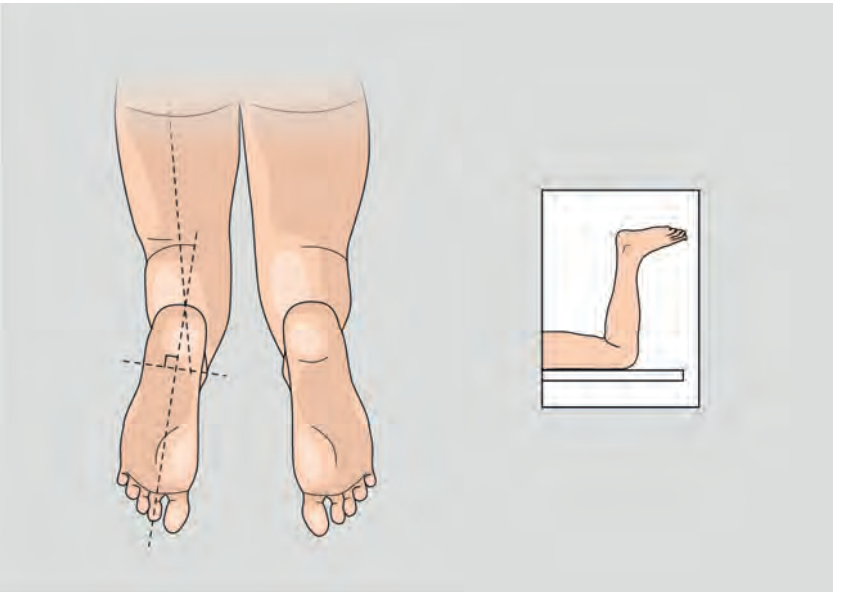

Figure 1.15
Transmalleolar axis.

The feet are assessed using the heel bisector, which intersects the second toe of the normal foot and medial displacement indicates metatarsus adductus (Figure 1.16).

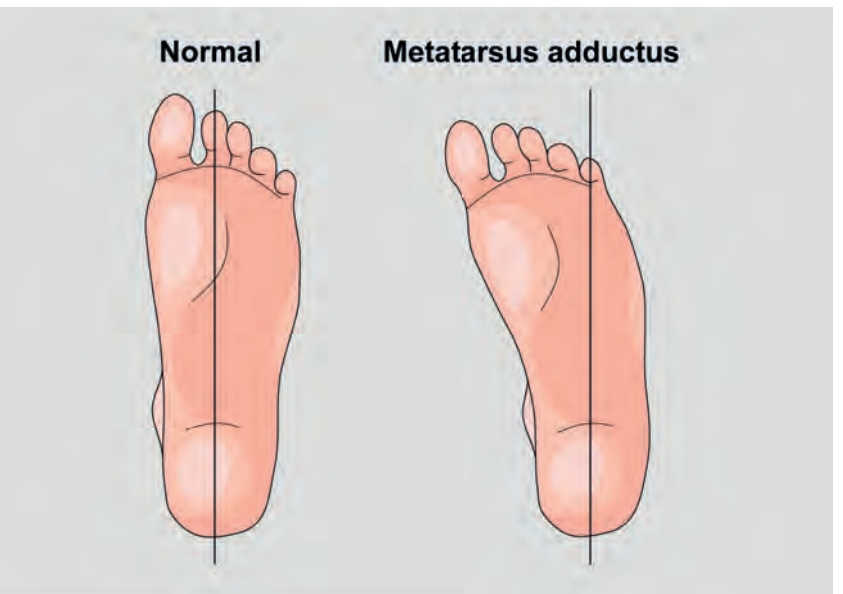

Figure 1.16
Heel bisector line.

An abnormal rotational profile can involve an overall reduction in the arc of rotation or a normal total range with reduction of the internal/external rotation component, with a complementary increase in the external/internal rotation component. This may be asymptomatic in the developing child unless the difference is substantial. Small changes in rotation in the skeletally mature patient, however, are often problematic and usually follow a fracture or osteotomy.

Leg-length discrepancy

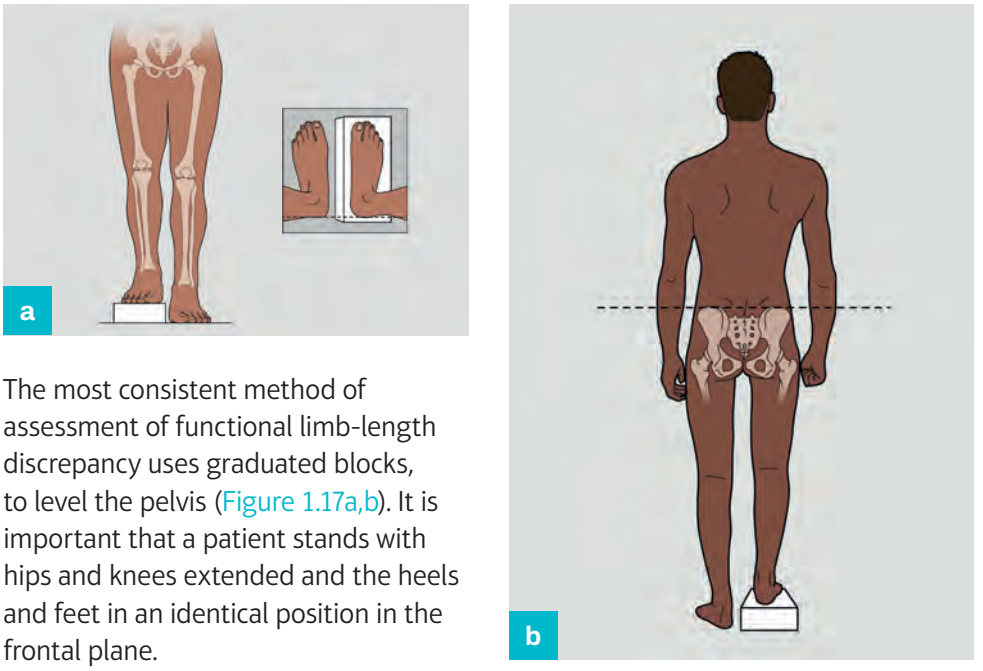

Figure 1.17 (a,b) Assessment of limb-length difference using graduated blocks.

The most consistent method of assessment of functional limb-length discrepancy uses graduated blocks, to level the pelvis (Figure 1.17a,b). It is important that a patient stands with hips and knees extended and the heels and feet in an identical position in the frontal plane.

If there is a fixed contracture, with flexion of the hip, knee or ankle, the limbs should be arranged in a symmetrical position, but this can present considerable difficulties with fatigue and balance.

Measurement of limb-length discrepancy relies on localisation of the anterior superior iliac spine (ASIS), the highest point of the iliac crests or posterior superior iliac spines (PSIS). Confirming that the pelvis is level is subjective and it is generally accepted that the PSIS is a more reproducible method. The height of a block that produces a level pelvis is equal to the functional leg-length discrepancy.

Limb length is estimated in the supine patient by the measured distance between ASIS and medial malleolus, with both legs placed in neutral alignment (Figure 1.18).

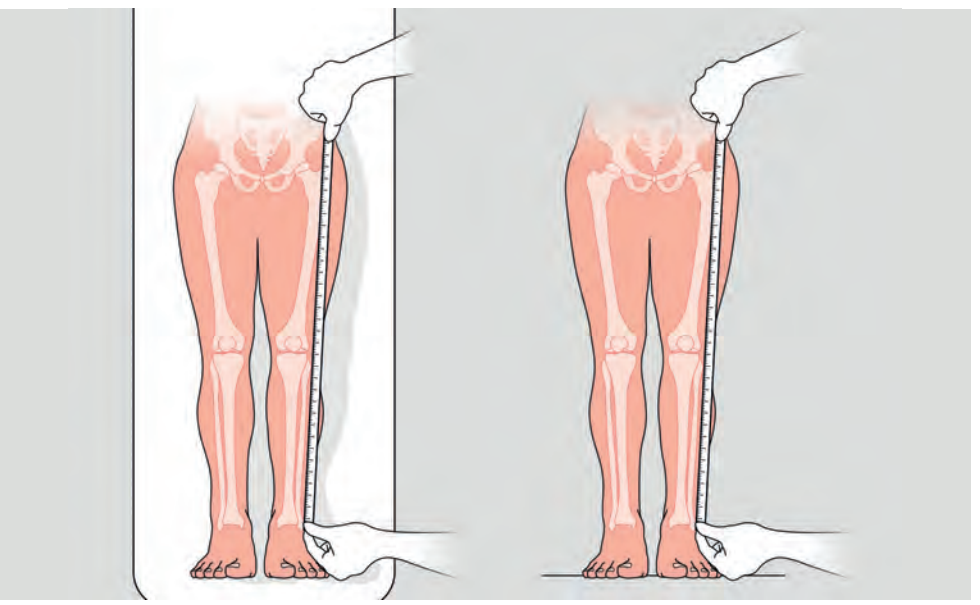

Figure 1.18 Measurement of leg length.

Assessment of the total length of the lower limb requires measurement to the sole of the foot and this should be included, particularly if there is ankle or hindfoot involvement. The presence of deformity at the hip or knee is accommodated by placing the normal extremity in a symmetrical position.

The length of the femur is also assessed in the supine position with the hips flexed to 90°, the knees together and the heels off the bed (Figure 1.19).

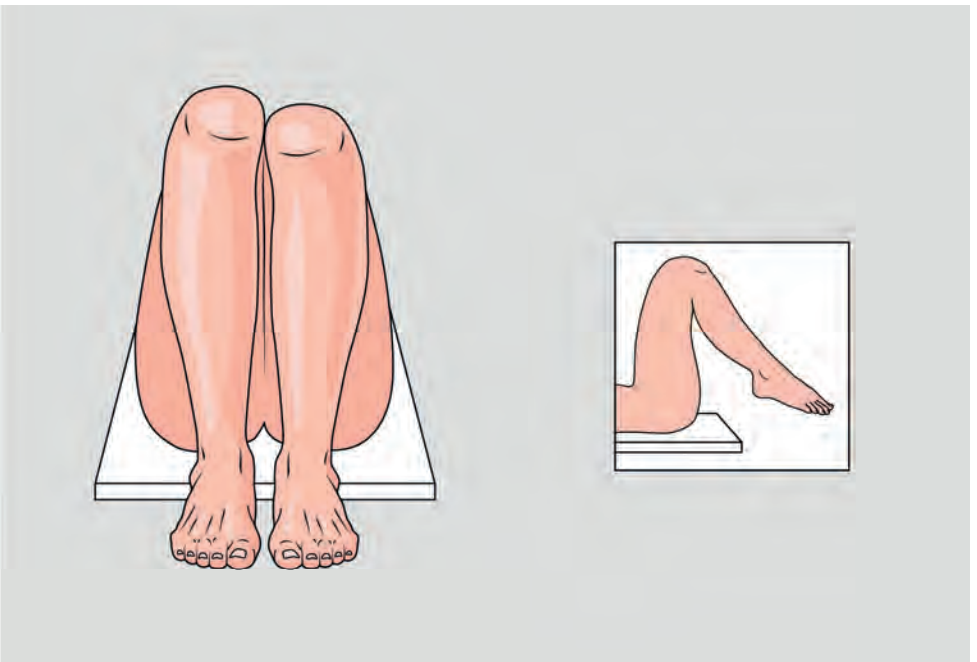

Figure 1.19
Assessment of femoral length.

Although it is conventional to assess the tibial length with the patient supine, it is more accurate to assess in the prone patient with the hip and ankle in a neutral position and the knee flexed to 90° (Figure 1.20). This can be conducted in association with assessment of the rotational profile. The measured difference at the medial malleoli represents the contribution from the tibia and the difference in heel heights represents the additional contribution from the hindfoot.

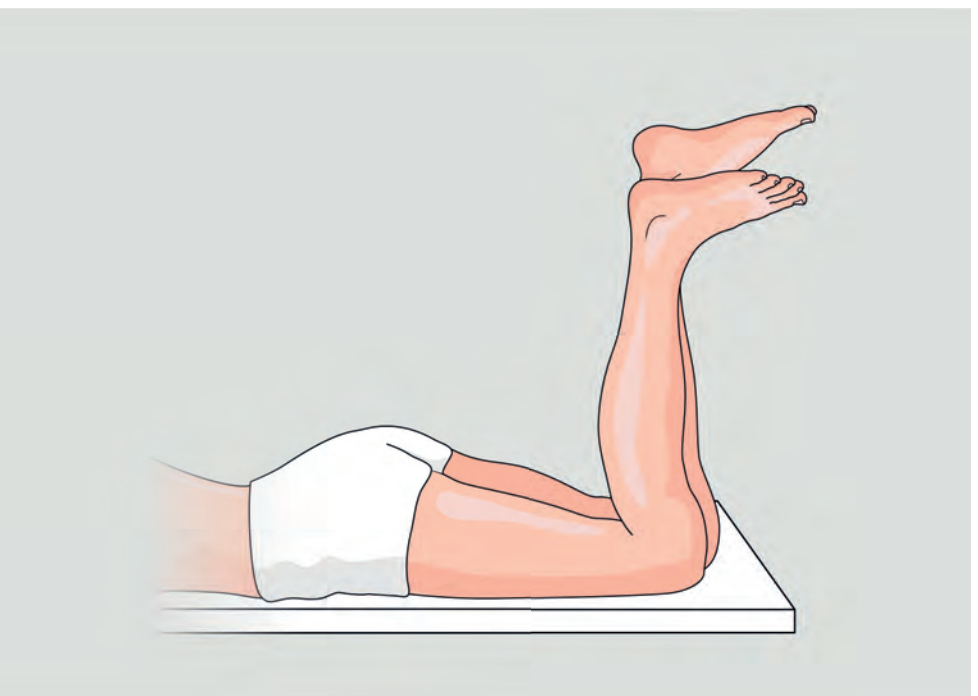

Figure 1.20
Assessment of tibial and hindfoot length.

Assessment of joints

Each joint adjacent to the site of deformity must be examined as part of the overall assessment of the limb. Joint stability should initially be evaluated in the standing position and as part of the assessment of walking.

Supine assessment involves identifying pain and demonstrating and recording the active and passive range of joint movement with the knee in extension and flexion.

Correctable deformity, particularly in the frontal plane, may be overlooked and the examination should also involve formal tests of ligament laxity and dynamic instability. This is particularly important in congenital reduction deformities. The presence of joint laxity in this group of conditions influences the available treatment options and is associated with additional morbidity during attempts at reconstruction. Joint ranges must be preserved. An evolving loss of passive range is a compelling reason to decrease the rate of surgical correction and may result in abandoning a procedure.

Compensatory contractures must be appreciated as they will continue after axis correction and, if fixed, will result in incomplete deformity correction. Fixed subtalar joint inversion is a common consequence of a long-standing tibial valgus and isolated correction of the axis of the tibia will result in fixed hindfoot varus. Compensatory strategies for long-standing limb shortening include tiptoeing on the short side, with knee and hip flexion of the long leg. These joints may not return to normal after limb equalisation and identification of fixed contractures is an important part of the evaluation.

Soft-tissue assessment

The clinical examination must include assessment of individual peripheral nerves including motor function, mapping areas of cutaneous sensation, evaluation of sympathetic function and the presence of nociceptive or neuropathic pain.

Peripheral arterial pulses must be evaluated, documented and, if necessary, verified with a Doppler probe. Where abnormalities are identified, referral for specialist investigation is necessary prior to limb reconstruction.

The condition of the non-skeletal tissues has a fundamental effect on the management options and outcome following limb reconstruction. The effect of the soft-tissue envelope is equally important in reconstruction of congenital and traumatic deformity, but there are subtle differences in assessment.

Skin cover in congenital limb reduction is generally normal, but the field defect results in loss of pliability of the myo-fascial units that impedes surgical lengthening.

The condition of the skin and subcutaneous elements is often abnormal following limb trauma, as a consequence of direct injury, surgical approach or complications, particularly infection. The soft tissues on the concave side of a deformity are at risk, particularly if adherent to deeper structures including bone, and will be under tension during deformity correction.

The soft-tissue envelope must be comprehensively assessed prior to surgical intervention and this will inform decisions including the site of osteotomy and rate of correction (Figure 1.21). Soft-tissue tethering, skin grafts and local and free tissue transfer may preclude incisions for osteotomies, obviate internal fixation or require elevation as part of a surgical strategy.

Figure 1.21
Assessment of the soft-tissue envelope.

Evidence of complications including compartment syndrome must be identified in a post-traumatic deformity as fibrotic muscle will be uncompliant and attempted correction of angular deformity and length will produce joint contractures.

KEYPOINTS

- Components of a clinical history relevant to the assessment of skeletal deformity
- Differences in emphasis between paediatric and adult cases
- Differences in emphasis between congenital and acquired deformity
- Assessment of :
  - Skeletal proportions
  - Lower-limb rotation
  - Limb shortening
  - Foot and ankle
  - Soft-tissue envelope

CHAPTER

2

Radiological evaluation of lower-limb deformity

Elizabeth Moulder and Gamal Hosny

Introduction

Radiographs are used to identify the site and geometry of skeletal abnormality to determine the axis of the limb and individual segments. They also provide information on bone quality and the cause of the deformity. Clinical examination is, however, of fundamental importance in the assessment of limb deformity and sophisticated radiographic analysis is redundant in isolation. This chapter will describe how to produce standardised radiographs and will outline additional investigations that may be required in specific circumstances. The common pitfalls associated with the radiological assessment of limb deformity will be discussed, with practical advice on how to avoid them.

General principles

When the patient is positioned between an X-ray source and an image receptor, the tissue densities determine the differential X-ray absorption, which is detected by the receptor to create a greyscale image. Digital radiology has become the gold standard and can be performed using computed radiography (CR) or direct digital radiography (DDR) techniques. This allows remote access and digital processing of images to alter contrast and exposure. Software packages can also be used with picture archiving and communication systems (PACS) to measure and manipulate the images required for deformity planning.

X-rays travel in a straight line, divergent from their source, and this results in magnification of the final image. Magnification is the ratio of the detector and object distance from the source. The closer the object is to the X-ray source, the greater the resultant magnification (Figure 2.1).

The patient should therefore be placed as close to the detector as possible and the distance between the X-ray tube and detector should be as far as is practical, with a typical distance of 305 cm. It can be difficult to place the patient with an external fixator or joint deformity close to the detector and this will result in a magnification error.

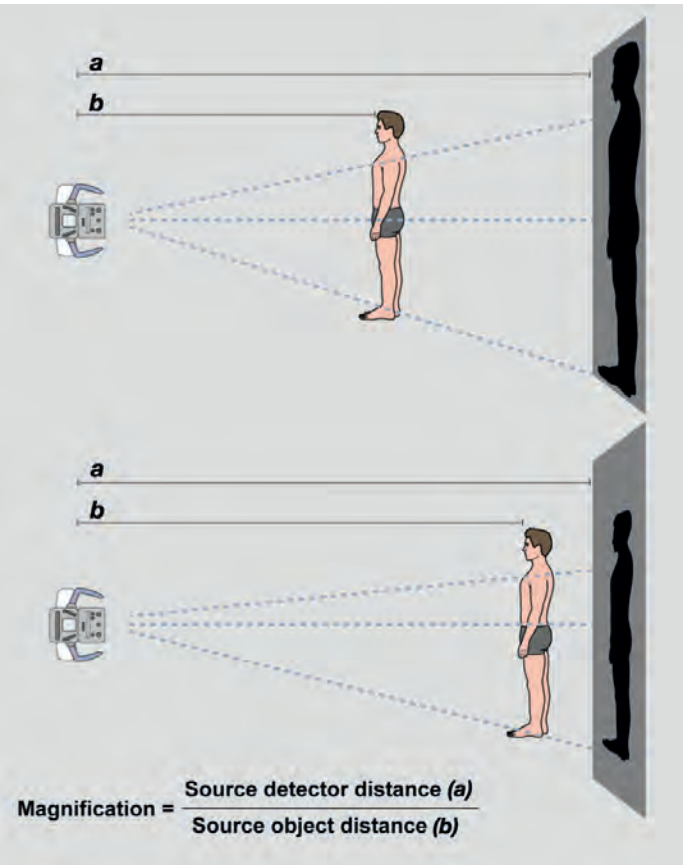

Figure 2.1
Divergent X-rays result in magnification of the object in the final image.

Magnification will not affect the measurement of angles but affects the measurement of distances and will introduce an error. Accurate distance measurement is necessary for pre-operative planning of an osteotomy level, determination of mounting parameters for a hexapod fixator or measuring the dimensions of a distraction site. Magnification can be estimated using commercially available scalars but any radio-opaque object of known dimensions, positioned in the same plane as the bone in the antero-posterior (AP) and lateral views, will suffice (Figure 2.2a,b).

Figure 2.2
Correct positioning of the limbs and scalar ball for the AP view **(a)** and lateral view **(b)**.

Imaging software will often automatically detect a scalar ball and adjust for magnification (Figure 2.3).

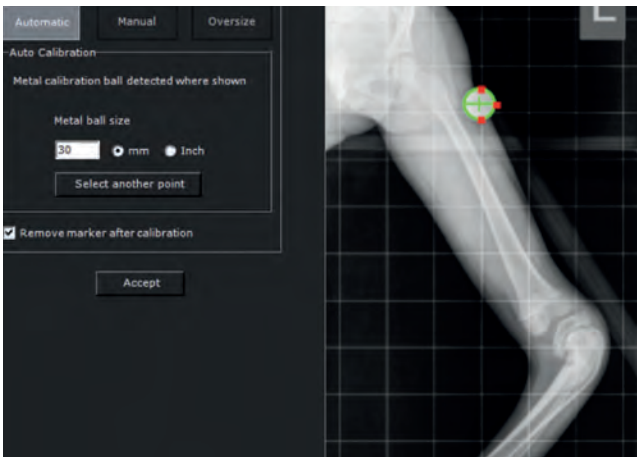

Figure 2.3
Image calibration using a scalar ball.

For the example shown in Figure 2.4, a manual method to account for magnification uses the ratio between the actual (30 mm) and measured (34.2 mm) diameter of the scalar ball, but any object of known dimension of can used as an alternative.

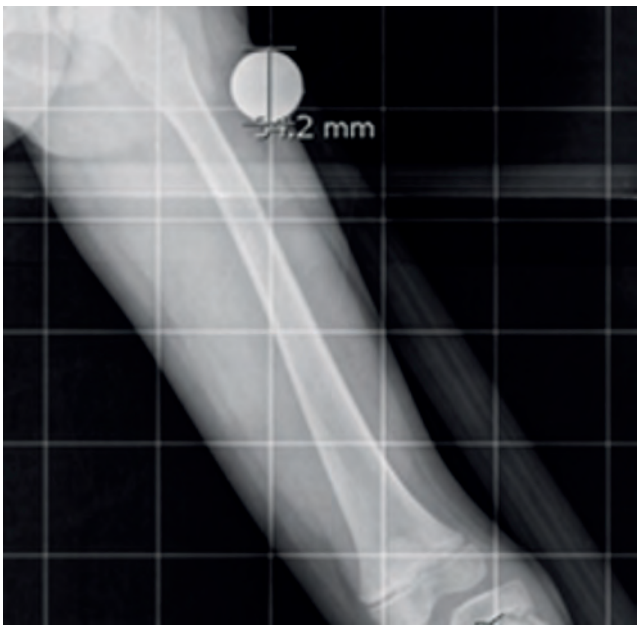

Figure 2.4
Manual calculation of the magnification multiplier.

$$\text{Magnification multiplier} = \frac{\text{Known object size}}{\text{Measured image size}}$$

$$\text{Magnification multiplier} = \frac{30.0}{34.2}$$

$$\text{Magnification multiplier} = 0.88$$

A magnified image will result in a conversion factor, which is then used to correct all linear measurements for that radiograph. The result should be <1 and measurements of length are multiplied by this ratio. It is important to consider the AP and lateral images separately, as the magnification will be different in each plane.

Assessment of torsion

The nomenclature used to describe the axial plane is imprecise and, for the purpose of this description, 'torsion' will be used for an angular deformity of the skeleton in the axial plane and 'rotation' to describe the movement of a joint. Torsion is difficult to quantify radiologically, particularly if the deformity is distributed throughout the whole limb, and clinical examination is the primary method of assessment. Axial computed tomography (CT) imaging can be used to assess the torsional profile in patients with suspected deformity (Figure 2.5). The conventional approach is to obtain axial images of both legs at the trochanteric and condylar levels of the femur, the proximal tibia and the ankle malleoli. Analysis is, however, subjective and may be inaccurate if there is a coexisting angular or translational deformity, even when image analysis software is used.

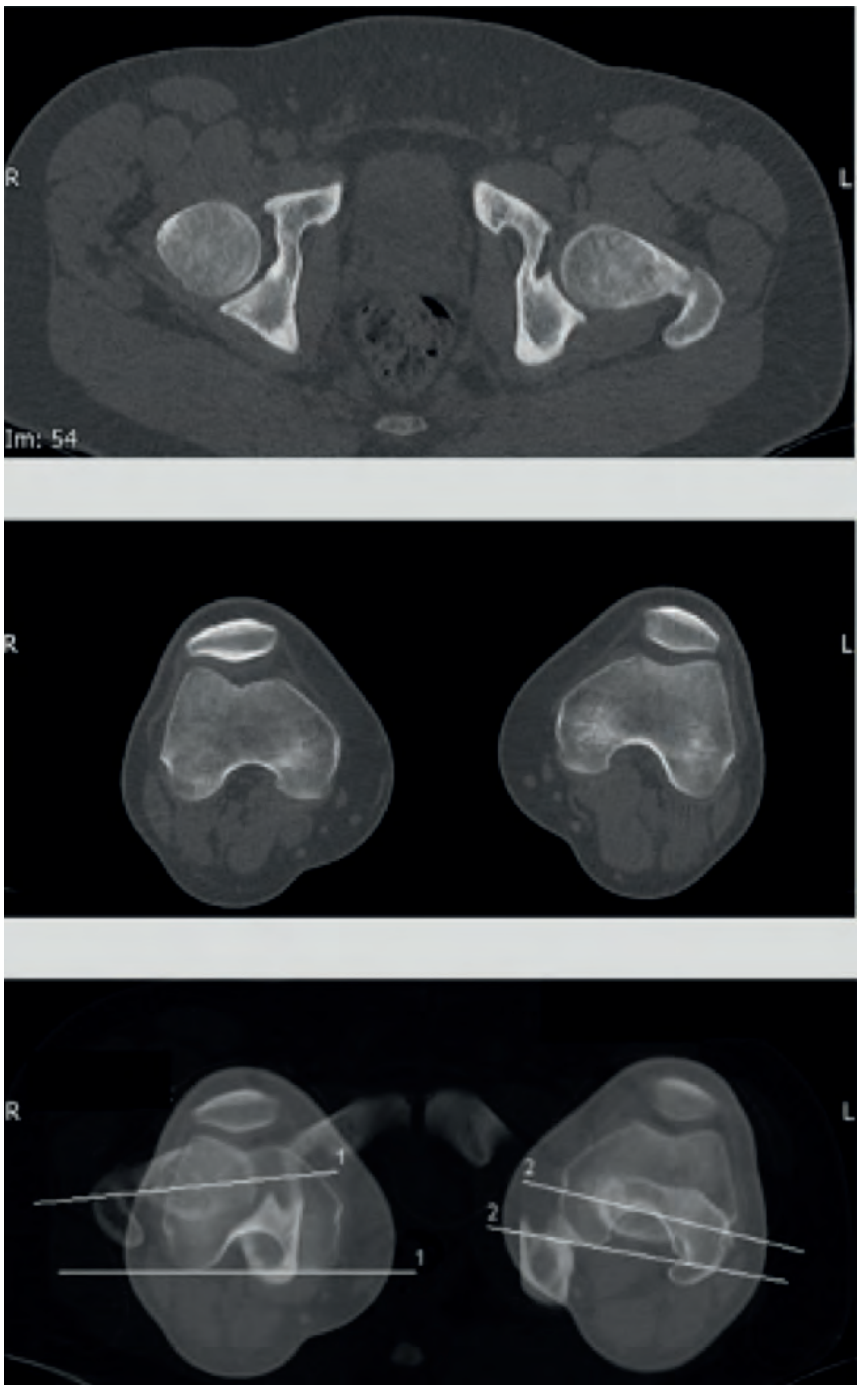

Figure 2.5
Torsional abnormality demonstrated by axial CT scanning.

Radiographs for limb deformity analysis

The baseline radiographic images for deformity assessment are a standing AP and a perpendicular lateral view of both legs (Figure 2.6a,b).

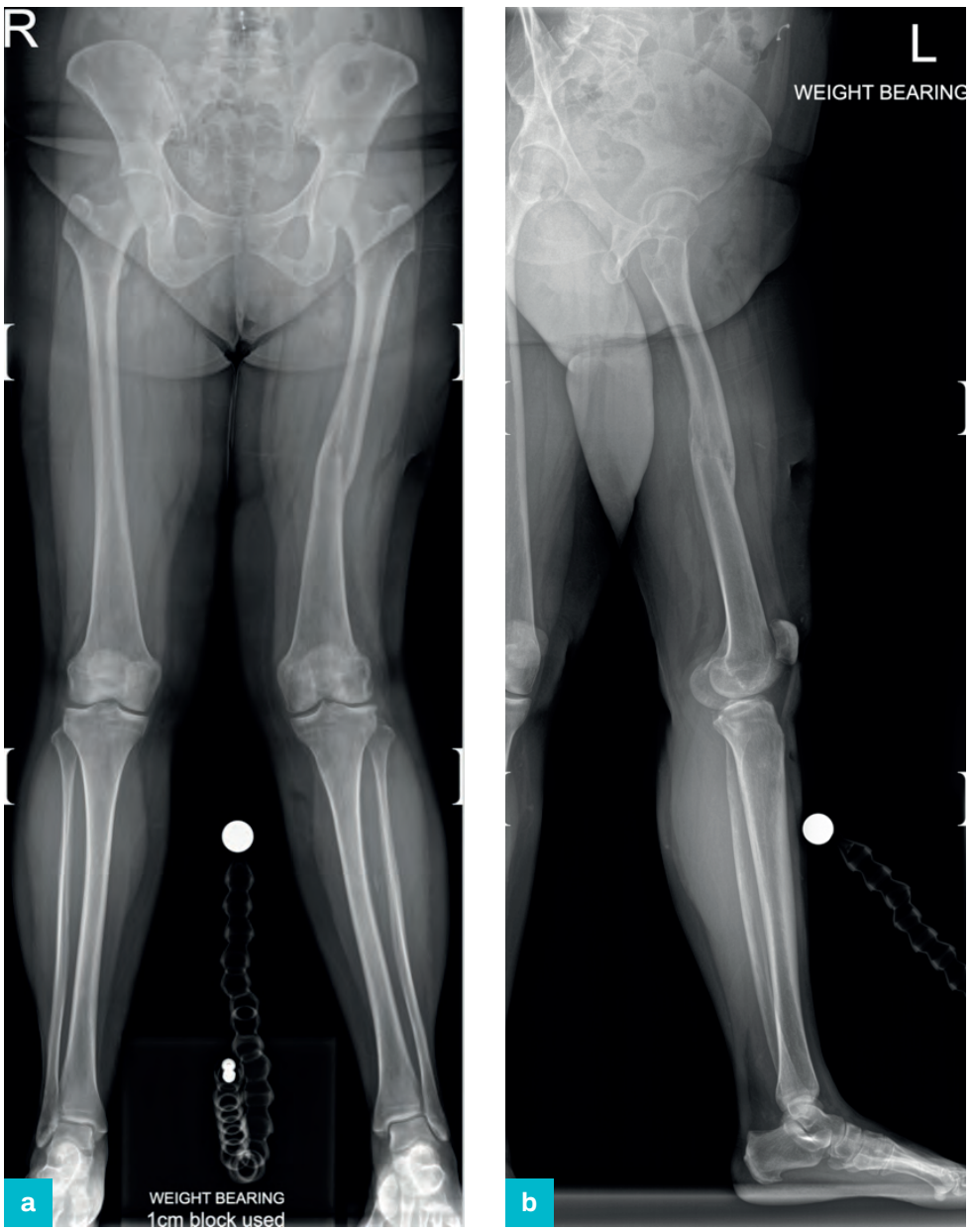

Figure 2.6
(a) Standing AP and **(b)** standing lateral radiographs.

Dedicated images of specific bone segments or joints may also be necessary and are determined by the individual clinical circumstances. Digital radiography uses a fluoroscopic sensor and the cassettes used in conventional radiology are: 13 × 18 cm; 18 × 24 cm; 24 × 30 cm; 20 × 40 cm; 30 × 40 cm; 35 × 35 cm; 35 × 43 cm; 30 × 90 cm. Long-leg films are commonly obtained with a 1 m cassette for children and 1.3 m cassette for adults. The following diagrams are intended to demonstrate the principles of image acquisition. They do not specify the cassette sizes or source to plate distances as these are variable and are dictated by factors including local protocols and patient size.

Standing AP view

A patient may alter their stance to compensate for a deformity and this should be identified as part of the clinical assessment. The position of the limb in a standing alignment radiograph will influence the radiological projection and therefore the apparent geometry of the skeleton. The standing AP view should demonstrate both legs and include the iliac crests to the ankle joints, with the patella facing forward (Figure 2.7a,b). If there is a leg-length discrepancy, the pelvis must be levelled, with blocks under the short limb. It is necessary for the radiographer to appreciate the exact requirements for this view and an efficient nomenclature should be agreed to streamline the process of ordering of this radiograph.

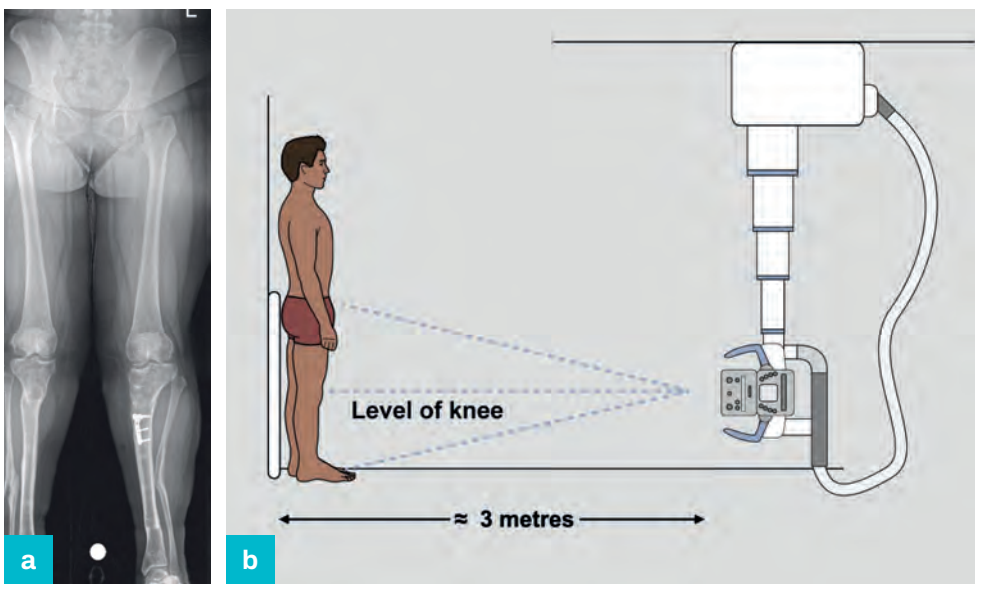

Figure 2.7 (a,b) AP long-leg radiograph.

Patient positioning

It is important to ensure that both legs are placed as close to the detector as possible, to reduce the magnification error. If one leg is placed further forward, due to a flexion deformity or an external fixator, the leg lengths and width will appear to be unequal.

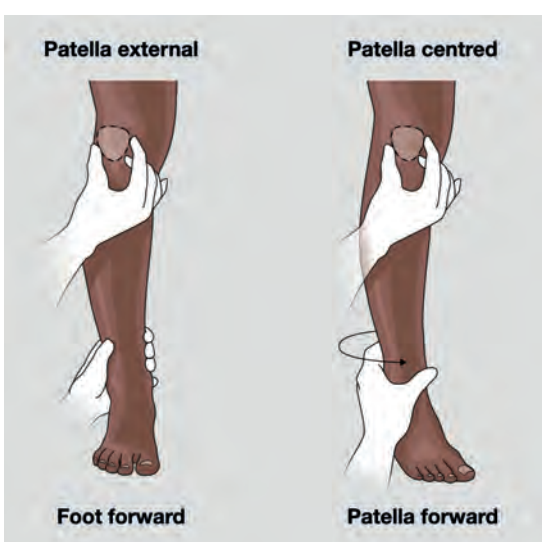

Figure 2.8 The patellar position is used to orientate the limb correctly.

A standard standing knee radiograph is taken with the foot facing forward and this is the default position that a radiographer will use. Standing alignment radiographs for deformity planning are independent of the position of the foot. A true frontal image of the knee will generate a reproducible projection, which is required for accurate deformity assessment and can be compared with previous and subsequent images. This is usually produced by positioning the limb with the patella facing forward (Figure 2.8). It is useful to palpate the patella and delineate it with skin marker pen,

especially when there is considerable deformity, with the required position of the limb demonstrated to the patient and the radiographer.

Radiographs obtained in a non-standardised manner are prone to measurement error and a patella-forward position is required to produce the true representation of deformity in the frontal plane (Figure 2.9a,b).

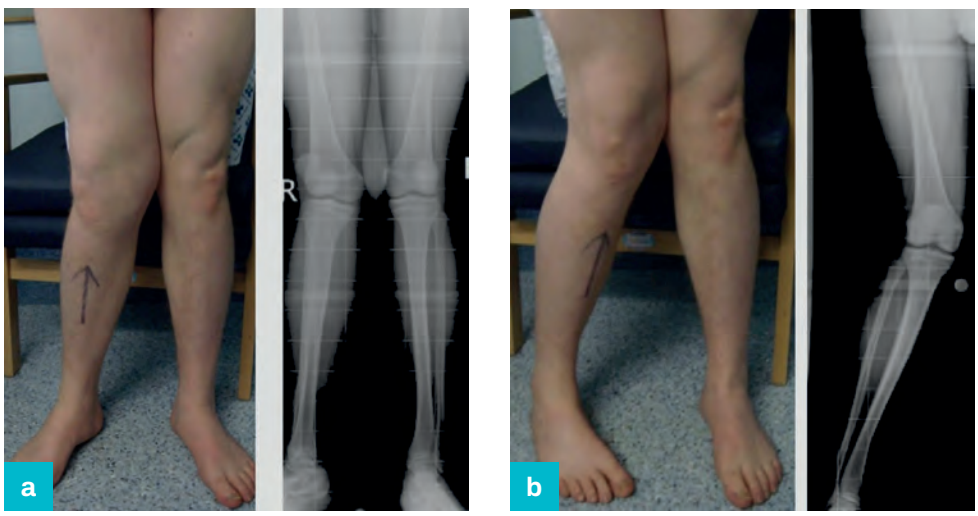

Figure 2.9
Effect of limb position on radiological alignment:
(a) foot forward;
(b) patella forward.

If the patello-femoral joint is abnormal, particularly if the patella is subluxed or dislocated in extension, the plane of movement of the knee should be determined by flexion and extension of the knee. The true lateral radiograph is obtained with the beam set at 90° to this position (Figure 2.10).

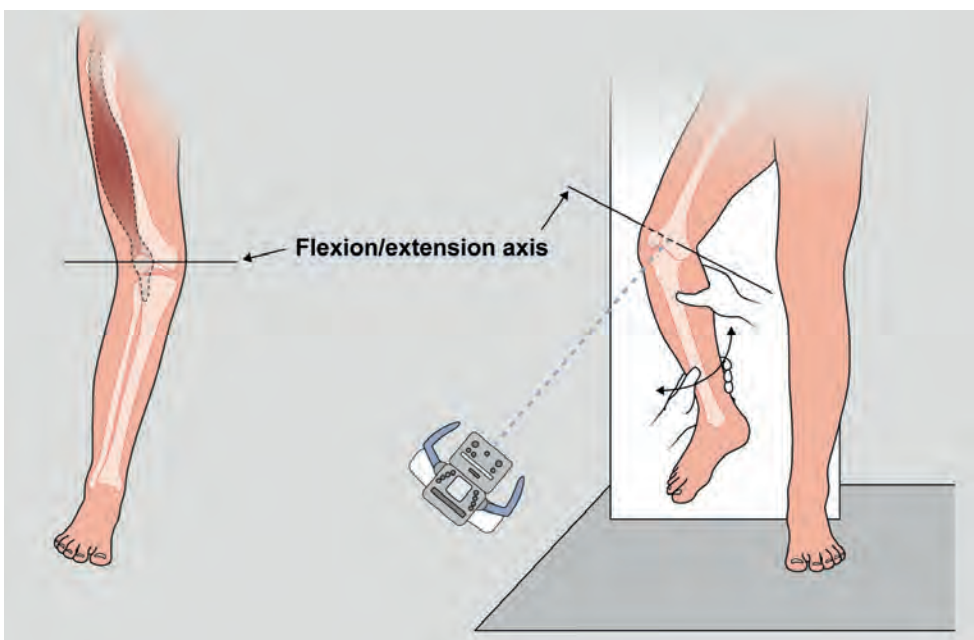

Figure 2.10
Determination of the true axis in the presence of patellofemoral abnormality.

Patients will accommodate a limb-length inequality with a predictable set of compensatory strategies. These include lengthening the short leg with a tiptoe stance or shortening the long leg with a combination of flexion or hyperextension of the knee, dorsiflexion of the ankle and flexion of the hip. There may also be compensatory hindfoot valgus, pelvic tilt and scoliosis. These secondary deformities should be corrected if possible or compensated if fixed, to produce standard, reproducible radiographic images.

The anterior superior iliac spines are identified by palpation in a standing patient and a series of blocks are positioned under the short leg until the pelvis is level and flexible compensatory strategies are corrected. The radiographer should use the same blocks and corrected position of the limb for the long-leg films. If there are no fixed contractures, the height of the blocks is a good estimate of the total leg-length discrepancy (Figure 2.11a).

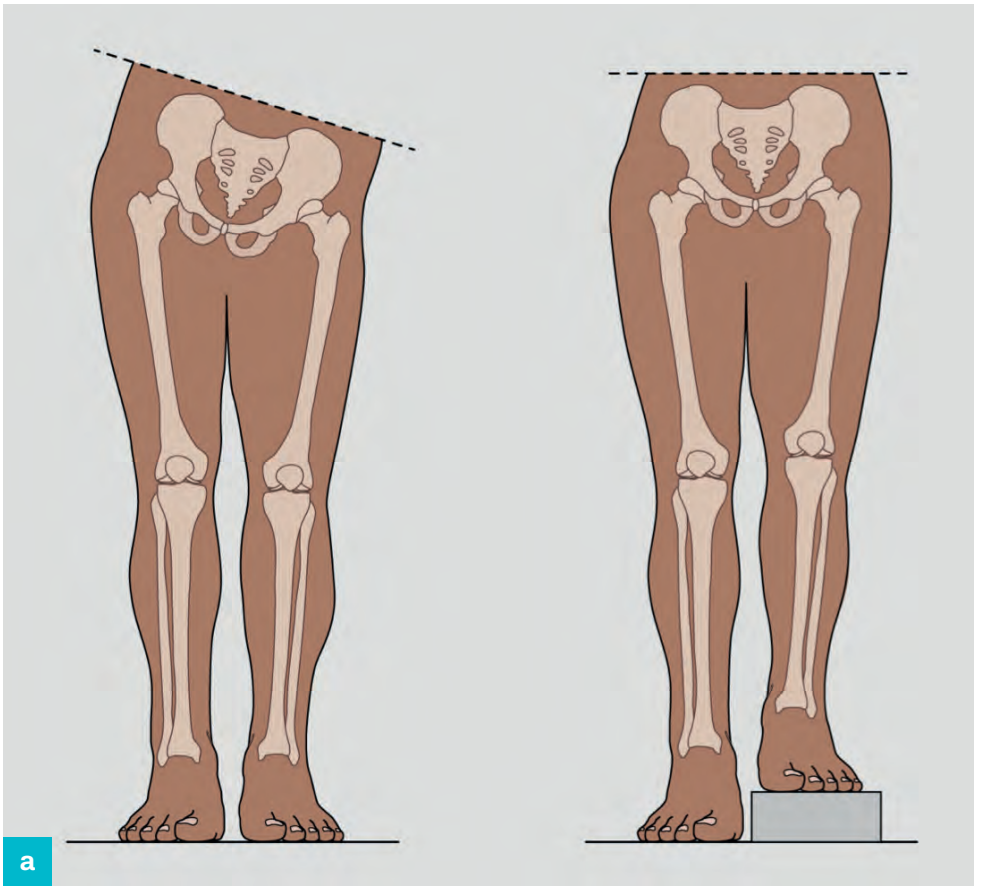

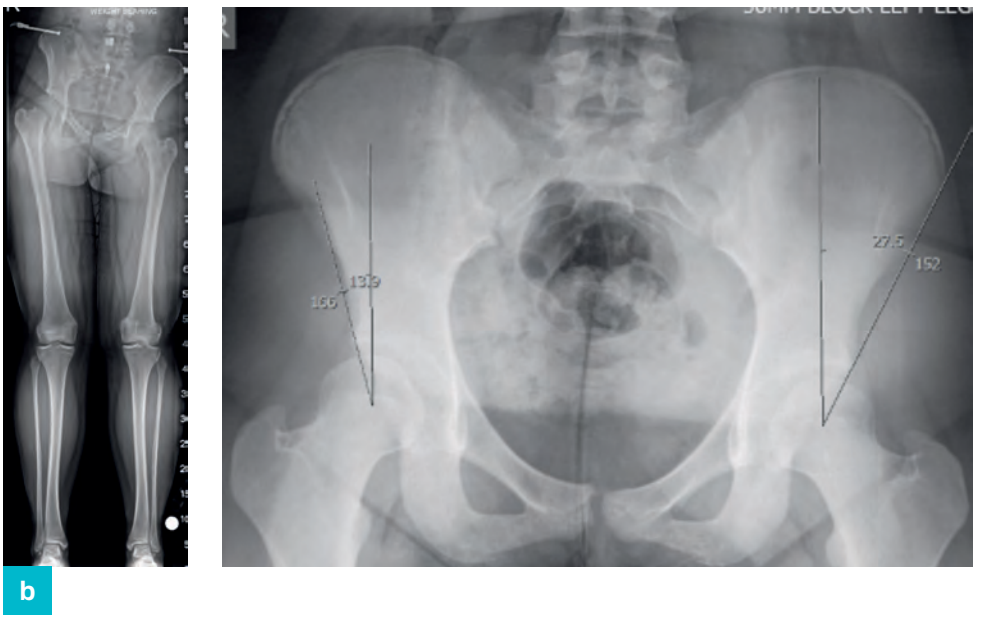

Figure 2.11
(a) Pelvis levelled using blocks under the short leg.
(b) A levelled radiograph of the pelvis is necessary to measure hip coverage.

If the pelvis remains in an oblique position for the radiographs, the hip of the long leg may appear to be abnormal and a centred pelvic radiograph may be necessary for further assessment (Figure 2.11b).

Joint line incongruity

Stress views, particularly of the knee (Figures 2.12a,b and 2.13a,b), are used to assess joint stability and determine whether this is flexible, due to ligamentous laxity, or fixed, due to joint incongruity.

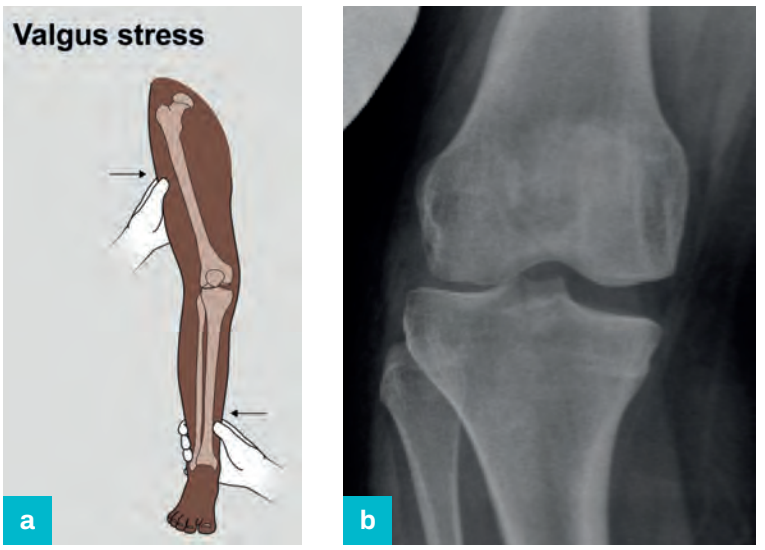

Figure 2.12 (a,b)
Valgus stress view.

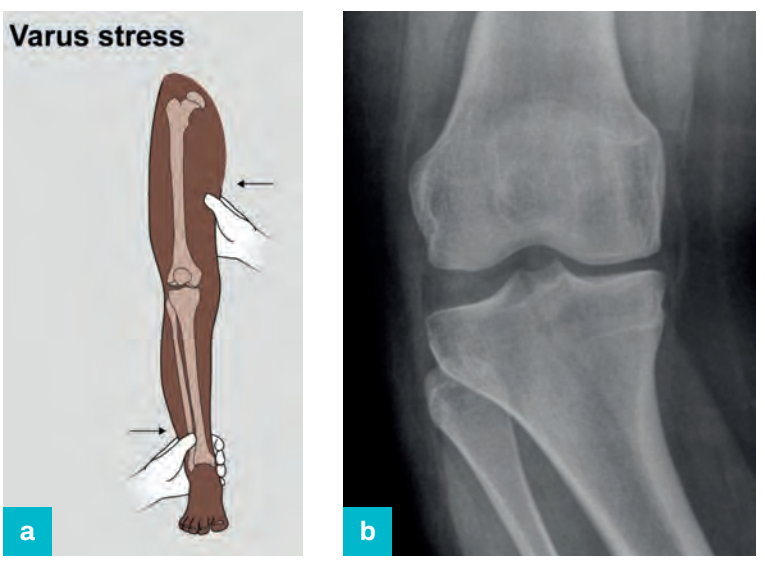

Figure 2.13 (a,b)
Varus stress view.

Figure 2.14
Centred AP radiograph demonstrating intra-articular deformity.

Plain radiographs, centred on a joint, are used to assess articular congruity (Figure 2.14). If the cause of incongruity is not accurately determined, subsequent correction of the deformity will be incomplete.

Standing lateral view

The standing lateral view should be obtained perpendicular to the AP view and ideally demonstrate the femoral head to the ankle joint. Comprehensive radiological assessment of deformity is a general requirement in surgical planning but, in some circumstances, complete lateral imaging is impractical and views of an individual bone segment will suffice.

Producing consistent lateral views can be challenging for the patient who may need assistance, including walking aids, to maintain the correct position. It is often useful to accompany the patient to assist the radiographer with this process.

Patient positioning

To obtain full-leg lateral views, the patient should be placed with the foot of the target limb parallel to the detector with the knee fully extended and the opposite hemipelvis externally rotated. This produces an image from the hip to the ankle and demonstrates any fixed knee flexion or hyperextension (Figure 2.15a,b).

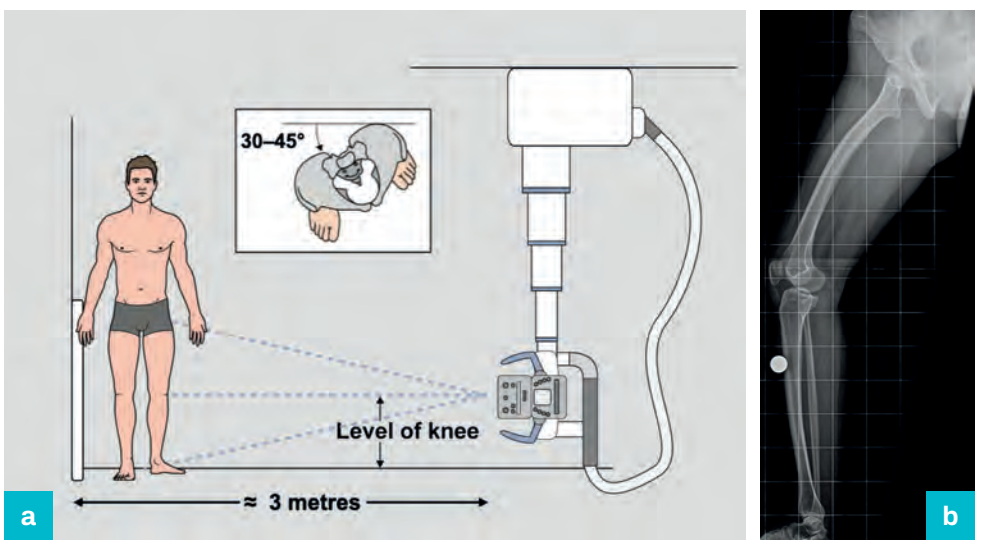

Figure 2.15 (a,b) Standing lateral long-leg radiograph.

A CT scanogram may be used to assess limb alignment, but these images are produced in the prone position and therefore they do not account for joint laxity and the effect of weight-bearing on the mechanical axis cannot be assessed. Full-body stereoradiographic imaging (EOS imaging) is an established technology and has the considerable advantage of low radiation dose and acquisition of weight-bearing images.

Radiology of individual segments

It is important that radiographs are requested with unambiguous instructions to ensure that usable images are produced routinely. There are nuanced differences in the information available from radiographs obtained with slightly different beam orientation and this is particularly relevant to parallax errors if a joint is peripherally placed.

The images for the femur are centred on the hip or knee (Figures 2.16 and 2.17).

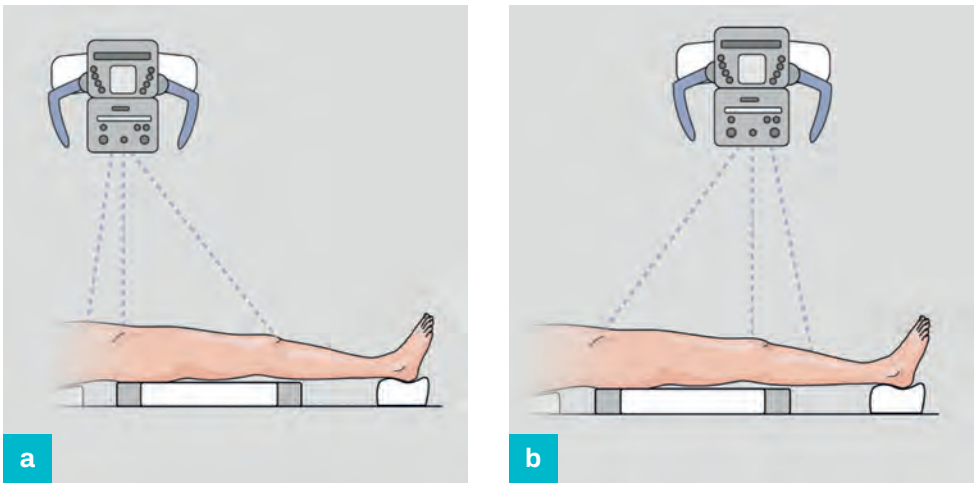

Figure 2.16
AP femoral radiograph
(a) centred on the hip;
(b) centred on the knee.

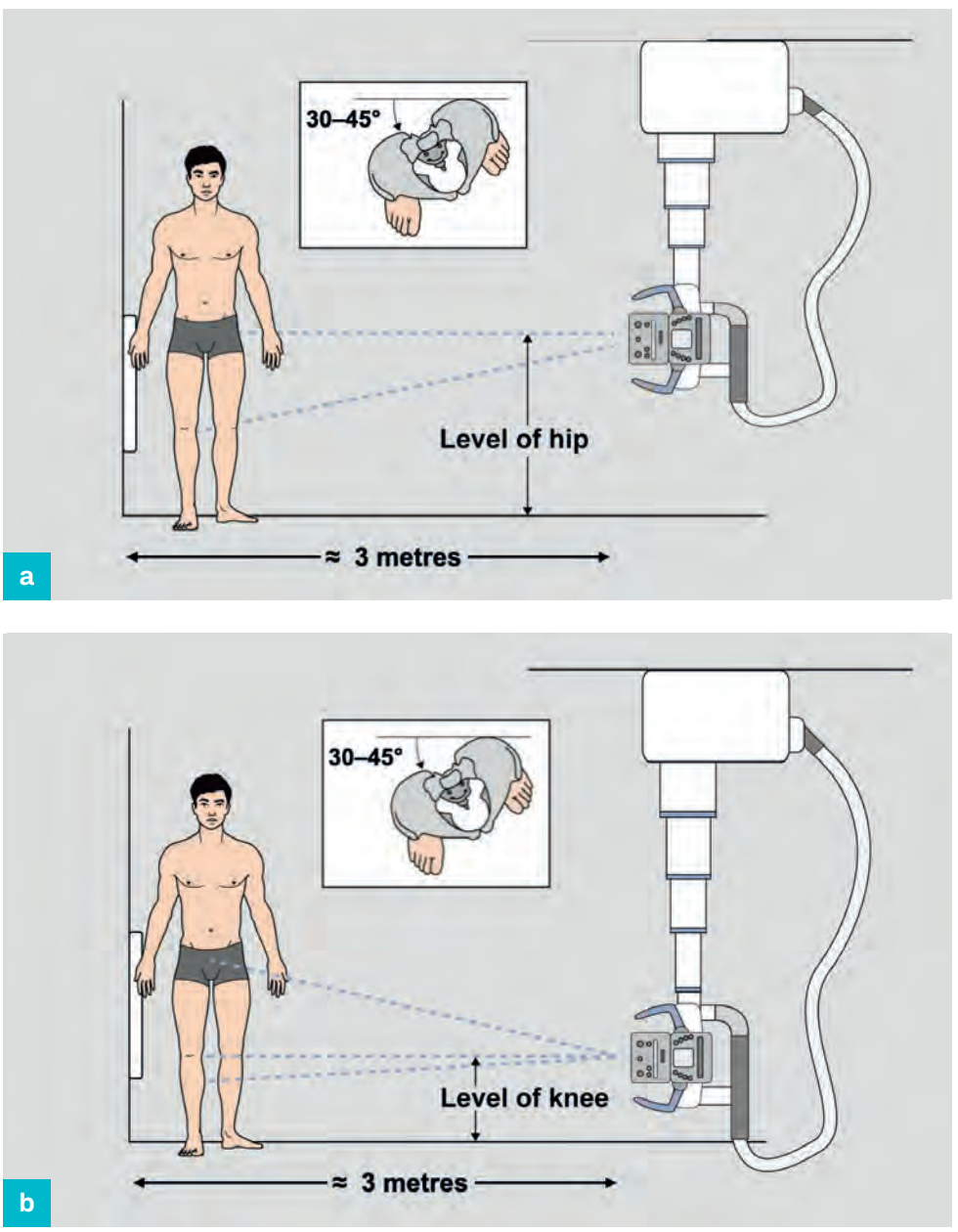

Figure 2.17
Standing lateral femoral radiograph
(a) centred on the hip;
(b) centred on the knee.

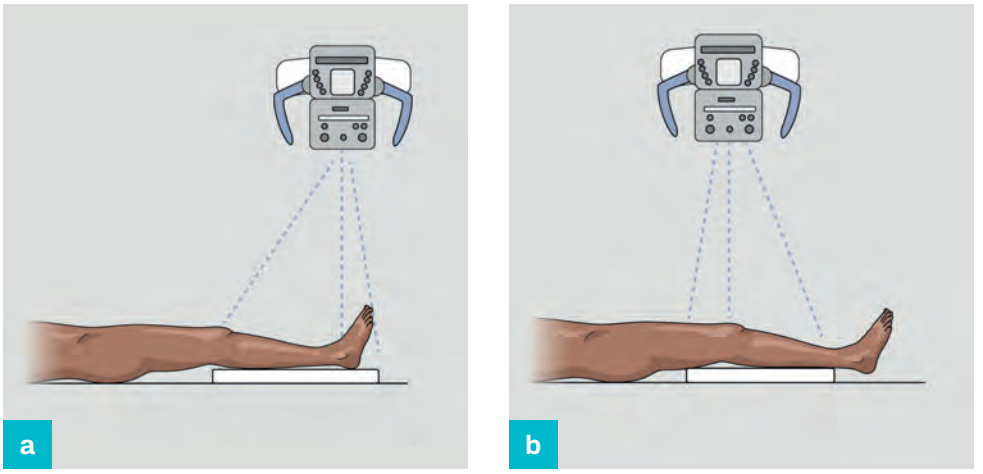

Figure 2.18
AP tibial radiograph **(a)** centred on the ankle; **(b)** centred on the knee.

The equivalent images for the tibia are centred on the knee or ankle (Figures 2.18a,b and 2.19a,b).

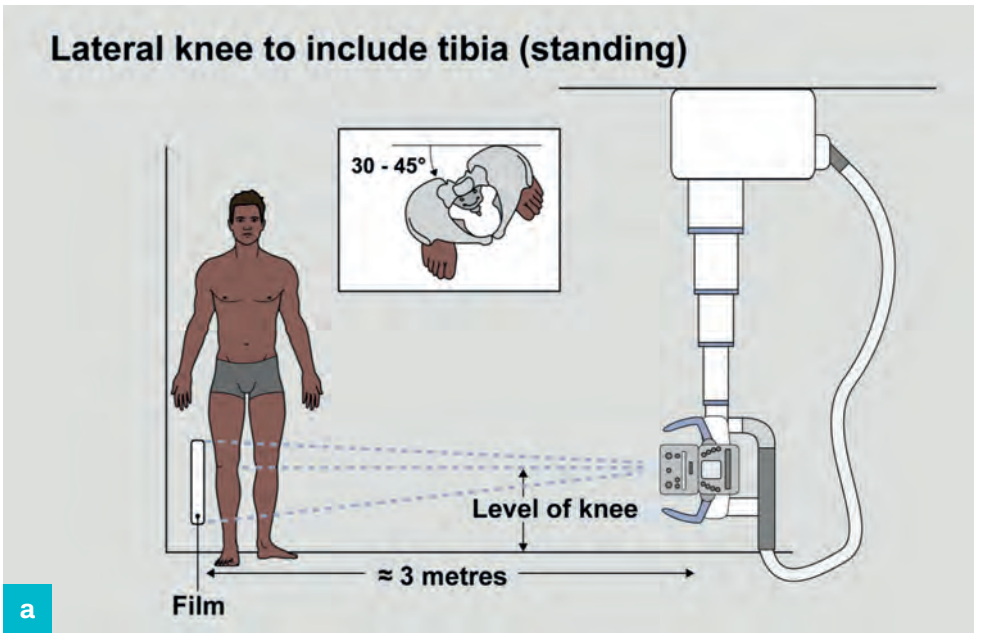

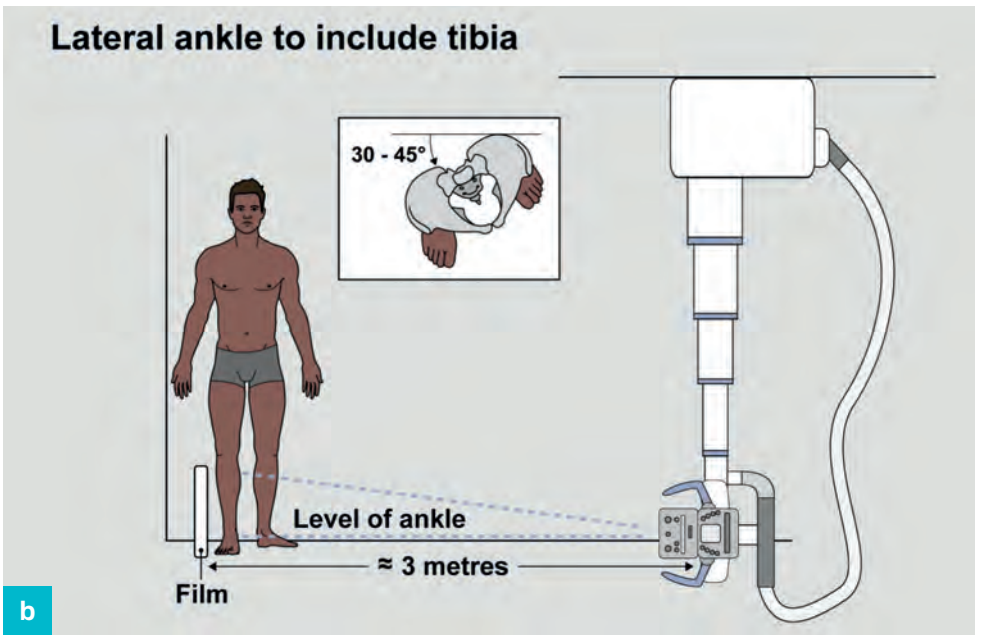

Figure 2.19
Standing lateral tibial radiograph **(a)** centred on the knee; **(b)** centred on the ankle.

Radiological evaluation of the foot and ankle

The baseline radiographic images for evaluation of ankle joint deformity are the AP ankle, AP mortise and mortise lateral views.

Standard AP view

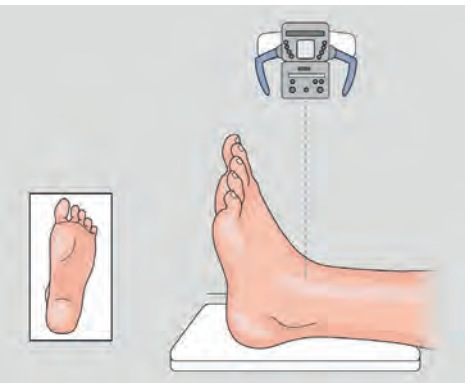

Figure 2.20 Standard AP ankle radiograph.

The standard AP ankle radiograph is taken with the foot facing forward with the beam perpendicular to the floor (Figure 2.20).

Weight-bearing AP ankle view

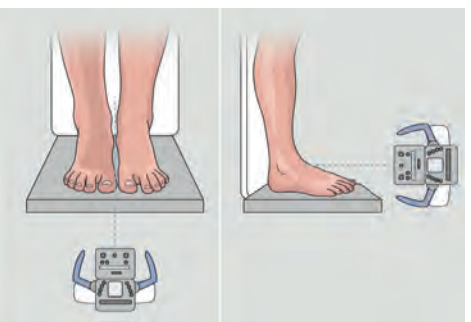

Figure 2.21 Weight-bearing AP ankle radiograph.

For a weight-bearing AP view, the patient stands on a 5 cm block with the beam parallel to the floor and the cassette behind the heels. This view is the most useful to demonstrate talo-tibial deformity (Figure 2.21).

AP mortise view

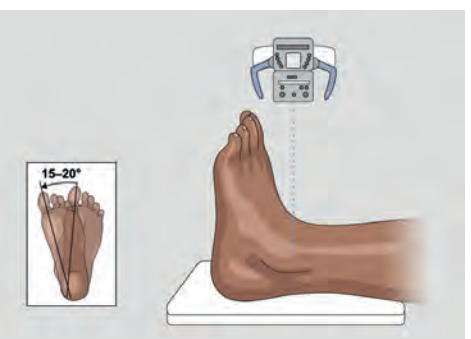

Figure 2.22 AP mortise radiograph.

The AP mortise view is taken with the limb in 15–20° internal rotation, to prevent fibular–tibial overlap, and is useful to assess the position of the talus and its relationship with the syndesmosis (Figure 2.22).

Mortise lateral view

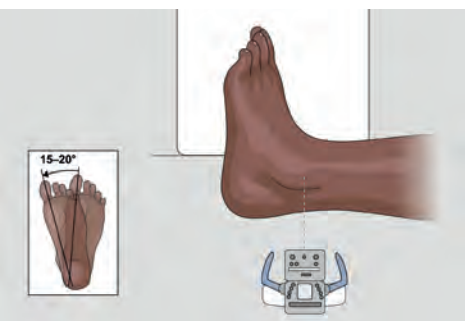

Figure 2.23 Mortise lateral radiograph.

The mortise lateral view is taken directly perpendicular to the AP mortise view (Figure 2.23). It is useful for the assessment of talar deformity and identification of osteophytes, which are an important consideration in deformity analysis and surgical planning. Identification of the joint orientation line is more straightforward using this projection because the malleoli overlap and the tibial plafond is therefore seen in maximum profile.

Distal tibial geometry is conventionally measured from an AP ankle radiograph, but differences in measurements from the AP mortise view have not been found to be significant and this, in combination with the mortise lateral view, may be used as an alternative for distal tibia deformity planning.

AP foot view

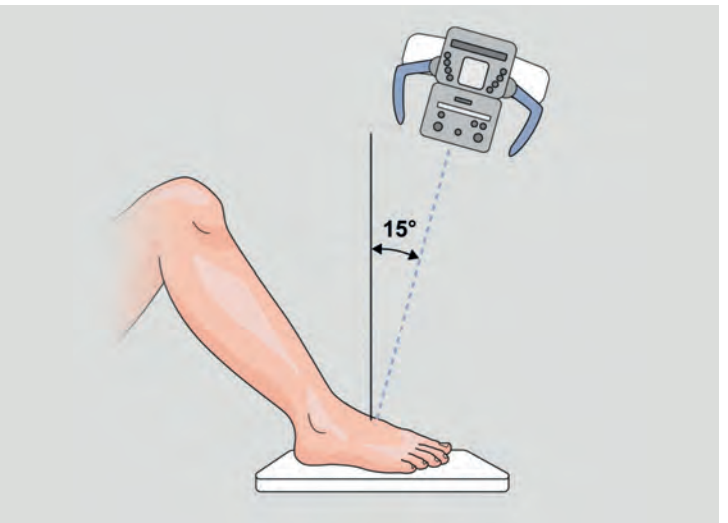

Figure 2.24
AP foot radiograph.

A non-weight-bearing AP view of the foot is obtained with the primary beam centred on the base of third metatarsal and angled 15° to the vertical (Figure 2.24).

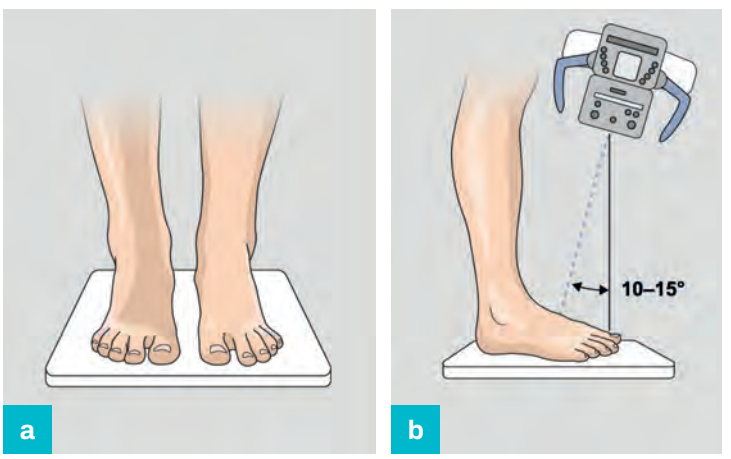

Figure 2.25 (a,b)
Weight-bearing AP radiograph.

The weight-bearing AP view is obtained with the primary beam centred on the base of third metatarsal and angled 15° to the vertical (Figure 2.25a,b).

Lateral foot view

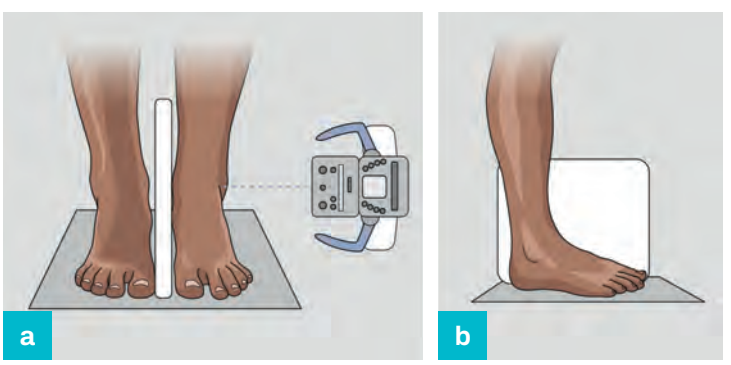

Figure 2.26 (a,b)
Weight-bearing lateral radiograph.

A lateral weight-bearing radiograph from the proximal tibia to the foot is the baseline image for assessment of sagittal foot deformity (Figure 2.26a,b).

If there is no deformity within the tibia, a radiograph from the mid-tibia is an acceptable alternative. If weight-bearing is not possible, then a simulated view should be obtained, with the foot supported against a block. If there is a fixed hindfoot deformity, the foot is positioned in a simulated weight-bearing position and a direct lateral view obtained (Figure 2.27).

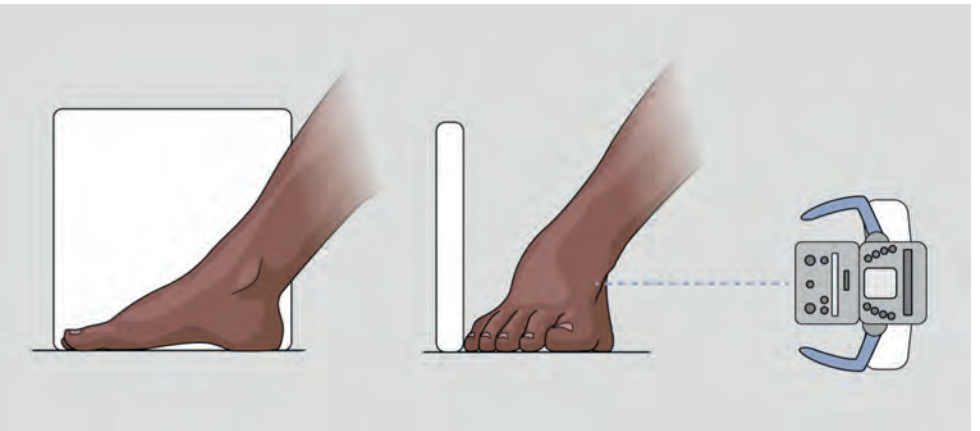

Figure 2.27
Simulated weight-bearing with fixed deformity.

Hindfoot deformity

Hindfoot abnormality is not visualised on long-leg films, and dedicated views should be obtained for deformity analysis and surgical planning. This minimises the overlap of the midfoot and ideally should be performed in a functional weight-bearing position. Non-weight-bearing imaging can be used for peri-operative planning when the patient is positioned on an operating table.

Long calcaneal axial view

The long calcaneal axial view demonstrates the relationship between the calcaneus, tibia and subtalar joint, and it can be obtained in a weight-bearing or supine position (Figure 2.28).

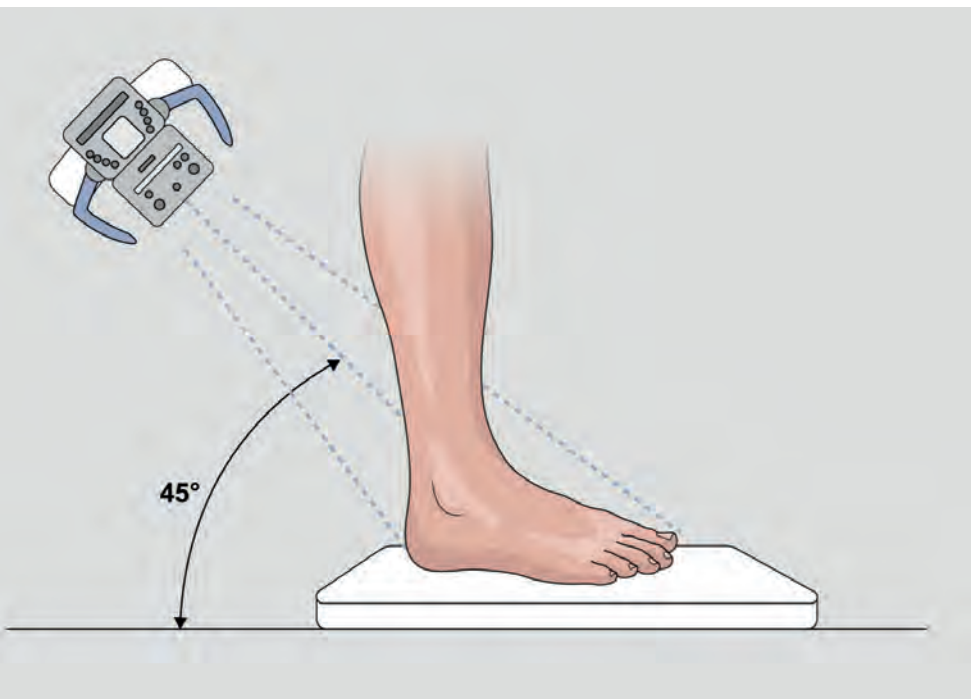

Figure 2.28
Long calcaneal axial view.

Hindfoot alignment view

The hindfoot alignment demonstrates the relationship between the ankle joint, calcaneus and tibia (Figure 2.29).

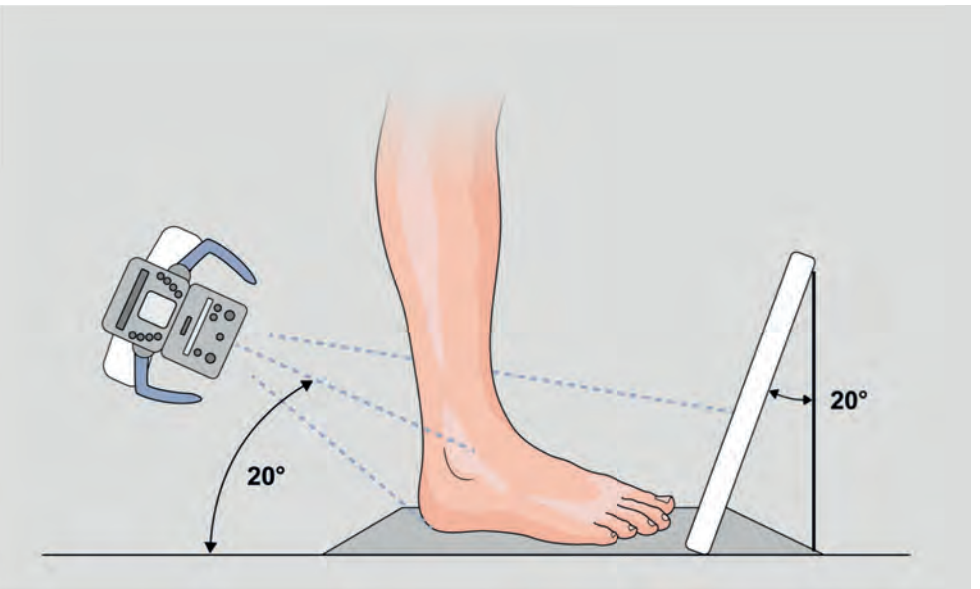

Figure 2.29 Hindfoot alignment view.

Special circumstances

Intra-operative radiographs

Commercially available radio-opaque grids can be used to assess the mechanical axis of the whole limb in an anaesthetised patient. If these are not available, an image intensifier can be used to identify the centre of the hip and ankle joints. A radio-opaque guide or diathermy cable is placed to connect these points and the position of the cable relative to the centre of the knee will demonstrate abnormalities in the mechanical axis (Figure 2.30a–c).

Some image intensifier screens will include measurement tools and, if unavailable, a smart phone with appropriate measurement apps can be used.

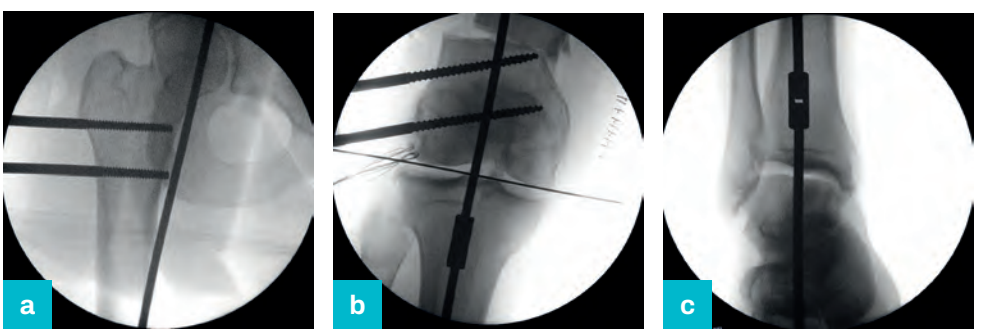

Figure 2.30 (a–c) Intra-operative radiographs to confirm alignment.

Post-operative radiographs

The principles of post-operative deformity analysis are identical and require full weight-bearing radiographs of the entire limb to measure the mechanical axis accurately.

This may not be practical in the immediate post-operative period, especially in patients who are unable to fully weight-bear. Digitally stitched radiographs of individual segments and CT scanograms may be used as an alternative. The post-operative radiographic evaluation of patients with an external fixator requires modification of usual practice and it is important to specify whether the fixator or bone segment is the area of interest (Figure 2.31).

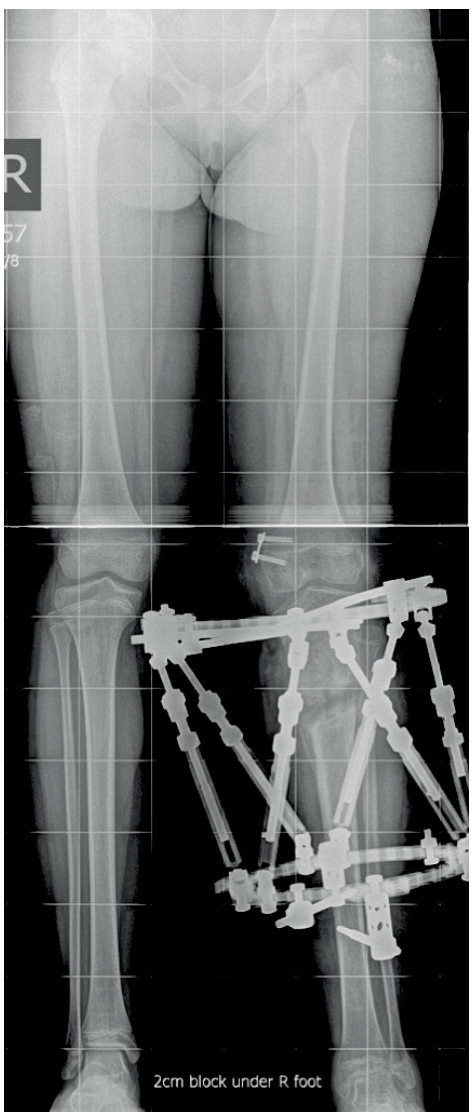

Figure 2.31
Post-operative radiograph with level pelvis and centred patella.

Post-operative imaging for hexapod use

Software-assisted hexapod correction uses a specified set of deformity and mounting parameters that are determined from plain radiographs. The radiograph should be reproducible to allow accurate measurements and include the full width of the external fixator ring. The image is centred on a specified ring and should include a magnification marker (Figure 2.32a,b). Images are performed with the beam parallel to this ring as it will appear as a linear structure from which perpendicular measurements can be taken. This ring should be specified as part of the imaging request for a beam-parallel image. Limb position should be specified with either the joint closest to the ring or a defined component of the external fixator facing forward, with perpendicular lateral views.

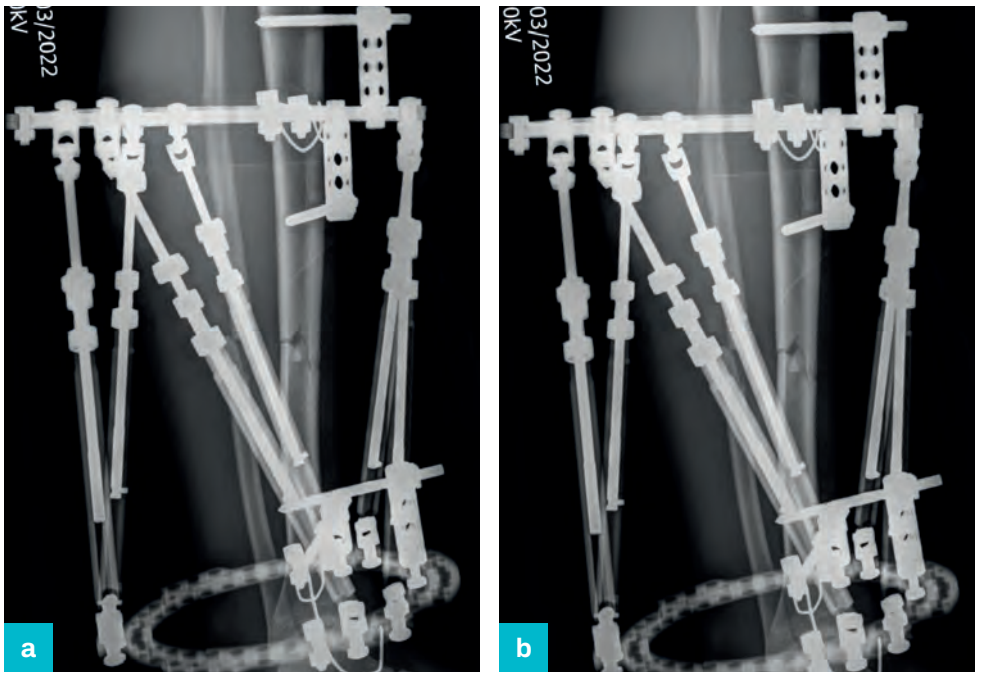

Figure 2.32
(a) Radiographic assessment for hexapod correction. **(b)** Radiograph centred on proximal ring.

While there is software available to compensate for incorrect positioning, it is useful to have standardised images for subsequent visual comparison.

When the deformity is corrected, the beam position relative to the external fixator ring is irrelevant and the area of interest in further imaging requests usually involves a specified bone segment (Figure 2.33a,b). This is to assess regenerate formation or fracture union and it may be necessary to remove the external fixator components in order to visualise the area of interest.

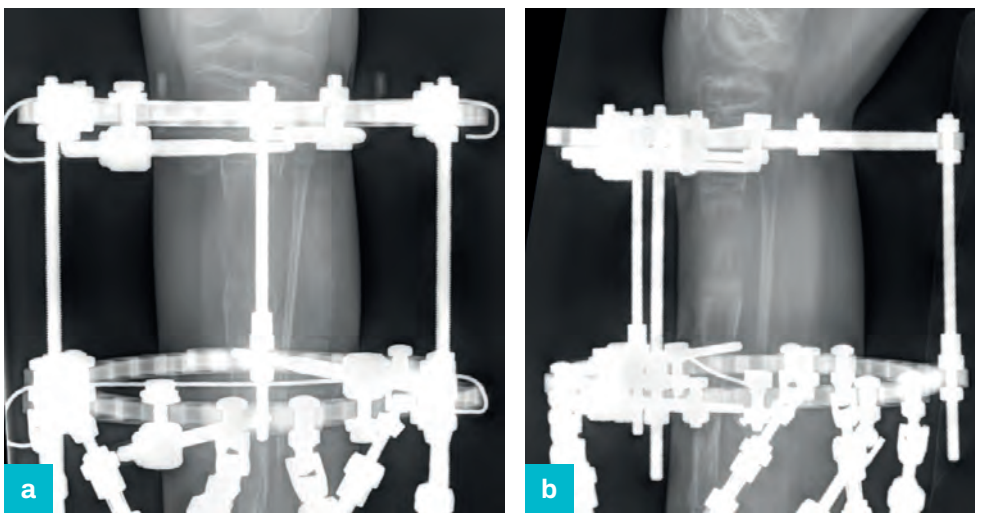

Figure 2.33 (a,b)
Radiographs centred on regenerate.

Oblique plane deformity

Deformity may not exist in the true AP or lateral plane, but in an oblique plane. This can be calculated using simple trigonometry and is described in detail in Chapter 7. The oblique plane can be identified by fluoroscopic screening in an awake patient or as part of peri-operative assessment.

The limb or image intensifier is rotated until the maximum deformity is identified and the orientation of the X-ray beam will define the plane of the deformity (Figure 2.34a,b). The corollary is that the image obtained perpendicular to this axis will demonstrate apparent elimination of the deformity and represents the axis of correction. This is discussed in greater detail in Chapter 7.

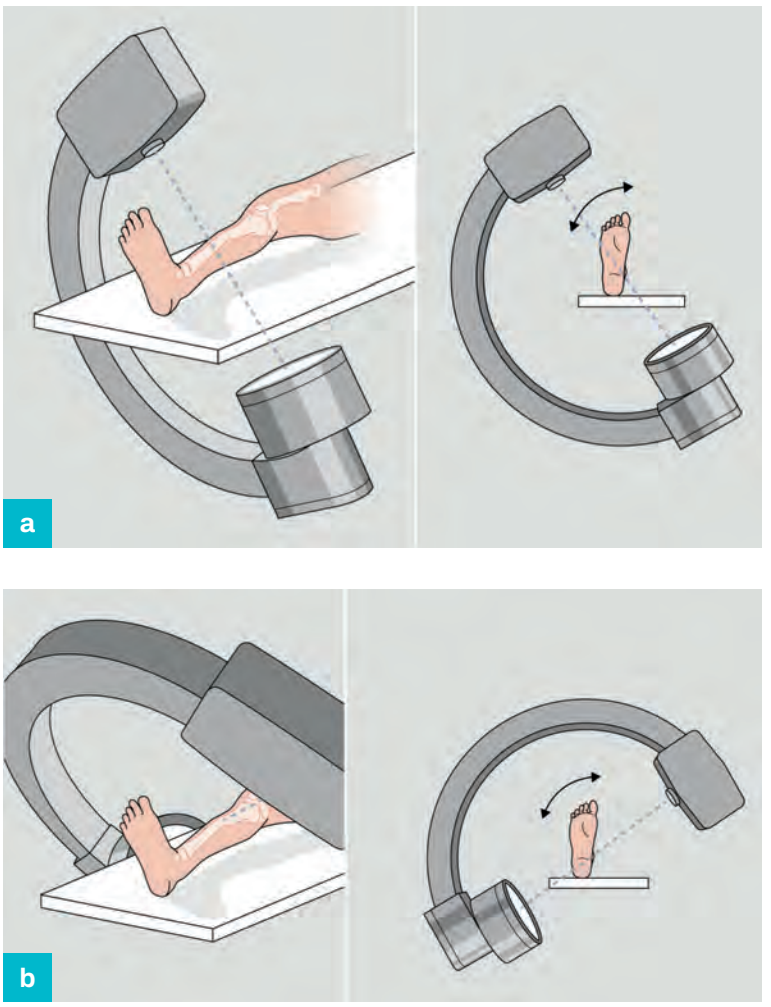

Figure 2.34 (a,b)
Oblique plane deformity analysis.

Deformity analysis software

Digital PACS usually contain software that allows measurement of angles and distance and permits reasonably sophisticated deformity analysis. Web- and tablet-based applications are also available and include TraumaCad®, (Brainlab, Munich, Germany), OrthoView™ (Materialise, Leuven, Belgium), HEX-ray (Orthofix, Lewisville, USA) and Bone Ninja (International Center for Limb Lengthening, Baltimore, USA). While these systems enable rapid and detailed analysis, they all require a detailed understanding of the conventions, vocabulary and geometry of deformity correction that is outlined in subsequent chapters.

Radiograph analysis with limited resources

Alternative methods of deformity analysis may be used in areas with limited resources.

The AP and lateral radiographs of separate parts of the limb and standing views of both knees are the minimum data set required for analysis.

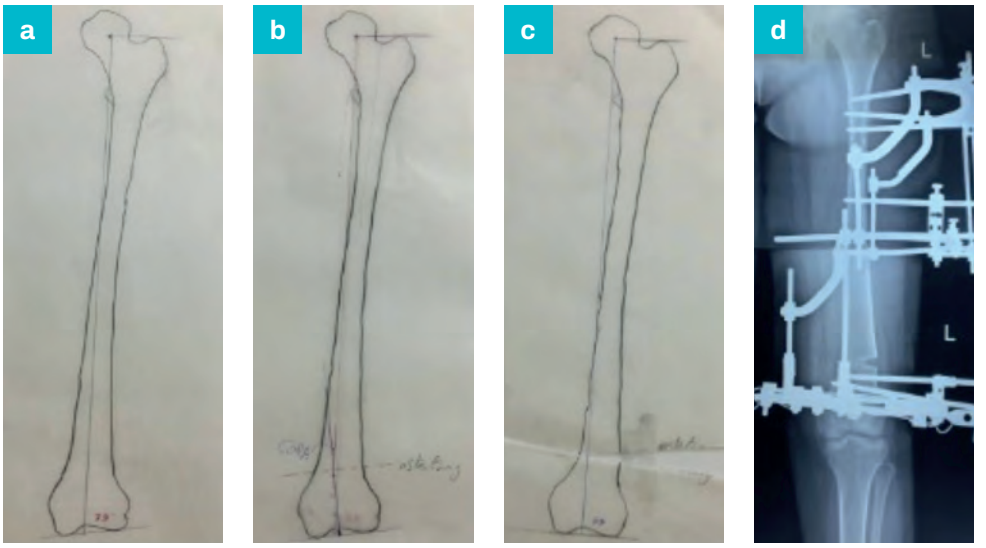

Figure 2.35
Deformity analysis without planning software:
(a) femur including mechanical axis planning lines;
(b) osteotomy site;
(c) simulated correction;
(d) post-operative radiograph.

A pencil, protractor and ruler are used directly on radiographic films or paper prints of digital images to plan deformity and simulate surgical correction (Figure 2.35a–d). Deformity analysis is conducted using the principles and techniques described in subsequent chapters, and the site of the proposed osteotomy is marked. The image is traced onto transparent paper which is cut with scissors to create the effect of an osteotomy and drawing pins are used to simulate a hinge. The sheet is manipulated to model the correction and conventional analysis is repeated to confirm a normal axis and full deformity correction.

KEYPOINTS

- The effect of magnification
- Assessment of torsion
- Joint instability
- Specific views to avoid parallex errors
- Radiology of individual segments
- Post-operative radiology
- Hexapod radiology
- Demonstrating the oblique plane
- Planning software

CHAPTER

3

Normal lower-limb geometry

Milind Chaudhary and Hemant Sharma

Introduction

The terminology in this book is conventional and uses directional descriptors including medial/lateral, superior/inferior, proximal/distal, cranial/caudal and dorsal/ventral. The standard anatomical position is assumed and is defined as standing, facing forward, with straight, slightly externally rotated legs, feet slightly apart, arms by the sides and palms facing forward.

- The *frontal (coronal) plane* produces anterior/posterior or dorsal/ventral components and the *lateral (sagittal) plane* produces left/right or medial/lateral components.
- The transverse plane runs parallel to the ground and produces proximal/distal or caudal/cranial components (Figure 3.1a,b).

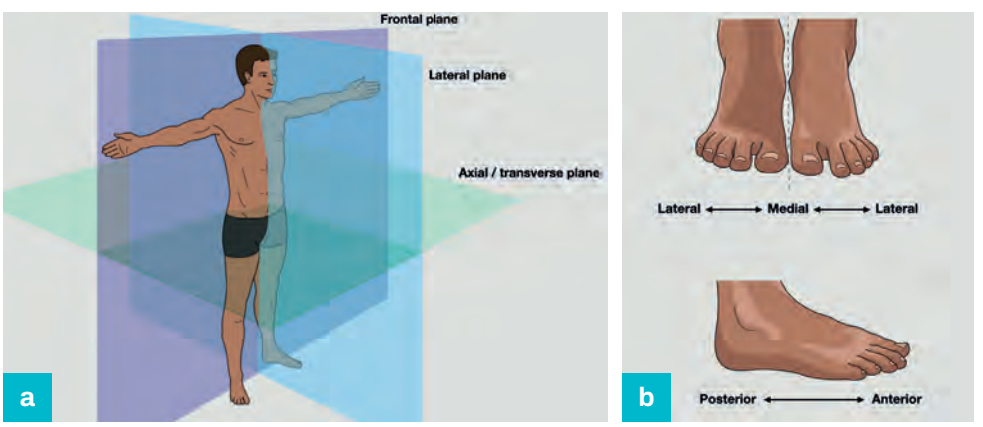

Figure 3.1 (a,b) The anatomical position with standard planes.

Lower-limb alignment

Characterisation of limb alignment relies on accurate identification of the geometric centre and orientation of the articular surface of the joints. These are determined in the frontal and lateral planes using radiographs, obtained in standardised positions (see Chapter 2).

Joint centres

The hip

The centre of the femoral head can be identified by a number of simple methods that depend on the type of radiograph. The use of templates has been superseded by the availability of digital imaging systems, often with tools that simplify this task. If these are not available, the point of intersection of any two radii in a spherical femoral head (Figures 3.2a and 3.3a) and the intersection of the major and minor radii in an ellipsoid femoral head (Figures 3.2b and 3.3b) will consistently localise the joint centre.

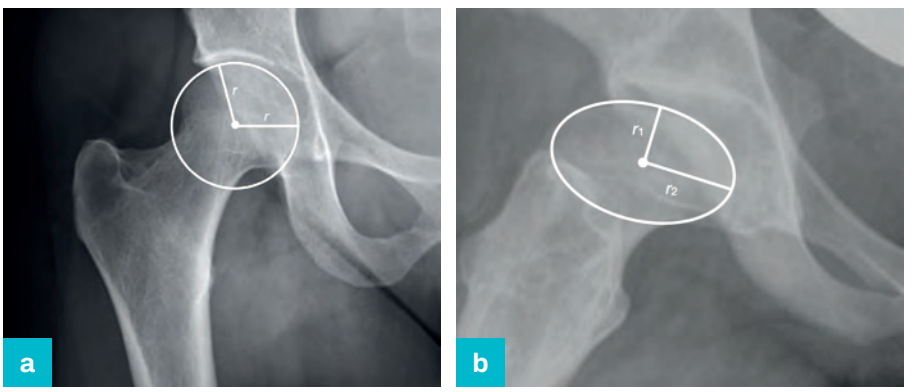

Figure 3.2
Localisation of the femoral head centre (frontal plane):
(a) spherical femoral head;
(b) ellipsoid femoral head.

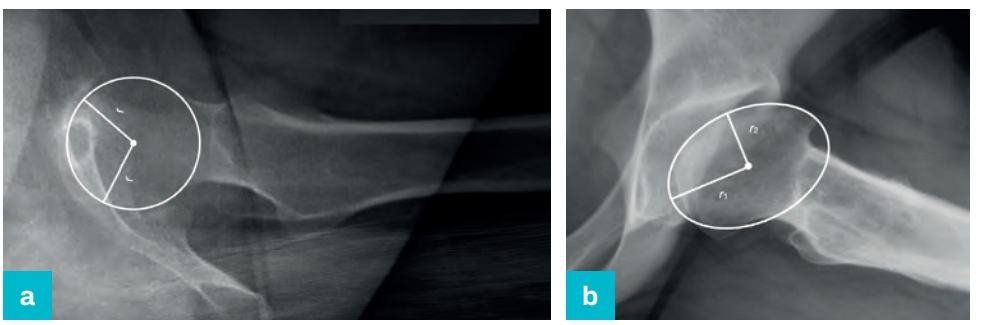

Figure 3.3
Localisation of the femoral head centre (lateral plane):
(a) spherical femoral head;
(b) ellipsoid femoral head.

The knee

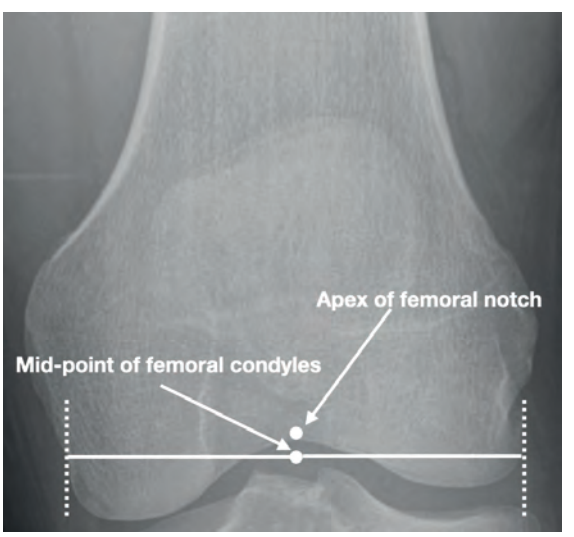

Figure 3.4
Localisation of the mid-point of the distal femur.

The centre of distal femur is localised in the frontal plane by identifying the apex of the femoral notch or the mid-point of the femoral condyles (Figure 3.4).

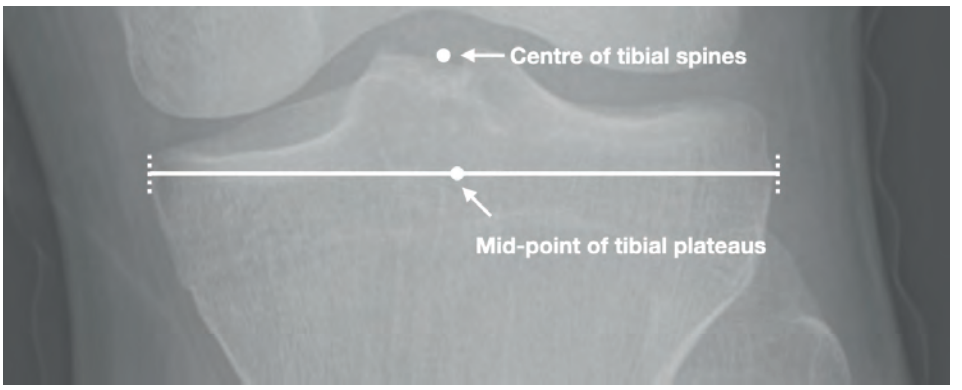

Figure 3.5
Localisation of the mid-point of the proximal tibia.

The centre of the proximal tibia is localised by identifying the centre of the tibial spines or the mid-point of the tibial plateaus (Figure 3.5).

The knee does not function as a fixed hinge and the lateral plane biomechanics are complex. Localisation of the joint centre is therefore difficult and, for the purpose of deformity analysis, is an approximation with the knee in full extension. In children, the centre of knee rotation is defined as the intersection of the posterior femoral cortex and the distal femoral physis (Figure 3.6a) and in adults as the intersection of the posterior femoral cortex and Blumensaat's line (Figure 3.6b).

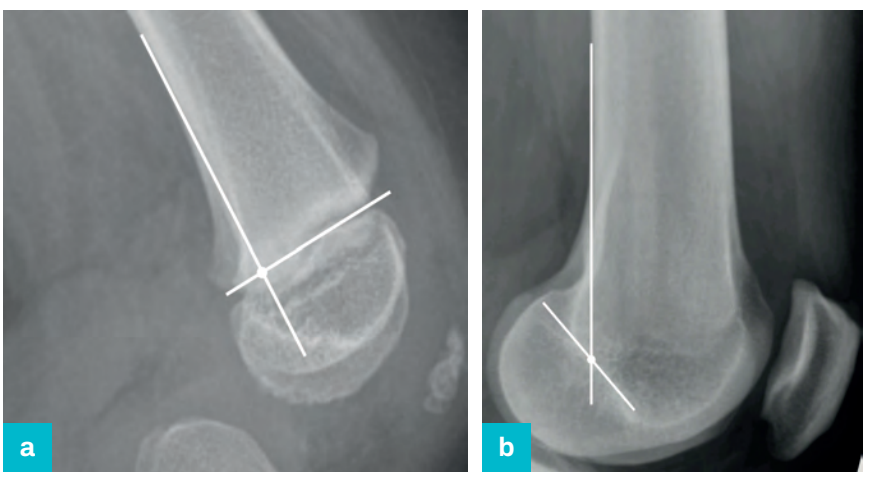

Figure 3.6
Localisation of the centre of knee rotation:
(a) in children;
(b) in adults.

The ankle

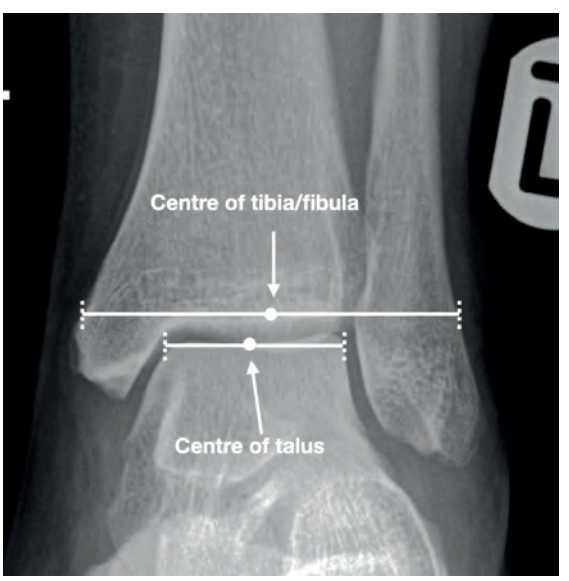

Figure 3.7
Localisation of the mid-point of the ankle (frontal).

The centre of the ankle is represented in the frontal plane by the centre of the talus or the mid-point of the combined width of tibia and fibula at the level of the ankle (Figure 3.7).

Figure 3.8
Localisation of the mid-point of the ankle (lateral).

The centre of the ankle in the lateral plane is represented by the mid-point of the distal articular surface (Figure 3.8).

Figure 3.9
Localisation of the centre of ankle rotation.

The centre of rotation of the ankle is, by convention, taken as the tip of the lateral process of the talus (Figure 3.9).

Joint orientation

The hip

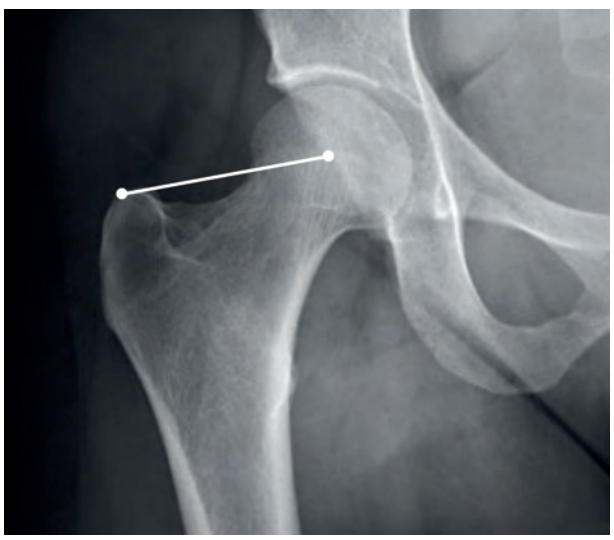

Figure 3.10
Frontal hip joint line.

The normal femoral head is spherical and the relationship of the tip of the greater trochanter to the centre of the femoral head is used as a surrogate to demonstrate the orientation of the hip joint in this plane (Figure 3.10).

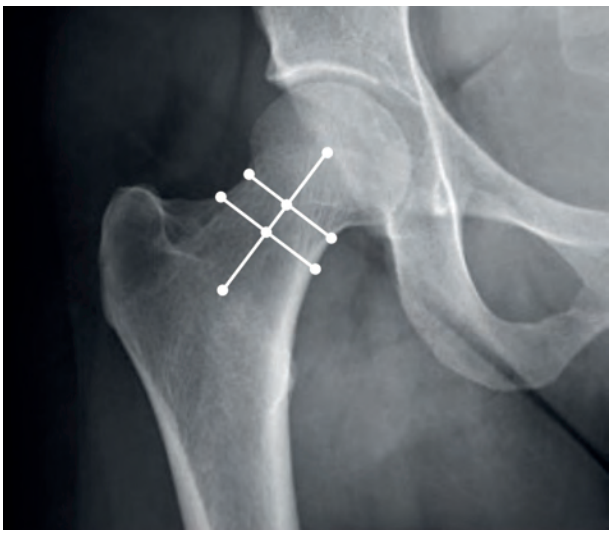

Figure 3.11
Frontal neck bisector line.

The neck bisector line can also be used to represent the position of the hip joint. This is the line between the mid-point of the femoral neck and the centre of the femoral head (Figure 3.11).

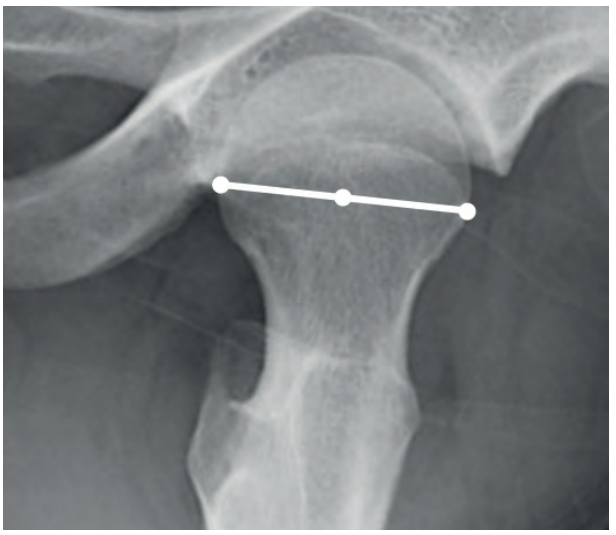

Figure 3.12
Lateral hip joint line.

The line between the point of intersection of the physeal scar and joint surface is used to represent the orientation of the hip joint in the lateral plane (Figure 3.12).

The knee

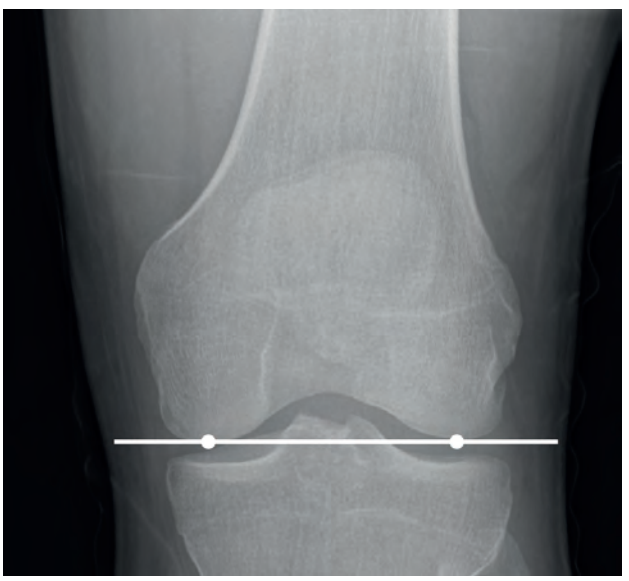

Figure 3.13
Frontal knee joint line (femoral).

The distal femoral joint surface is represented in the frontal plane by the tangent to the most distal points on the convexity of the medial and lateral condyles (Figure 3.13).

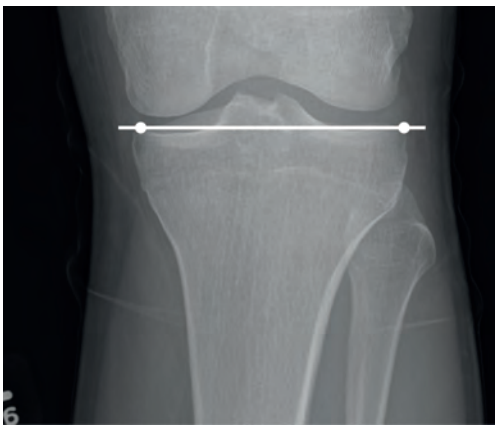

Figure 3.14
Frontal knee joint line (tibial).

The tibial component of the knee joint in the frontal plane is represented by the line of best fit drawn between the medial and lateral tibial plateaus (Figure 3.14).

Figure 3.15
Knee joint line convergence angle.

The angle formed between the joint orientation lines on opposite sides of the knee is termed the joint line convergence angle (JCA). The normal JCA is 0° (±2°) (Figure 3.15).

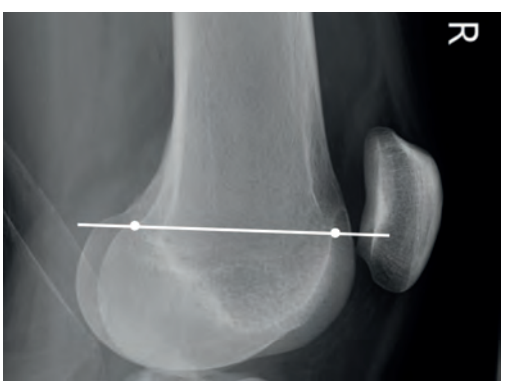

Figure 3.16
Lateral femoral knee joint line (growth plate closed).

A line between the points where the femoral condyles join the anterior and posterior distal femoral metaphysis represents the orientation of the distal femur in the lateral plane (Figure 3.16).

Figure 3.17
Lateral femoral knee joint line (growth plate open).

In the skeletally immature patient, the joint orientation line is located between the anterior and posterior margins of the growth plate (Figure 3.17).

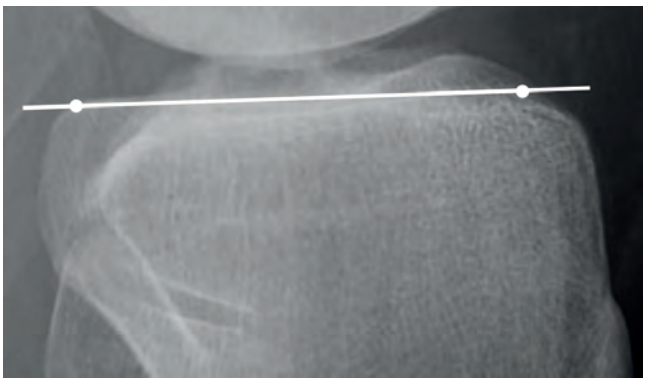

Figure 3.18
The medial condyle is concave and the lateral condyle is convex. The line of best fit is drawn and represents the lateral tibial knee joint line.

In the lateral plane, the tibial component of the knee joint is represented by the line of best fit along the superimposed medial and lateral plateaus (Figure 3.18).

The ankle

Figure 3.19
Frontal ankle joint line.

The orientation of the ankle in the frontal plane is represented by a line drawn across the surface of the tibial plafond or the talar dome (Figure 3.19).

Figure 3.20
Lateral ankle joint line.

In the lateral plane, the joint surface is represented by a line that joins the posterior lip to the anterior lip of the distal tibia (Figure 3.20).

Limb mechanical axis

Frontal plane

In the frontal plane, the mechanical axis of the limb is represented by a line that joins the centre of the femoral head to the centre of the ankle (Figure 3.21a).

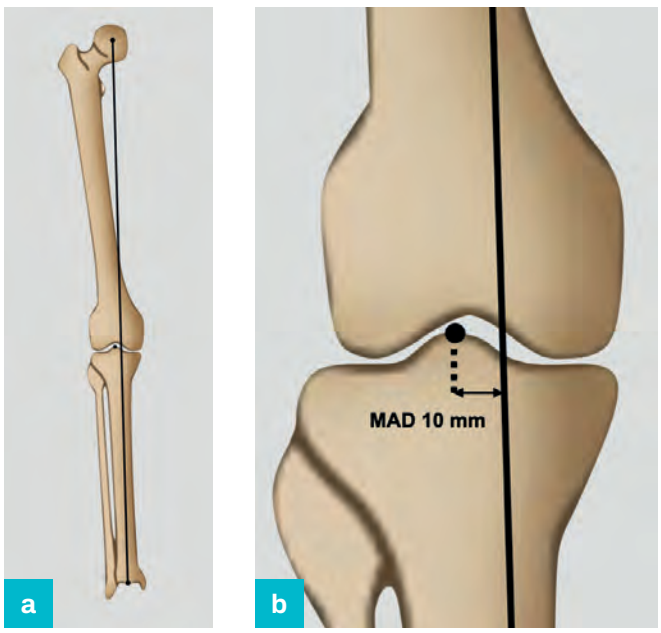

Figure 3.21 (a,b) Frontal mechanical axis.

The horizontal distance between the centre of the knee and the mechanical axis is referred to as the mechanical axis deviation (MAD). The mechanical axis is normally located medial to the centre of the knee with a population average of 10 mm (Figure 3.21b).
Medial displacement infers an overall apex lateral (varus) limb alignment and lateral displacement infers an overall apex medial (valgus). It is not possible to localise deformity to an individual bone without further analysis.

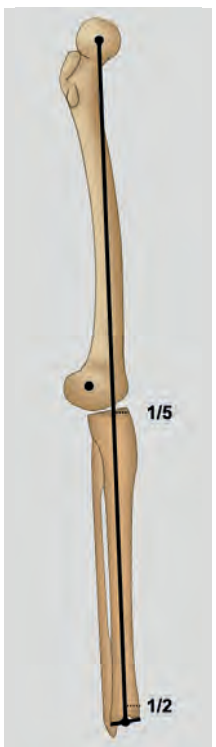

Figure 3.22 Lateral mechanical axis.

Lateral plane

The lateral mechanical axis is represented by a line from the centre of the hip to the centre of the ankle and passes just anterior to the centre of rotation of the knee when the knee is fully extended (Figure 3.22).

Joint orientation angles

The angle subtended at the intersection of an axis and a joint line describes joint orientation (Figures 3.23a,b and 3.24a,b). The angle <90° is used by convention and each angle is assigned an abbreviated title that depends on the location ([F]emoral or [T]ibial), position ([P]roximal or [D]istal) and the plane ([A]nterior, [P]osterior, [M]edial or [L]ateral). If there is a difference in the angle produced by the mechanical and the anatomical axis, the prefix [m] or [a] is also added.

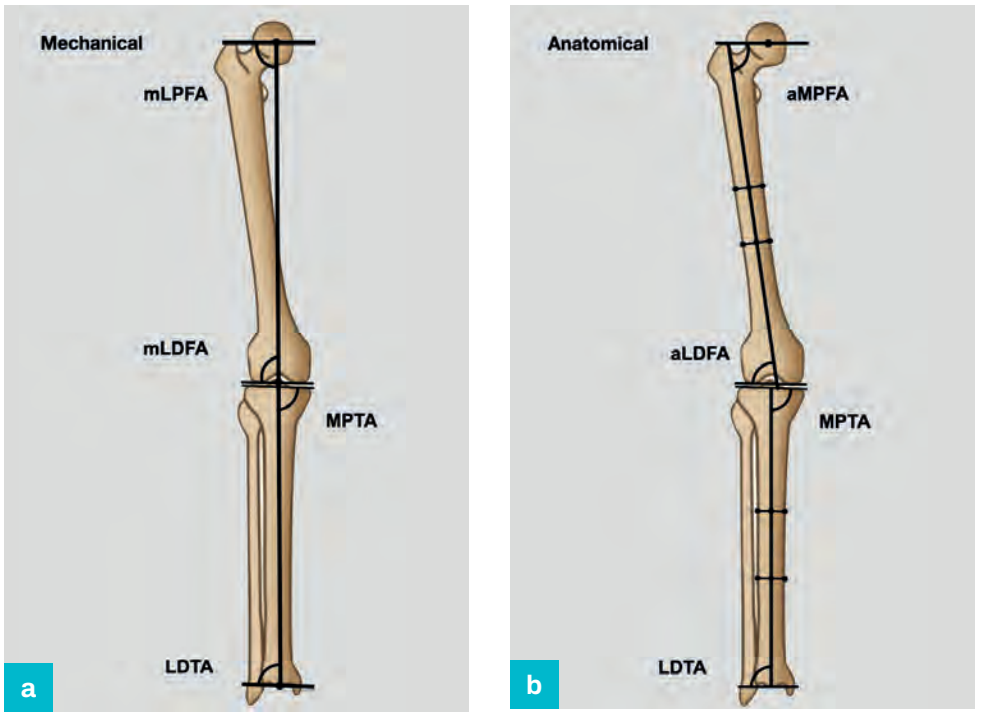

Figure 3.23
Frontal angles:
(a) mechanical;
(b) anatomical.

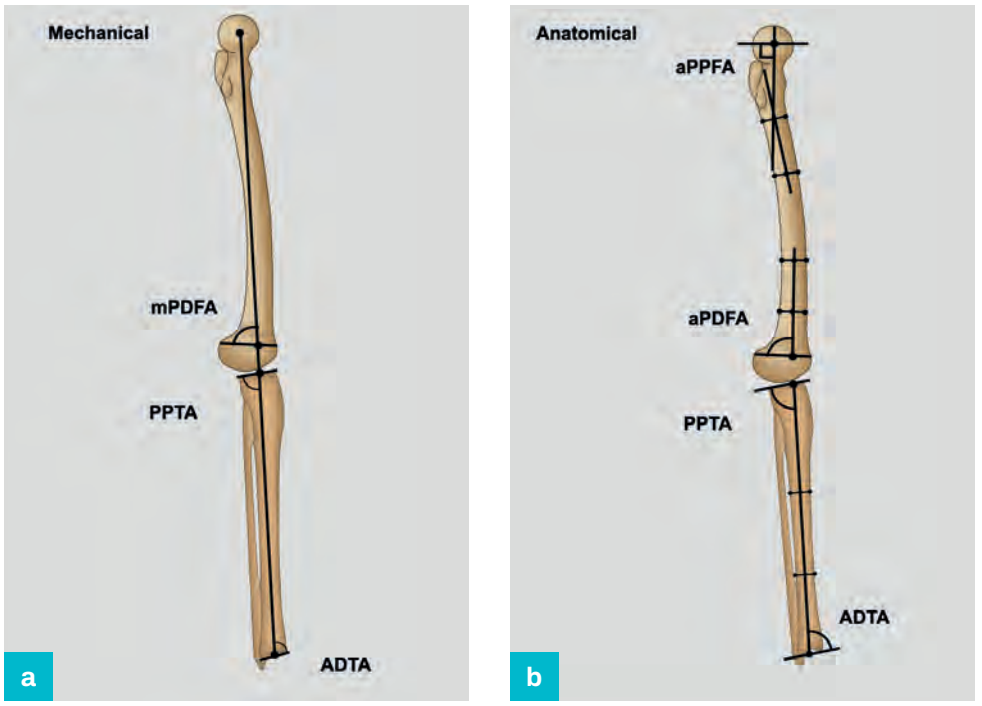

Figure 3.24
Lateral angles:
(a) mechanical;
(b) anatomical.

The femur

The hip joint is offset from the femoral shaft, which directly affects load transmission through the limb and introduces a difference in the mechanical and the anatomical axis. Geometry in frontal plane may be described using either axis, but it is important to note that this produces different values for the angles between the axis and joint lines.

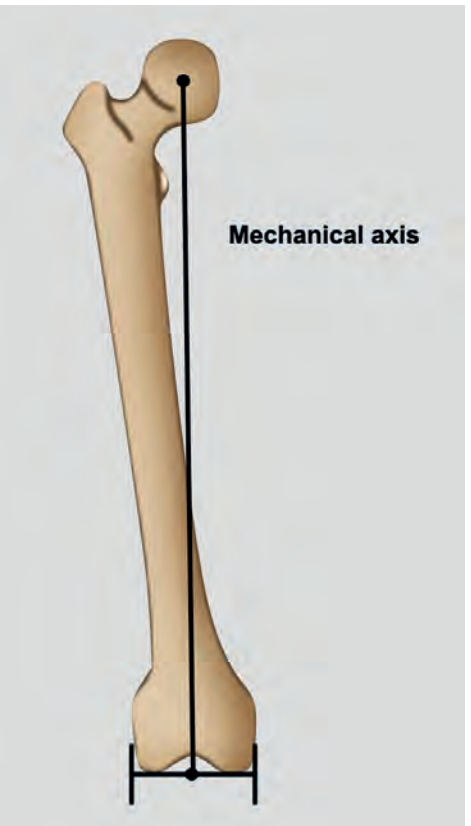

Figure 3.25
Femoral mechanical axis (frontal).

The mechanical axis of the femur is represented in the frontal plane by a single line that connects the centre of the femoral head and mid-point of the distal femur (Figure 3.25).

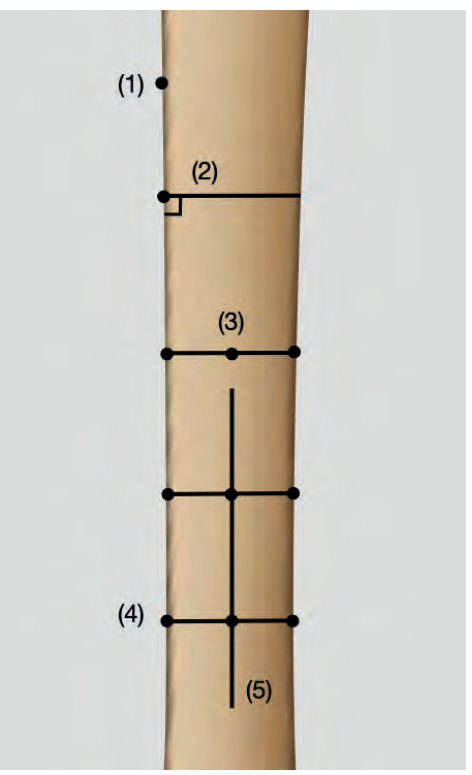

Figure 3.26
Localisation of the mid-diaphyseal point.

The anatomical axis of any long bone is defined by a single mid-diaphyseal line (Figure 3.26). This is identified at a representative position on the diaphysis (marked (1)) and a line (2) is constructed that is perpendicular to the diaphysis at this point. The mid-point of this line is measured and marked (3).

This is repeated at a second representative position on the diaphysis (4) and the mid-points of these lines are joined by a line representing the anatomical axis of the segment (5).

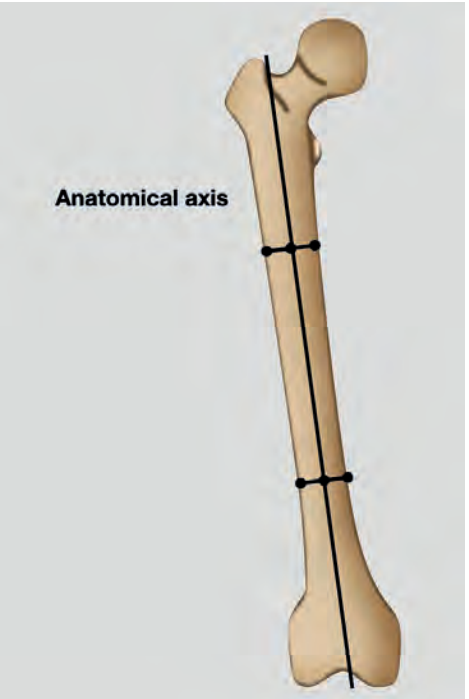

Figure 3.27
Femoral anatomical axis (frontal).

The frontal plane, femoral anatomical axis is identified by constructing lines that are perpendicular to the diaphysis in the upper and lower third and identifying the mid-points. The axis is represented by a line that joins these mid-points (Figure 3.27).

The joint orientation lines intersect the axis at each end of the bone to produce a series of angles that define the normal geometry and localise deformity in the abnormal limb.

Measurements generated from the mechanical axis

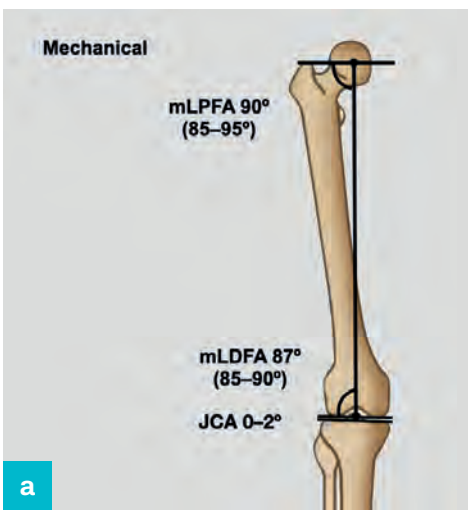

Figure 3.28
Normal values for the femur in the frontal plane:
(a) mechanical;
(b) anatomical.

The frontal hip joint line (Figure 3.28a) intersects the proximal mechanical axis to produce the mechanical lateral proximal femoral angle (mLPFA).

The normal range for the mLPFA is 85–95° and the population normal is 90°. The distal femoral joint line (Figure 3.28a) intersects the mechanical axis to produce the mechanical lateral distal femoral angle (mLDFA). The normal range for the mLDFA is 85–90° and the population normal is 87°.

Measurements generated from the anatomical axis

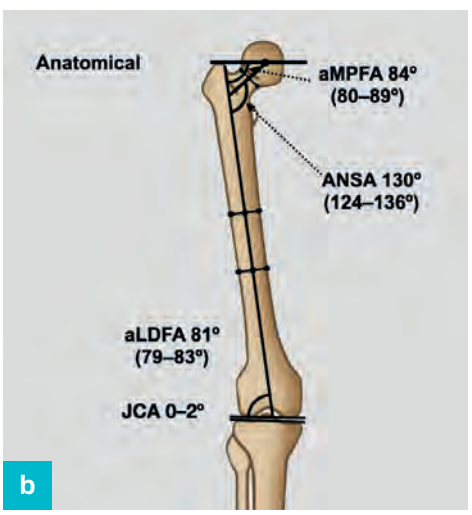

The frontal hip joint line (Figure 3.28b) intersects the proximal anatomical axis to produce the anatomical medial proximal femoral angle (aMPFA).

The normal range for the aMPFA is 80–89° and the population normal is 84°.

The line between the centre of the femoral head and mid-point of the femoral neck intersects the proximal anatomical axis to produce the anterior neck shaft angle (ANSA) (Figure 3.28b).

The normal range for the ANSA is 124–136° and the population normal is 130°.

The distal femoral joint line (Figure 3.28b) intersects the anatomical axis to produce the anatomical lateral distal femoral angle (aLDFA).

The normal range for the aLDFA is 79–83° and the population normal is 81°.

The tibia

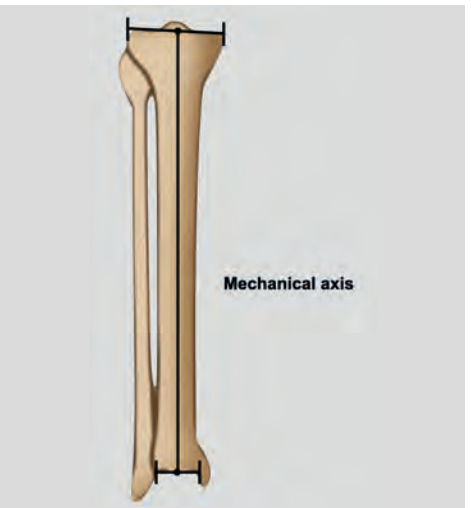

Figure 3.29 Tibial mechanical axis (frontal).

The mechanical axis of the tibia in the frontal plane is represented by a line that joins the centres of the knee and ankle (Figure 3.29).

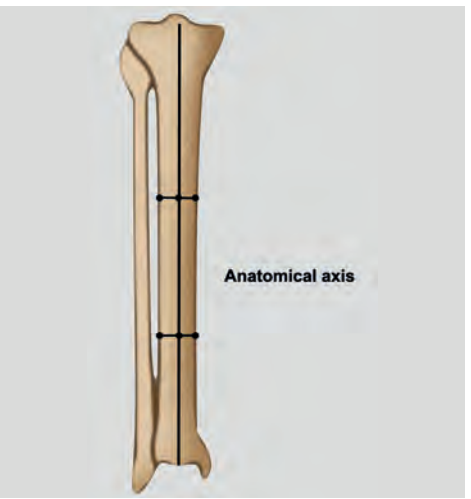

Figure 3.30 Tibial anatomical axis (frontal).

The anatomical axis of the tibia in the frontal plane is identified by a line joining the diaphyseal mid-point at two levels (Figure 3.30).

Figure 3.31 Normal values for the tibia in the frontal plane: **(a)** mechanical; **(b)** anatomical.

The orientation of the tibial component of the knee joint in the frontal plane is represented by a line that joins the most proximal extent of the medial and lateral tibial plateaus and intersects the axes to produce the medial proximal tibial angle (MPTA) (Figure 3.31 a,b).

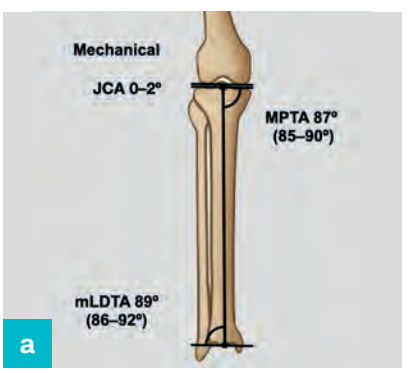

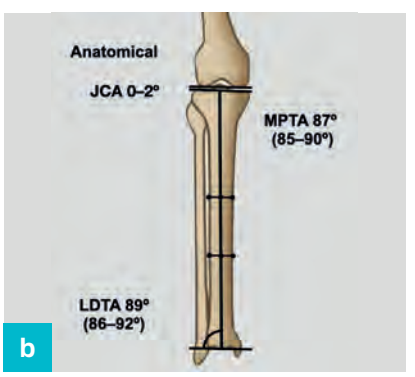

The tibial mechanical and anatomical axes are parallel in the frontal plane, with the mechanical axis located slightly lateral to the mid-diaphysis and this angle is identical for each axis. The angles subtended by the mechanical and anatomical axes are identical, and the use of a prefix is redundant. There are, however, subtle but important differences in evaluating peri-articular deformity and the use of the mechanical axis is recommended.

The normal range for the MPTA is 85–90° and the population normal is 87°.

The orientation of the ankle joint in the frontal plane is represented by the tibial plafond or superior surface of the talus and intersects the axes to produce the lateral distal tibial angle (LDTA) (Figure 3.31). The value of this angle is also identical for the anatomical and mechanical axis and the use of the prefix is also redundant.

The normal range for the LDTA is 86–92° and the population normal is 89°.

Lateral plane

Femur

Mechanical axis

Figure 3.32
Lateral femoral mechanical axis.

Due to the morphology of the femur and effect of knee flexion, the definition of the lateral mechanical axis of the individual bones is a compromise and is referred to as the modified mechanical axis.

The modified mechanical axis of the femur in the lateral plane is represented by a line between the centre of the femoral head and a point 1/3 of the length of a line drawn from the anterior to the posterior cortex at the level of the open physis in a child or physeal scar following skeletal maturity (Figure 3.32).

The proximal lateral mechanical axis is not generally used in clinical practice.

The mechanical axis intersects distally with the joint orientation line to produce the mechanical posterior distal femoral angle (mPDFA) (Figure 3.32).

The normal range for the mPDFA is 79–87° and the population normal is 83°.

Anatomical axis

The femur is bowed in the lateral plane, with a radius of curvature of approximately 1 metre, and cannot be described by a single axis line. The anatomical axis of the proximal and distal segments are therefore considered individually and are identified by constructing lines that are perpendicular to the femoral diaphysis in the upper and lower third and identifying the mid-points.

The point of intersection between the lateral proximal femoral joint orientation line and mid-point of the femoral neck forms the proximal posterior femoral angle (PPFA) and this is 90° in the normal hip.

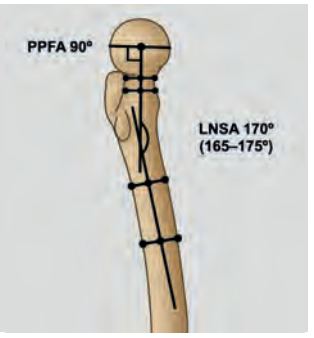

Figure 3.33
Lateral neck shaft angle.

The line between the centre of the femoral head and mid-point of the femoral neck intersects the proximal lateral anatomical axis to produce the lateral neck shaft angle (LNSA) (Figure 3.33).

The normal range for the LNSA is 165–175° and the population normal is 170°.

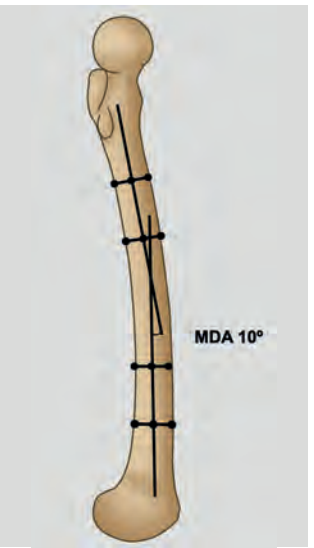

Figure 3.34
Mid-diaphyseal angle.

The proximal and distal anatomical axes intersect to produce the mid-diaphyseal angle (MDA), with a population mean of 10° (apex anterior) (Figure 3.34).

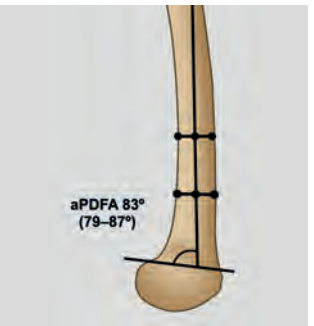

Figure 3.35
Proximal distal femoral angle.

The axis of the lower third bisects the line that represents the distal physeal scar at the junction between the anterior 1/3 and posterior 2/3 to form the anatomical proximal distal femoral angle (aPDFA) (Figure 3.35).

The normal range for the aPDFA is 79–87° and the population normal is 83°.

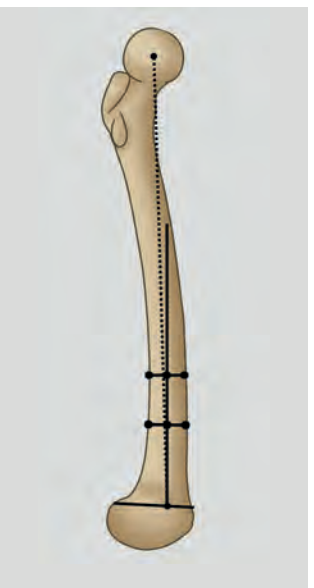

Figure 3.36
Lateral mechanical (-----) and anatomical axes (___).

The distal mid-diaphyseal axis is within 1° of the lateral mechanical axis line and the joint orientation angle derived from the anatomical and mechanical axes is identical for practical purposes and the use of the prefix (m) or (a) is redundant (Figure 3.36).

There are, however, subtle but important differences in evaluating peri-articular deformity and the use of the modified mechanical axis, with the joint angles derived from the anterior 1/3 of the joint orientation line, is more accurate.

Figure 3.37
Tibial mechanical axis (lateral).

Tibia

Mechanical axis

The modified mechanical axis of the tibia is taken as a line between the junction of the anterior 1/5 of the lateral proximal tibial joint orientation line and centre of the tibial plafond (Figure 3.37).

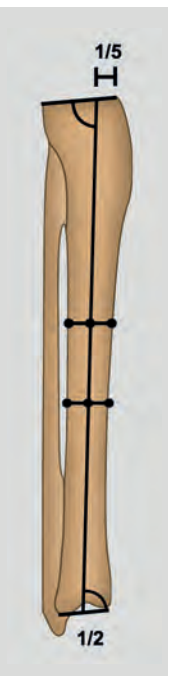

Figure 3.38
Tibial anatomical axis (lateral).

Anatomical axis

The lateral anatomical axis is identified by a line joining the diaphyseal mid-point at two levels. This also intersects the proximal tibial joint line at the anterior 1/5 of the lateral proximal tibial joint orientation line and the lateral distal tibial joint line at the centre of the tibial plafond (Figure 3.38).

These lines are coincident and either can be used for deformity planning. The joint orientation angles derived from the anatomical and mechanical axes are identical and the use of the prefix (m) or (a) is redundant.

The axes intersect the proximal lateral joint orientation line to form the posterior proximal tibial angle (PPTA) (Figure 3.39a,b).

The normal range for the PPTA is 77–84° and the population normal is 81°.

The axes intersect the lateral ankle joint orientation line to form the anterior distal tibial angle (ADTA).

The normal range for the ADTA is 78–82° and the population normal is 80°.

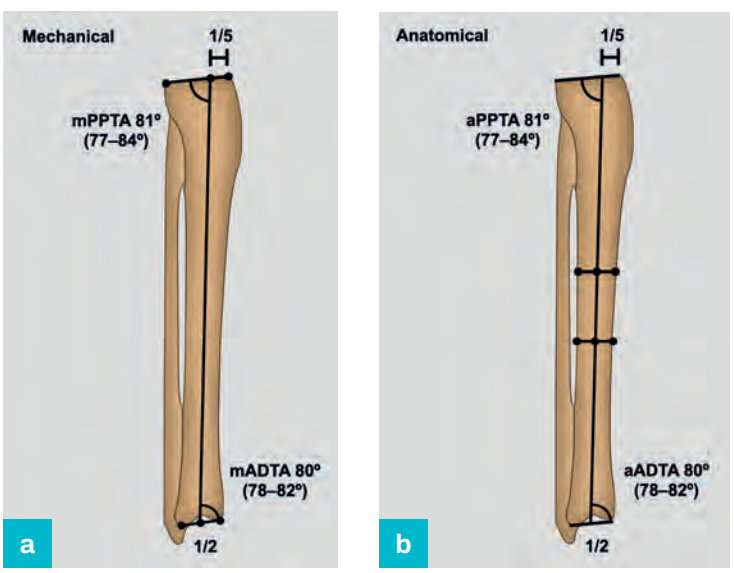

Figure 3.39
Normal values for the tibia in the lateral plane: **(a)** mechanical; **(b)** anatomical.

KEYPOINTS

- Terminology used in deformity planning
- Methods of identification of joint centres and articular surfaces
- Construction of limb and segment axis lines
- Measurement of joint orientation
- Normal femoral and tibial configuration
- Population normal values

CHAPTER

4

The frontal plane

Ross Muir and Reggie Hamdy

Introduction

This chapter describes contemporary methods used to define the location and magnitude of frontal plane lower limb deformities. The ability to systematically assess normal and abnormal geometry is essential for accurate deformity planning and relies on an accepted vocabulary and system of acronyms that are introduced in this chapter. Geometric principles that are used to describe the alignment of the lower limbs and identify deformity are introduced for evaluation in the frontal plane.

Lower limb mechanical axis

The mechanical axis of the lower limb is the vector along which the force generated by the weight of the body is transferred from the point where the limb meets the ground to the point where the limb joins the torso. The proximal extent is defined as the centre of the hip joint and the distal extent as the centre of the weight-bearing surface of the talar dome (see Chapter 3). This is more accurately represented by the area of contact of the sole of the foot with the ground but measurement would require specialised force plates and pressure sensors and is not appropriate for normal clinical practice.

Mechanical axis deviation

In the normal human lower limb, the frontal plane mechanical axis passes just medial to the centre of the knee joint. This will lie further from the centre of the knee joint if there is a frontal plane deformity. The perpendicular distance from the axis to the centre of the knee is defined as the mechanical axis deviation (MAD). This provides an initial estimate of the magnitude and direction of the deformity.

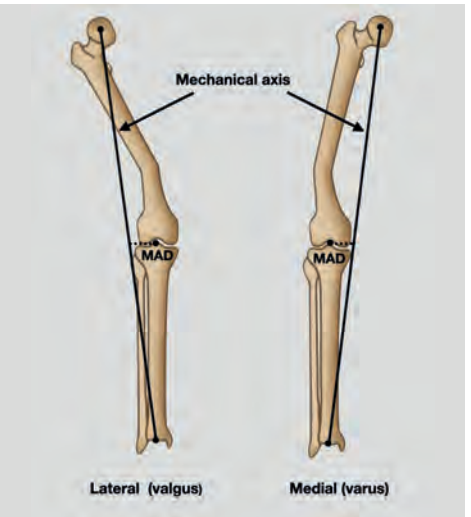

Figure 4.1
Lateral (valgus) and medial (varus) MAD (femoral deformity).

A deformity of the femur (Figure 4.1) and/or tibia (Figure 4.2) will produce an overall lateral or medial MAD.

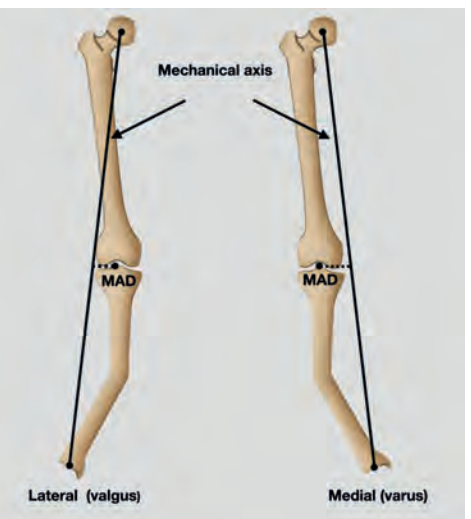

Figure 4.2
Lateral (valgus) and medial (varus) MAD (tibial deformity).

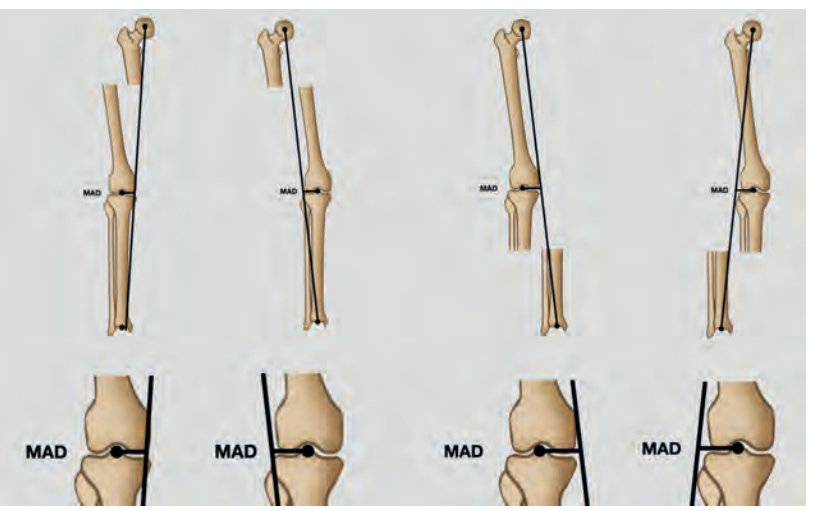

Figure 4.3
The effect of translation on the MAD.

Pure translation deformities of the femur or tibia will produce opposite effects on the MAD. A lateral translation deformity of the femur will displace the MAD medially; a lateral translation deformity of the tibia will displace the MAD laterally (Figure 4.3).

Mechanical and anatomical axes (femur and tibia)

Each lower limb segment can be defined by either a mechanical or an anatomical axis, which are fundamentally different in the femur and broadly similar in the tibia. Consistent use of either the mechanical or the anatomical axis is important during analysis to avoid errors in the assessing and planning deformity correction.

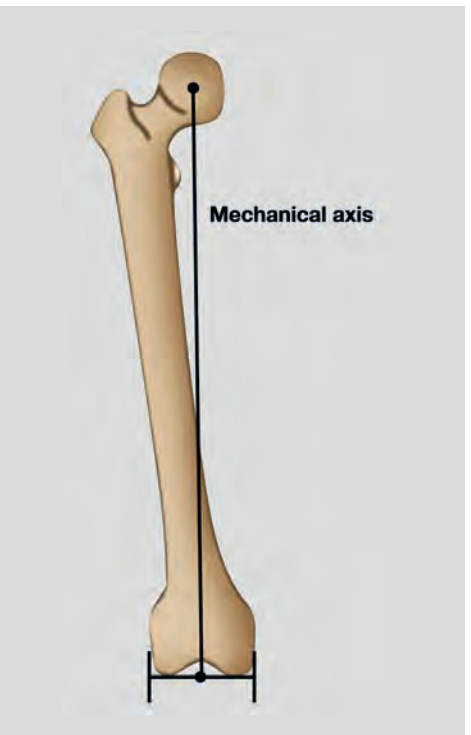

Figure 4.4
Femoral frontal mechanical axis.

The mechanical axis of an individual bone is conceptually similar to the mechanical axis of the limb as a whole and is represented by a line between the centre of the two joints, along which forces are transmitted during weight-bearing. In the femur, this is represented by the line that joins the centre of the femoral head to the centre of the distal femoral condyles (Figure 4.4).

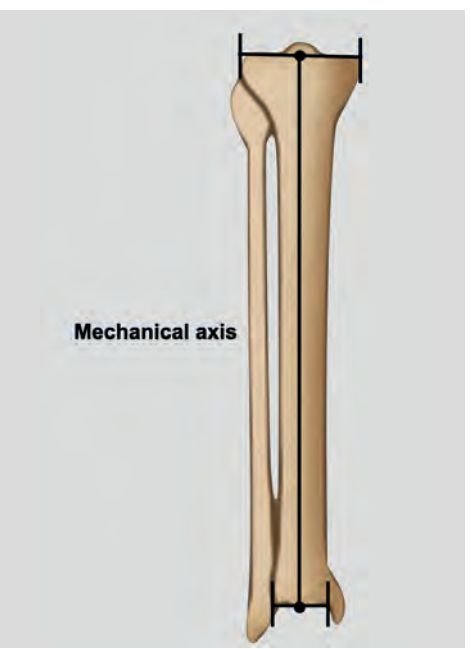

Figure 4.5
Tibial frontal mechanical axis.

In the tibia, it is represented by the line that joins the mid-point of the tibial plateau to the mid-point of the tibial plafond (Figure 4.5).

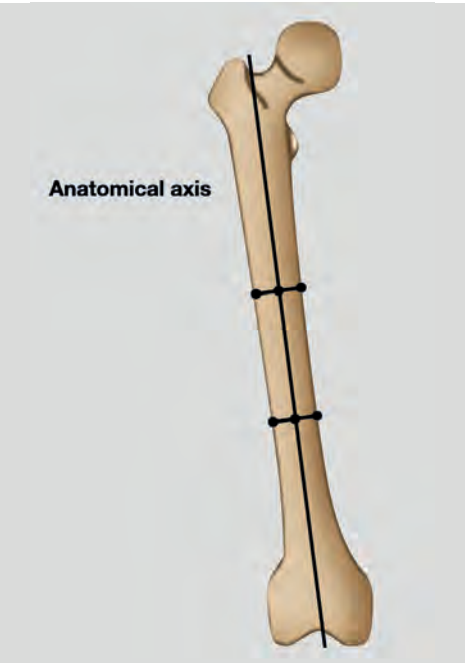

Figure 4.6
Femoral frontal anatomical axis.

The anatomical axis is represented by the line that bisects the diaphysis and is therefore easier to visualise. It is drawn by marking the mid-point of the diameter of the diaphysis at two points along its length and drawing a line joining, and extending beyond, these points.

The femoral anatomical axis (Figure 4.6) should exit proximally through the piriformis fossa and distally just medial to the mid-point of the intercondylar notch. This is the line along which a straight intramedullary nail should be inserted.

Anatomical to mechanical angle

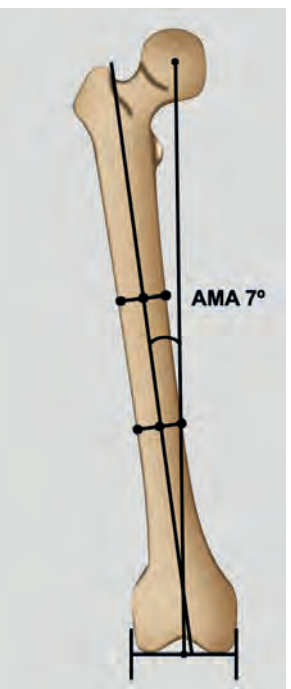

Figure 4.7
Anatomical to mechanical angle.

In the normal adult femur, the anatomical and mechanical axis lines diverge proximally by an average of 7°, because of the lateral offset of the proximal femoral diaphysis caused by the femoral neck. This angle is referred to as the anatomical to mechanical angle (AMA) (Figure 4.7).

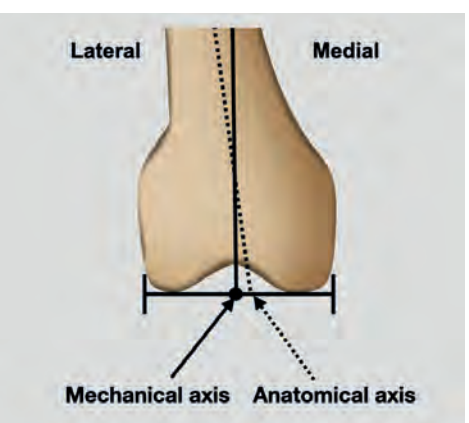

Figure 4.8
Relationship between the distal mechanical and anatomical axes and the distal joint line.

The mechanical and anatomical axes cross just above the condyles as, by definition, the mechanical axis passes through the middle of the knee, whereas the anatomical axis passes from the middle of the diaphysis, to reach a point approximately 10 mm medial to the mechanical axis at the level of the knee, in the lateral aspect of the medial femoral condyle (Figure 4.8).

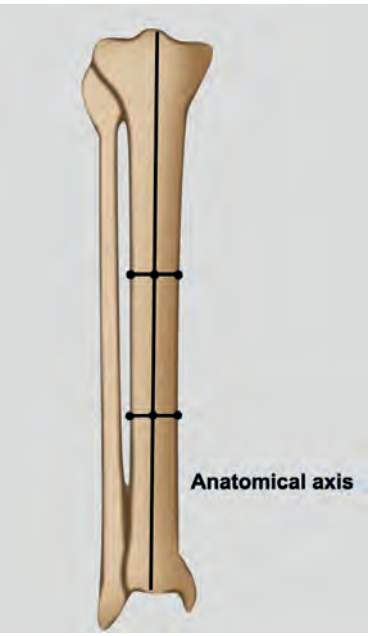

Figure 4.9
Tibial frontal anatomical axis.

The anatomical axis of the normal adult tibia should exit proximally through the medial tibial spine and distally through the centre of the talus. It is also the line along which a straight intramedullary nail should be inserted (Figure 4.9).

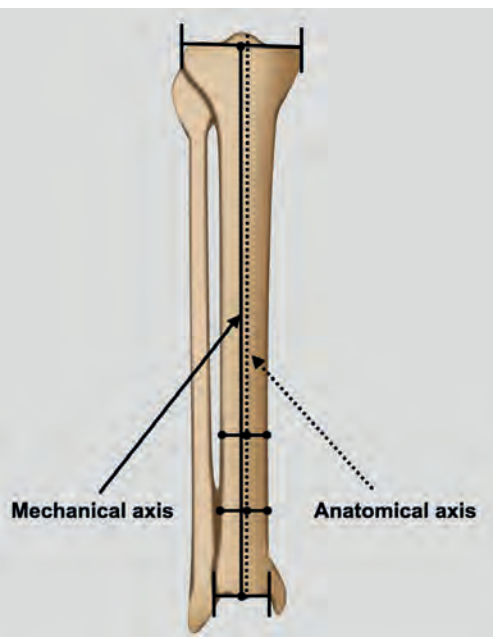

Figure 4.10
Tibial mechanical and anatomical axes.

The tibial mechanical and anatomical axes are virtually collinear and, for practical purposes, can be considered to be identical (Figure 4.10).

Joint orientation

In the normal standing position and during the stance phase of normal gait, the ankle joint line is approximately parallel to the ground and perpendicular to the mechanical axis. The knee joint line is approximately 3° to the ground in the frontal plane, with even distribution of forces across the weight-bearing surfaces of these hinged joints.

Significant deviations from this normal pattern will produce uneven loading of the joints, leading to cartilage damage in areas with increased contact stress. A common example, in clinical practice, is an increased rate of progression of medial compartment osteoarthritis in proportion to amount of varus malalignment and is the basis for high tibial osteotomy as an option for treatment.

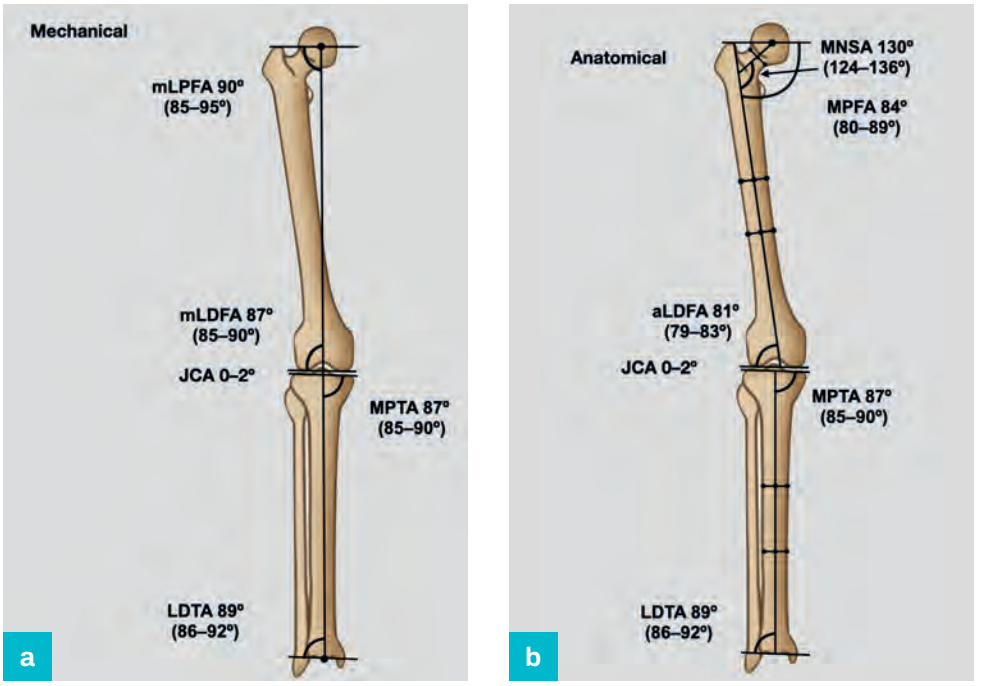

Figure 4.11
Joint orientation angles:
(a) mechanical;
(b) anatomical.

The convention and normal values for the joint orientation angles measured in the lower limb are discussed in Chapter 3 and illustrated in Figure 4.11a,b.

Osteotomy geometry

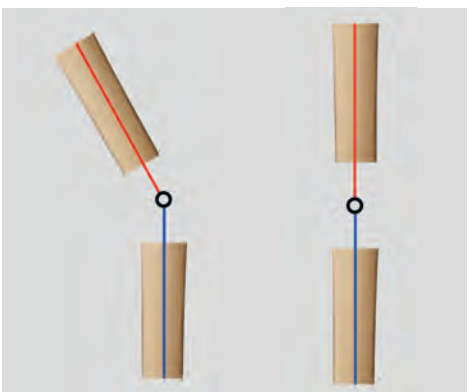

Figure 4.12
Correction at the apex of deformity.

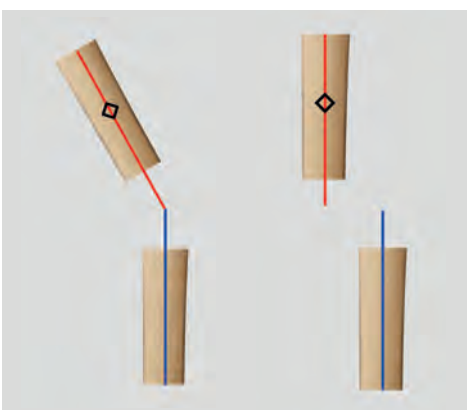

Figure 4.13
Correction at an alternative point results in obligatory translation.

The fundamental principle of deformity analysis involves identification of the axis of the segments of deformity, whether this includes the whole limb or the individual skeletal components. The essence of deformity correction is realignment of these axes to restore normal geometry, referenced to the contralateral side or the population average. This requires an understanding of the geometry and mechanics of a simple hinge and the language that has developed to describe it.

The point of intersection of the proximal and distal axes of the deformity is the point about which angular correction occurs, resulting in collinear alignment of the proximal and distal axes, without producing a secondary translation deformity (Figure 4.12).

The convention used in all subsequent illustrations represents the proximal axis as a red line, the distal axis as a blue line, an intercalary axis as a green line and the point of intersection of the proximal and distal segmental axes by the symbol ○ If angular correction occurs at a point that does not correspond to the point of intersection of the axes, realignment will occur with translation (Figure 4.13).

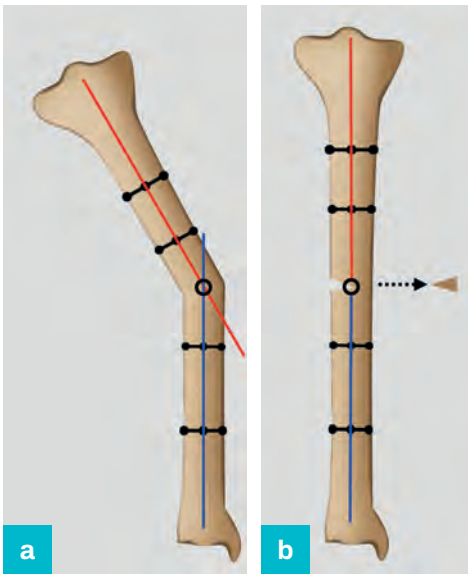

Figure 4.14 (a,b)
Correction of tibial diaphyseal deformity at the intersection of the proximal and distal axes (neutral axis).

Correction at the point of intersection of the axes results in correction without length change and requires excision of a segment of bone on the concave side of the diaphysis (Figure 4.14a,b).

Transverse bisector line

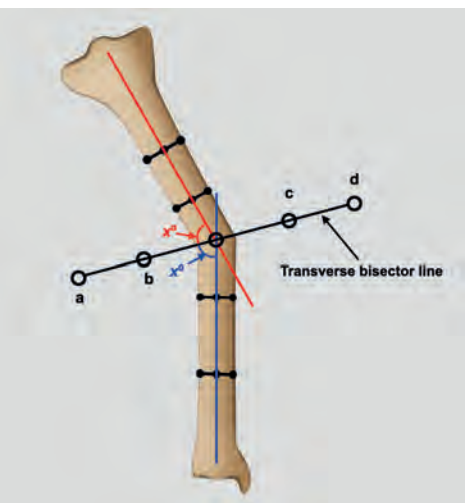

Figure 4.15
The location of apices along a transverse bisector line.

The line that bisects the angle formed at the intersection of the proximal and distal axes is termed the transverse bisector line (tBL) (Figure 4.15) and a simple hinge located anywhere on this line will restore the axis of the bone.

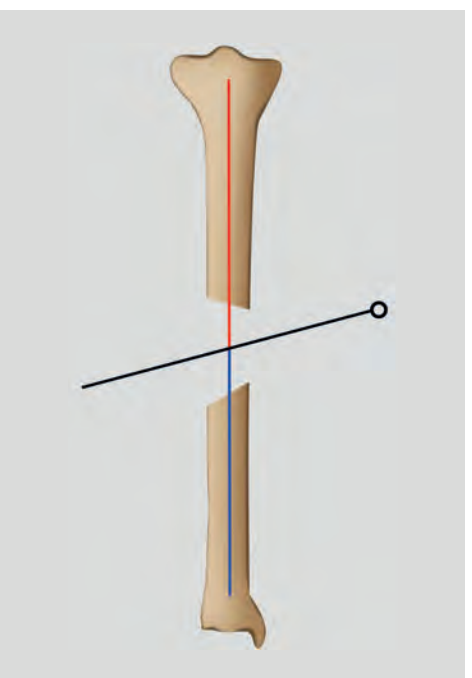

Figure 4.16
Correction on the convex side will result in axis correction with lengthening.

Correction on the convex side of the deformity will produce an opening wedge and add length (Figure 4.16).

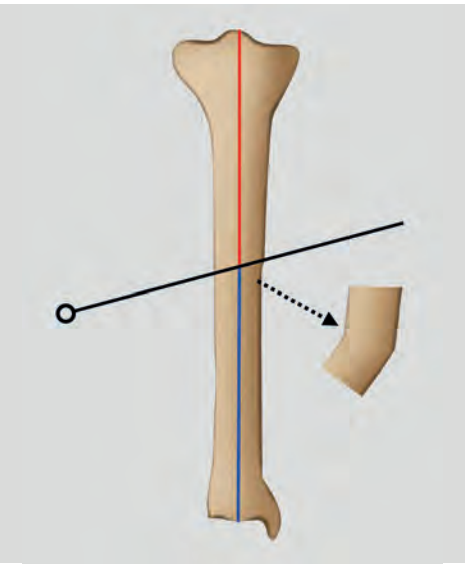

Figure 4.17
Correction on the concave side will result in axis correction with shortening.

Correction on the concave side of the deformity will produce a closing wedge and result in shortening (Figure 4.17).

Hinge and osteotomy position

The position of an externally applied hinge and the osteotomy site can be altered to suit the clinical environment. This is important if the point of intersection of the proximal and distal segment axes is adjacent to a joint surface or is situated in an area of abnormal bone or soft tissue. The relationship between the point of intersection of the axes, the osteotomy level and position of an external hinge determines the final geometry of the bone. This has been codified as *Paley's osteotomy rules* and detailed understanding is crucial, particularly if internal fixation is planned.

Osteotomy geometry

1 *The point of intersection of the axes, osteotomy and externally applied hinge is coincident.* Realignment will occur without displacement (Figure 4.18a,b) and all forms of internal or external fixation are possible, as there is no translation.

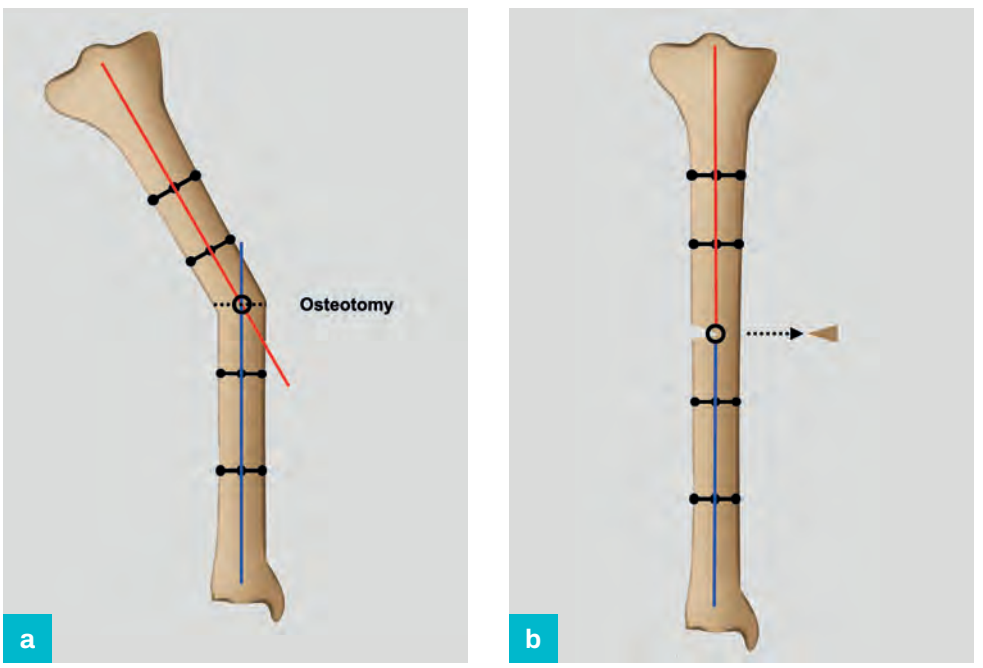

Figure 4.18
(a) The point of intersection of the axes, hinge point and osteotomy are coincident.
(b) Collinear realignment occurs without translation.

2 *The hinge is placed at the point of intersection of the axes but the osteotomy is distant from this.* Normal axial alignment will be restored but translation will be present at the osteotomy site (Figure 4.19a,b). This is useful for peri-articular deformities when an osteotomy is performed away from the joint to produce a bone segment sufficiently large for fixation.

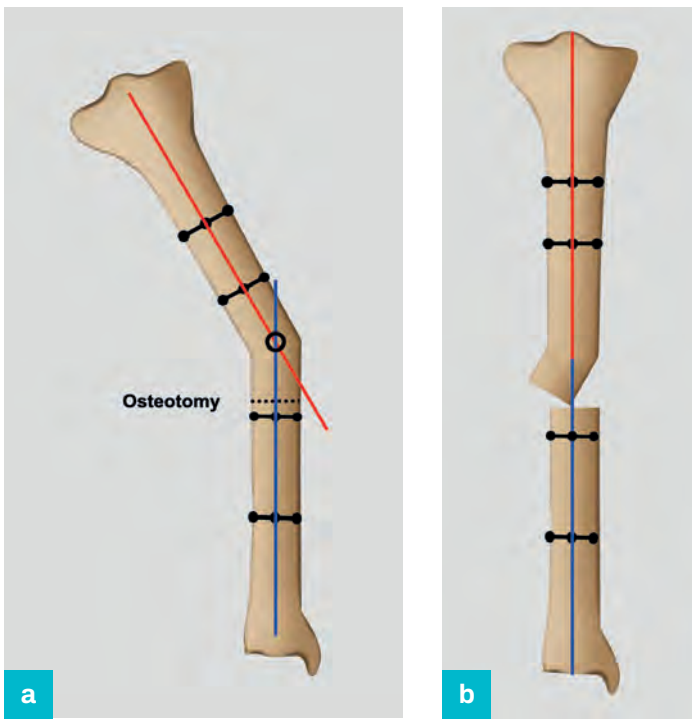

Figure 4.19
(a) A hinge is placed at the point of intersection of the axes with an osteotomy distant to this.
(b) Collinear realignment occurs with translation at the osteotomy.

3 *The hinge is placed away from the point of intersection of the axes.* Realignment of the axes will occur with the distal axis parallel, but not collinear, to the proximal axis. This will result in axis deviation (Figure 4.20a,b) due to a secondary translation deformity. This is often unintentional due to incorrectly placed hinges but may be used deliberately to correct pre-existing translation deformities.

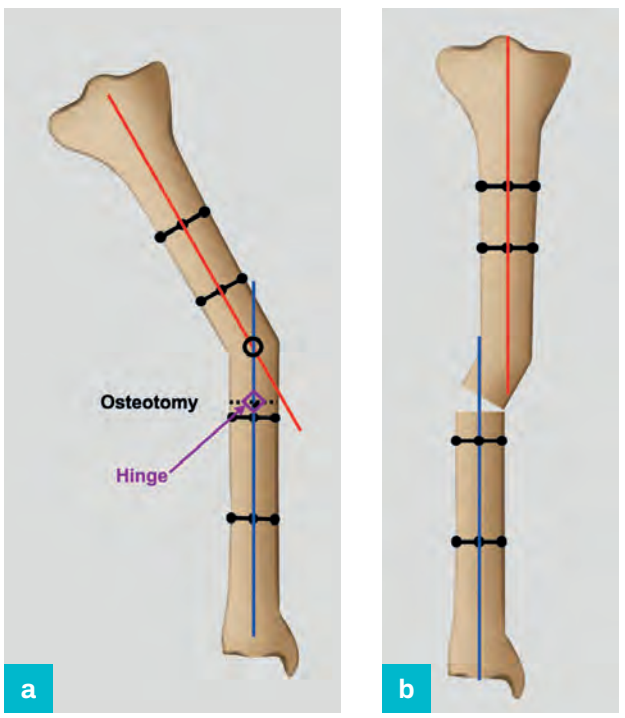

Figure 4.20
(a) The point of intersection of the axes, osteotomy and externally applied hinge are at different levels.
(b) Collinear realignment does not occur because of obligatory translation.

Uni-apical vs multi-apical deformity

Deformity occurs either at a single level (uni-apical) or at multiple levels (multi-apical) within a single bone. Deformities may also be present in both the femur and the tibia and their effects on the MAD may be summative or may neutralise.

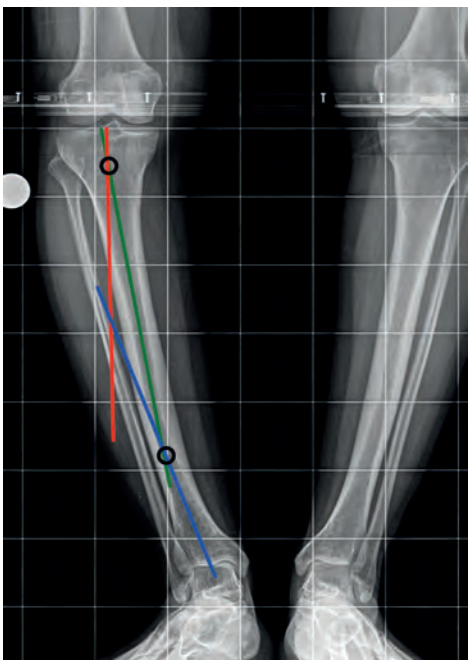

Figure 4.21
Multi-apical deformity.

A multi-apical deformity (Figure 4.21) or an angular deformity with associated translation (Figure 4.22) should be suspected when the point of intersection of the axes is not at the obvious apex or the proximal and distal axes intersect outside the bone. While this may be obvious, it is often subtle and easily overlooked unless a systematic approach is used.

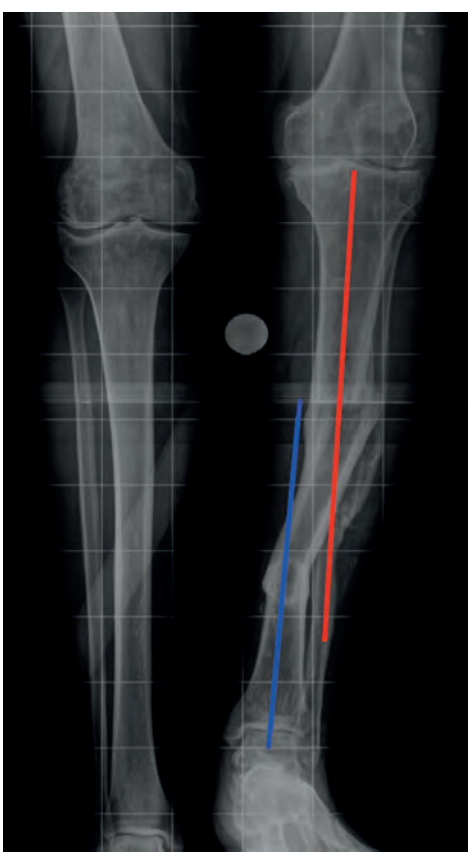

Figure 4.22
Angulation and translation deformity.

Each segment of a deformed long bone has its own axis, which must be identified to allow planning for accurate surgical correction. Analysis must be performed in a systematic fashion to avoid overlooking translation, multi-apical and subtle additional deformities.

If the contralateral leg is normally aligned, this should be used to provide representative values to mitigate individual variation within the population. If there is bilateral limb deformity or if radiographs are not available, population normal values are used as an alternative.

Deformity evaluation

The sequence of evaluation is organised as follows:

1. Confirm that deformity is present by identification of an abnormal limb axis.
2. Identify which bone(s) is (are) involved by measuring the joint orientation angles and comparing to contralateral or population normal values.
3. Locate the site of the deformity by reconstruction of the proximal and distal axes.
4. Determine the magnitude and direction of deformity at each level at the point of intersection of the axes.
5. Assess joint involvement.

Frontal mechanical axis evaluation

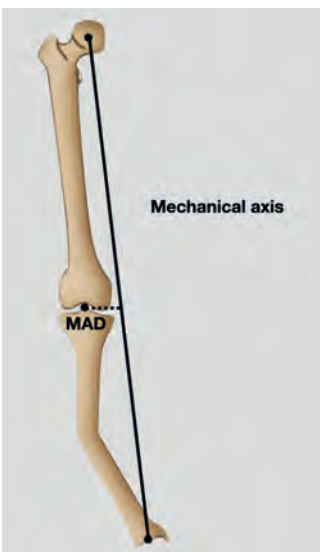

Figure 4.23
Medial MAD (varus).

A line is drawn from the centre of the femoral head to the centre of the tibial plafond. This defines the mechanical axis of the limb and should pass through the centre or just medial to the centre of the knee.

The MAD is measured as the perpendicular distance from the mechanical axis to the centre of the knee (Figure 4.23).

A medial MAD deviation greater than 10 mm and anything lateral is abnormal.

Figure 4.24
Normal mechanical axis in the presence of obvious deformity.

If the mechanical axis is normal (Figure 4.24), malorientation of one or more joints remains a possibility and evaluation of joint orientation is mandatory before frontal plane deformity can be excluded. It is also possible that rotation or lateral plane deformity is present and evaluation of these planes is also essential (see Chapters 5 and 6).

Joint orientation evaluation

Mechanical axis

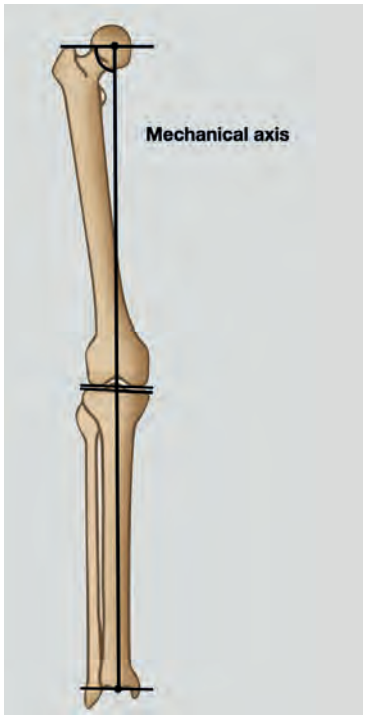

Figure 4.25
Joint orientation lines.

The joint orientation lines for the hip, knee and ankle are drawn (Figure 4.25).

Figure 4.26
Normal mLPFA.

The mLPFA is measured. The population normal is 90° (85–95°). If the measurement is abnormal, there is a deformity in the proximal femur (Figure 4.26).

Figure 4.27
Normal mLDFA.

The mLDFA is measured. The population normal is 88° (85–90°). If the measurement is abnormal, there is a deformity in the distal femur (Figure 4.27).

Figure 4.28
Normal MPTA.

The MPTA is measured. The population normal is 87° (85–90°). If the measurement is abnormal, there is a deformity in the proximal tibia (Figure 4.28).

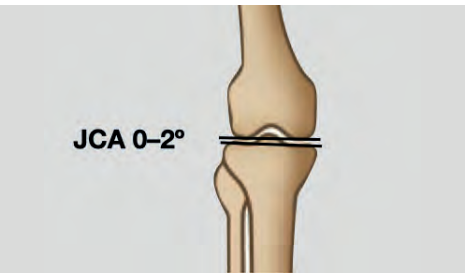

Figure 4.29
Normal JCA.

The joint convergence angle (JCA) is measured. The normal range is 0–2°. If the measurement is abnormal, there is incongruity in the knee joint contributing to the deformity (Figure 4.29).

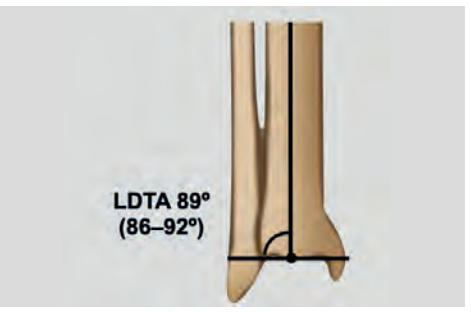

Figure 4.30
Normal LDTA.

The LDTA is measured. The population normal is 89° (86–92°). If the measurement is abnormal, there is a deformity in the distal tibia (Figure 4.30).

Anatomical axis

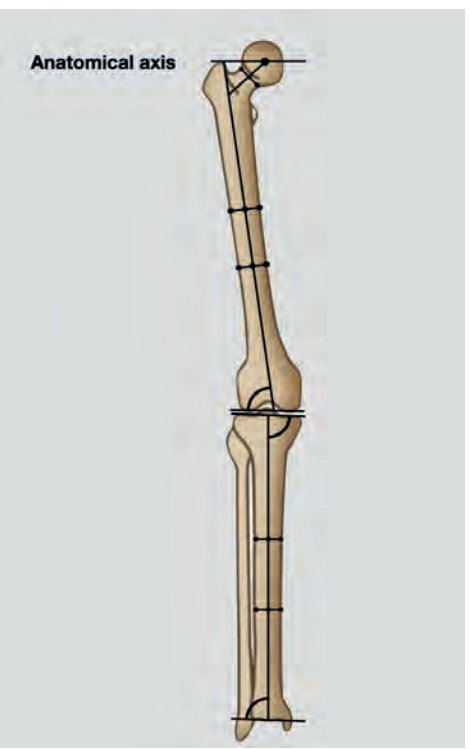

Figure 4.31
Joint orientation lines.

The joint orientation lines for the hip, knee and ankle are drawn (Figure 4.31).

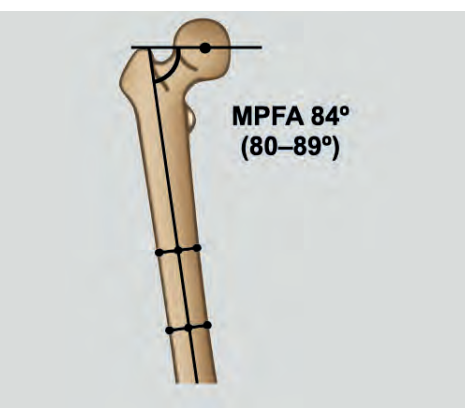

Figure 4.32
Normal aMPFA.

The aMPFA is measured. The population normal is 84° (80–89°). If the measurement is abnormal, there is deformity in the proximal femur (Figure 4.32).

Figure 4.33
Normal MNSA.

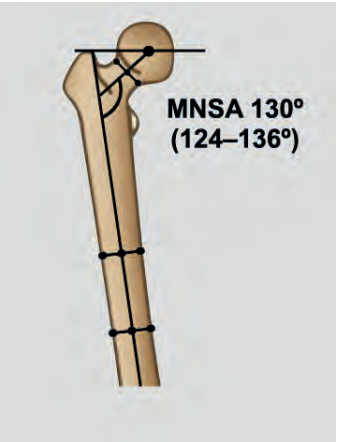

The medial neck shaft angle (MNSA) is measured. The population normal is 130° (124–136°). If the measurement is abnormal, there is deformity in the proximal femur (Figure 4.33).

Figure 4.34
Normal aLDFA.

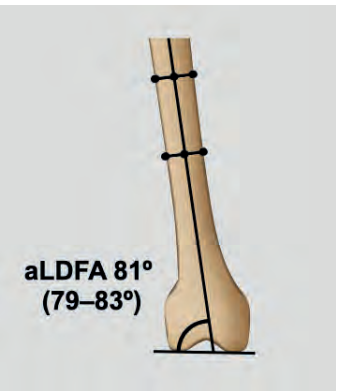

The aLDFA is measured. The population normal is 81° (79–83°). If the measurement is abnormal, there is a deformity in the distal femur (Figure 4.34).

Figure 4.35
Normal MPTA.

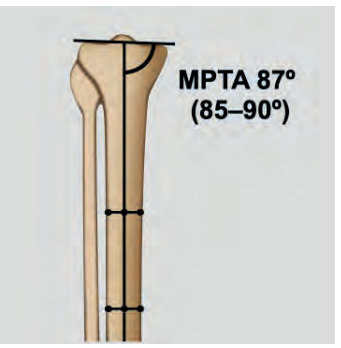

The MPTA is measured. The population normal is 87° (85–90°). If the measurement is abnormal, there is a deformity in the proximal tibia (Figure 4.35).

Figure 4.36
Normal JCA.

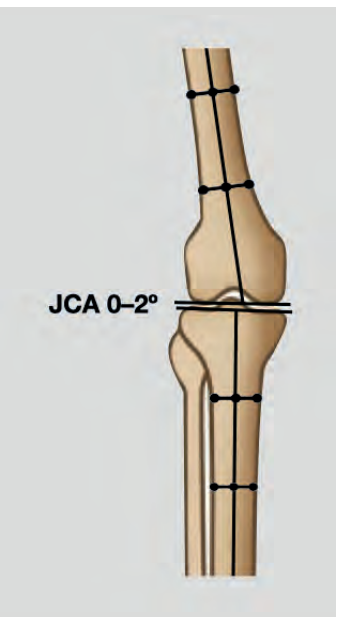

The JCA is measured. The normal range is 0–2°. If the measurement is abnormal, there is incongruity in the knee joint contributing to the deformity (Figure 4.36).

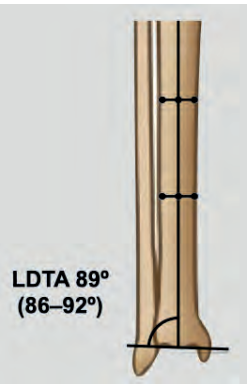

Figure 4.37
Normal mLDTA.

The LDTA is measured. The population normal is 89° (86–92°). If the measurement is abnormal, there is a deformity in the distal tibia (Figure 4.37).

Location of the site of deformity

When a deformity has been recognised and localised to an individual bone, the position of the deformity within the bone is identified. This can be performed using either the mechanical or the anatomical axis. If the deformity is obviously diaphyseal, drawing the anatomical axis of the proximal and distal segments is more straightforward but will overlook peri-articular and metaphyseal deformities. In the following examples, the use of the anatomical axis is described for femoral and tibial deformity. The use of the mechanical axis and evaluation of peri-articular deformity is considered in the chapters dealing with the individual bones.

Femoral anatomical axis planning

Figure 4.38
Proximal femoral anatomical axis.

The joint orientation line of the proximal femur and the mid-diaphyseal line, representing the proximal anatomical axis, is drawn (Figure 4.38).

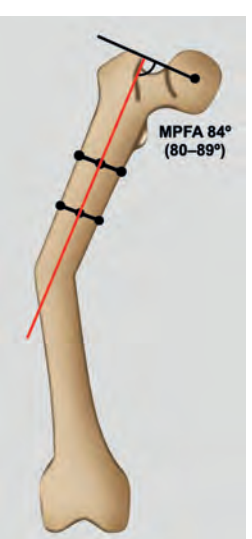

Figure 4.39
Normal proximal femur.

Joint orientation, relative to the mid-diaphyseal line, is checked (Figure 4.39).

The MPFA is normal excluding proximal peri-articular deformity.

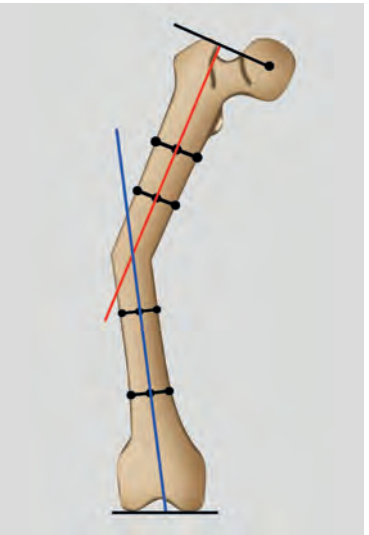

Figure 4.40
Distal femoral anatomical axis.

The joint orientation line of the distal femur and the distal mid-diaphyseal line, representing the anatomical axis of the distal femur, is drawn (Figure 4.40).

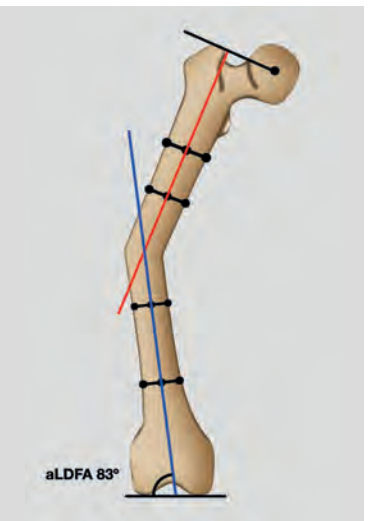

Figure 4.41
Normal distal femur.

Joint orientation, relative to the mid-diaphyseal line, is checked (Figure 4.41).

The aLDFA is normal excluding distal peri-articular deformity.

The point of intersection of the proximal and distal axes represents the point about which neutral correction of deformity will occur (Figure 4.42).

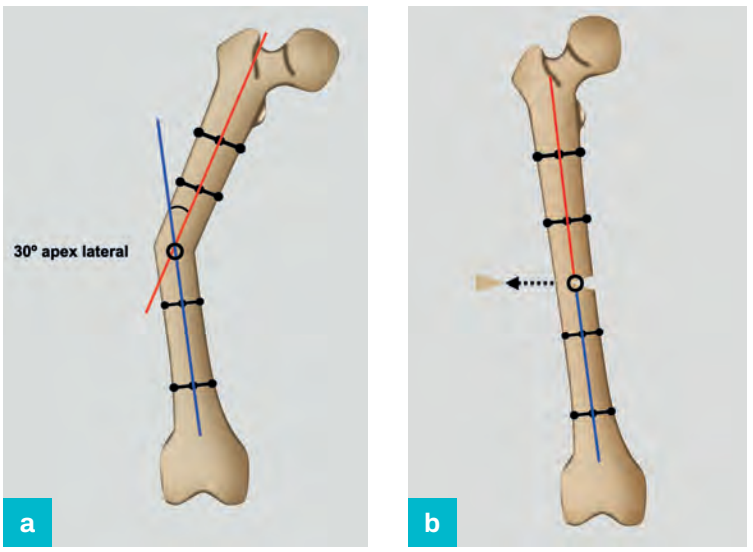

Figure 4.42 (a,b)
30° apex lateral femoral diaphyseal deformity.

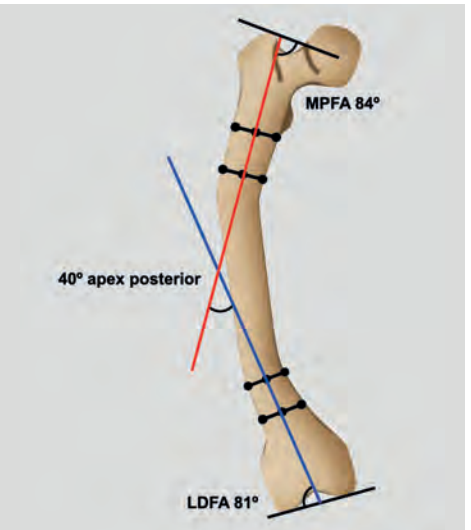

Figure 4.43
Anatomical axes intersect outside the bone.

If the anatomical axes intersect outside the bone, the deformity must be multi-apical or associated with translation (Figure 4.43).

In this case, it is necessary to draw in a third line along the anatomical axis of the intercalated segment and identify where it meets the anatomical axes at either end, representing the points of correction of each component of the deformity. The sum of the individual components is identical to the magnitude of the initial deformity (Figure 4.44a,b).

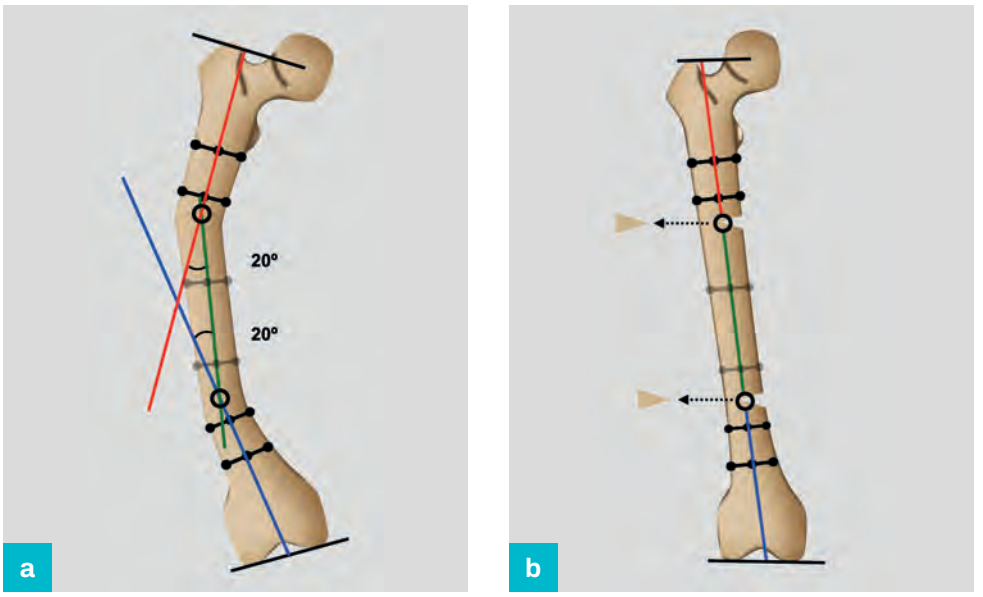

Figure 4.44
(a,b) Correction of multiple-level deformity using an intercalary axis.

Tibial anatomical axis planning

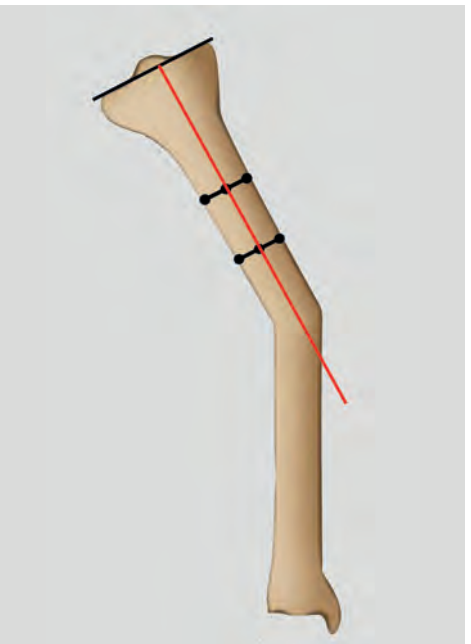

Figure 4.45
Proximal tibial anatomical axis.

The joint orientation line of the proximal and the mid-diaphyseal line, representing the proximal anatomical axis, is drawn (Figure 4.45).

Figure 4.46
Normal proximal tibia

Joint orientation, relative to the mid-diaphyseal line, is checked (Figure 4.46).

The MPTA is normal, excluding proximal peri-articular deformity.

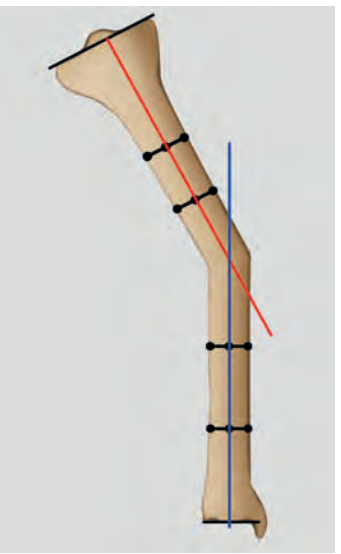

Figure 4.47
Distal tibial anatomical axis.

The joint orientation line of the distal tibia and the distal mid-diaphyseal line, representing the anatomical axis of the distal tibia, is drawn (Figure 4.47).

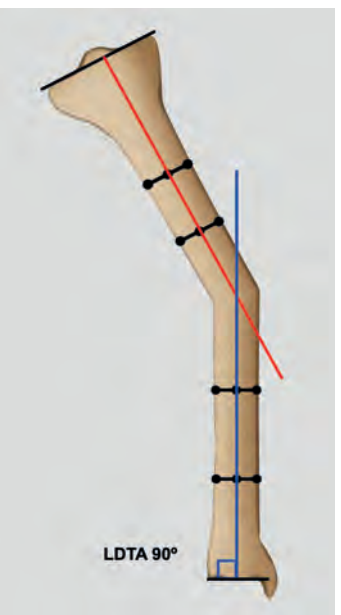

Figure 4.48
Normal distal tibia.

Joint orientation, relative to the mid-diaphyseal line, is checked (Figure 4.48).

The aLDTA is normal, excluding distal peri-articular deformity.

The point of intersection of the proximal and distal axes represents the point about which neutral correction of deformity will occur (Figure 4.49a,b).

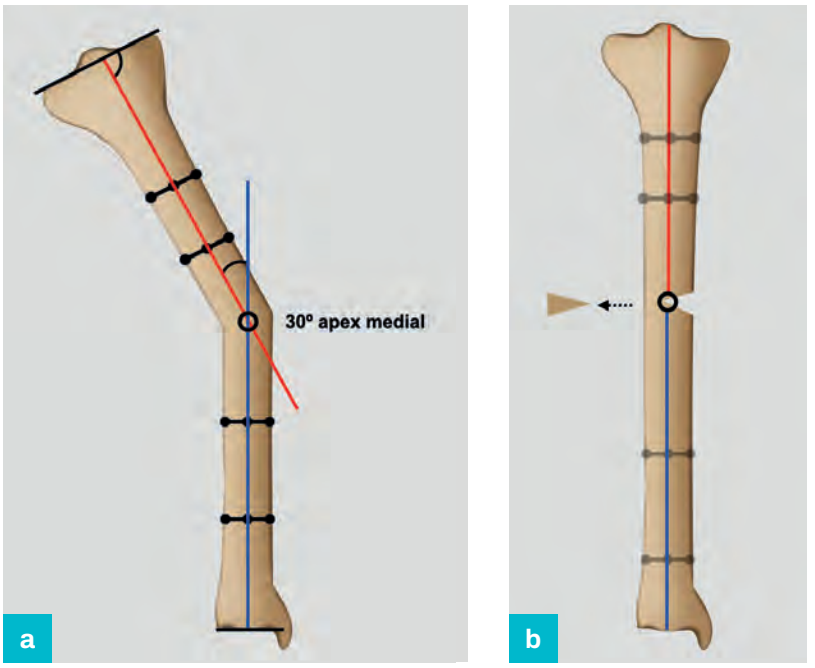

Figure 4.49 (a,b) Correction of 30° apex medial tibial diaphyseal deformity.

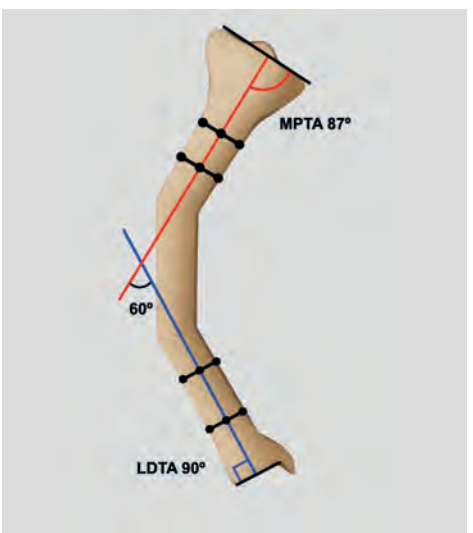

Figure 4.50 Anatomical axes intersect outside the bone.

If the anatomical axes intersect outside the bone, the deformity must be multi-apical or associated with translation (Figure 4.50).

In this case, it is also necessary to draw in a third line along the anatomical axis of the intercalated segment and identify where it meets the anatomical axes at either end, representing the points of correction of each component of the deformity. The sum of the individual components is identical to the magnitude of the initial deformity (Figure 4.51a,b).

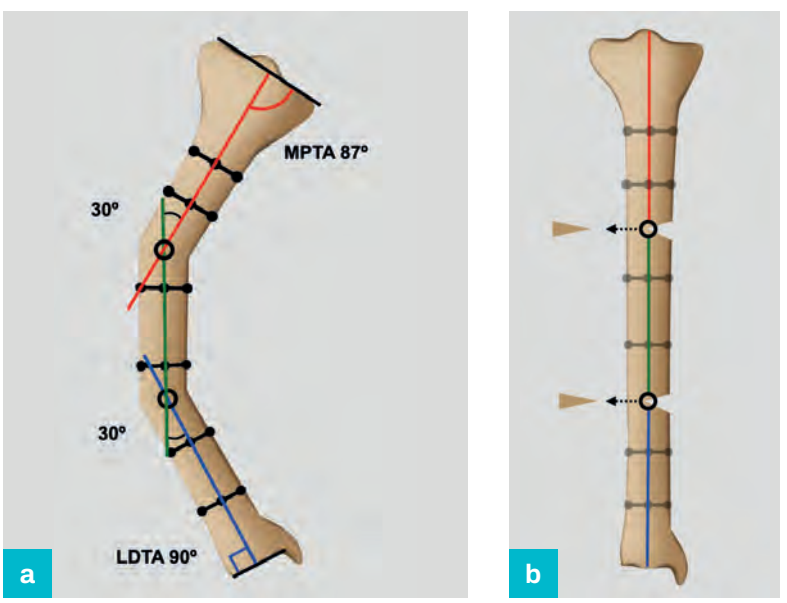

Figure 4.51 (a,b) Correction of multiple-level deformity using an intercalary axis.

Compensatory deformity

Frontal plane deformities occur perpendicular to the plane of motion of the knee joint and cannot be compensated by altering knee joint position. Hip adduction or abduction and hindfoot inversion or eversion may be utilised to achieve normal contact between the foot and ground and to position the foot vertically beneath the hip joint. This reduces contact pressures with the ground and reduces the moment arm of deforming forces during weight-bearing. The position of the joints can be mobile or become partly or completely fixed.
The whole limb and spine should therefore be examined as a routine part of planning for deformity correction (see Chapter 1) and compensatory deformities should be identified and quantified. Mobile compensatory deformities will correct spontaneously after correction of a primary deformity. Partially flexible and fixed compensatory deformities must be taken into consideration as part to the overall planning exercise.

KEYPOINTS

- The mechanical axis of the lower limb and mechanical axis deviation
- The frontal plane mechanical and anatomical axes of the femur and tibia
- Lower limb joint orientation angles and variations from normal
- The geometry of lower limb frontal plane deformity
- The differences between uni-apical and multi-apical deformities
- The relationship between apex of deformity, level of osteotomy and site of correction
- Compensatory deformity

CHAPTER

5

The lateral plane

David Rowland and Alexander Cherkashin

Introduction

Knee movement occurs predominately in the lateral plane and affects the position of the hip and ankle during the normal gait cycle. While malalignment is tolerated because all three joints move in this plane, characterisation of deformity is more complex because of this arrangement. Conventional analysis considers the static limb in maximum extension, but a dynamic component must also be considered to ensure that analysis is clinically relevant. This chapter considers how the standard principles of evaluation of limb alignment are modified to identify lateral plane deformity. This initially considers the overall alignment with a modification of the evaluation of malalignment and introduces the modified mechanical axis. Individual segments are analysed to determine the contribution from the femur and tibia, and methods of identifying the components of the deformity from the joints and soft tissues are also discussed.

General evaluation

Clinical examination is an important precursor to deformity analysis in general and lateral plane evaluation in particular (see Chapter 1). The hip, knee and ankle must be carefully assessed, particularly as fixed hip and knee flexion and fixed ankle plantarflexion may be overlooked. A fixed compensatory contracture may be accentuated following deformity correction and contribute to loss of function.

Evaluation of the lower limb in the lateral plane requires a standardised standing lateral radiograph with the knee in maximum extension (see Chapter 2). Scanners such as the EOS system can produce standing, simultaneous frontal and lateral images of the whole body or an anatomical segment. There is a lower-dose option for paediatric patients which further reduces the radiation exposure, and this technology is likely to form an important part of deformity evaluation as it becomes generally available.

Lateral plane mechanical axis

The lateral mechanical axis of the lower limb is assessed by drawing a line from the centre of the hip to the centre of the ankle.

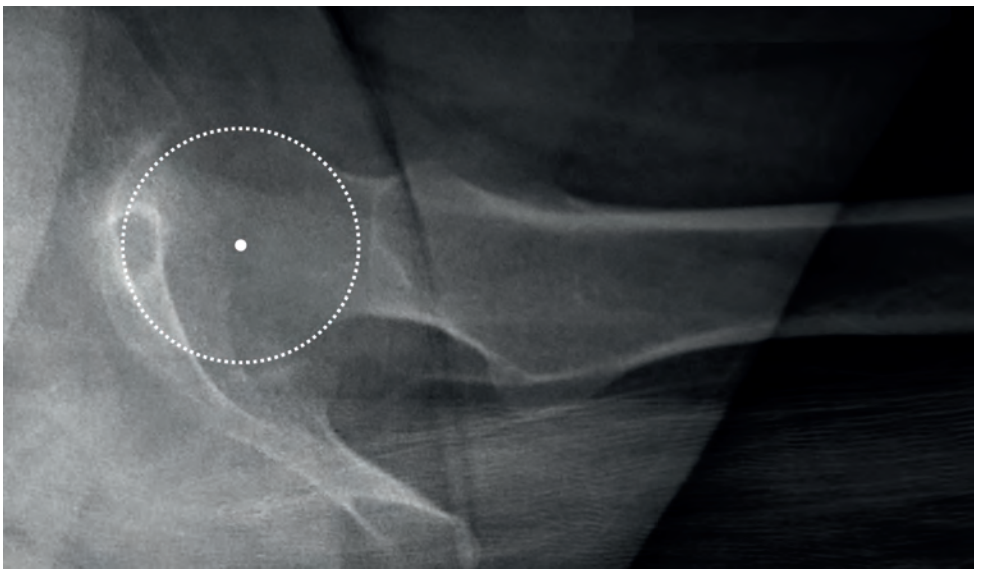

Figure 5.1
Localisation of the femoral head centre.

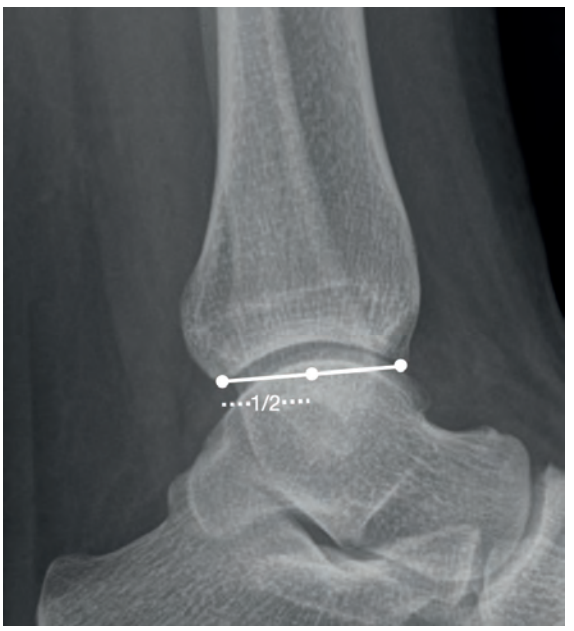

Figure 5.2
Localisation of the mid-point of the ankle (lateral plane).

The centre of the hip is located at the centre of the femoral head, in a true lateral radiograph (Figure 5.1).

The centre of the ankle in the lateral plane is located at the mid-point of the distal tibial articular surface (Figure 5.2).

Figure 5.3
Normal lateral plane alignment.

In full extension, the mechanical axis will pass just anterior to the centre of rotation of the normal knee and remain within the distal femur (Figure 5.3).

In a skeletally immature patient, the centre of rotation of the knee is located at the intersection of the femoral physis with the posterior femoral cortex (Figure 5.4a) and in the adult at the intersection of the posterior femoral cortex and Blumensaat's line (Figure 5.4b).

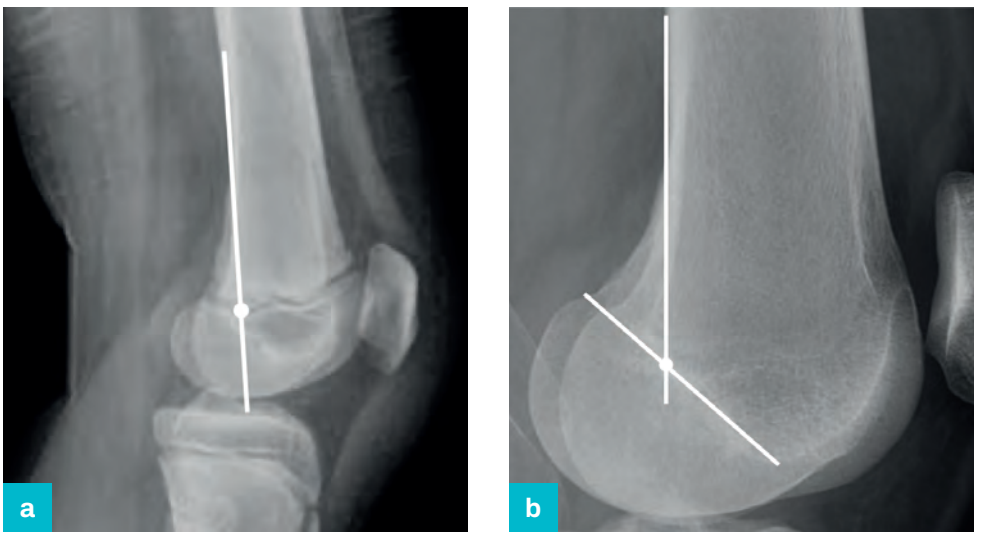

Figure 5.4 Centre of knee rotation: **(a)** skeletally immature; **(b)** adult.

During a normal gait cycle, the posterior capsule, cruciate ligaments and hamstrings limit extension during stance phase. The axis normally passes just anterior to the centre of knee rotation, locking the knee in extension and reduces the muscular effort associated with standing. The position of the lateral mechanical axis can be deliberately translated anteriorly by altering the gait pattern. This is an important compensatory mechanism for patients with quadriceps weakness in conditions including sciatic nerve injury, myelomeningocele and poliomyelitis.

The sequence of evaluation is identical to the frontal plane and is organised as follows:

1. Confirm that deformity is present by identification of an abnormal limb axis.
2. Identify which bone(s) is (are) involved by measuring the joint orientation angles and comparing to contralateral or population normal values.
3. Locate the site of the deformity by reconstruction of the proximal and distal axes.
4. Determine the magnitude and direction of deformity at each level at the point of intersection of the axes.
5. Assess joint involvement.

Lateral mechanical axis evaluation

The lateral mechanical axis is constructed to confirm the presence of deformity.

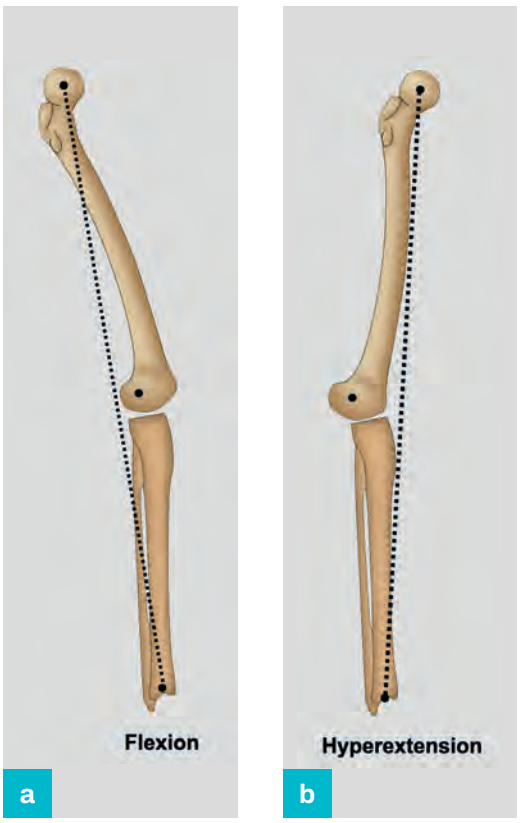

Figure 5.5 (a,b) Knee flexion and hyperextension deformity.

- *If the axis lies posterior to the centre of knee rotation*, due to growth arrest, fracture mal-union, gastrocsoleus or hamstring contracture, there will be an overall flexion deformity.
- *If the mechanical axis is significantly anterior to the centre of rotation of the knee*, due to muscle weakness, growth arrest, fracture mal-union or incompetence of the posterior soft tissue structures, there will be a hyperextension deformity (Figure 5.5a,b).

The extent of the overall deformity is initially assessed by drawing lines that follow the anterior cortex of the distal femur and of the proximal tibia.

The anterior cortical lines are collinear in a normal limb and the acute angle at their intersection is a measurement of the overall flexion or extension deformity (Figure 5.6a–c).

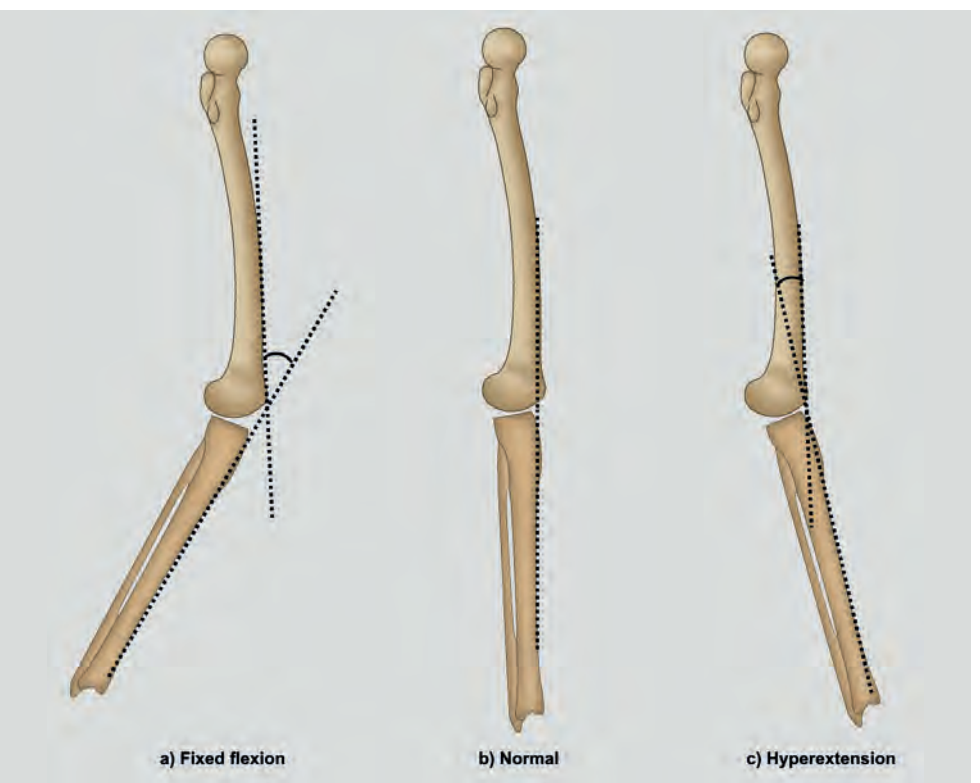

Figure 5.6 Anterior cortical lines in **(a)** fixed flexion, **(b)** normal limb and **(c)** hyperextension.

The width of the femoral condyles and tibial plateau are drawn and mid-points are marked to assess subluxation or dislocation of the knee joint. The mid-points are usually aligned in extension and a discrepancy of >3 mm is indicative of subluxation.

- *Anterior cruciate ligament injury* results in anterior subluxation and is the basis for the anterior drawer and Lachman test.
- *Posterior cruciate ligament injury* results in posterior subluxation, producing posterior sag and is the basis for the posterior drawer test (Figure 5.7a–c).

Figure 5.7
Joint centres in **(a)** anterior subluxation, **(b)** normal limb and **(c)** posterior subluxation.

The femur

Modified mechanical axis

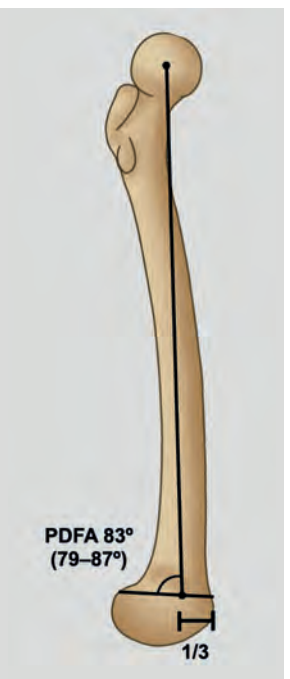

Figure 5.8
Femoral modified mechanical axis (lateral).

The proximal femoral mechanical axis is difficult to localise in the lateral plane and is rarely used in clinical practice.

The modified mechanical axis of the femur in the lateral plane is represented by a line between the centre of the femoral head and a point at the anterior 1/3 of the distal femoral joint orientation line.

The axis intersects distally with the joint orientation line to produce the posterior distal femoral angle (PDFA) (Figure 5.8). The normal range for the PDFA is 79–87° and the population normal is 83°.

Anatomical axis

Proximal femur

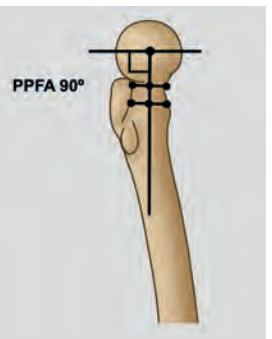

Figure 5.9
Proximal posterior femoral angle.

The anatomical axis of the proximal femur is identified by constructing the proximal 1/3 diaphyseal bisector line.

The proximal femoral joint orientation line is represented by a line that connects the anterior and posterior extent of the physeal scar and intersects the femoral neck bisector to form the proximal posterior femoral angle (PPFA) (Figure 5.9). This is 90° in the normal hip; >90°< is abnormal.

Figure 5.10
Anterior neck shaft angle.

The line between the centre of the femoral head and mid-point of the femoral neck intersects the proximal lateral anatomical axis to produce the anterior neck shaft angle (ANSA) (Figure 5.10). The normal range for the ANSA is 165–175° and the population normal is 170°.

Distal femur

The anatomical axis of the distal femur is identified by constructing the distal 1/3 diaphyseal bisector line. The distal mid-diaphyseal line also intersects the distal femoral joint orientation line at a point at the anterior 1/3 of the distal femoral joint orientation line to produce the posterior distal femoral angle (PDFA). The distal mid-diaphyseal line is within 1° degree of the lateral modified mechanical axis line and the joint orientation angle derived from the anatomical and mechanical axes is identical for practical purposes; the use of the prefix (m) or (a) is redundant (Figure 5.11).

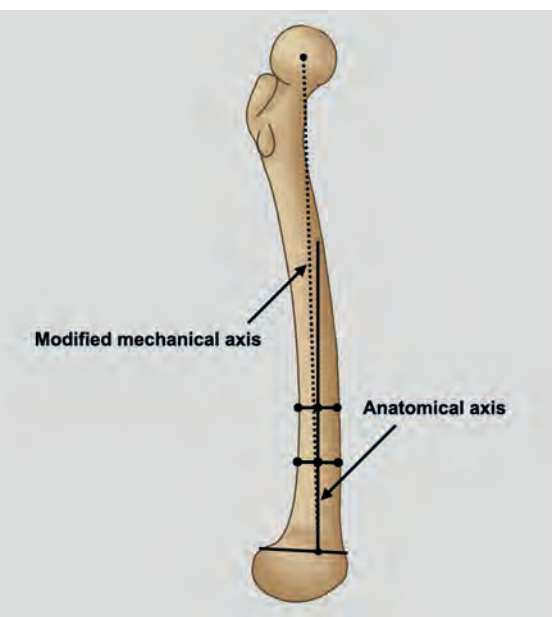

Figure 5.11
Modified mechanical and anatomical axis.

Figure 5.12
Mid-diaphyseal angle.

The intersection of the proximal and distal mid-diaphyseal lines occurs in the middle ⅓ of the normal femur and forms the mid-diaphyseal angle (MDA). The normal femoral MDA is an apex anterior angle with a population normal of 10° (Figure 5.12).

Proximal femoral deformity

If the ANSA is outside the population normal range of 160–175°, either an apex posterior (recurvatum) (<160°) or an apex anterior (procurvatum) (>175°) deformity is present (Figure 5.13).

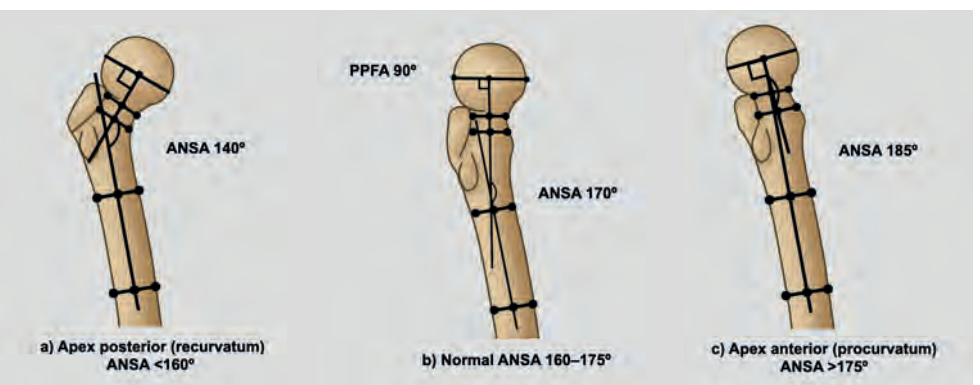

Figure 5.13
Proximal femoral lateral alignment in **(a)** apex posterior (recurvatum), **(b)** normal limb and **(c)** apex anterior (procurvatum).

The ANSA in the example in Figure 5.14 is 140° and is therefore abnormal (Figure 5.14a).

A line representing the normal ANSA is drawn from the normal point of intersection. This uses the contralateral measurement if the deformity is confined to one leg or the population normal of 170° if both legs are involved, or if radiographs are not available (Figure 5.14b).

This intersects the proximal mid-diaphyseal line at the level of the deformity indicating a 30° apex posterior deformity of the proximal femur (Figure 5.14c).

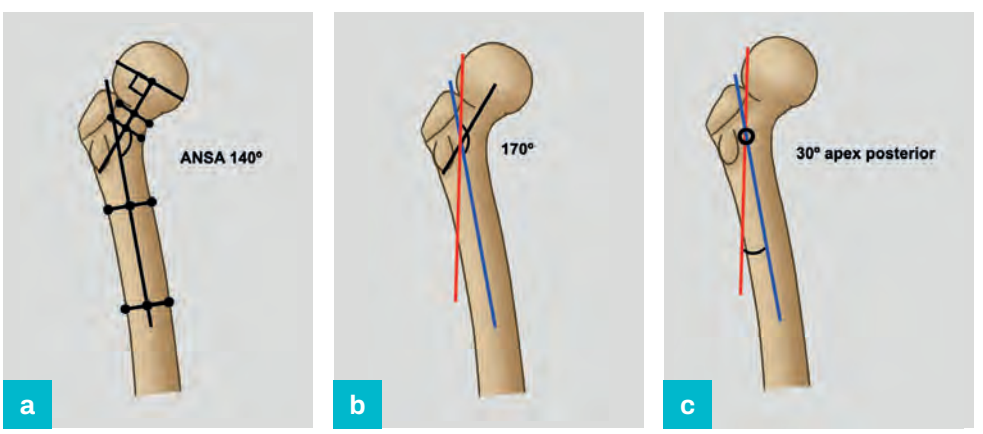

Figure 5.14
Proximal femoral deformity.
(a) Identification of abnormal ANSA.
(b) Normal ANSA drawn in.
(c) 30° apex posterior deformity.

Distal femoral deformity

If the PDFA is outside the population normal range of 79–87°, either an apex anterior (procurvatum) (<79°) or an apex posterior (recurvatum) (>87°) deformity is present (Figure 5.15).

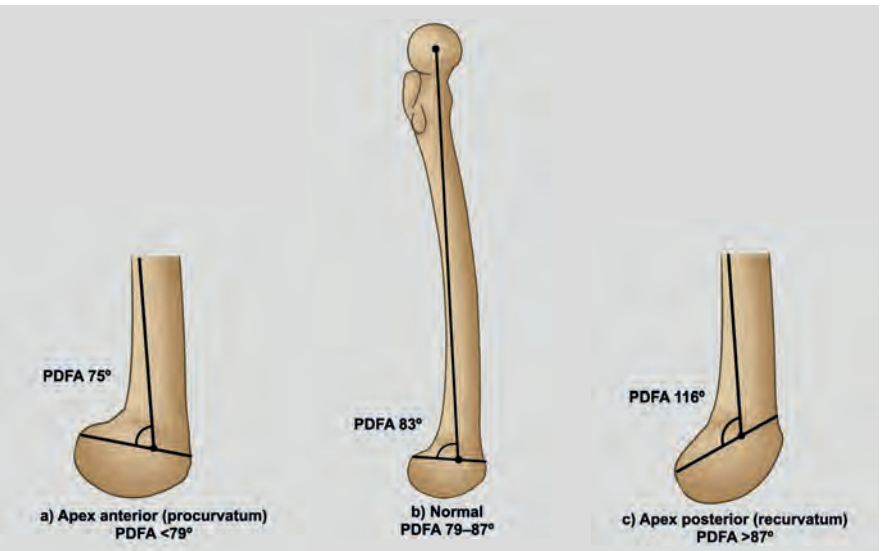

Figure 5.15 Distal femoral lateral alignment in **(a)** apex anterior (procurvatum); **(b)** normal limb and **(c)** apex posterior (recurvatum).

The PDFA in the example in Figure 5.16 measures 68° and is therefore abnormal (Figure 5.16a).

A line representing the normal PDFA is drawn from the normal point of intersection at the anterior 1/3 of the distal femoral joint orientation line. This uses the contralateral measurement if deformity is confined to one leg or the population normal of 83° if both legs are involved, or if radiographs are not available (Figure 5.16b).

This intersects with the distal mid-diaphyseal line at the level of the joint orientation line indicating a 15° apex anterior deformity of the distal femur (Figure 5.16c).

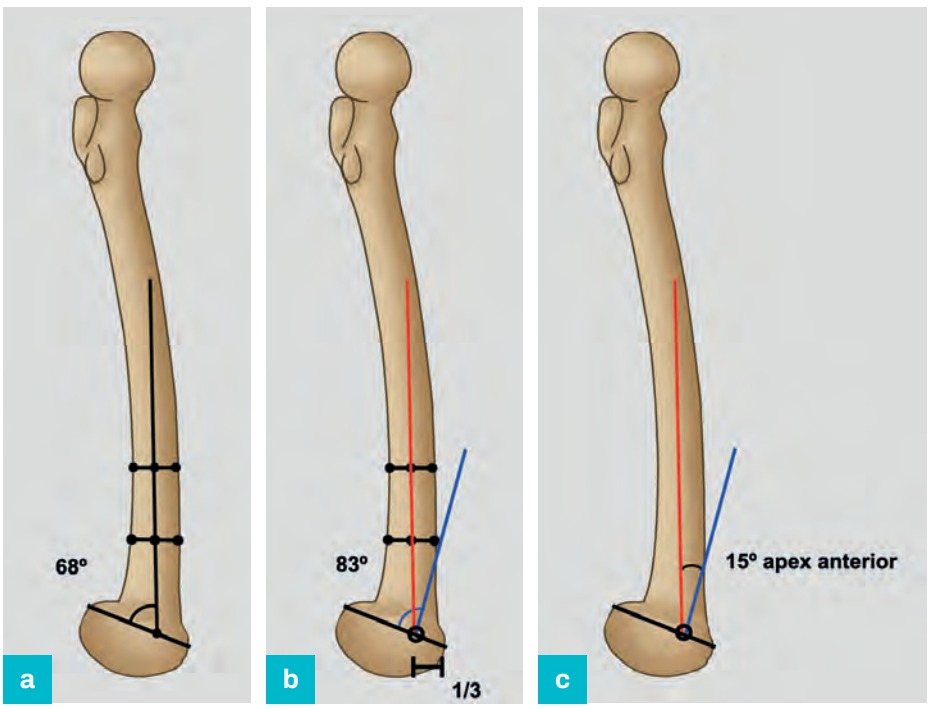

Figure 5.16 Distal femoral deformity. **(a)** Identification of abnormal PDFA. **(b)** Normal PDFA drawn in. **(c)** 15° apex anterior deformity.

Diaphyseal femoral deformity

The proximal anatomical axis and the neck bisector line confirm normal proximal femoral anatomy (ANSA = 170° = normal) (Figure 5.17a).

The distal mid-diaphyseal line and distal femoral joint orientation line confirm normal distal femoral anatomy (PDFA = 83°) with a 40° apex anterior diaphyseal angle (Figure 5.17b).

The proximal mid-diaphyseal line intersects the distal axis at the apex of the clinically obvious deformity, confirming that there is no additional component due to translation or rotation. The angle between the proximal and distal axes at the point of intersection is 40°. The normal femur has a mid-diaphyseal apex anterior (procurvatum) of 10° and the deformity is therefore 30° apex anterior (Figure 5.17c).

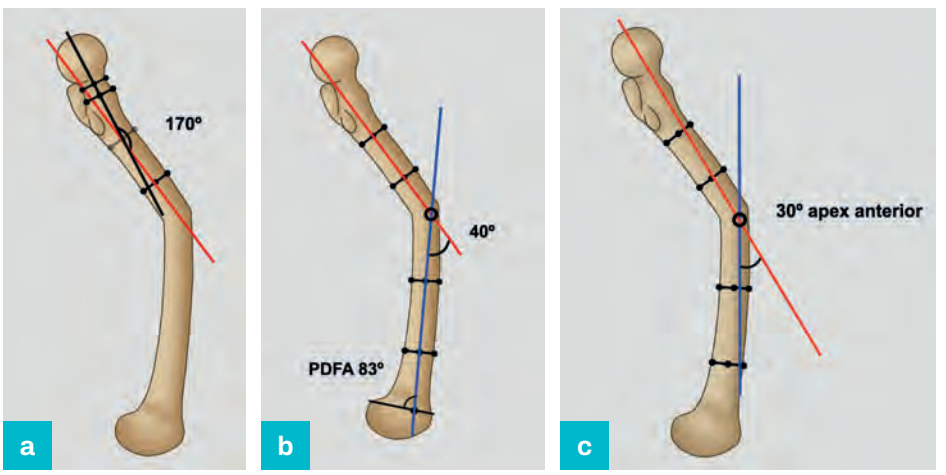

Figure 5.17
Diaphyseal femoral deformity.
(a) Identification of normal ANSA.
(b) Measurement of PDFA and apex anterior diaphyseal angle.
(c) 30° apex anterior deformity.

Clinical example 5.1 Treatment of congenital short femur

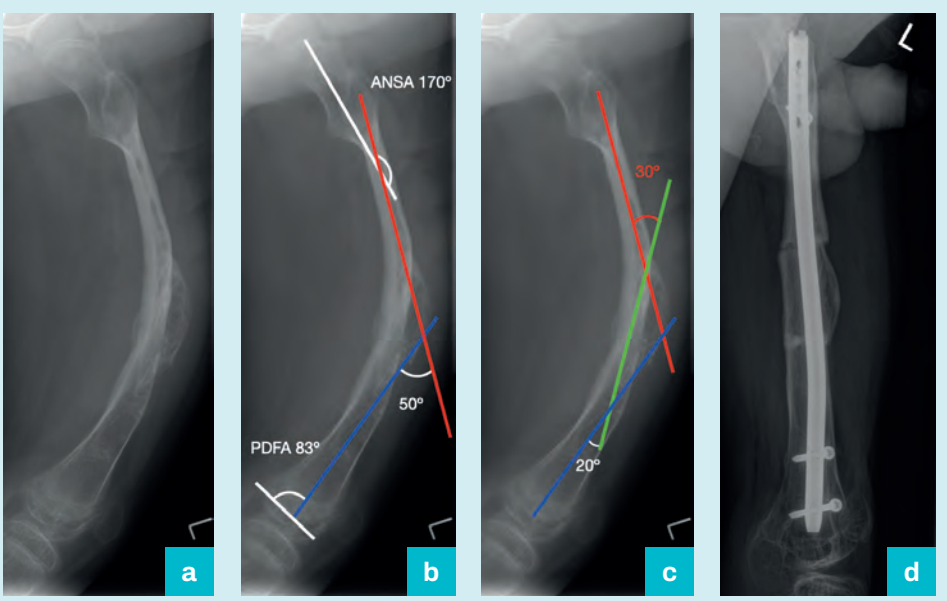

a Lateral radiograph of a patient with a congenital short femur with an apex anterior deformity following lengthening complicated by fracture and delayed union.

b The neck (white), proximal (red) and distal (blue) axes are drawn. In this case, the ANSA and PDFA are normal and the point of intersection of the mid-diaphyseal lines is outside the bone, indicating more than one apex of diaphyseal deformity.

c Intercalary axis demonstrating proximal and distal deformity. An additional mid-diaphyseal line has been drawn (green) to resolve this to a 30° proximal apex anterior component and 20° distal apex anterior distal component. The actual deformity is 40° to account for an expected 10° apex anterior (procurvatum) in the normal femoral diaphysis.

d Two-level osteotomy with intramedullary fixation. This was treated with osteotomies at each predetermined apex, stabilised with a lateral entry femoral nail.

The tibia

Modified mechanical axis

Figure 5.18
Tibial mechanical axis (lateral).

The modified mechanical axis of the tibia is taken as a line between the anterior 1/5 of the lateral proximal tibial joint orientation line and the centre of the tibial plafond (Figure 5.18).

Anatomical axis

Figure 5.19
Tibial anatomical axis (lateral).

The lateral anatomical axis is identified by lines joining the diaphyseal mid-point at two levels. This also intersects the anterior 1/5 of the proximal tibial joint line and the mid-point of the tibial plafond (Figure 5.19).

The modified mechanical and anatomical axes are coincident for the lateral tibia, the proximal and distal joint orientation angles are identical and the use of the prefix (m) or (a) is redundant.

The modified mechanical and anatomical axis intersects the proximal tibial joint orientation line to form the proximal posterior tibial angle (PPTA). The normal range for the PPTA is 77–84° and the population normal is 81°.

If the PPTA is outside these limits, either an apex anterior or procurvatum (<77°) or an apex posterior or recurvatum (>84°) deformity is present (Figure 5.20a–c).

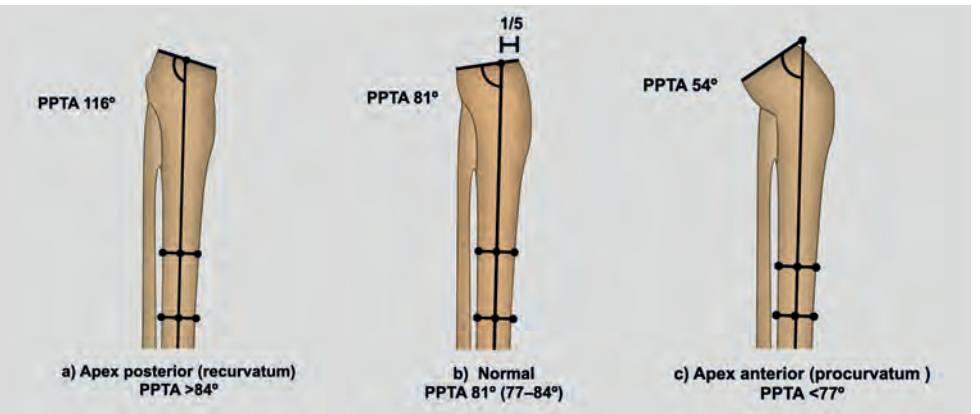

Figure 5.20
Proximal tibial sagittal alignment in **(a)** apex posterior (recurvatum), **(b)** normal limb and **(c)** apex anterior (procurvatum).

The modified mechanical and anatomical axis intersects the distal joint line at its mid-point to form the anterior distal tibial angle (ADTA). The normal range for the ADTA is 78–82° and the population normal is 80°.

If the ADTA is outside these limits, then either an apex anterior or plantarflexion (>82°) or an apex anterior or dorsiflexion (<78°) deformity is present (Figure 5.21).

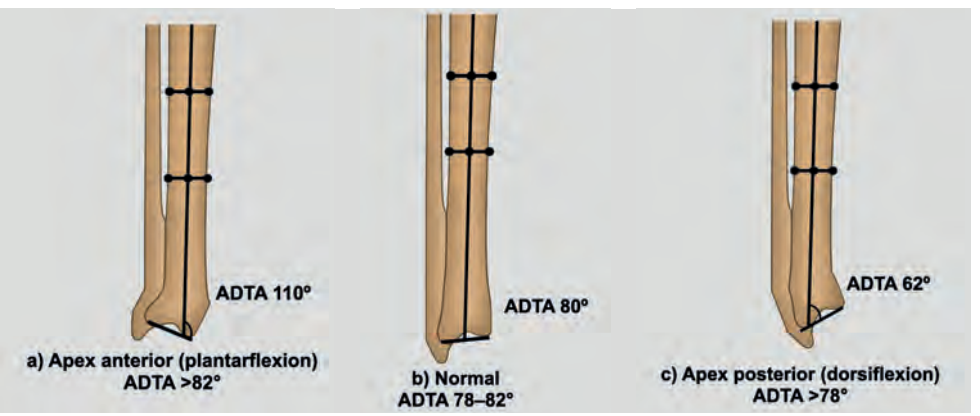

Figure 5.21
Distal tibial lateral alignment in **(a)** apex anterior (plantarflexion), **(b)** normal limb and **(c)** apex posterior (dorsiflexion).

Proximal tibial deformity

The PPTA in the example in Figure 5.22 measures 60° and is therefore abnormal (Figure 5.22a).

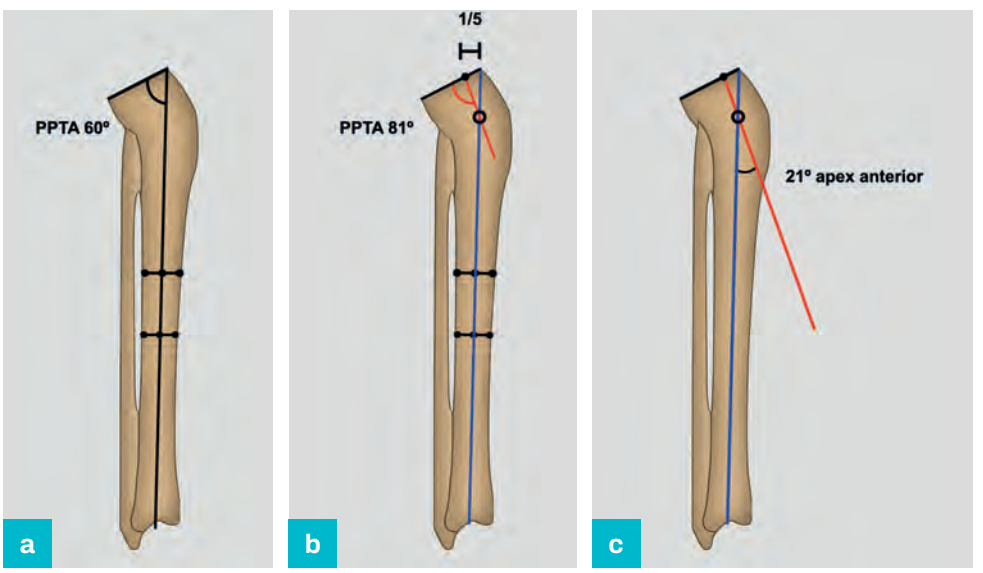

Figure 5.22
Proximal tibial deformity.
(a) Identification of abnormal PPTA.
(b) Normal PPTA drawn in.
(c) 21° apex anterior deformity.

A line representing the normal PPTA is drawn from the normal point of intersection. This uses the contralateral measurement if deformity is confined to one leg or the population normal of 81° if both legs are involved, or if radiographs are not available (Figure 5.22b).

This intersects with the axis line indicating a 21° apex anterior deformity of the proximal tibia (Figure 5.22c).

Distal tibial deformity

The ADTA in the example in Figure 5.23 measures 50° and is therefore abnormal (Figure 5.23a).

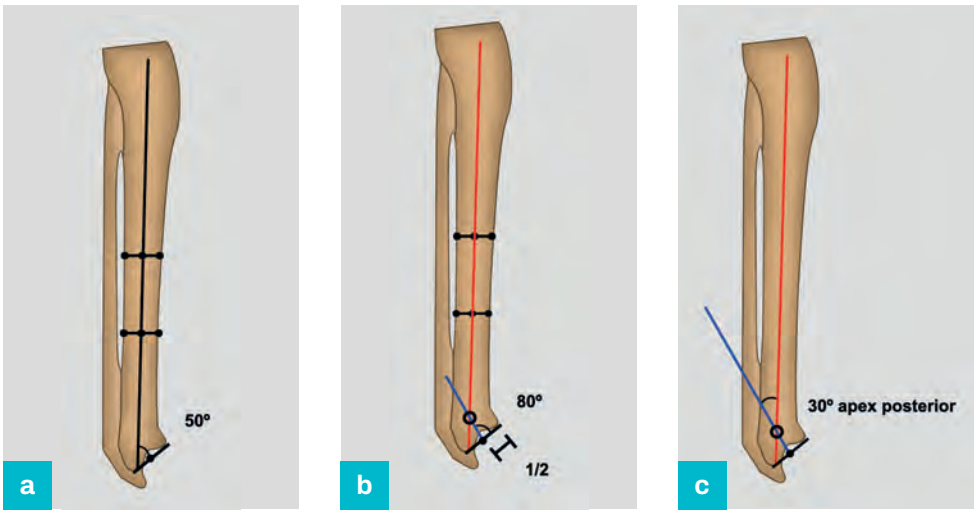

Figure 5.23
Distal tibial deformity.
(a) Identification of abnormal ADTA.
(b) Normal ADTA drawn in.
(c) 30° apex posterior deformity.

A line representing the normal ADTA is drawn from the normal point of intersection. This uses the contralateral measurement if the deformity is confined to one leg or the population normal of 80° if both legs are involved, or if radiographs are not available (Figure 5.23b).

This intersects with the axis line indicating a 30° apex posterior deformity (Figure 5.23c).

Diaphyseal tibial deformity

Mid-diaphyseal and joint orientation lines are constructed (Figure 5.24a).

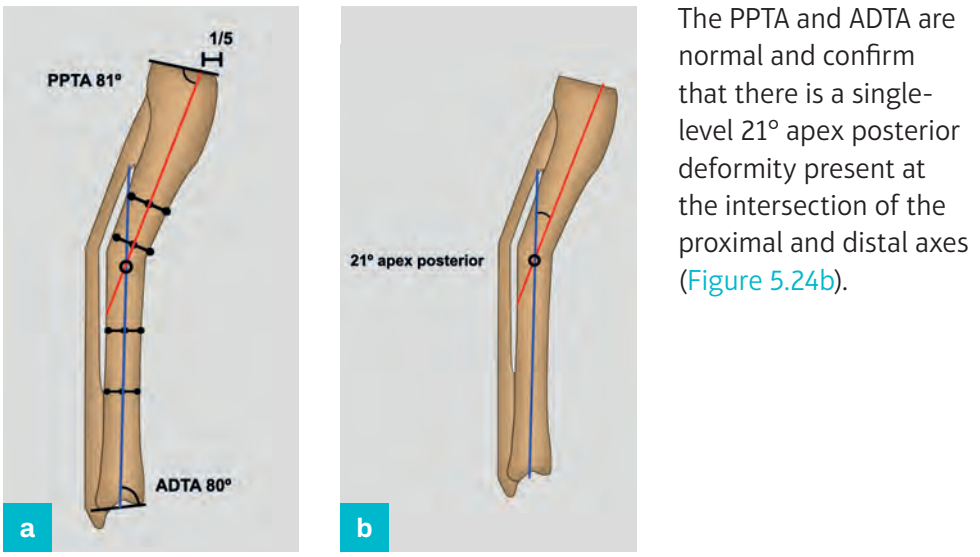

Figure 5.24
Diaphyseal tibial deformity.
(a) Mid-diaphyseal and joint orientation lines.
(b) 21° apex posterior deformity.

The PPTA and ADTA are normal and confirm that there is a single-level 21° apex posterior deformity present at the intersection of the proximal and distal axes (Figure 5.24b).

Clinical example 5.2 Correction of posteromedial tibial deformity

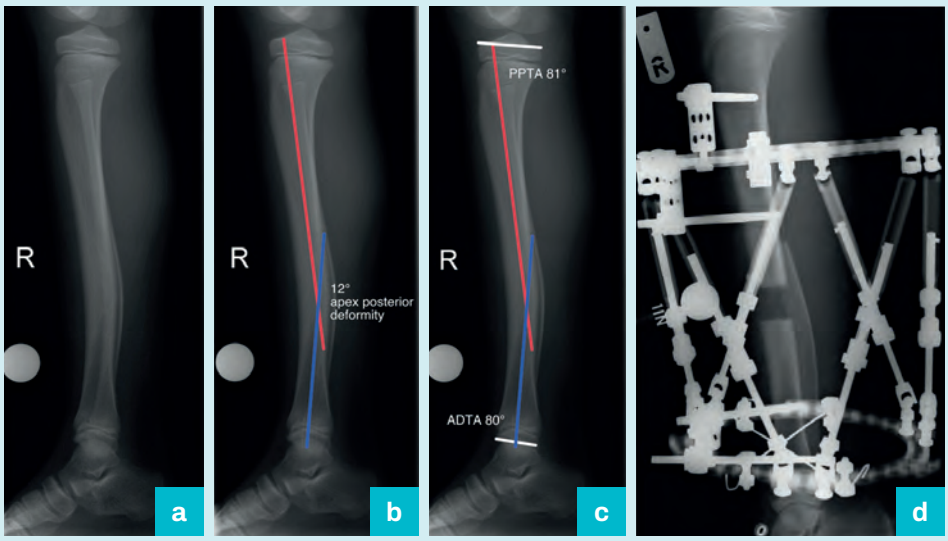

a The lateral radiograph demonstrates a posteromedial tibial deformity with 4 cm shortening.

b The proximal (red) and distal (blue) axes are drawn. These mid-diaphyseal lines indicate a 12° apex posterior diaphyseal deformity.

c The joint orientation angles (PPTA and ADTA) are normal.

d This was treated by an osteotomy at the predetermined apex with a circular fixator to correct all deformity parameters (hexapod correction).

Peri-articular knee deformity

A lateral plane knee deformity may be caused by femoral deformity, tibial deformity, soft tissue contracture/laxity, or a combination of any of these components. Complex combinations of peri-articular knee deformity can be evaluated using a systematic approach, considering the individual effect of the distal femoral and proximal tibial components and determining the additional effect of the joint and soft tissues.

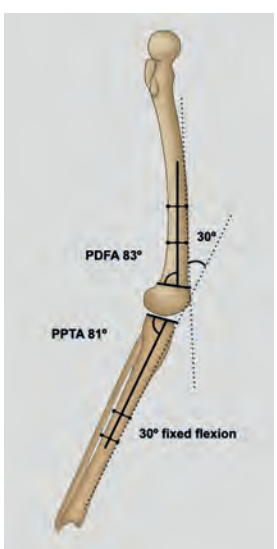

Figure 5.25
Joint contracture with normal PDFA and PPTA.

The six examples in Figures 5.25–5.30 illustrate a 30° deformity, demonstrated by the acute angle formed between the anterior cortical lines.

Joint contracture with normal PDFA and PPTA

The PDFA and PPTA are normal, excluding a distal femoral or proximal tibial abnormality. This confirms that the deformity is due to a soft tissue contracture, which is confirmed by clinical examination (Figure 5.25).

Distal femoral deformity

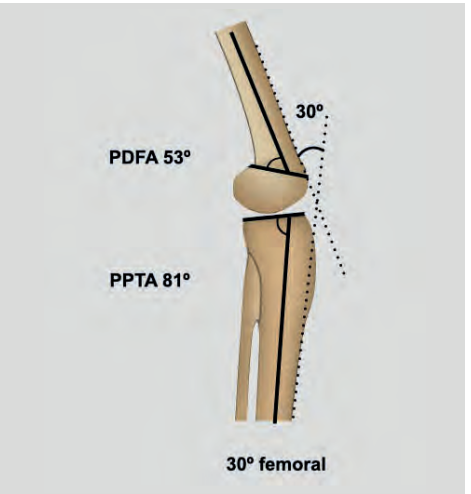

Figure 5.26
Distal femoral deformity.

The PPTA is normal, excluding a proximal tibial deformity. The PDFA is 53°, demonstrating a 30° distal femoral deformity and confirming that the soft tissues are not adding to the deformity (Figure 5.26).

Distal femoral deformity with joint contracture

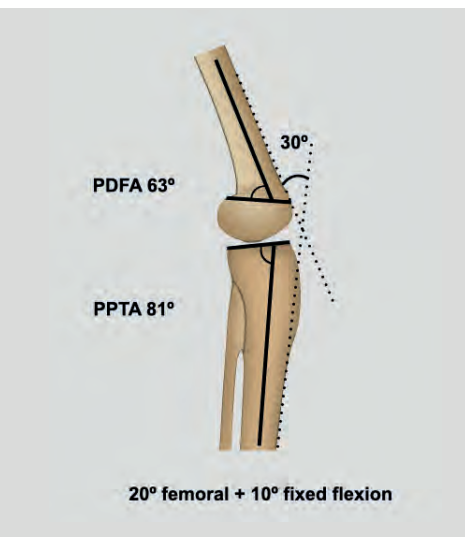

Figure 5.27
Distal femoral deformity with joint contracture.

The PPTA is normal, excluding a proximal tibial deformity. The PDFA is 63°, demonstrating a 20° distal femoral deformity, which does not fully account for the measured overall deformity of 30°. There must therefore be a flexion contracture contributing the remaining 10° of the deformity, which is confirmed by clinical examination (Figure 5.27).

Distal femoral and proximal tibial deformity

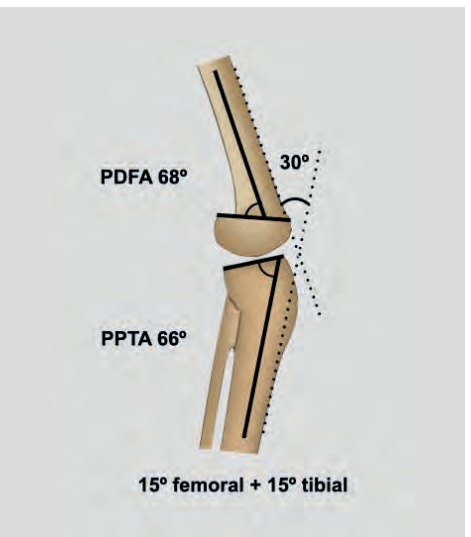

Figure 5.28
Distal femoral and proximal tibial deformity.

The PDFA is 68° and PPTA is 66°, each contributing 15° to the measured overall deformity of 30° and confirming that the soft tissues are not adding to the deformity (Figure 5.28).

Proximal tibial deformity

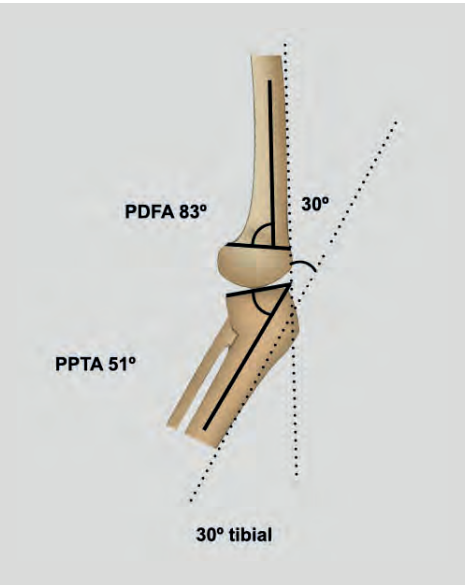

Figure 5.29
Proximal tibial deformity.

The PDFA is normal, excluding a distal femoral deformity. The PPTA is 51° demonstrating a 30° proximal tibial deformity and confirming that the soft tissues are not adding to the deformity (Figure 5.29).

Distal femoral deformity with joint laxity

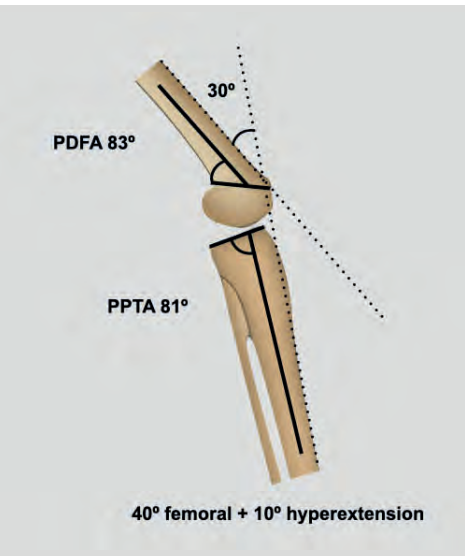

Figure 5.30
Distal femoral deformity with joint laxity.

The PPTA is normal, excluding a proximal tibial deformity. The PDFA is 43° demonstrating a 40° distal femoral deformity, which does not account for the measured overall deformity of 30°. There must therefore be 10° knee hyperextension, which is confirmed by clinical examination (Figure 5.30).

Clinical example 5.3 Distal femoral and proximal tibial growth arrest

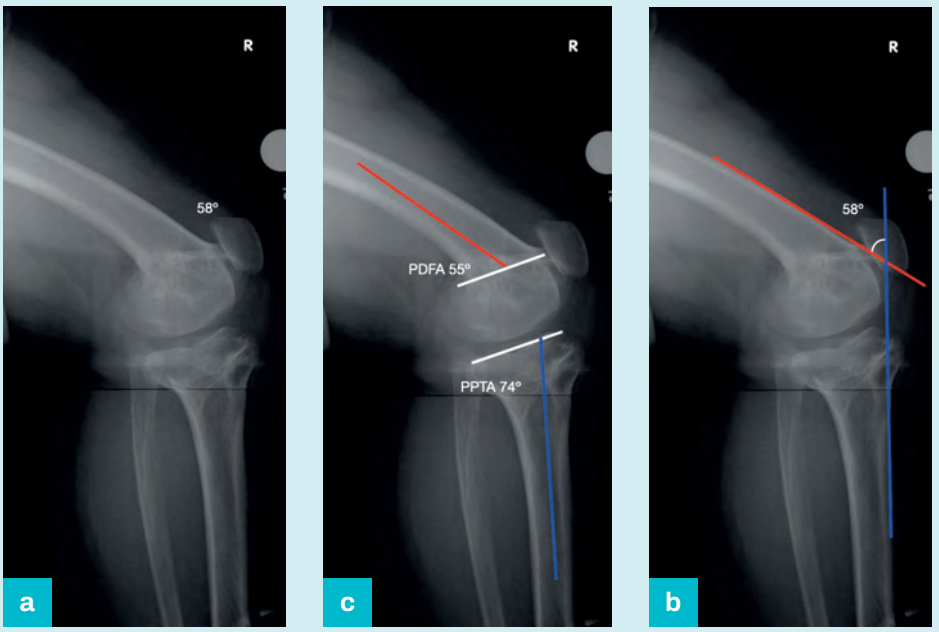

a The radiograph demonstrates the lateral view of the right knee in maximum extension in a patient with distal femoral and proximal tibial growth arrest following meningococcal septicaemia.

b The anterior cortical lines of the distal femur and proximal tibia indicate an apex anterior deformity of 58°.

c The modified mechanical axes and joint orientation lines are constructed as described in previous sections.

PDFA = 55° (normal = 83°) indicating 28° apex anterior distal femoral deformity.

PPTA = 74° (normal = 81°) indicating 7° apex anterior proximal tibial deformity.

The remaining 23° is therefore due to a knee joint contracture.

KEYPOINTS

- Measurement of lateral malalignment
- Evaluation of flexion/extension deformity using anterior cortical lines
- Identification of the anatomical and modified mechanical axis
- Identification of abnormal limb segments using joint orientation angles
- Identification of peri-articular deformity and the contribution from the soft tissues
- Identification of combined diaphyseal and peri-articular deformity

CHAPTER

6

The axial plane

David Goodier and Nikolaos Giotakis

Introduction

The terms torsion and rotation are used interchangeably to describe angulation in the axial plane and translation can refer to an increase or decrease in the length of a segment or limb. This chapter will refer to angular deformity in the axial plane as torsion, joint movement as rotation and translation as short or long, long or short, medial or lateral.

Limb-length discrepancy is less commonly a functional problem in the upper limbs unless it is particularly severe or combined with other deformities. Torsional deformities in the upper limbs can be a significant functional issue particularly in the forearm, where the relationship between the radius and the ulna is complex.

Lower-limb length discrepancy is due to either a real or apparent difference between the lengths, or a significant abnormality of equal length. Short stature or excessive height may result in difficulties with mobility, education and employment, in addition to psychosocial issues. Limb-length discrepancy may be present at birth, predicted in the growing child or occur as a consequence of trauma, infection or surgical treatment. An uncorrected discrepancy of greater than 10 mm in the lower limbs may be associated with back pain and may benefit from correction, with a spectrum of approaches ranging from simple orthotics to extensive surgery.

Lower-limb torsional abnormalities leading to patellar maltracking commonly present with anterior knee pain that can prove refractory to conservative treatment. Internal torsional deformities are less well tolerated and, although there is no evidence to correlate the onset of osteoarthritis to torsional malalignment, noticeable deformities are often poorly tolerated.

Radiological examination

Recent developments in X-ray detection have led to low-dose systems that produce simultaneous 2D images of the whole body. The technology is based on an ultrasensitive, multi-wire proportional chamber that substantially reduces the

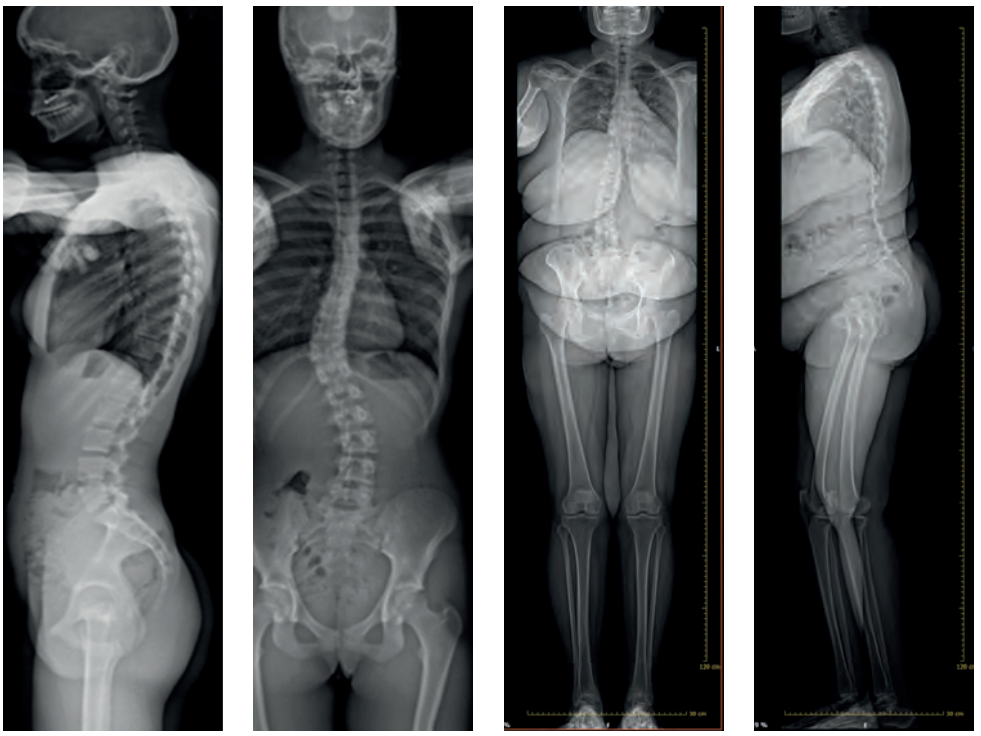

Figure 6.1
3D whole body scan (with permission Prof. B. Garg, All India Institute of Medical Sciences, New Delhi).

X-ray dose, generating a whole-body scan in approximately 20 seconds (Figure 6.1). The images are taken in functional positions, including standing, with 3D reconstruction of the skeleton by stereo-radiography, and this allows accurate evaluation of limb alignment and length in the load-bearing limb.

CT scanning may be necessary for accurate evaluation of torsional alignment using corresponding axial images at the hip, distal femur, proximal tibia and ankle. Lines are drawn along the femoral neck, the posterior line of the distal femoral condyles, the proximal tibia and the malleolar axis and are used to measure torsion in each segment (Figure 6.2). This is associated with considerable inter- and intra-observer measurement error and clinical evaluation is essential in the evaluation of rotational deformities (see Chapter 1).

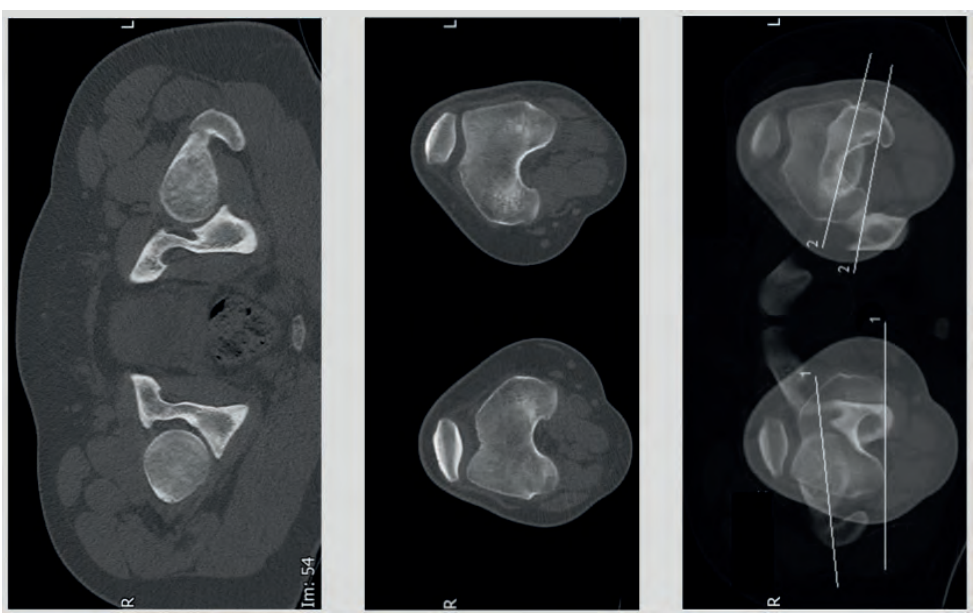

Figure 6.2
CT evaluation of torsion.

Long leg alignment view

This is the standard initial investigation and requires a modification in technique for the evaluation of leg-length discrepancy. A reference scale should be included and a calibration sphere or ruler is commonly used. The image is obtained with calibrated blocks to support the short limb and includes the iliac blades. This will identify pelvic obliquity and compensatory deformities that may influence the correction strategy. The limb must be positioned to ensure that the patella is facing forwards, as described in Chapter 2 (Figure 6.3a,b).

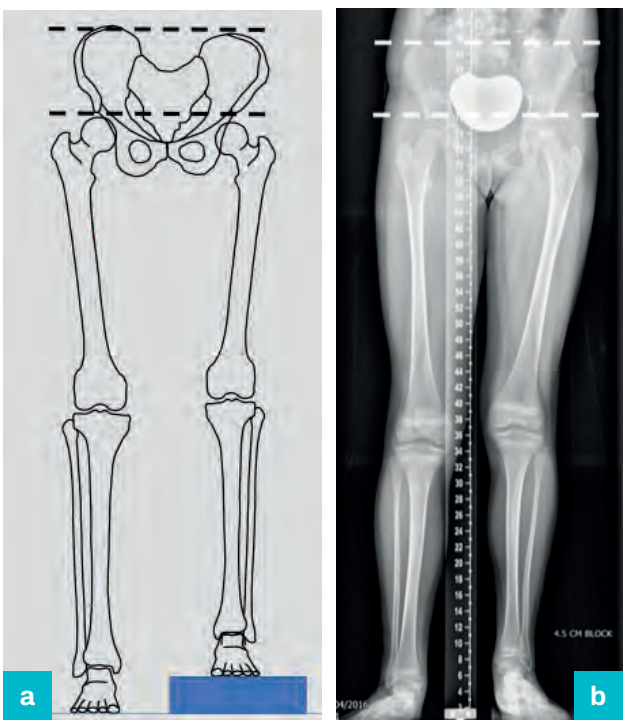

Figure 6.3 (a,b)
Pelvis levelled using blocks under the short leg.

It is also important to include the contribution from the hindfoot, particularly in congenital limb shortening, and this is overlooked if analysis simply measures the long bone lengths (Figure 6.4a,b).

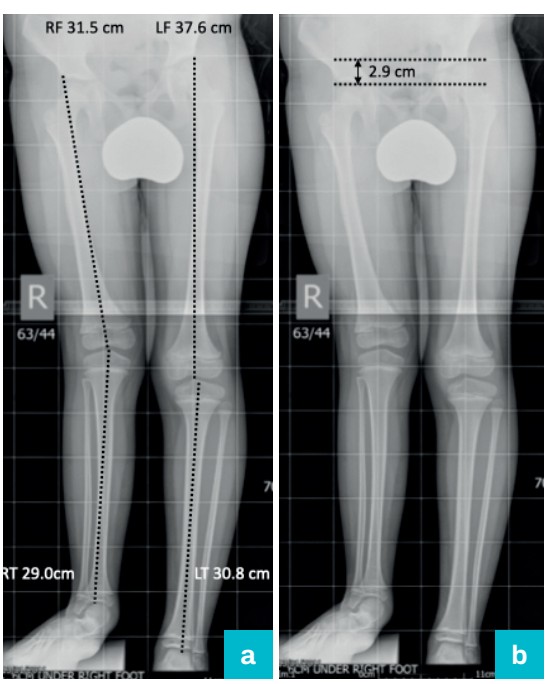

Figure 6.4
(a) Combined femoral and tibial lengths (right 60.5 cm, left 68.4 cm, LLD 7.9 cm).
(b) Accounting for hindfoot shortening (block 6 cm, residual difference 2.9 cm, LLD 8.9 cm).
LLD: leg-length discrepancy.

There is also a potential to underestimate the discrepancy if the iliac blades are used as a reference point if the hemi-pelvis is involved. The true discrepancy is therefore identified by combining the block height and residual difference at the hip.

The thoraco-lumbar spine may also be included to evaluate spinal alignment and simulate the effect of limb length equalisation on these abnormalities (Figure 6.5a,b).

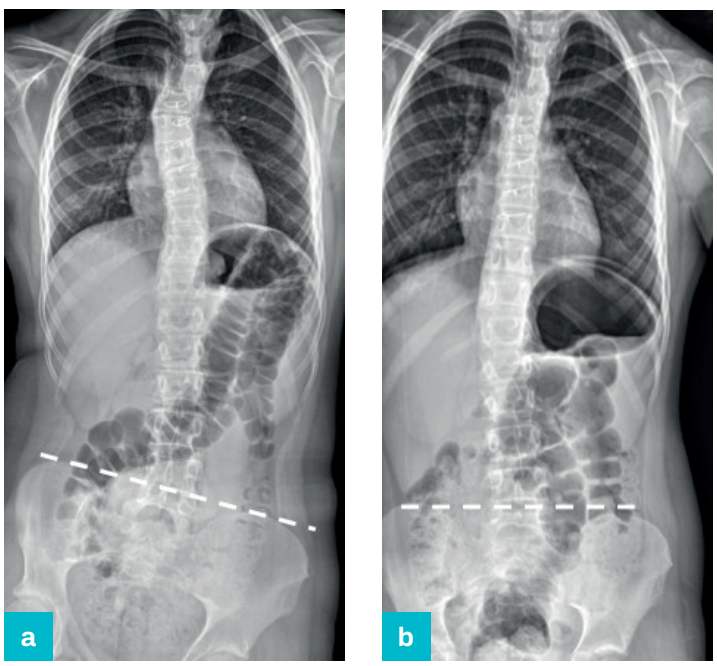

Figure 6.5
(a) Pelvis oblique.
(b) Pelvis level.

Measurement errors

Magnification errors will occur if the distance from the X-ray source to the plate, bone to plate and the location of a ruler or calibration sphere are not standardised. A reference marker placed in front of the patient is magnified and this effect is greater if the marker is out of the plane of the X-ray beam.

Magnification errors will occur if the distance from the X-ray source to the detector and bone to the detector is not standardised. The nearer the beam is to the patient, the greater the magnification error (Figure 6.6).

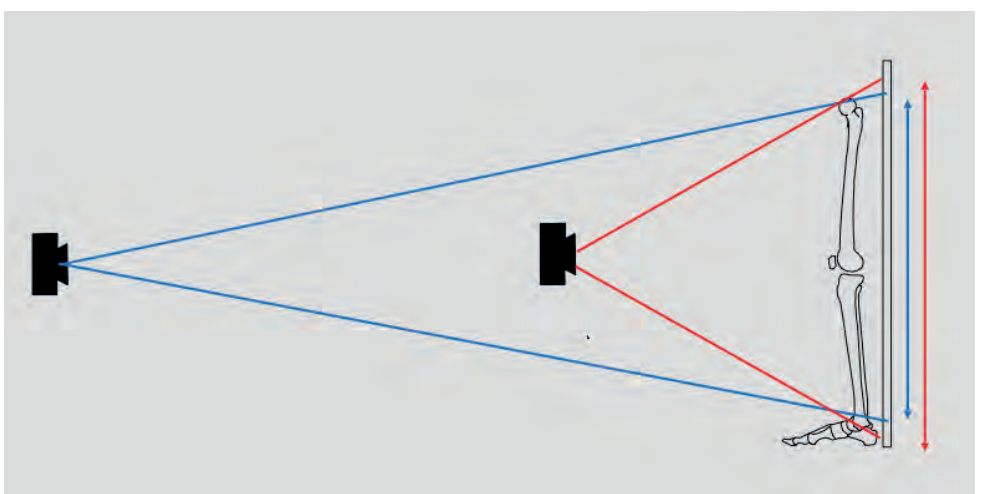

Figure 6.6
The effect of the position of the X-ray source on magnification.

The standing AP radiograph will overestimate shortening if there is a significant sagittal plane deformity, due to a bone abnormality or joint contracture. One of the most common causes is a flexion contracture of the knee leading to foreshortening of the radiographic image. If a flexion contracture has occurred during treatment, the true length can be calculated from measurement of the length of the untreated segment. Lengthening of the tibia can lead to tightness in the gastrocnemius and produce a knee flexion contracture and a foreshortened view on the long leg radiograph. The femur will be foreshortened by a similar amount and calculation of the ratio of pre-operative femoral length to current apparent length will give a multiplier that can be applied to the apparent tibial length (Figure 6.7).

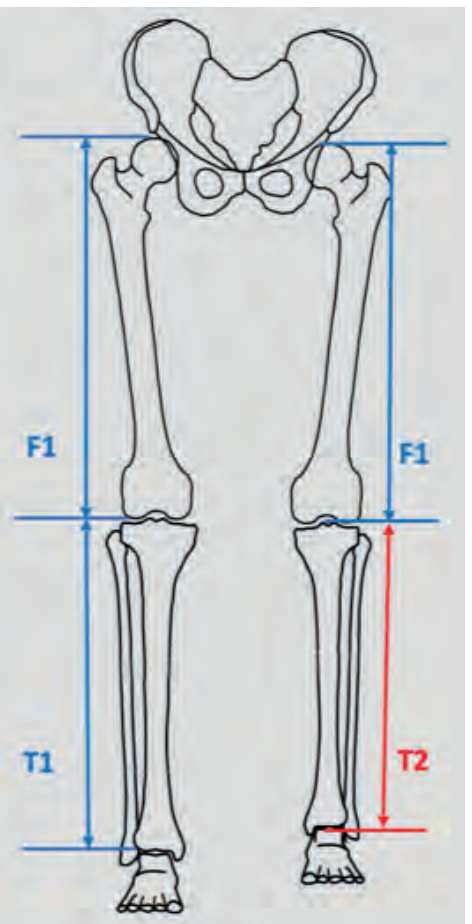

Figure 6.7
Confirmation of equal femoral length on pre-operative radiographs.

Figure 6.8
Calculation of the foreshortening error in fixed knee contracture.

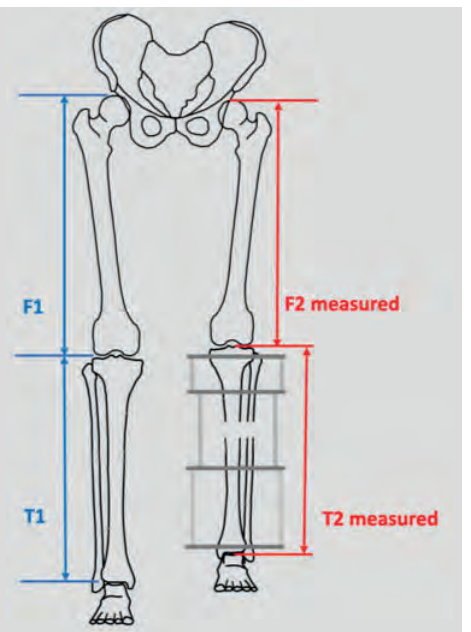

F1/F2 measured = True T2/T2 measured

True T2 = (F1 × T2 measured)/F2 measured

In the example in Figure 6.7, equal femoral lengths are confirmed in the pre-operative radiograph. Tibial lengthening results in a fixed knee contracture, producing a foreshortened image of the left femur and tibia (Figure 6.8). The amount of foreshortening is a function of the degree of knee flexion and will therefore affect each segment equally. The true length can be calculated using simple ratios.

An alternative method of correction uses a simple trigonometric evaluation based on hip and knee flexion angle, but the accuracy decreases with increasing flexion deformity (Figure 6.9).

Figure 6.9 (a,b)
Calculation of true femoral/tibial length.

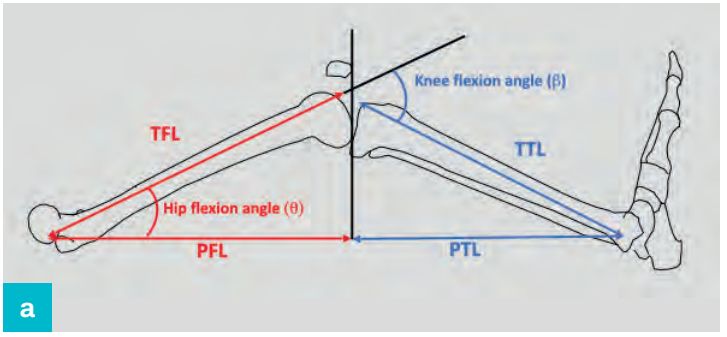

True femoral length (TFL) can be calculated from the projected femoral length (PFL) with the hip flexion angle (θ):

$PFL/TFL = \cos \theta$

$TFL = \cos \theta/PFL$

True tibial length (TTL) can be calculated from the projected tibial length (PTL) with a hip flexion angle θ and knee flexion angle β:

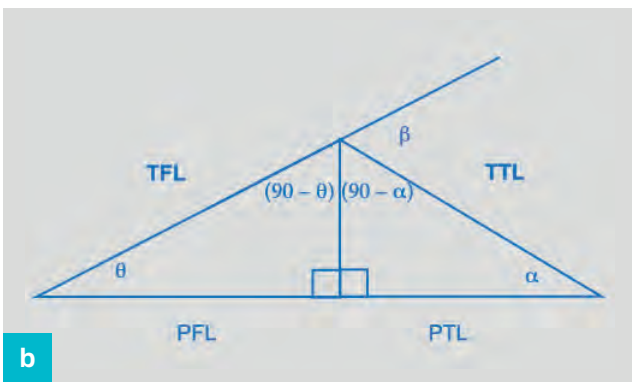

$(90-\theta)+(90-\alpha)+\beta = 180$

$\alpha = \beta - \theta$

$TTL = PTL/\cos\alpha$

The relationship between angular correction and length

Angular deformity in the frontal and lateral plane is inevitably associated with shortening in the axial plane. Correction of angulation with an opening wedge osteotomy will produce lengthening and this can be utilised as part of a strategy to correct shortening (Figure 6.10 a–c). The length gained is a function of the angular deformity and can be calculated by simple trigonometry.

r = length of proximal segment; θ = angular deformity; x = length gain

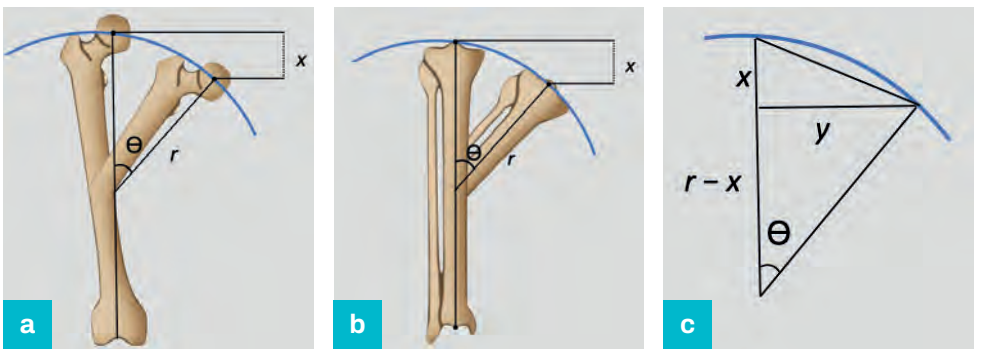

Figure 6.10 (a–c)
Calculation of length gain associated with angular correction.

Length of chord = $2r.\sin[\theta/2]$

$x^2 + y^2 = (2r.\sin[\theta/2])2$ (by Pythagoras)

$(r - x)2 + y2 = r^2$ (by Pythagoras)

$r^2 + x^2 - 2xr + y^2 = r^2$

$x^2 + y^2 = 2xr$

Therefore $2xr = (2r.\sin[\theta/2])^2$

$x = (2r.\sin[\theta/2])^2/2r$

Length increase associated with correction along a transverse bisector

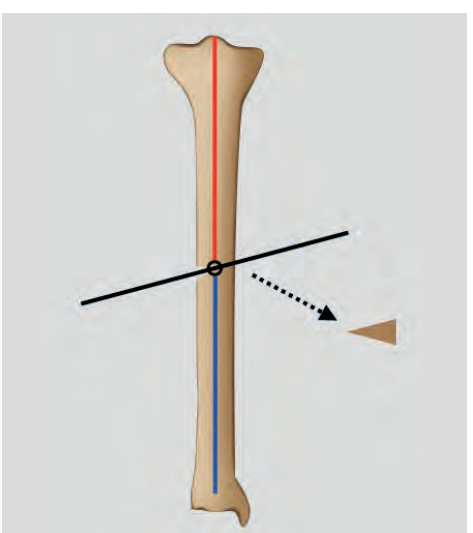

Figure 6.11
Correction at the apex of deformity results in correction of the axis without changing length.

If the correction is centred at the point of intersection of the axis lines, a neutral correction requires resection of the convex corner and will occur with no change in length (Figure 6.11).

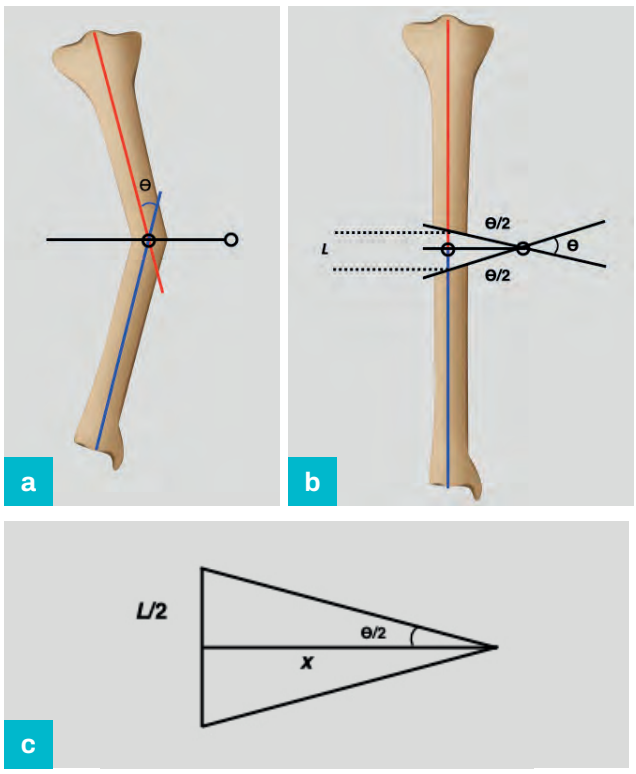

Figure 6.12 (a,b) Correction on the convex side of the transverse bisector line will result in axis correction with lengthening. **(c)** Calculation of the length increase.

If the correction is centred on the convex side of the deformity, correction will produce an opening wedge and add length (Figure 6.12).

The length increase can be calculated by simple trigonometry (Figure 6.12c):

L = increase in length

x = mid-diaphysis–apex distance

θ = deformity

$L/2 = x \tan(\theta/2)$

$L = 2[x \tan(\theta/2)]$

The 'structure at risk'

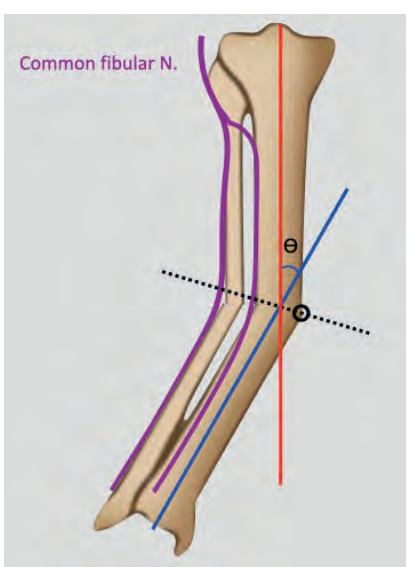

Figure 6.13 The fibular nerve is a structure at risk in correction of tibial valgus.

An appreciation of the increase in length of the neurovascular structures is crucial to avoid injury during deformity correction. This is not usually an issue with femoral correction because of the normal excursion of the sciatic nerve. The common fibular nerve, however, is at risk of neurapraxia with rapid correction of tibial valgus deformity because it is tethered at the neck of the fibula and has a very short excursion (Figure 6.13). The fibula is situated lateral and posterior to the tibia and correction of apex medial (valgus) angulation of the tibia will cause lengthening of both bones.

The degree of lengthening of a 'structure at risk' can be calculated from the distance between the structure and the apex of the angular deformity using simple trigonometry (Figure 6.14a,b).

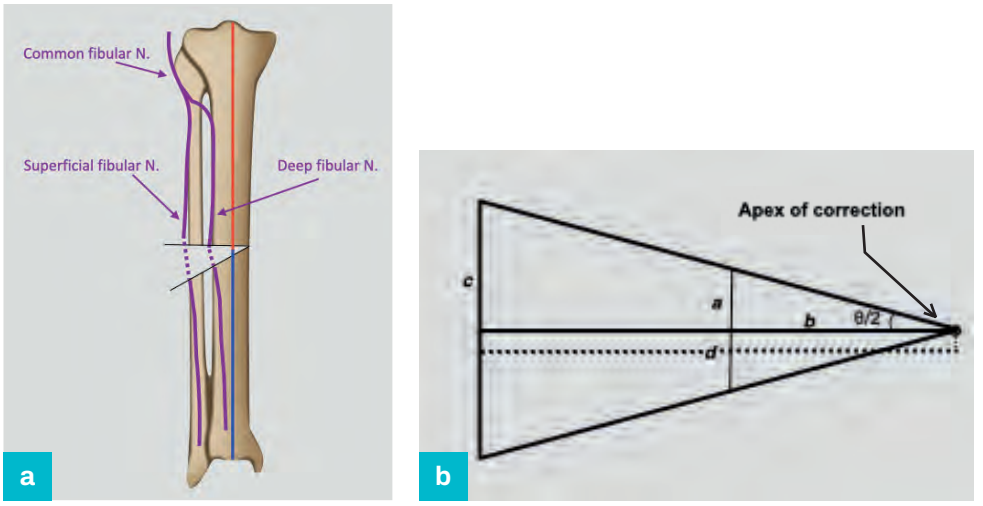

Figure 6.14
(a) Elongation of the fibular nerve associated with correction of valgus tibial deformity.
(b) Calculation of the length increase of a 'structure at risk'.

The opening wedge is composed of two right-angled triangles.

a = increase in length of concave surface/2
b = apex – concave surface
$2c$ = increase in length of structure at risk/2
d = apex – structure at risk

$a/b = c/d = \tan\theta$
$a.d/b = c$

If a is x mm
c = $x.d/b$ m

If the length of the convex cortex increases by x mm, the length of the structure at risk increases by x.(d/b) mm. If the rate of correction produces an increase in length of 1 mm/day at the concave cortex, the structure at risk will elongate at a rate of:

$$\left(\frac{\text{Distance apex of correction to structure at risk}}{\text{Distance apex to concave cortex}}\right) \text{mm/day}$$

The distance to the structure at risk may be increased in an oblique plane deformity. The calculation is identical but must include oblique plane deformity parameters, which are described in Chapter 7. Software-based correction often includes an automated evaluation and modifies the rate of correction to accommodate a structure at risk.

Axial deformity planning

Axial deformity planning requires careful clinical evaluation, combined with a stepwise, systematic evaluation of the available imaging. Magnification and other errors of projection should be identified as a precursor to deformity planning. The relevant segments are initially identified from the long leg radiograph. The mechanical axis of the leg is drawn and measured from the centre of the hip to the centre of the ankle.

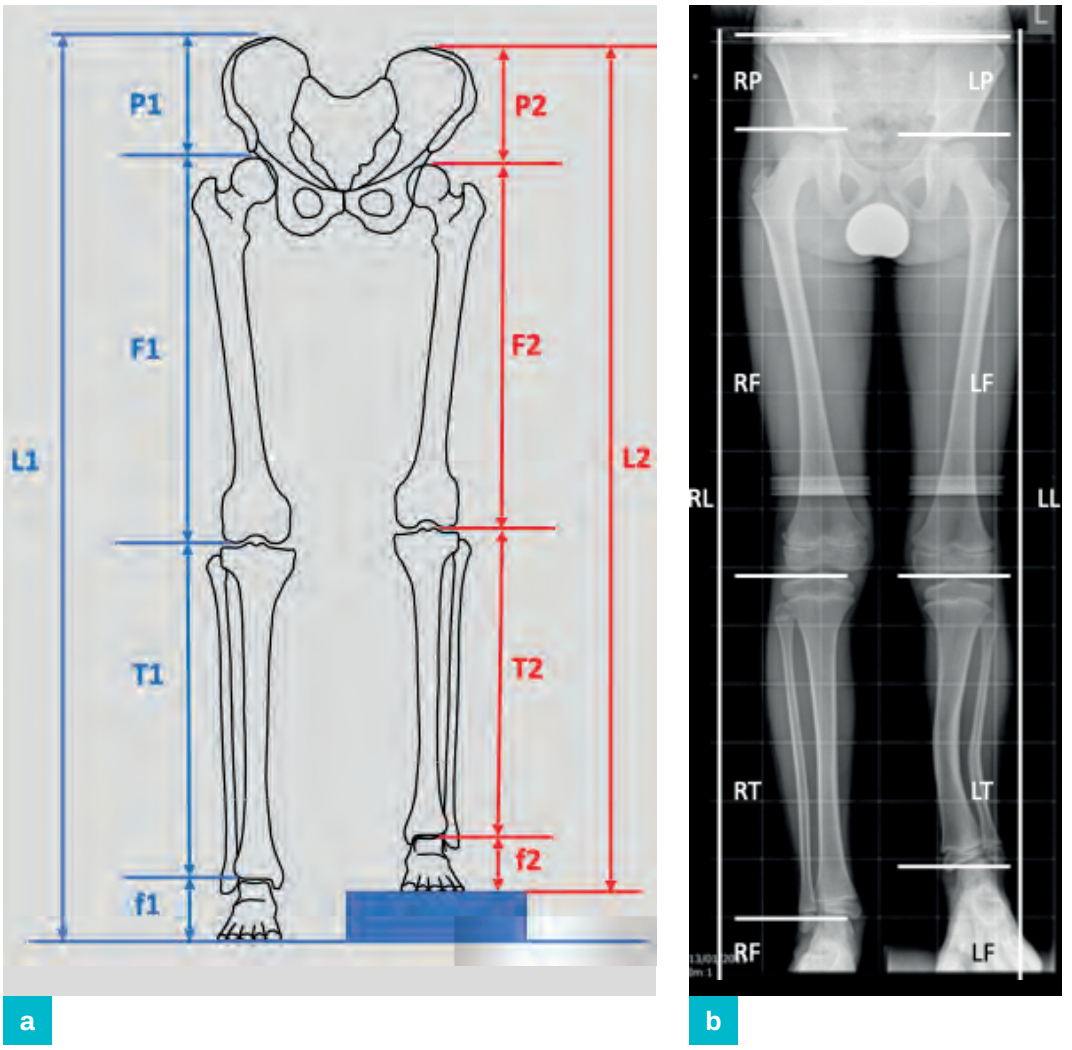

Figure 6.15 (a,b) Total limb length accounting for each anatomical segment.

Measurement of the whole leg from the sole of the foot (ground or top of block) to pelvic brim will determine any other areas of shortening. The contribution of foot height, tibial length, femoral length, pelvic size, and joint contractures should be assessed individually, and recorded separately (Figure 6.15 a,b).

In the skeletally immature patient, there are difficulties associated with incomplete ossification of conventional reference points, in addition to the specifics of the underlying diagnosis. There may be complete or partial failure of formation of key structures, which may require further evaluation with MRI scanning and hip arthrography and examination under anaesthetic may be necessary, particularly in the very young patient (Figure 6.16 a,b).

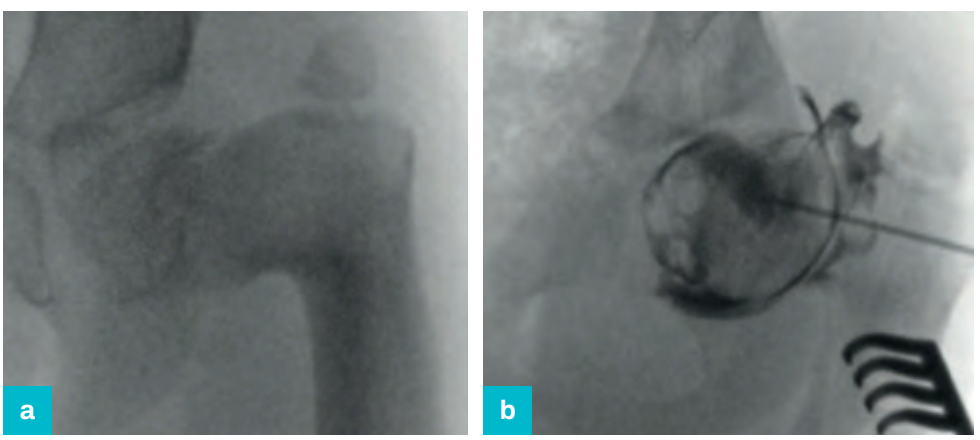

Figure 6.16 (a,b) Arthrogram to define femoral and acetabular morphology in congenital short femur.

This will inform management decisions, which can range from surgical equalisation with growth modulation by epiphysiodesis to complex joint reconstruction with staged surgical lengthening and ablative surgery with prosthetic solutions.

Prediction of future growth

In the immature skeleton, it is important to evaluate leg length discrepancy at presentation, in addition to predicting likely progression with growth. This requires an estimation of future growth and involves determination of current 'bone age', which differs from chronological age in a non-linear manner. This is based on identification of ossification patterns on a plain radiograph of the hand and wrist using the Greulich and Pyle method or Tanner and Whitehouse method or elbow using the Sauvegrain method.

Ultrasound evaluation and automated systems can improve accuracy and reproducibility and estimation based on cervical vertebral growth can also be used but involves greater radiation exposure. These methods provide an estimate of current bone age and therefore growth remaining, but factors including gender, onset of puberty, family history and metabolic disease must also be considered.

Prediction of maturity leg-length discrepancy

Children have an ability to compensate for minor limb-length discrepancies; however, discrepancies greater than 10 mm may cause symptoms in some patients. The general aim of management is to produce functionally equal leg lengths at the time of skeletal maturity and the most efficient surgical method is to arrest longitudinal growth in the peri-pubertal phase with an epiphysiodesis. This is a technically straightforward procedure, but the main difficulty is the determination of the correct time for intervention.
Historic datasets have been used to estimate remaining growth, and calculations are usually based on data collected by Anderson and Green. This involved a semi- longitudinal cohort study of children aged between 5 and 18 years and 84% had contralateral poliomyelitis with measurements taken from the unaffected 'normal' limbs. This is a potentially significant confounding factor and, with the additional effect of improvements in child health and nutrition in the developed world over the last 50 years, there are concerns that these historic datasets are no longer relevant.

Menelaus identified the unpredictability of leg-length discrepancy due to variable pathology and warned against the assumption that the growth inhibition of the short leg or the annual increase in discrepancy of the leg lengths is constant.

Shapiro categorised distinct patterns of growth disturbance that were dependent on the aetiology and identified a linear pattern in congenital lower limb abnormality (Figure 6.17). This allows more accurate prediction for this group and, while estimation using the approaches described in subsequent paragraphs is accepted practice, this should be used with caution in non-linear patterns due to the inherent and unknown inaccuracies.

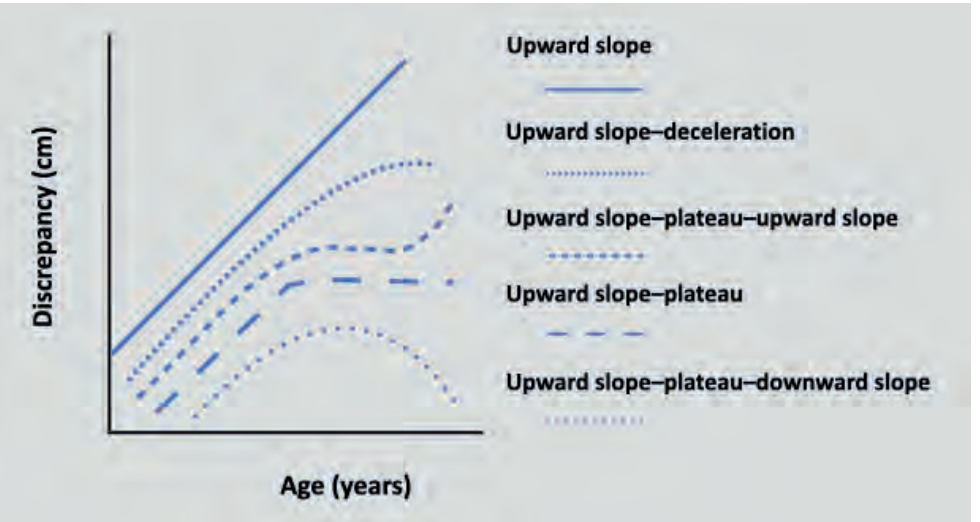

Figure 6.17 Shapiro classification of developmental patterns.

A number of techniques to estimate the leg-length difference at skeletal maturity have been described since the 1940s, each making different assumptions about the available data. There are, however, errors of up to 2 cm in the prediction of final leg length with the Anderson and Green, and Menelaus and Moseley methods.

Moseley's straight-line graph

This method was published by Moseley in 1977. It relies on annual limb radiographs and skeletal age measurements.

The following example (Table 6.1, Figures 6.18–6.20) represents the evaluation of a female patient presenting at an estimated skeletal age of 7, with 2 cm distributed shortening in the left leg. The patient was followed for 3 years with annual evaluation of skeletal age and leg length.

Table 6.1 Example data for application of Moseley's straight-line graph method

Age (years)	7	8	9	10
Right leg (cm)	59.4	63.2	68.8	74.0
Left leg (cm)	57.4	60.5	65.5	70.2

The following stages are required to assess the timing of epiphysiodesis.

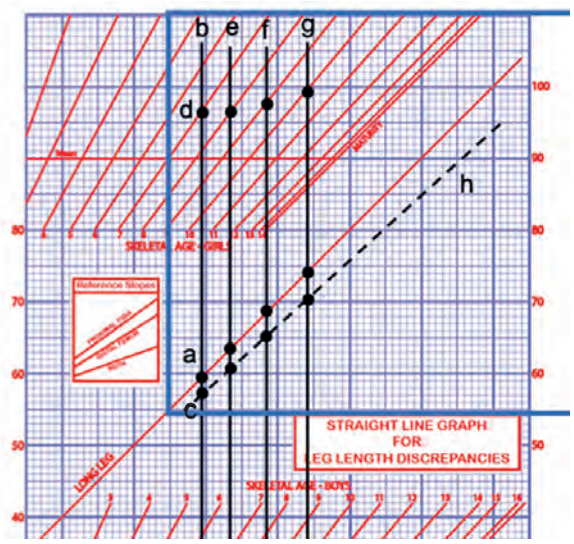

Figure 6.18 Moseley 1: evaluation of past growth.

1 *Evaluation of past growth* (Figure 6.18)

- **a** The point representing the length of the long leg is plotted on the 'long-leg line'.
- **b** A vertical line is drawn at this point.
- **c** The point representing the length of the short leg is plotted on the vertical line.
- **d** Skeletal age is marked on the appropriate nomogram.
- **e–g** Identical steps are repeated at each clinical evaluation.
- **h** The line of best fit is drawn through the short-leg points, to represent growth of this leg.

2 *Prediction of future growth* (Figure 6.19)

- **i** The line of best fit is drawn for the skeletal age points, representing the growth percentile.
- **j** A vertical line is drawn at the point of intersection with the maturity line, representing the end of growth.

The points of intersection of the two growth lines represent the predicted leg lengths and leg-length discrepancy at maturity.

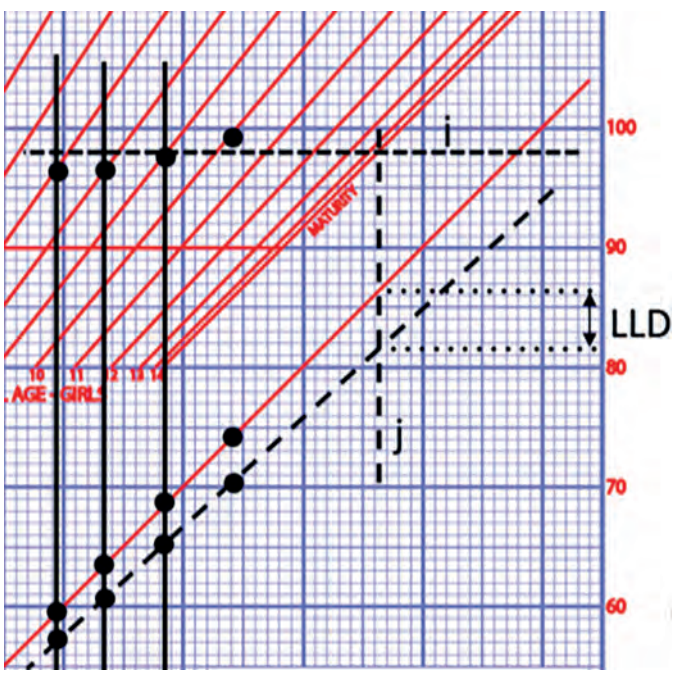

Figure 6.20 Moseley 2: prediction of future growth.

3 *Prediction of the effect of surgery* (Figure 6.20)

The effect of epiphysiodesis is simulated by a series of lines, drawn parallel to reference lines:

k Distal femur and proximal tibia.

l Proximal tibia.

m Distal femur.

n The growth trajectory is altered by distal femoral epiphysiodesis at the time of the most recent evaluation to equalise limb lengths at skeletal maturity.

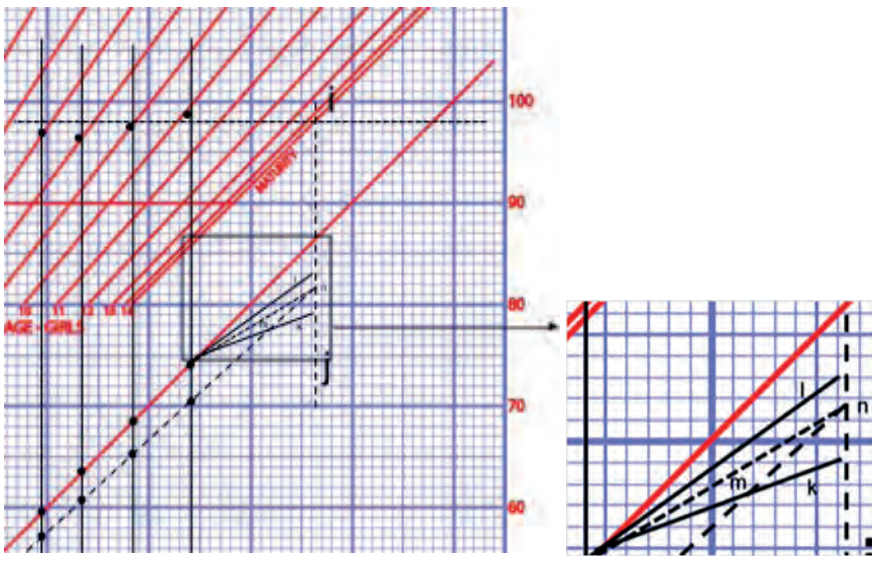

Figure 6.20
Moseley 3: prediction of the effect of surgery.

The effect of lengthening (not illustrated) is simulated by drawing a line parallel to the short leg line, separated by the planned gain in length.

The arithmetic method

Menelaus described a non-graphical arithmetic method, which was based on clinical measurements and not reliant on radiology. The fundamental assumption was that boys reach skeletal maturity at 16 years, girls at 14 years and that the distal femur (10 mm) and proximal tibia (6 mm) predictably contribute to longitudinal growth in patients older than 8 years. This was the basis for an alternative graphic method of prediction described by Eastwood and Cole (Eastwood DM 1995).

Table 6.2
Example data for application of the Eastwood and Cole arithmetic method

The following example (Table 6.2, Figures 6.21–6.22) considers a male patient presenting at a chronological age of 5, with 2.7 cm distributed shortening in the right leg. The patient was followed annually for 3 years with clinical evaluation of leg-length discrepancy.

Age (years)	5	6	7	8
Leg-length discrepancy	2.7	3.0	3.3	3.6

The following stages are required to assess the timing of epiphysiodesis, using the Eastwood and Cole graph.

1 *Prediction of future growth* (Figure 6.21)

a–d The clinically measured limb length discrepancy is plotted against chronological age at each visit.

e The line of best fit is constructed and extended.

f A vertical line is drawn at $x = 16$ years to represent the expected age of male skeletal maturity.

g Maturity leg-length discrepancy.

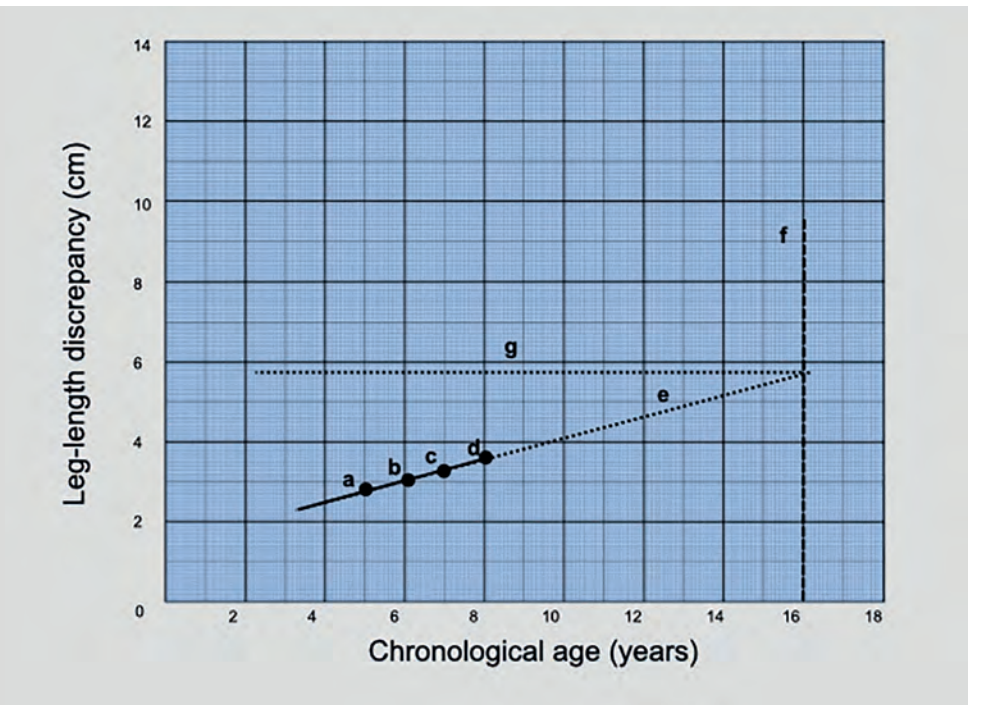

Figure 6.21
Eastwood and Cole 1: prediction of future growth.

2 *Prediction of the effect of surgery* (Figure 6.22)

The effect of epiphysiodesis is simulated by a series of lines, drawn parallel to reference lines:

h Distal femur and proximal tibia.

i Proximal tibia.

j Distal femur.

The growth trajectory is altered by distal femoral epiphysiodesis aged 9 years 4 months (k), or combined distal femoral and proximal tibial epiphysiodesis aged 12 years (l) to equalise limb lengths at skeletal maturity. Tibial epiphysiodesis (m) would have been necessary aged 6 years and is no longer relevant.

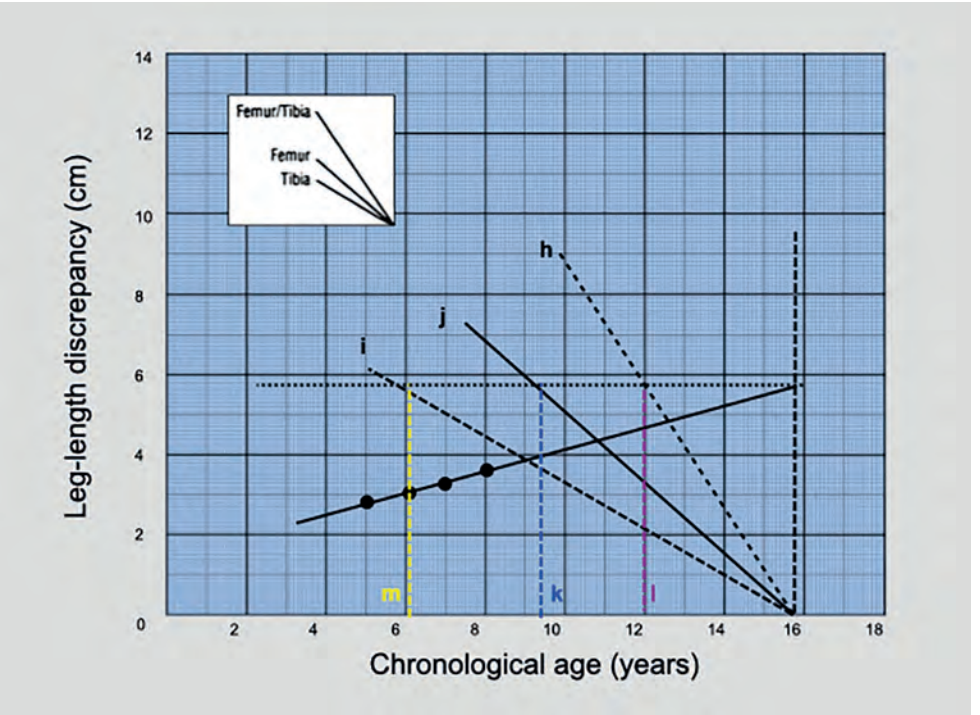

Figure 6.22
Eastwood and Cole 2: prediction of the effect of surgery.

The multiplier method

Recent improvements in methods of calculation have been based on more sophisticated mathematical algorithms, but the quality of the original data remains the rate-limiting step. The multiplier method described by Aguilar and Paley is regarded as the most sophisticated and accurate method of evaluation. This is, however, associated with a mean error of 1.1 cm in the individual evaluation of the lengths of the tibia and femur.

Leg-length multiplier = *L*m/*L*
Where *L*m = predicted leg length at skeletal maturity
L = leg length at their current age

The method uses tables representing the annual multipliers for males and females and the calculation relies on clinical evaluation of individual segment lengths and the chronological age. Table 6.3 shows lower-limb multipliers.

Figure 6.23
Leg-length discrepancy in 7-years 5-month-old boy.

The leg-length discrepancy in the example of a 7 years 5-month-old male in Figure 6.23) is 2.9 cm + block height of 6 cm under right foot = 8.9 cm. Using the multiplier from the table for a boy of this age:

*L*m = 8.9 × 1.52 = 13.5 cm

The predicted maturity discrepancy is therefore 13.5 cm and this allows planning for leg equalisation with 5 cm femoral lengthening now, a second 5 cm femoral lengthening aged 10–13 years and a distal femoral epiphysiodesis aged 13.

Separate tables are available for tibia, femur, upper limb, achondroplasia and height. A multiplier app is available as a free download.

Table 6.3
Lower-limb multipliers for boys and girls

Age (years + months)	Multiplier	
	Boys	Girls
Birth	5.080	4.630
0 + 3	4.550	4.155
0 + 6	4.060	3.725
0 + 9	3.600	3.300
1 + 0	3.240	2.970
1 + 3	2.975	2.750
1 + 6	2.825	2.600
1 + 9	2.700	2.490
2 + 0	2.590	2.390
2 + 3	2.480	2.295
2 + 6	2.385	2.200
2 + 9	2.300	2.125
3 + 0	2.230	2.050
3 + 6	2.110	1.925
4 + 0	2.000	1.830
4 + 6	1.890	1.740
5 + 0	1.820	1.660
5 + 6	1.740	1.580
6 + 0	1.670	1.510
6 + 6	1.620	1.460
7 + 0	1.570	1.430
7 + 6	1.520	1.370
8 + 0	1.470	1.330
8 + 6	1.420	1.290
9 + 0	1.380	1.260
9 + 6	1.340	1.220
10 + 0	1.310	1.190
10 + 6	1.280	1.160
11 + 0	1.240	1.130
11 + 6	1.220	1.100
12 + 0	1.180	1.070
12 + 6	1.160	1.050
13 + 0	1.130	1.030
13 + 6	1.100	1.010
14 + 0	1.080	1.000
14 + 6	1.060	NA
15 + 0	1.040	NA
15 + 6	1.020	NA
16 + 0	1.010	NA
16 + 6	1.010	NA
17 + 0	1.000	NA

References

Aguilar JA, Paley D, Paley J et al. (2005). Clinical validation of the multiplier method for predicting limb length at maturity, part I. J Pediatr Orthop 25(2): 186–191.

Eastwood DM, Cole WG. (1995). A graphic method for timing the correction of leg-length discrepancy. J Bone Joint Surg Br 77(5): 743–747.

Moseley CF. (1977). A straight-line graph for leg-length discrepancies. J Bone Joint Surg Am 59(2): 174–179.

Shapiro F. Developmental patterns in lower-extremity length discrepancies. J Bone Joint Surg Am. 1982 Jun; 64(5): 639–51).

Westh RN, Menelaus MB. (1981). A simple calculation for the timing of epiphysial arrest: a further report. J Bone Joint Surg Br. Feb; 63-B (1):117–9.

KEYPOINTS

- Radiological evaluation involves plain radiographs, CT and stereo-radiography
- Radiological evaluation includes the spine, pelvis and foot
- Measurement errors associated with magnification and relative foreshortening
- Length change associated with angular correction
- The ‘structure at risk’
- Patterns of growth
- Prediction of future growth

CHAPTER

7

The oblique plane

Bilal Jamal and Simon Royston

Introduction

Radiological evaluation is based on bi-planar imaging, which by convention is assessed with antero-posterior (AP) and lateral radiographs. These are representative of a deformity that often exists in a separate, oblique plane. There are difficulties associated with visualising this pattern of deformity as it requires a fundamental change in the perception of three-dimensional space. The introduction of hexapod fixators, with virtual hinges and software-based analysis, has made calculation of the magnitude and orientation of this plane less important. Understanding the conceptual and mathematical basis for the oblique plane is, however, crucial for analysis and correction of long bone deformity and this chapter will provide practical instruction on methods in common use.

Radiology of the oblique plane

Identification and description of long bone deformity in the frontal and lateral planes have been considered in Chapter 4 and 5.

A pure apex medial (valgus) or apex lateral (varus) deformity exists exclusively in the frontal plane. An X-ray beam directed along this plane will produce a lateral radiograph, which will demonstrate normal alignment. An AP radiograph is perpendicular to the plane of this deformity and will demonstrate the extent of deformity.

A pure apex anterior (procurvatum) or apex posterior (recurvatum) deformity exists exclusively in the lateral plane. An X-ray beam directed along this plane will produce an AP radiograph, which will demonstrate normal alignment. A lateral radiograph is perpendicular to the plane of this deformity and will demonstrate the extent of deformity.

Deformity usually exists in a single oblique plane that is neither frontal nor lateral, with components that are seen seperately by AP and lateral radiographs.

The following example illustrates a right tibial diaphyseal deformity (Figures 7.1–7.4). Conventional radiographs demonstrate 30° apex medial and 35° apex anterior components (Figures 7.1a,b and 7.2a,b respectively).

This is incorrectly referred to as a bi-planar deformity because there is only one deformity, which occurs in an oblique plane.

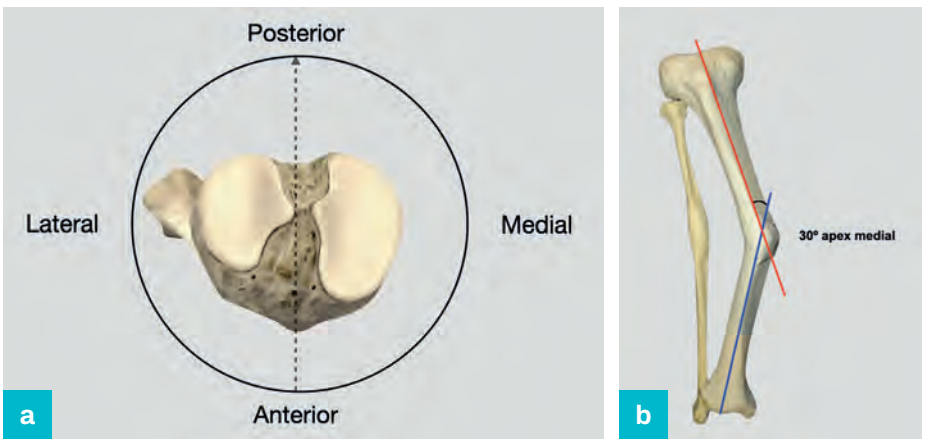

Figure 7.1 (a,b) AP view demonstrating 30° apex lateral deformity.

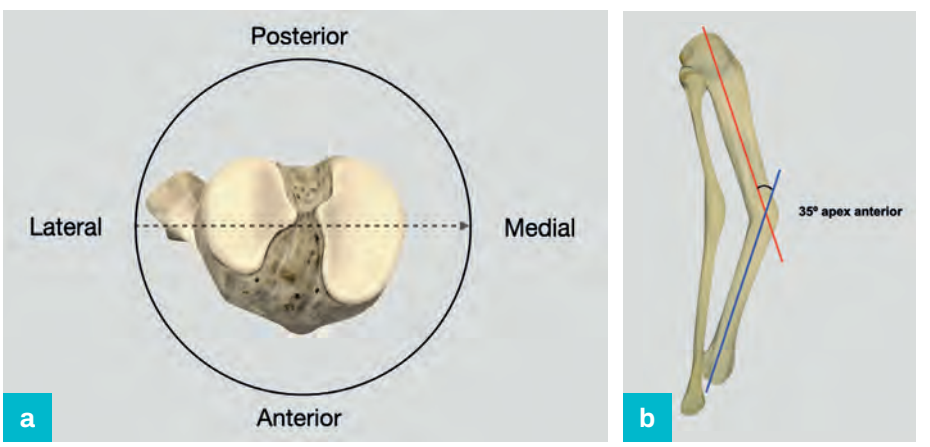

Figure 7.2 (a,b) Lateral view demonstrating 35° apex anterior deformity.

A radiograph that is in the plane of the deformity will eliminate the deformity. (Figure 7.3a,b).

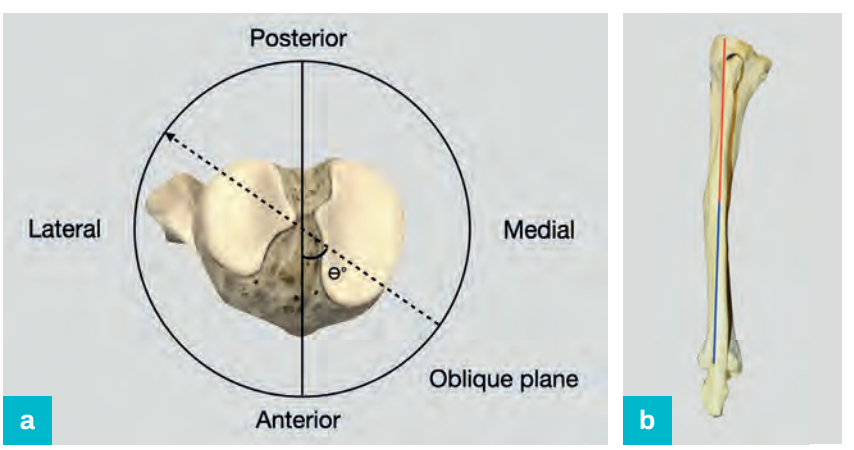

Table 7.3 (a,b) Oblique plane view, demonstrating no apparent deformity. The angle Θ°, between this view and the true AP view represents the orientation of the single oblique plane

A radiograph taken perpendicular to this plane demonstrates the maximum deformity, which is greater than that demonstrated in either the AP or lateral projection. This also represents the correction axis for an externally applied hinge (Figure 7.4a,b).

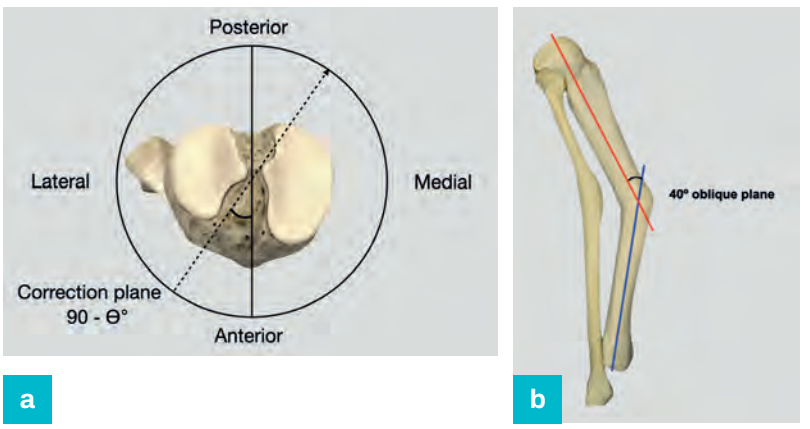

Figure 7.4 (a,b) Orthogonal view demonstrates a 40° deformity.

Radiographic method of description of an oblique plane deformity

The most straightforward method of demonstrating an oblique plane deformity is by direct visualisation, using radiographs orientated in the oblique plane. This can be conducted with either an awake patient in a fluoroscopy suite or an anaesthetised patient with an image intensifier. It provides a straightforward method of peri-operative assessment, particularly for correction using fixed hinges.

The limb is placed in a true AP position, with the patella facing forwards and produces an AP radiograph (Figure 7.5a–c).

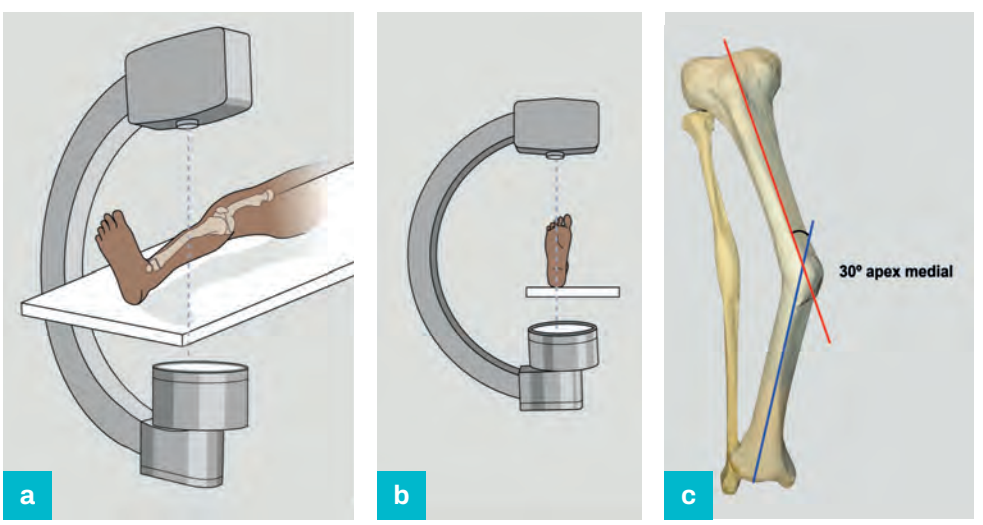

Figure 7.5 (a–c) True AP view.

The C-arm is rotated to eliminate the deformity and the orientation of the C-arm represents the oblique plane (Figure 7.6a–c).

Figure 7.6 (a–c)
Oblique plane view.

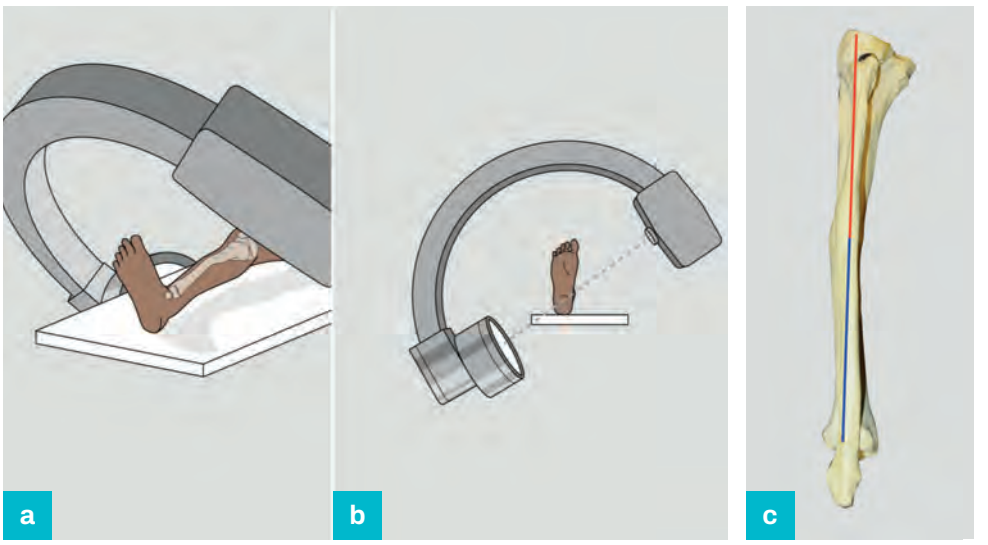

If the C-arm is rotated by 90°, the true deformity will be demonstrated and is also the axis of correction using a physical hinge (Figure 7.7a–c).

Figure 7.7 (a–c)
Orthogonal view.

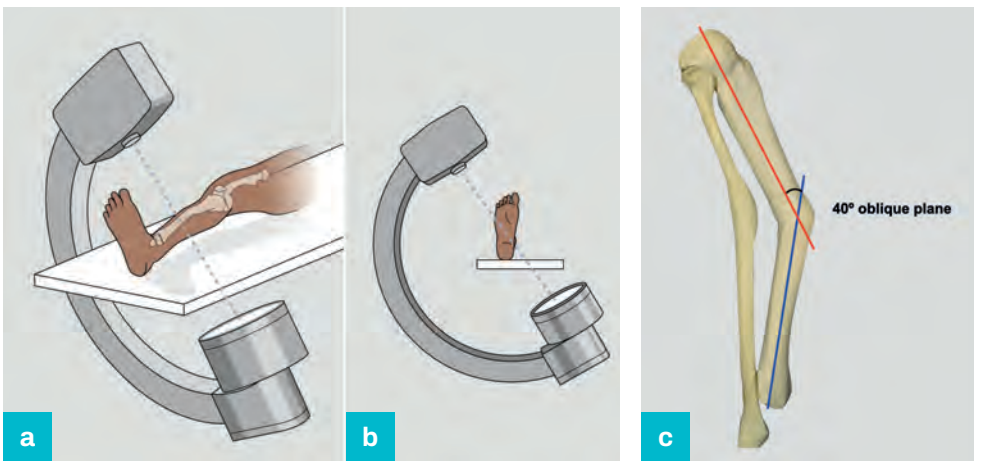

Defining an oblique plane angular deformity

The characteristics of an oblique plane angular deformity can be estimated by a simple graphic method or calculated with an approach that requires no more than a basic understanding of the geometry of right-angled triangles (Figure 7.8).

Figure 7.8
Geometry of right-angled triangles.

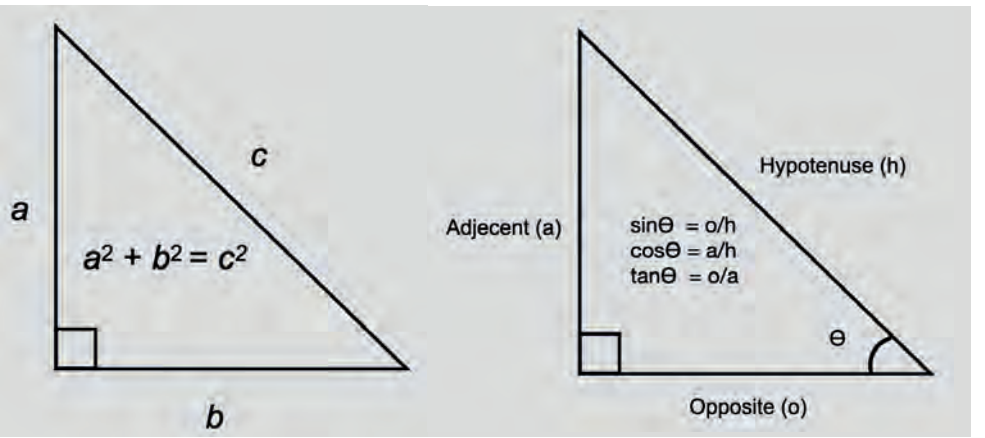

Graphic method

A graph is constructed with the x-axis representing the frontal plane and the y-axis representing the lateral plane and each is identified by the direction of the apex of angulation. The grids for left and right legs are mirror images and orientated to represent the appearance looking from the knee to the foot (Figure 7.9).

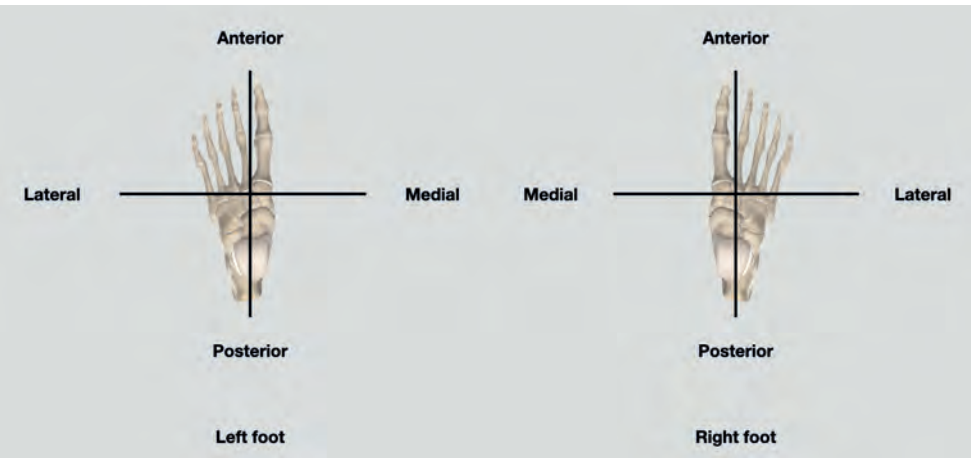

Figure 7.9
Axes representing left and right legs.

The magnitude of angulation measured on the AP (x-axis) and lateral (y axis) are marked, with 1 mm representing 1°, drawn in the direction that corresponds to the apex of angulation.

Example 1 (Figure 7.10)

This example considers a right 20° apex lateral / 25° apex anterior tibial deformity and 1 mm = 1° (Figure 7.10a). A 20 mm line is therefore drawn along the 'lateral' part of the x-axis and a 25 mm line is drawn along the 'anterior' part of the y-axis.

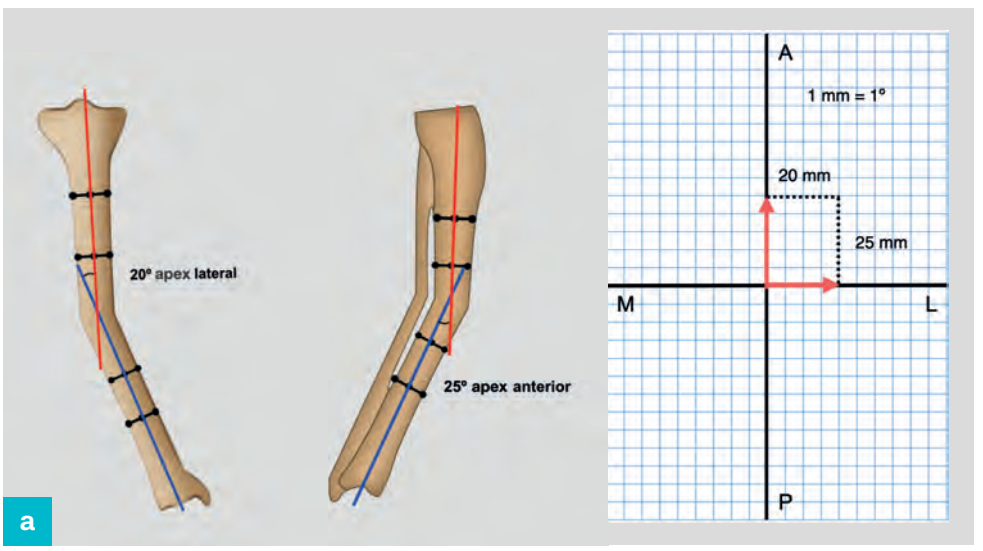

Figure 7.10 (a–c)
Analysis of a right 20° apex lateral / 25° apex anterior tibial deformity.

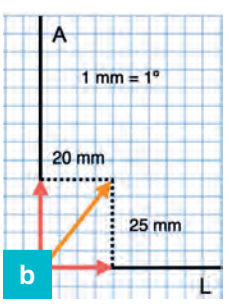

These two lines represent adjacent sides of a rectangle, which is completed with two additional lines. A line is drawn from the origin to the diagonally opposite point on this rectangle. The length of the diagonal represents the magnitude and the angle Θ, to the x-axis, describes the plane of deformity (Figure 7.10b).

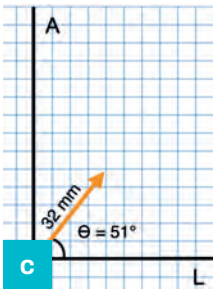

Each square represents 5 mm, 1 mm is equivalent to 1°, the true magnitude of the deformity measures 32 mm and is therefore 32°.

The angle Θ represents the direction of the deformity in relation to the lateral plane and measures 51° (Figure 7.10c).

The true deformity therefore has a magnitude of 32°and is orientated 51° to the lateral plane.

Trigonometric method

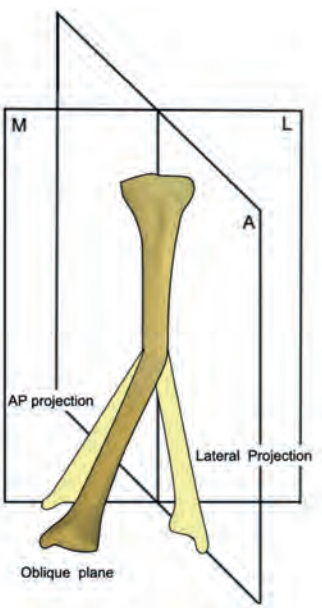

Figure 7.11
Schematic representing the AP and lateral projections of an oblique plane deformity.

Orthogonal radiographs of an oblique plane deformity will produce AP and lateral projections of the true deformity (Figure 7.11). The deformity measured from each projection can be used to calculate the magnitude and direction of an oblique plane deformity.

These projections are represented by right-angled triangles in each of the AP, lateral and oblique planes (Figure 7.12).

- The deformity in the AP plane is represented by angle AP.
- The deformity in the lateral plane is represented by angle Lat.
- The deformity in the oblique plane is represented by angle Obl, and the orientation of the oblique plane, with reference to the frontal plane, is represented by angle α (Figure 7.12b).

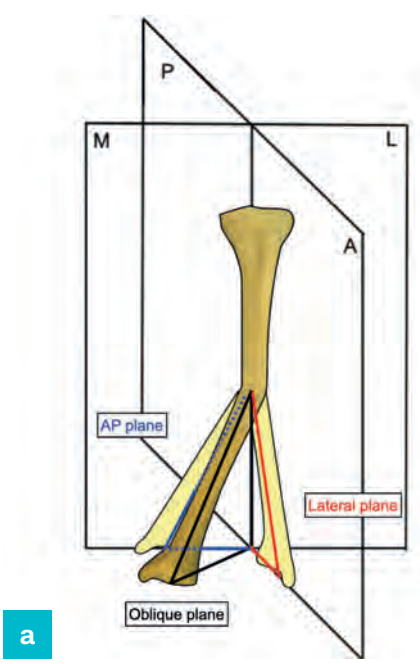

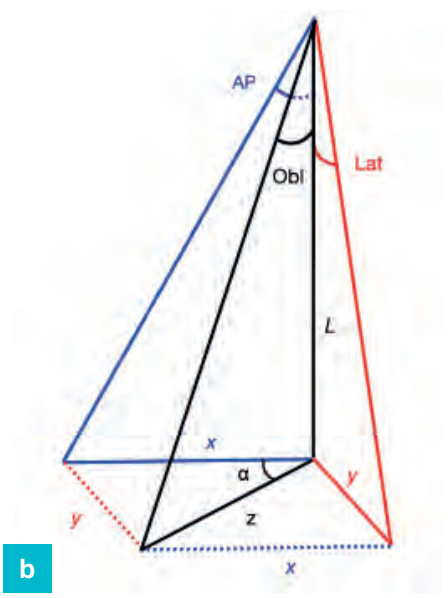

Figure 7.12 (a,b)
The components of the deformity are represented by three right-angled triangles.

$\tan(AP) = x/L$
$x = \tan(AP) \times L$
$\tan(Lat) = y/L$
$y = \tan(Lat) \times L$
$\tan \alpha = y/x$
$= \frac{\tan(Lat) \times L}{\tan(AP) \times L}$
$\alpha = \tan^{-1} \frac{\tan(Lat)}{\tan(AP)}$

This represents the orientation of the oblique plane, with reference to the lateral plane.

$z^2 = x^2 + y^2$ (by Pythagoras)
$z^2 = \tan^2(AP) \times L^2 + \tan^2(Lat) \times L^2$
$z^2 = L^2 \times (\tan^2(AP) + \tan^2(Lat))$
$z^2/L^2 = (\tan^2(AP) + \tan^2(Lat))$
$\tan(Obl) = z/L$
$\tan^2(Obl) = z^2/L^2$
$\tan^2(Obl) = (\tan^2(AP) + \tan^2(Lat))$
$Obl = \tan^{-1}\sqrt{(\tan^2(AP) + \tan^2(Lat))}$

This represents the magnitude of deformity in the oblique plane.

Example 1: Complete trigonometric method

AP deformity = 20°
tan(AP) = 0.364
Lateral deformity = 25°
tan(Lat) = 0.466

Magnitude
$= \arctan \sqrt{(\tan^2(AP) + \tan 2(Lat))}$
$= \arctan \sqrt{((0.364)^2 + (0.466)^2}$
$= \arctan \sqrt{(0.132 + 0.217)}$
$= \arctan \sqrt{0.349}$
$= \arctan 0.591$
30.6°

Orientation
$= \arctan (\tan(Lat)/\tan(AP))$
$= \arctan (\tan 25/\tan 20)$
$= \arctan (0.446/0.364)$
$= \arctan (1.225)$
50.8°

Example 2 (Figure 7.13)

This example considers a right 30° apex medial / 40° apex posterior tibial deformity and 1 mm = 1° (Figure 7.13a). A 30 mm line is therefore drawn along the 'medial' part of the x-axis and a 40 mm line is drawn along the 'posterior' part of the y-axis and the adjacent sides of a rectangle are inserted.

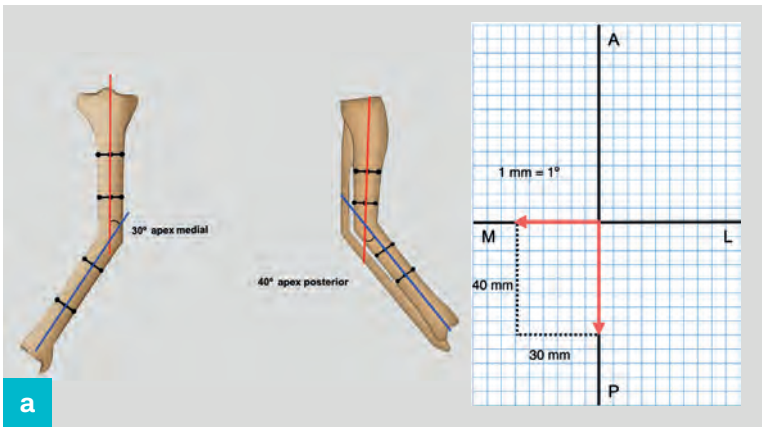

Figure 7.13 (a–c) Analysis of a right 30° apex medial / 40° apex posterior tibial deformity.

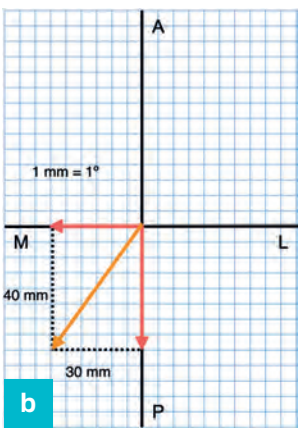

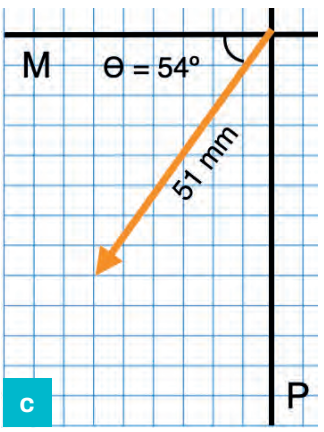

A line is drawn from the origin to the point diagonally opposite on this rectangle (Figure 7.13b).

Each square represents 5 mm and1 mm is equivalent to 1°. The true magnitude of the deformity measures 51 mm and is therefore 51°.

The angle Θ between the diagonal and the x-axis measures 54° (Figure 7.13c).

The true deformity therefore has a magnitude of 51° and is orientated at 54° to the lateral plane.

Example 2: Complete trigonometric method

AP deformity = 30°
tan(AP) = 0.577
Lateral deformity = 45°
tan(Lat) = 1

Magnitude = arctan $\sqrt{(\tan^2(AP) + \tan^2(Lat))}$
= arctan $\sqrt{(0.577)^2 + (1)^2}$
= arctan $\sqrt{(0.333 + 1)}$
= arctan $\sqrt{1.333}$
= arctan 1.155
49.1°

Orientation = arctan (tan(*Lat*)/tan(*AP*))
= arctan (1/0.577)
= arctan 1.733
60.0°

Example 3 (Figure 7.14)

This considers a left 15° apex medial / 45° apex posterior tibial deformity and 1 mm = 1°. Note that the lateral axis lines are reversed (Figure 7.14a). A 15 mm line is therefore drawn along the 'medial' part of the x-axis and a 45 mm line is drawn along the 'posterior' part of the y-axis and the adjacent sides of a rectangle are inserted.

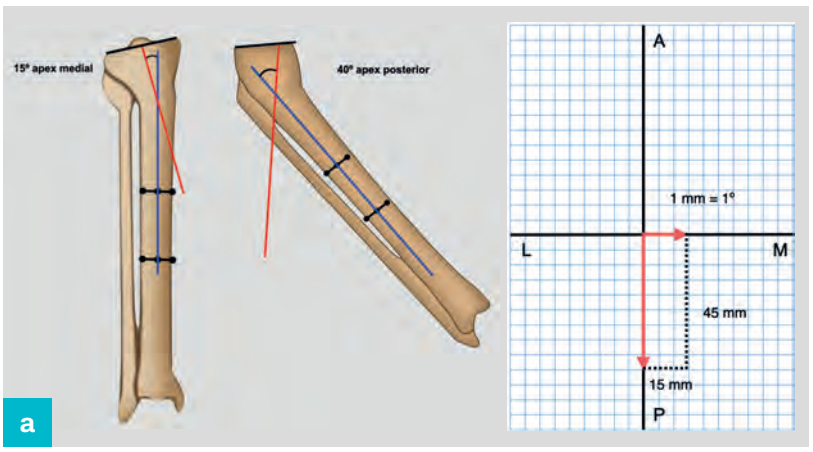

Figure 7.14 (a–c)
Analysis of a left 15° apex medial / 45° apex posterior tibial deformity.

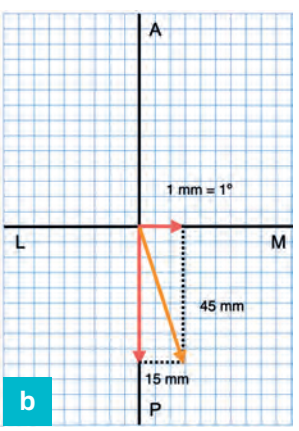

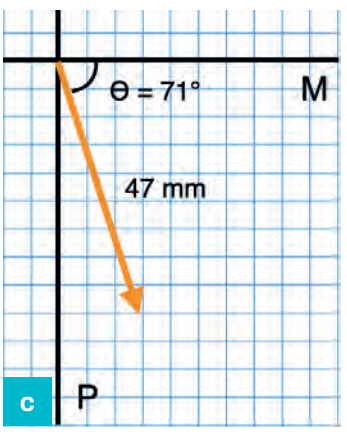

A line is drawn from the origin to the point diagonally opposite on this rectangle (Figure 7.14b).

Each square represents 5 mm and 1 mm is equivalent to 1°. The true magnitude of the deformity measures 47 mm and is therefore 47°.

The angle Θ between the diagonal and x-axis measures 71° (Figure 7.14c).

The true deformity therefore has a magnitude of 47° and is orientated 71° to the lateral plane.

Example 3: Complete trigonometric method

AP deformity = 15°
tan(AP) = 0.268
Lateral deformity = 45°
tan(Lat) = 1

Magnitude = arctan $\sqrt{(\tan^2(AP) + \tan^2(Lat))}$
= arctan $\sqrt{(0.268)^2 + (1)^2}$
= arctan $\sqrt{(0.072 + 1)}$
= arctan $\sqrt{1.072}$
= arctan 1.035
45.0°

Orientation = arctan 1/(0.268)
= arctan 3.731
75.0°

Variance between graphic and trigonometric methods

The graphic method has the advantage of simplicity but makes assumptions that are inaccurate with larger angular deformities. Oblique plane formulae are based on tangents, which increase in an approximately linear pattern from 0 to 45°. A graphic approximation can therefore be used without clinically important error for deformity <45° in either plane. The estimated deformity parameters compared to those derived from the more accurate trigonometric method in the series of tibial deformities detailed in the examples above illustrates this variance (Table 7.1).

Tibia deformity	Graphic (°)	Trigonometric (°)
Example 1		
Magnitude	32	30.6
Orientation	51	50.8
Example 2		
Magnitude	51	49.1
Orientation	54	60.0
Example 3		
Magnitude	47	45.0
Orientation	71	75.0

Defining a translation deformity

Graphic method

Translation is described as displacement of a distal segment relative to the proximal segment. Spinal deformity is described in reverse as is deformity proximal to the humeral and femoral neck, and this is relevant to the description of the slipped epiphysis. A graphic method, identical to angular deformity, can also be used to determine translation in an oblique plane.

A graph is constructed with the x-axis representing the frontal plane and the y-axis representing the lateral plane. Each axis is labelled to correspond to the direction of translation. The grids for left and right legs are mirror images and orientated to represent the appearance looking from the knee to the foot.

The magnitude of translation measured on the AP (x-axis) and lateral (y-axis) is marked, with 1 mm being equivalent to 3 mm translation. This is drawn in a direction that corresponds to the direction of translation.

The example in Figure 7.15 represents a right tibia with 24 mm lateral / 21 mm posterior translation. A line is drawn to scale along the 'lateral' part of the x-axis and the 'posterior' part of the y-axis. These two lines represent adjacent sides of a rectangle, which is completed with two additional lines (Figure 7.15a).

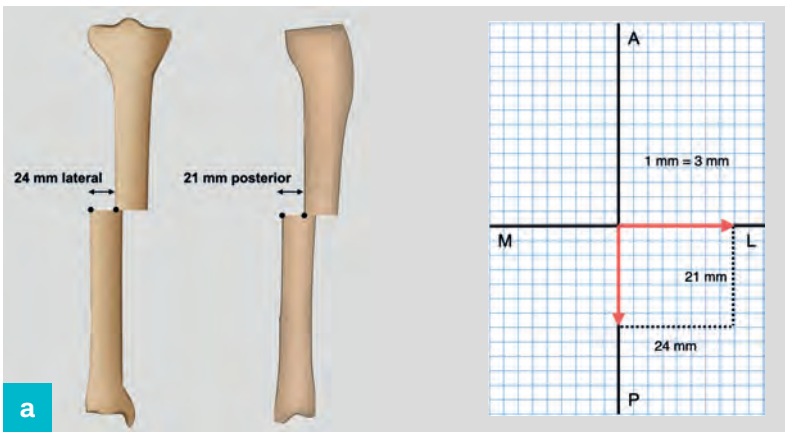

Figure 7.15 (a–c) Analysis of a 24 mm lateral / 21 mm posterior translation deformity of the right tibia.

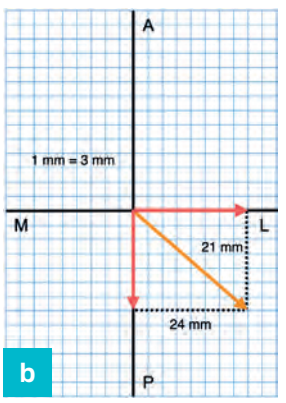

A line is then drawn from the origin to the point diagonally opposite on this rectangle (Figure 7.15b).

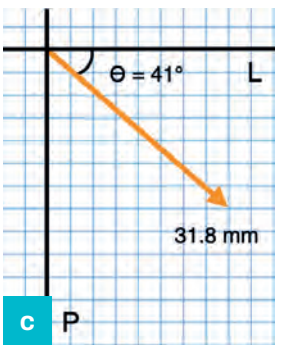

The length of this diagonal represents the magnitude of translation in the oblique plane. In Figure 7.15c, each 1 mm square represents 3 mm translation and in this example measures 10.6 mm. The true magnitude of the deformity is therefore 31.8 mm.

The angle Θ, between the arrow representing the magnitude of the deformity and the y-axis, is measured. This represents the relationship of the deformity to the lateral plane and measures 41°.

Simultaneous correction of angulation and translation

Radiological images, presented in standard AP and medio-lateral planes, are simple representations of bone segments in 3D space. Accurate analysis of the relationship of these segments is necessary to describe the structural abnormalities encountered following fracture displacement and mal-union. This requires an ability to describe the positions of the individual components in mathematical terms and is the essence of projective geometry.

This is a unique field in mathematics and is most commonly described as the evaluation of the space in which geometrical objects exist and act and is the conceptual basis for the understanding of automated deformity correction and fracture reduction using devices including a hexapod external fixator. Chasles recognised that the movement of any solid involves only rotation and translation and defined the three-dimensional axes about which these occurred (Figure 7.16). An understanding of projective geometry allows a mathematical description of three-dimensional deformity and application of Chasles' theorem and axis can be used to establish the position and direction of the vectors required for simultaneous correction of all components. This is of fundamental importance for automated fracture reduction or deformity correction and forms the basis for simultaneous correction of all components of complex skeletal deformity using a hexapod external fixator.

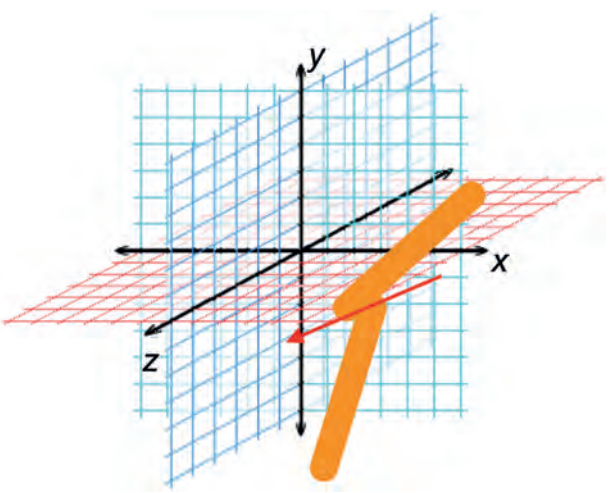

Figure 7.16
Chasles' axis. Simultaneous correction of all components of deformity occurs along a single axis.

KEYPOINTS

- The conceptual basis for the oblique plane
- Radiographic method of oblique plane description
- Defining an oblique plane angular deformity
  - Graphic method
  - Trigonometric method
- Variance between graphic and trigonometric methods
- Translation deformity
- Simultaneous correction of angulation and translation

CHAPTER

8

The femur

Peter Calder and Mick Dennison

Introduction

This chapter will describe methods used to define the location and magnitude of frontal and lateral plane deformity in the femur using either the mechanical or anatomical axis, highlighting differences in calculation and utilisation. Analysis of femoral deformity is complicated by the offset of the femoral neck, which is responsible for a difference in the axes. The reader should be familiar with the general concepts of deformity correction and a stepwise approach to whole limb deformity evaluation should be undertaken prior to specifically evaluating deformities in the femur. This ensures that contributory deformities elsewhere in the limb are appreciated and their effects on the weight-bearing axis are defined.

Frontal plane evaluation

Frontal plane deformity planning in the femur is complicated by the medial offset of the femoral head from the shaft. This causes the mechanical axis, which by definition passes between the joint centres of the hip and the knee, to diverge proximally from the anatomical axis, which by definition is mid-diaphyseal. The angle subtended by the axes is termed the anatomical to mechanical axis angle (AMA). The population mean AMA is 7° and will generate important errors if planning methods are mixed (Figure 8.1a–c).

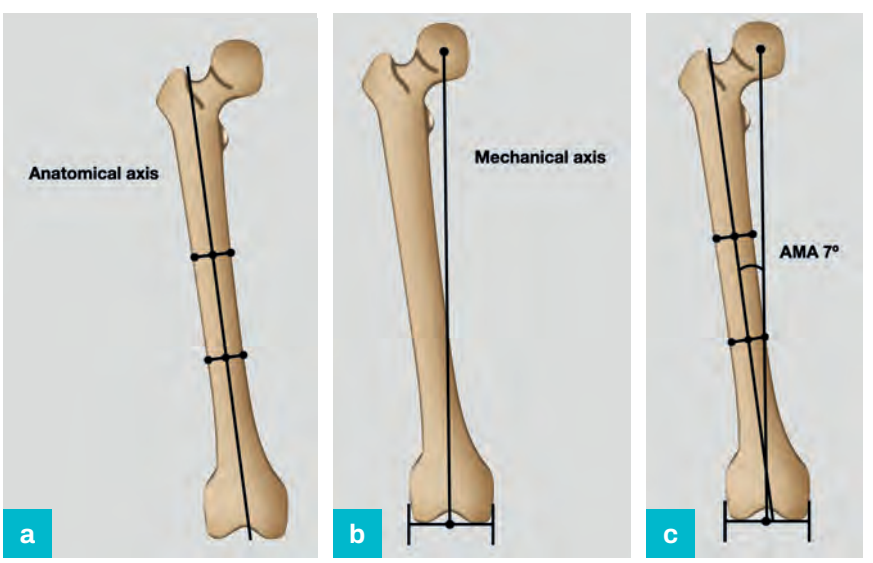

Figure 8.1 (a–c) Anatomical to mechanical axis angle.

Use of the anatomical axis is more straightforward and is appropriate for obvious diaphyseal deformity. It is, however, inaccurate for assessing metaphyseal and peri-articular deformity, particularly if the segment is short, and mechanical access planning is more reliable and therefore recommended.

Mechanical axis planning

Femoral mechanical axis planning in the frontal plane initially involves construction of a line between the hip and knee joint centres and measuring the mechanical lateral proximal femoral angle (mLPFA) and mechanical lateral distal femoral angle (mLDFA). Abnormality of either angle indicates that deformity is present in the femur and requires separate evaluation of the proximal and distal segmental axes.

Proximal mechanical axis reconstruction

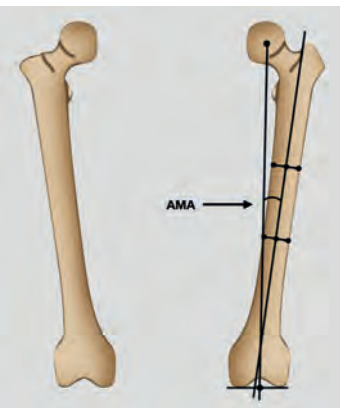

Figure 8.2
Patient-specific AMA.

The mechanical axis of the proximal femur is reconstructed to confirm normal anatomy or identify deformity. In cases of developmental, post-traumatic or post-surgical alteration of trochanteric height, it may not be possible to construct the mLPFA and, in either case, the anatomical axis and AMA can be used to reconstruct the mechanical axis.

In the example in Figure 8.2, it is not possible to construct a joint orientation line, due to an abnormality of the greater trochanter. The patient-specific AMA is calculated by constructing the mechanical and anatomical axes on radiographs of the normal left femur. If there is bilateral deformity or radiology is not available, the population normal (7°) is used instead.

The mid-diaphyseal line is located and a parallel line that passes through the femoral head is constructed on the abnormal femur (Figure 8.3a).

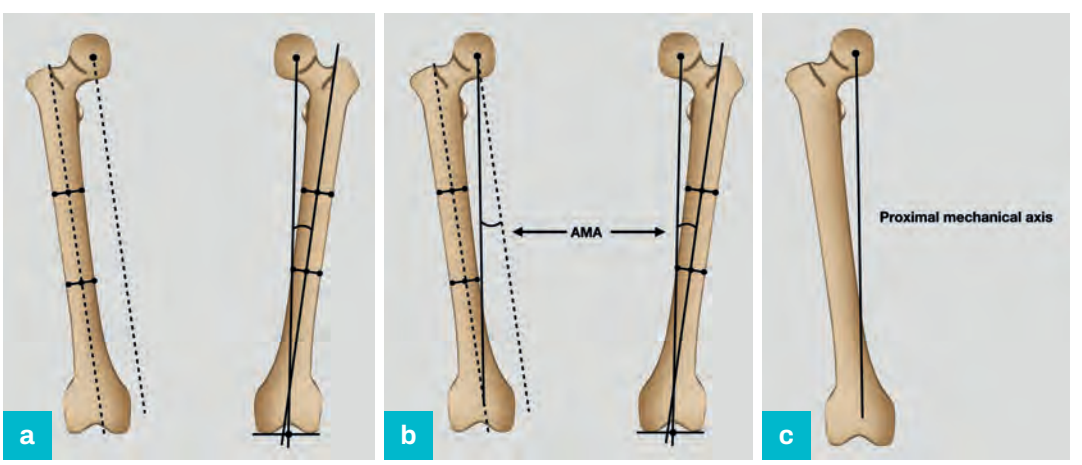

Figure 8.3 (a–c)
Proximal mechanical axis reconstruction.

A further line is constructed from the centre of the femoral head at an angle equal to the normal AMA (Figure 8.3b) and this represents the proximal mechanical axis (Figure 8.3c). This is an alternate angle and equality is a property of parallel lines.

Distal mechanical axis reconstruction

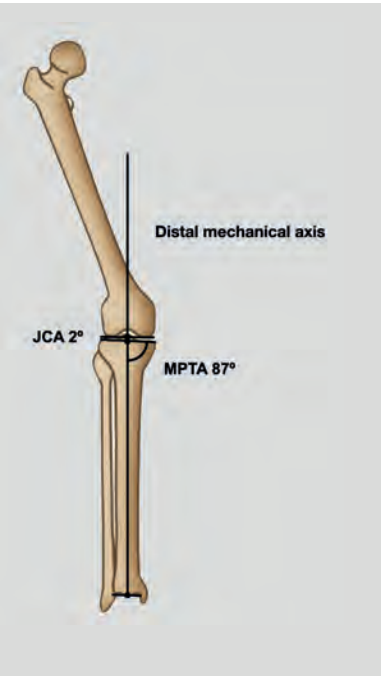

Figure 8.4
Distal mechanical axis reconstruction.

The mechanical axes of the normal tibia and femur pass through the knee joint centre and are collinear with the overall mechanical axis of the limb. The tibial mechanical axis can therefore be extended proximally to reconstruct the distal femoral mechanical axis, provided there is no tibial or joint abnormality (Figure 8.4). This requires initial confirmation that the MPTA and JCA are normal and there is no joint subluxation.

Proximal deformity

Initial analysis demonstrates a normal MAD with normal tibial geometry. Deformity cannot be excluded until analysis of both bones has been undertaken. In the example in Figure 8.5, proximal femoral peri-articular deformity will not obviously displace the limb axis and will be overlooked, unless formal analysis is completed (Figure 8.5a).

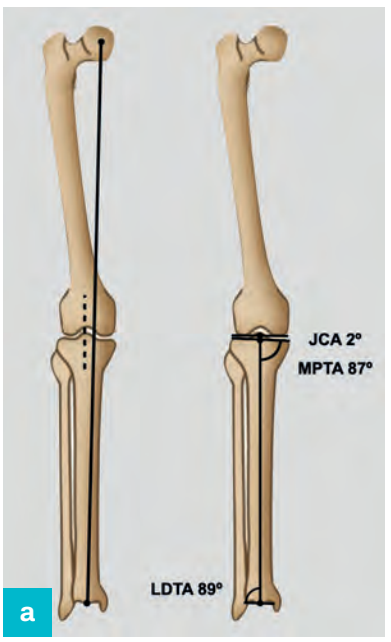

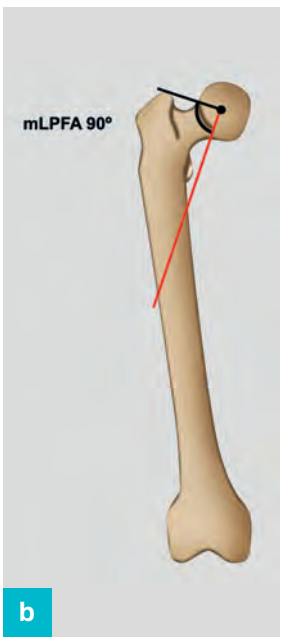

Figure 8.5
Proximal deformity: analysis.
(a) Identification of mechanical axis abnormality and normal tibial geometry.
(b) Reconstruction of the proximal mechanical axis.

The proximal segment mechanical axis is reconstructed from the proximal joint orientation line using the using the patient-specific mLPFA. If this is unavailable due to bilateral deformity or lack of appropriate radiology, the population normal of 90° is used (Figure 8.5b).

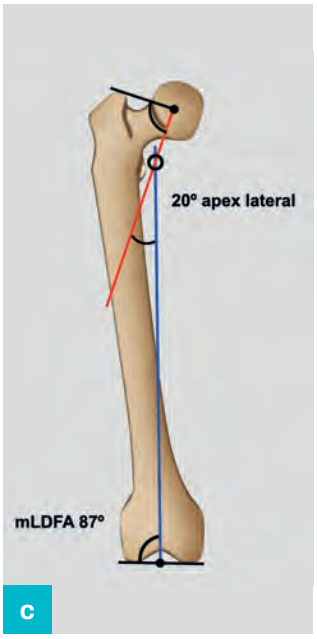

Figure 8.5
Proximal deformity: analysis.
(c) 20° apex lateral proximal deformity.

The distal segment mechanical axis is reconstructed from the distal joint orientation line using the using the patient normal mLDFA. If this is unavailable due to bilateral deformity or lack of appropriate radiology, the population normal of 87° is used (Figure 8.5c). The point of intersection of the proximal and distal axes identifies a 20° apex lateral deformity but is positioned medially because of the mechanical axis offset. This corresponds with the visible deformity, excluding an additional translation or multi-apical deformity.

Distal deformity

Initial analysis demonstrates an abnormal MAD with normal tibial geometry and therefore confirms a femoral deformity (Figure 8.6a).

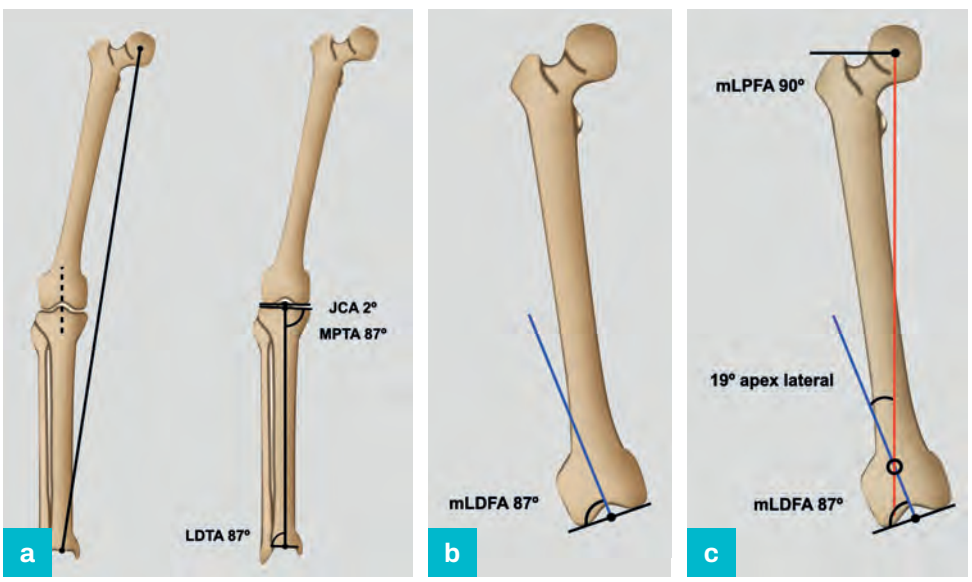

Figure 8.6
Distal deformity: analysis.
(a) Identification of mechanical axis abnormality and normal tibial geometry.
(b) Reconstruction of the distal mechanical axis.
(c) 20° apex lateral distal deformity.

The distal segment mechanical axis is reconstructed from the distal joint orientation line using the using the patient normal mLPFA. If this is unavailable due to bilateral deformity or lack of appropriate radiology, the population normal of 87° is used (Figure 8.6b).

The proximal segment mechanical axis is reconstructed from the proximal joint orientation line using the patient normal mLPFA. If this is unavailable due to bilateral deformity or lack of appropriate radiology, the population normal of 90° is used (Figure 8.6c). The point of intersection of the proximal and distal axes identifies a 19° apex lateral deformity. This corresponds with the visible deformity, excluding an additional translation or multi-apical deformity.

Diaphyseal deformity

Initial analysis demonstrates an abnormal limb mechanical axis, normal tibial geometry and therefore identifies a deformity in the femur (Figure 8.7a).

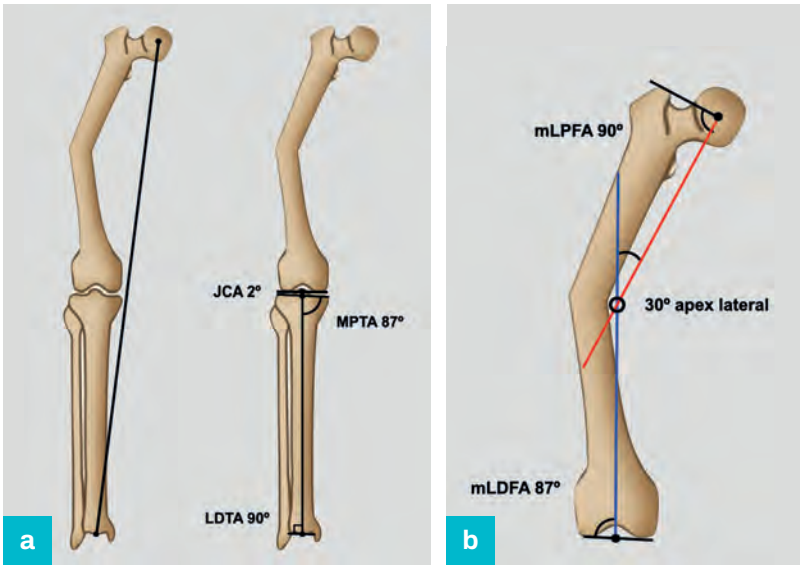

Figure 8.7
Diaphyseal deformity: analysis. **(a)** Identification of mechanical axis abnormality and normal tibial geometry. **(b)** 30° apex lateral diaphyseal deformity.

The proximal and distal mechanical axes are reconstructed using the methods described in previous paragraphs with contralateral measurements referenced to the hip and knee joint orientation lines. If these are unavailable due to bilateral deformity or lack of appropriate radiology, the population normals are used. The point of intersection of the proximal and distal mechanical axes demonstrates a 30° apex lateral diaphyseal deformity but is positioned medially because of the mechanical axis offset (Figure 8.7b). This corresponds with the visible deformity, excluding an additional translation or multi-apical deformity.

Multi-apical deformity

If there is more than one deformity, the proximal and distal mechanical axes are derived from the joint orientation lines (Figure 8.8).

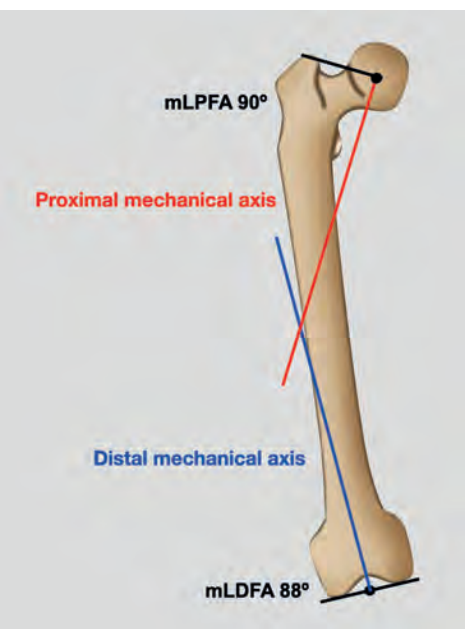

Figure 8.8
Identification of the proximal and distal mechanical axes in a multi-apical deformity.

The mechanical axis of the middle segment is derived by the method described in previous paragraphs (Figure 8.9a,b).

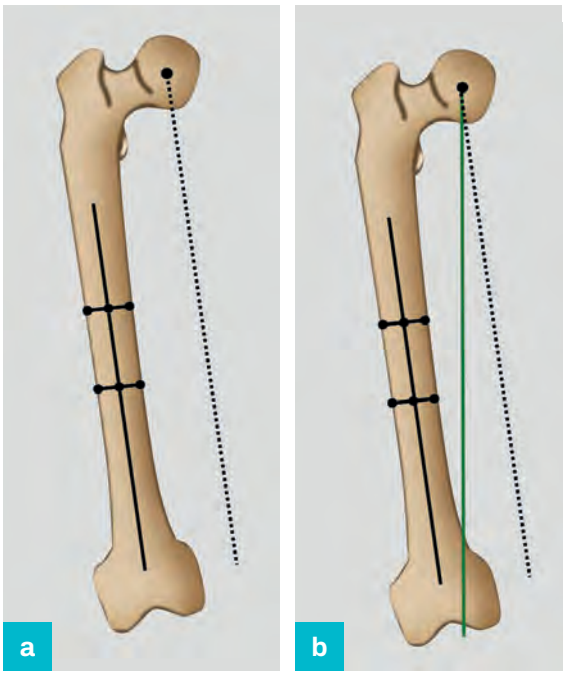

Figure 8.9 (a,b) Localisation of the middle segment mechanical axis.

The position of this line is flexible, provided it remains parallel to the mechanical axis, and is placed at an intersection that is located at the site of deformity (Figure 8.10a,b).

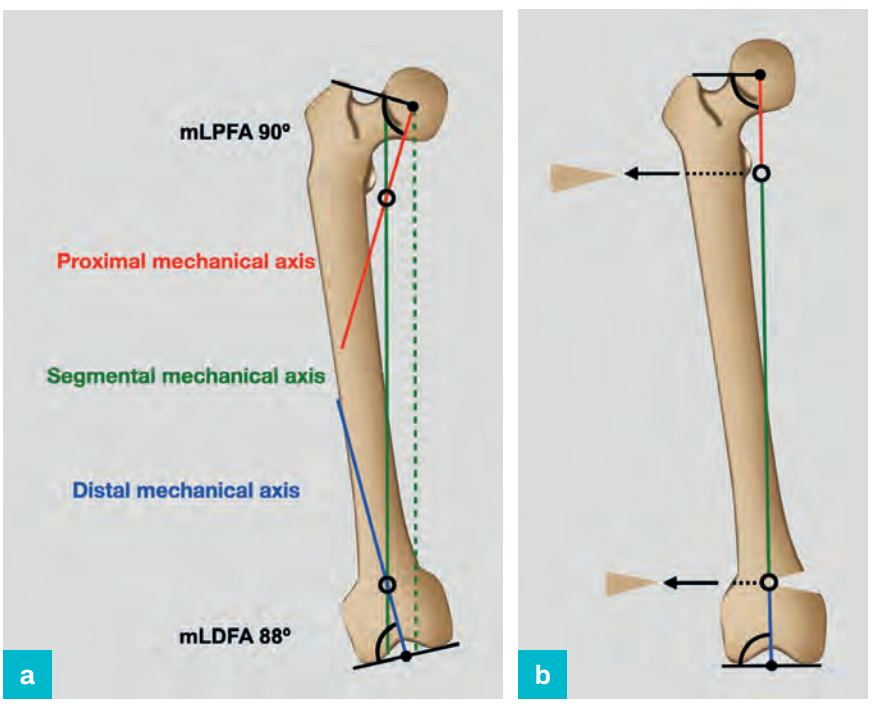

Figure 8.10 (a,b) Anatomical correction of a multi-apical deformity.

If the deformity is corrected at a different level, the mechanical axis is corrected with secondary deformity, which will preclude fixation with an intramedullary device (Figure 8.11a,b).

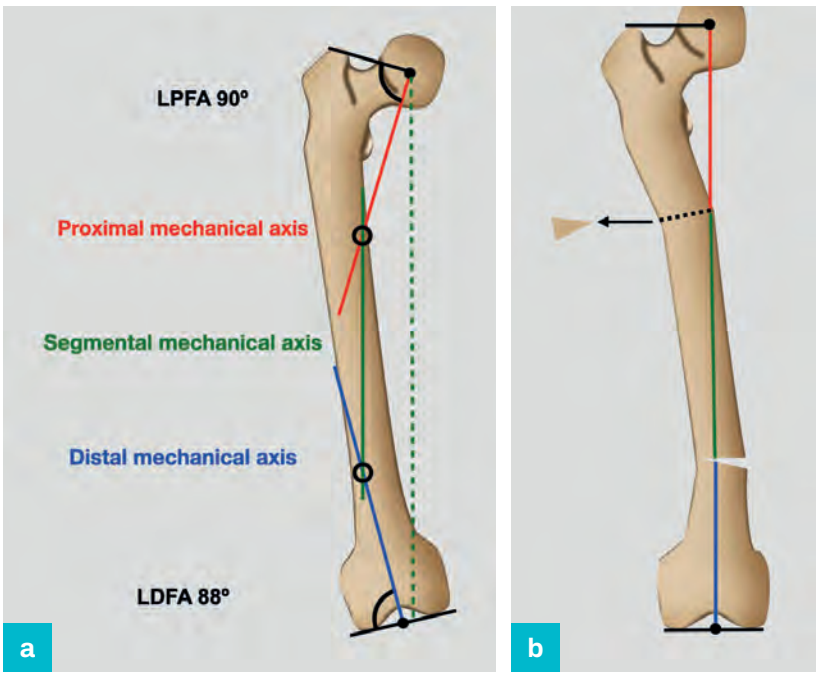

Figure 8.11 (a,b)
Axis realignment with secondary deformity.

Anatomical axis planning

Anatomical planning will underestimate subtle peri-articular malalignment if the segment is short and is less accurate than mechanical axis planning, which is recommended for peri-articular deformity. In the following examples (Figures 8.12–8.18), the initial evaluation demonstrates an axis abnormality with normal tibial geometry, localising deformity to the femur, and will not be illustrated separately.

Proximal deformity

The anatomical medial proximal femoral angle (aMPFA) is formed at the intersection of the hip joint orientation line and anatomical axis of the proximal diaphysis, represented by the proximal mid-diaphyseal line (Figure 8.12).

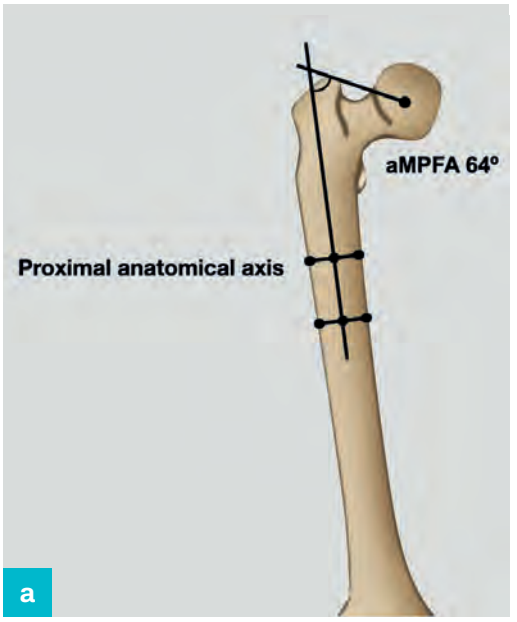

The aMPFA in this example is abnormal (64°) (Figure 8.12a) and the proximal anatomical axis is reconstructed using contralateral measurements, referenced to the hip joint orientation line at the normal point of intersection at the piriformis fossa.

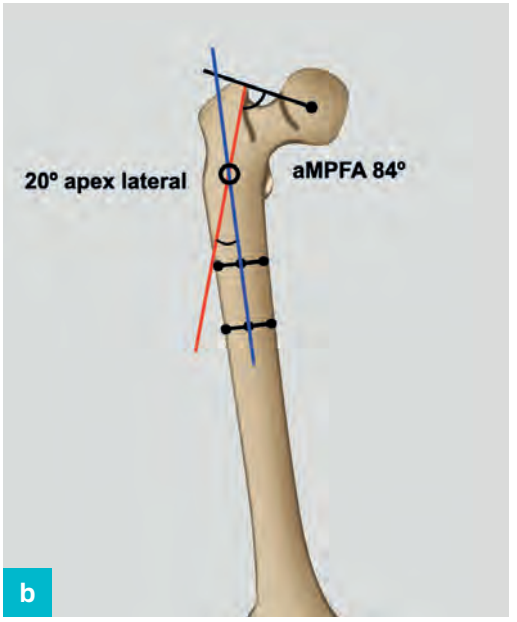

If these are unavailable, the population normal of 84° is used. The acute angle formed by the diaphyseal and reconstructed proximal segmental anatomic axes identifies a 20° apex lateral deformity (Figure 8.12b).

Figure 8.12
Proximal deformity: analysis.
(a) Identification of abnormal aMPFA.
(b) 20° apex lateral deformity.

Distal deformity

The anatomical lateral distal femoral angle (aLDFA) is formed at the intersection of the knee joint orientation line and the distal axis, represented by the distal mid-diaphyseal line. In the example in Figure 8.13, the aLDFA is abnormal (97°) (Figure 8.13a).

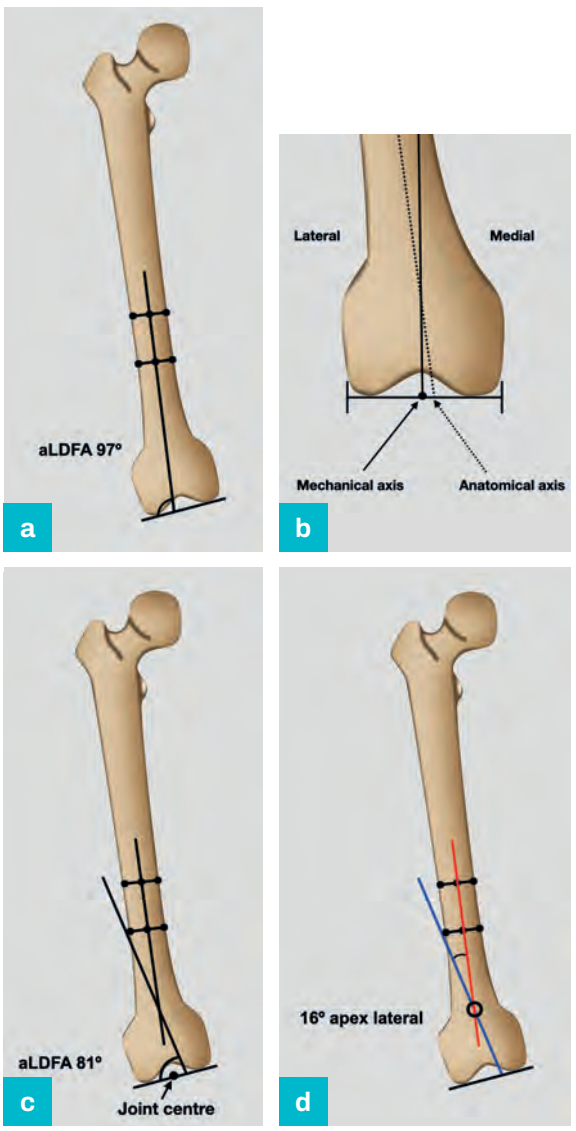

Figure 8.13
Distal deformity: analysis.
(a) Identification of abnormal aLDFA.
(b) Relationship between the distal mechanical and anatomical axes and the distal joint orientation line.
(c) Reconstruction of the distal anatomical axis.
(d) 16° apex lateral deformity.

The distal anatomical axis is reconstructed using contralateral measurements, referenced to the knee joint orientation line at the normal point of intersection.

The anatomical and mechanical axes cross just above the knee as, by definition, the mechanical axis passes through the middle of the knee, whereas the anatomical axis passes from the middle of the diaphysis to reach a point approximately 10 mm medial to the mechanical axis at the level of the knee, in the lateral aspect of the medial femoral condyle (Figure 8.13b).

The distal anatomical axis is reconstructed, using contralateral measurements referenced to the knee joint orientation line from this medial point (Figure 8.13c). If these are unavailable, the population normal of 81° is used. The acute angle formed at the intersection of proximal and reconstructed distal segmental anatomic axes identifies a 16° apex lateral deformity (Figure 8.13d).

Diaphyseal deformity

The proximal joint orientation line and adjacent anatomical axis are constructed (Figure 8.14a).

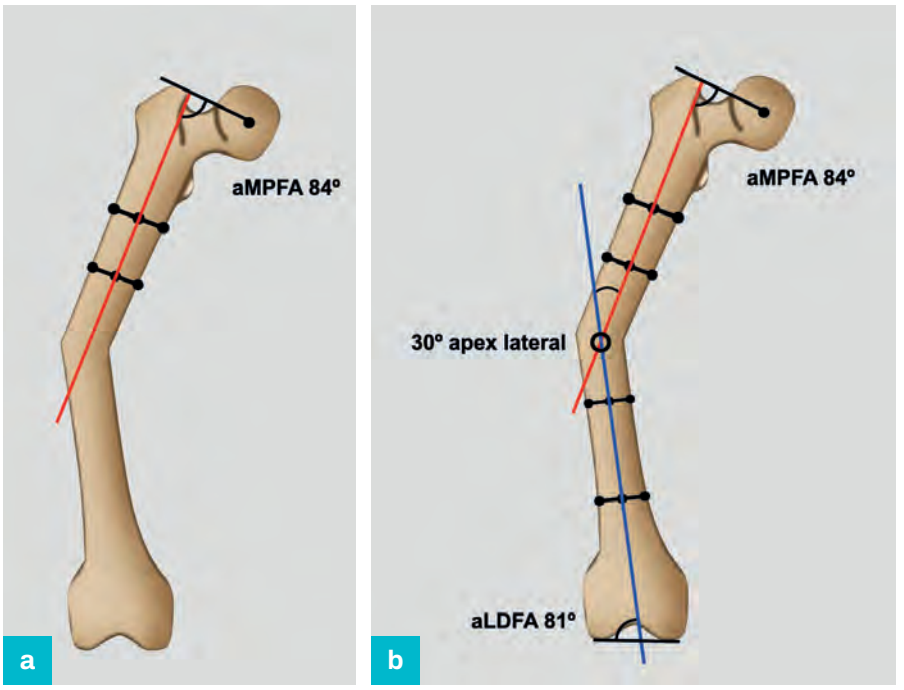

Figure 8.14 Diaphyseal deformity: analysis. **(a)** Proximal joint orientation line and anatomical axis. **(b)** Distal joint orientation line and anatomical axis in a 30° apex lateral diaphyseal deformity.

The distal joint orientation line and adjacent anatomical axis are constructed. The joint orientation angles are normal and the point of intersection of the proximal and distal anatomical axes corresponds to the visible level of a 30° apex lateral diaphyseal deformity (Figure 8.14b).

Multi-apical deformity

If the point of intersection of the proximal and distal components of the axis does not coincide with the anatomical deformity or is outside the femoral shaft, there is either multi-focal deformity or an associated translation.

Additional mid-diaphyseal line(s) will define additional deformities (Figure 8.15a), with correction of the deformity possible at each level (Figure 8.15b).

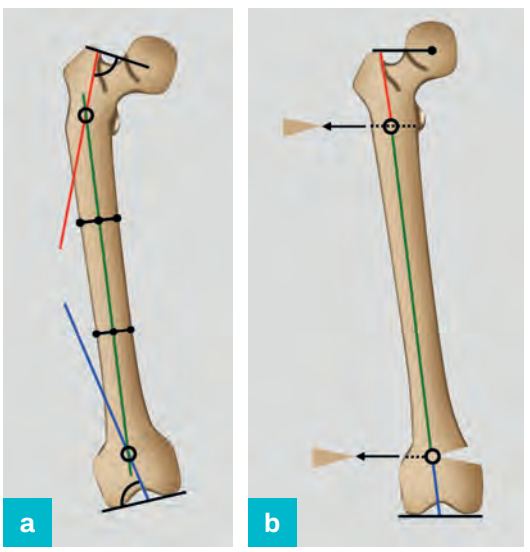

Figure 8.15 (a,b) Identification of multi-apical deformity.

If a single osteotomy is used to correct a multi-apical diaphyseal deformity, the axis will be reconstructed but a 'gull wing' profile is produced (Figure 8.16).

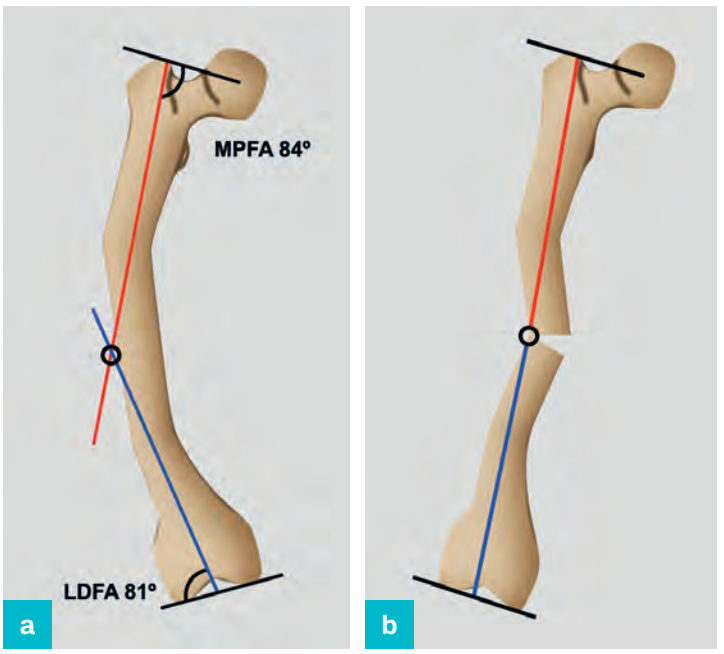

Figure 8.16 (a,b) Non-anatomical correction of multi-apical deformity.

Anatomical correction is achieved by identifying a series of apices with osteotomies at each site (Figure 8.17).

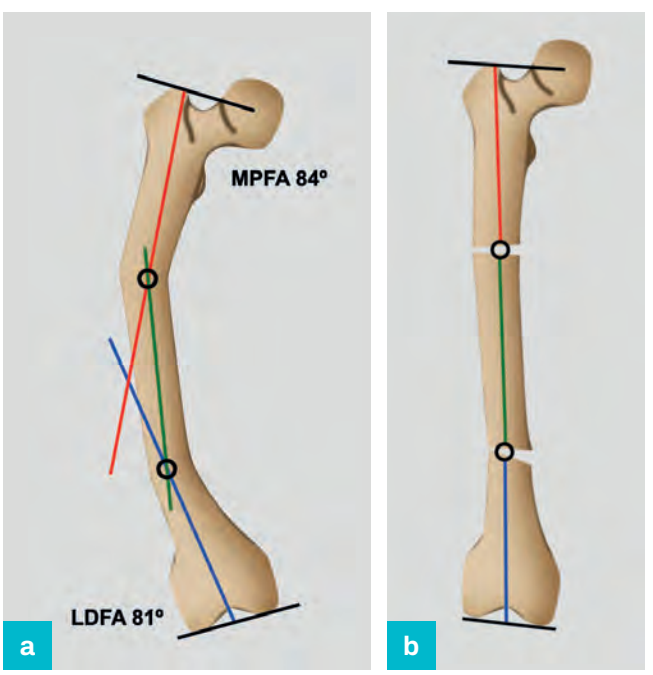

Figure 8.17 (a,b) Anatomical correction of multi-apical deformity.

Bowing

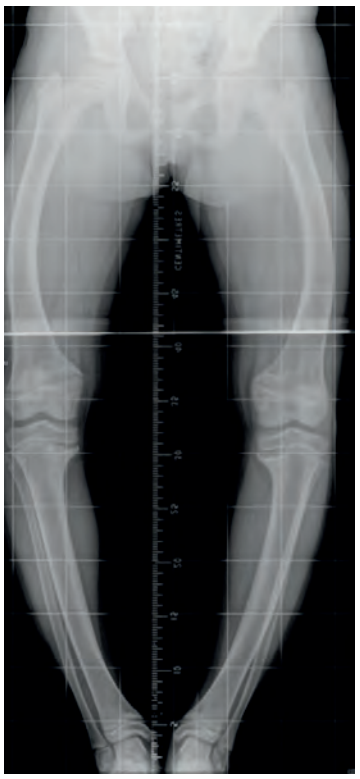

Figure 8.18 Multi-apical femoral deformity.

'Bowing' describes a multi-apical deformity, distributed throughout the diaphysis, which occurs in bone fragility (e.g. osteogenesis imperfecta), skeletal dysplasia (e.g. achondroplasia) and metabolic bone disease (e.g. X-linked rickets) (Figure 8.18).

A curve can be defined by an infinite number of straight lines and it is important to be pragmatic in clinical practice. In the example in Figure 8.19, correction involves resolution of the axis in addition to anatomical reconstruction of the femoral diaphysis.

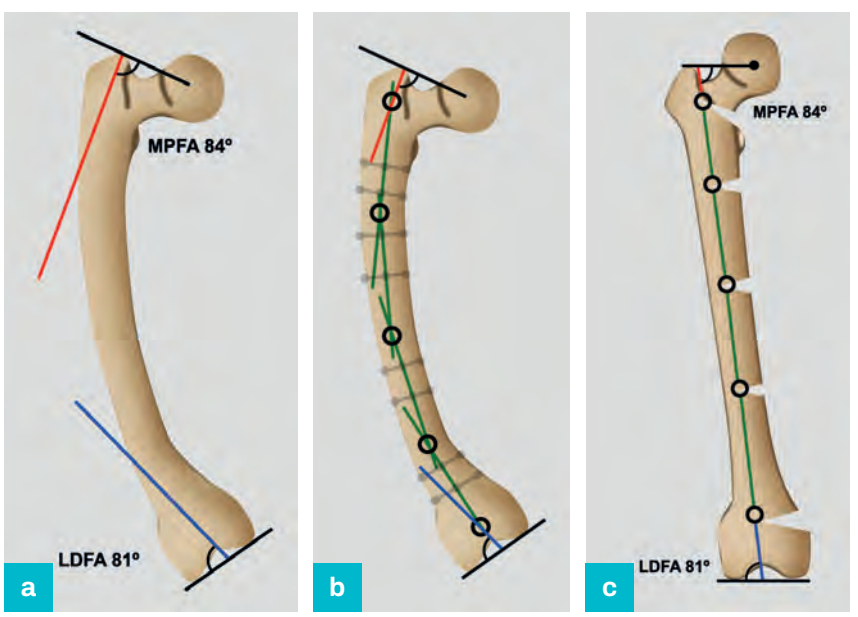

Figure 8.19 (a) Reconstruction of the proximal and distal joint orientation angles. **(b)** Diaphyseal bisector lines constructed for each segment identify multiple apices. **(c)** Realignment of the axis with anatomical reconstruction of the diaphysis.

This initially involves reconstruction of the proximal and distal joint orientation angles (Figure 8.19a).

Constructing additional bisector lines for each diaphyseal segment identifies multiple apices (Figure 8.19b).

Osteotomy at each apex results in realignment of the axis, in addition to anatomical reconstruction of the diaphysis. This is important in clinical practice, particularly if intramedullary fixation is planned (Figure 8.19c).

A more straightforward solution involves initially constructing the proximal and distal axis lines (Figure 8.20a).

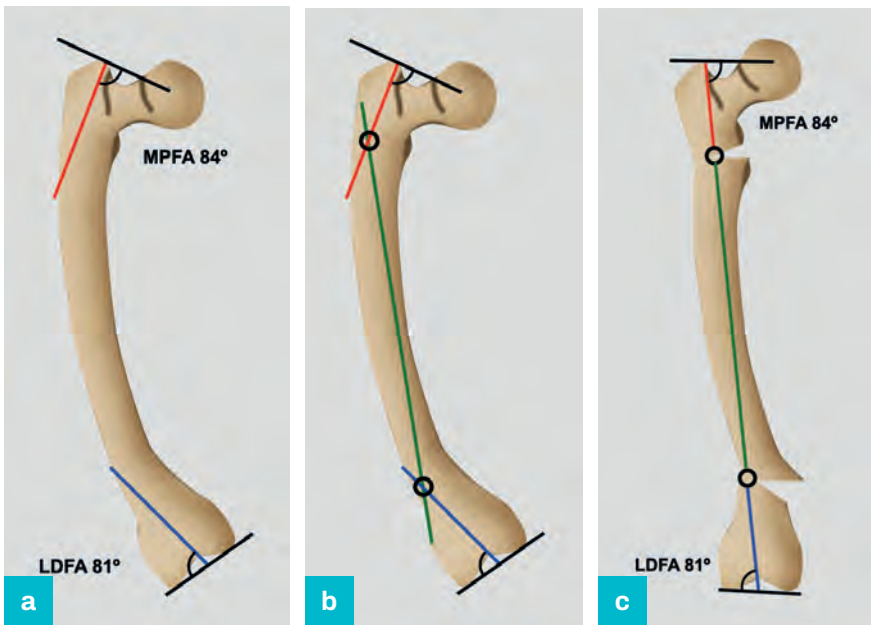

Figure 8.20 (a) Proximal and distal axis lines. **(b)** Additional axis line. **(c)** Axis reconstruction with residual anatomical deformity.

A further line is added and the points of intersection with the proximal and distal axes are marked (Figure 8.20b). The position of this line is variable and can be placed to accommodate the clinical circumstances, particularly the planned fixation.

Correction at these points will reconstruct the axis, but produce anatomical abnormalities, which will limit implant options (Figure 8.20c).

Anticipating the consequences of a planned correction can be achieved by drawing the deformity with tracing paper or using a computer-based system designed for this purpose (see Chapter 2).

Lateral plane evaluation

The proximal femur is difficult to image due to the superimposed pelvis and contralateral hip and femur. If an oblique image of the pelvis is used to isolate the proximal femur, this will affect the projection of the proximal geometry and will introduce measurement errors. The shape of the normal femur in this plane is a chord of a circle with a radius of approximately 1 metre and this presents difficulties localising the proximal mechanical axis. Deformity analysis in the lateral plane is therefore a compromise and uses a combination of anatomical and modified mechanical axis.

The proximal anatomical axis, neck bisector line and proximal femoral joint orientation line are used to describe the geometry of the proximal lateral femur. The modified mechanical axis is used to describe the distal femur. This is within 1° of the distal mid-diaphyseal line and the joint orientation angle derived from either axis is identical for practical purposes.

Proximal deformity

In the example in Figure 8.21, proximal femoral peri-articular deformity will not obviously displace the limb axis and will be overlooked unless formal analysis is completed. Initial analysis demonstrates a normal MAD with normal tibial geometry (Figure 8.21a). Deformity cannot be excluded until analysis of both bones has been undertaken.

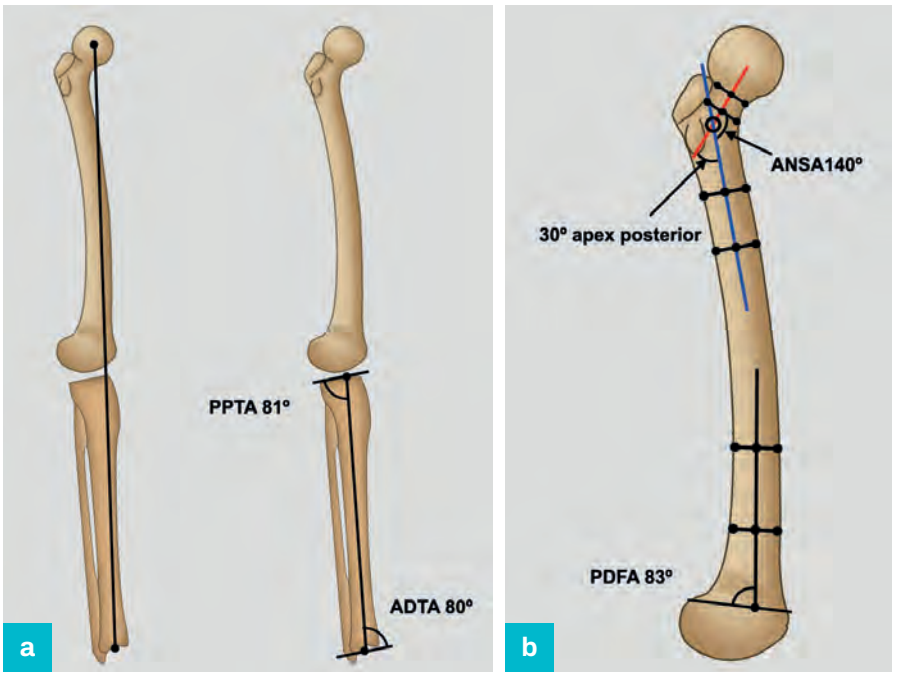

Figure 8.21
Proximal deformity: analysis.
(a) Identification of normal limb axis and tibial geometry.
(b) 30° apex posterior proximal femoral deformity.

The PDFA is normal, excluding distal deformity. The neck bisector and proximal anatomical axis intersect at the anterior neck shaft angle (ANSA), which is abnormal (140°), indicating a 30° apex posterior deformity (Figure 8.21b).

If the deformity is located in the femoral head or neck, the proximal axis is identified by the posterior proximal femoral angle (PPFA) and the distal axis by the neck bisector line. These are collinear in the normal femur and the point and angle of intersection indicate the site and magnitude of deformity.

In the example in Figure 8.22, the joint orientation line is abnormal due to the position of the femoral epiphysis and the intersection of the joint orientation line and neck bisector line demonstrates a 40° apex anterior deformity.

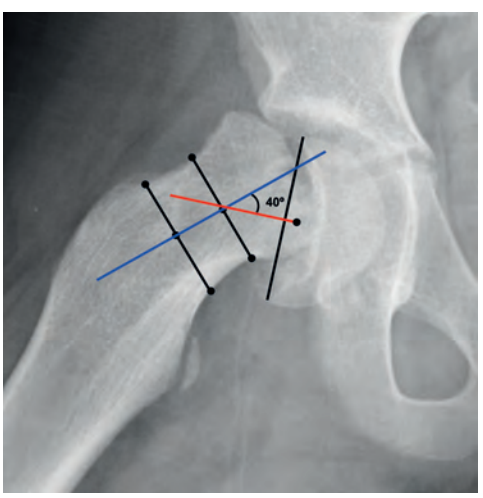

Figure 8.22
Slipped upper femoral epiphysis with 40° apex anterior deformity.

Distal deformity

Initial analysis demonstrates an abnormal limb mechanical axis, normal tibial geometry and therefore identifies a deformity in the femur (Figure 8.23a).

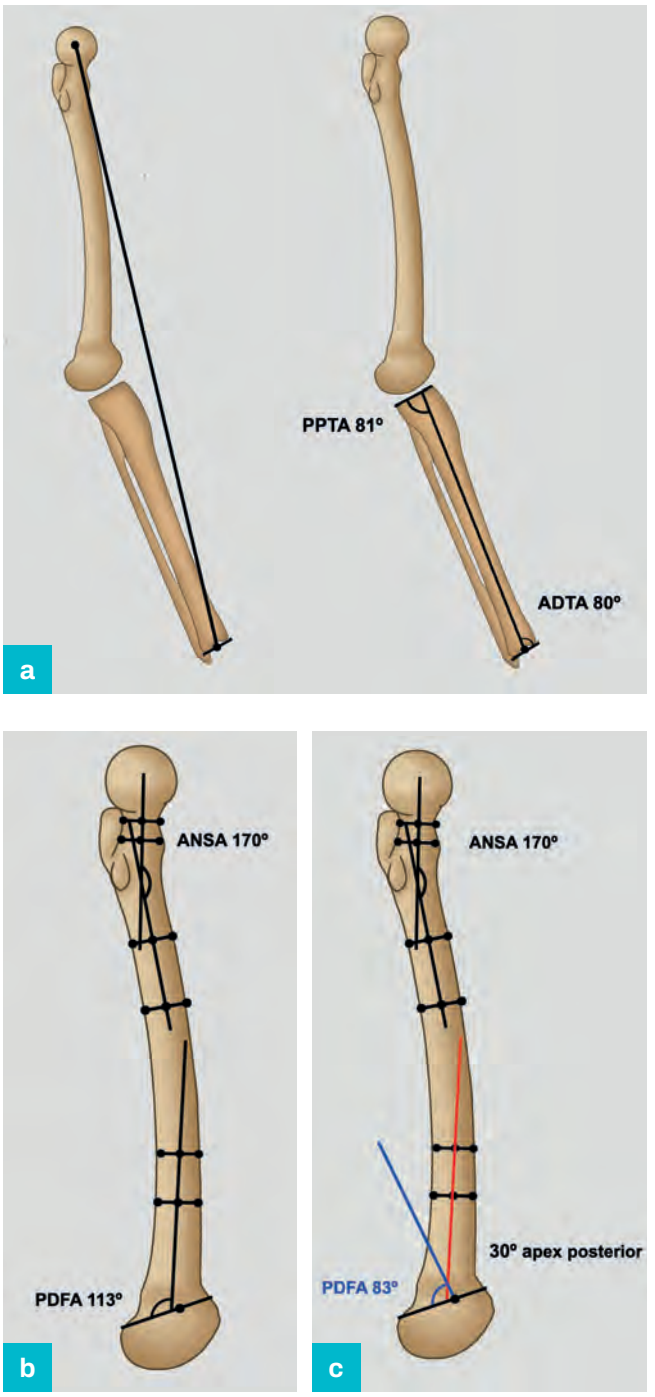

Figure 8.23
Distal deformity: analysis.
(a) Identification of abnormal limb axis and normal tibial geometry.
(b) Identification of abnormal PDFA.
(c) 30° apex posterior deformity.

The ANSA is normal, excluding proximal deformity. In this example, the PDFA is abnormal (113°), demonstrating distal peri-articular deformity (Figure 8.23b).

The distal modified mechanical axis is reconstructed using contralateral measurements, referenced to the knee joint orientation line at the normal point of intersection, 1/3 from the anterior cortex, using patient-specific angles. If these are unavailable due to bilateral deformity or lack of appropriate radiology, the population normal of 83° is used and identifies a 30° apex posterior deformity (Figure 8.23c).

Diaphyseal deformity

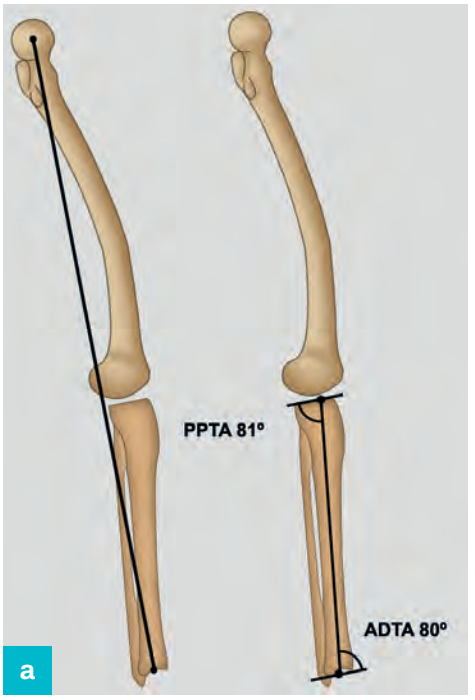

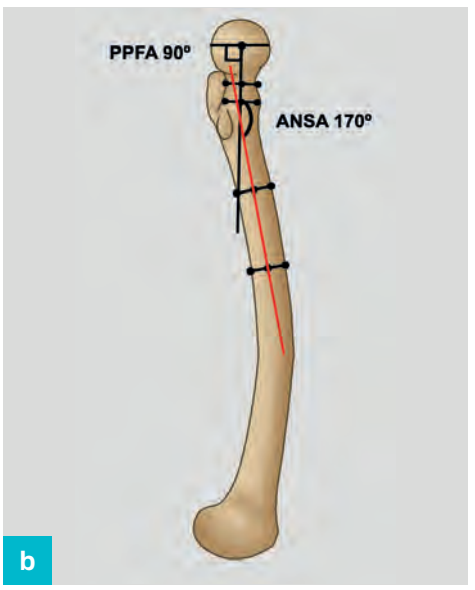

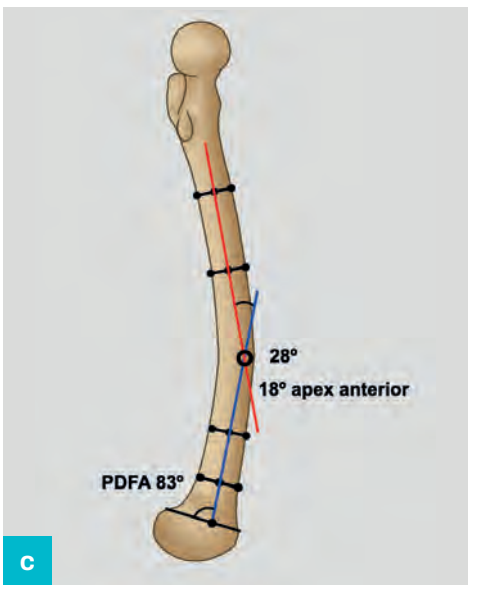

Figure 8.24 Diaphyseal deformity: analysis. **(a)** Identification of abnormal limb axis and normal tibial geometry. **(b)** Proximal joint orientation line, neck bisector and proximal anatomical axis. **(c)** 18° apex anterior single-level diaphyseal deformity.

Initial analysis demonstrates an abnormal limb mechanical axis, normal tibial geometry and therefore identifies a deformity in the femur (Figure 8.24a).

The proximal anatomical axis, neck bisector and proximal joint orientation lines are constructed. In this example, the PPFA and ANSA are normal, excluding proximal deformity (Figure 8.24b).

The distal anatomical axis and joint orientation line are constructed. The PDFA is normal, excluding distal deformity. The proximal and distal anatomical axes intersect at 28°, the contralateral or population normal mid-diaphyseal angle (MDA) (10°) is subtracted and the actual deformity is therefore 18° apex anterior (Figure 8.24c).

In subsequent examples, the initial evaluation has been performed and demonstrates an axis abnormality with normal tibial geometry, localising deformity to the femur, and will not be illustrated separately.

Multi-apical deformity

If the point of intersection of the mid-diaphyseal lines does not coincide with the visible anatomical deformity, or is outside the femoral shaft, there is either an associated translation or a multi-apical deformity (Figure 8.25a).

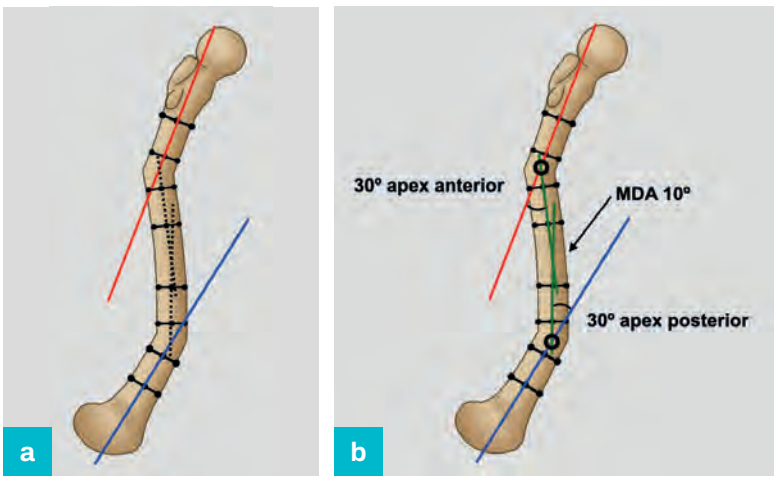

Figure 8.25
(a) Multi-apical lateral diaphyseal deformity.
(b) Resolution of multi-apical lateral diaphyseal deformity.

A mid-diaphyseal line can be drawn for each component of a multi-segmental deformity with an apex associated with each additional mid-diaphyseal line. When the magnitude of a deformity is measured, it is important that the normal 10° apex anterior MDA is appreciated, or the deformity will be overestimated by this amount.

In this example, correction of each deformity is performed with reference to the adjacent middle segment diaphyseal bisector and preserves the normal AMA (Figure 8.25b).

Bowing

'Bowing' in the lateral plane also describes multi-apical deformity, distributed throughout the diaphysis, which occurs in conditions including bone fragility disorders, skeletal dysplasia and metabolic bone disease.

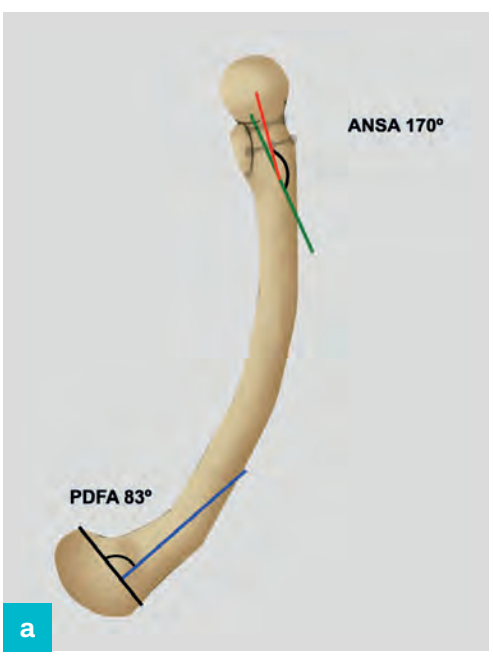

Figure 8.26
(a) Reconstruction of the proximal and distal joint orientation angles.

In the example in Figure 8.26, correction involves resolution of the axis in addition to anatomical reconstruction of the femoral diaphysis. This initially involves reconstruction of the proximal and distal joint orientation angles (Figure 8.26a).

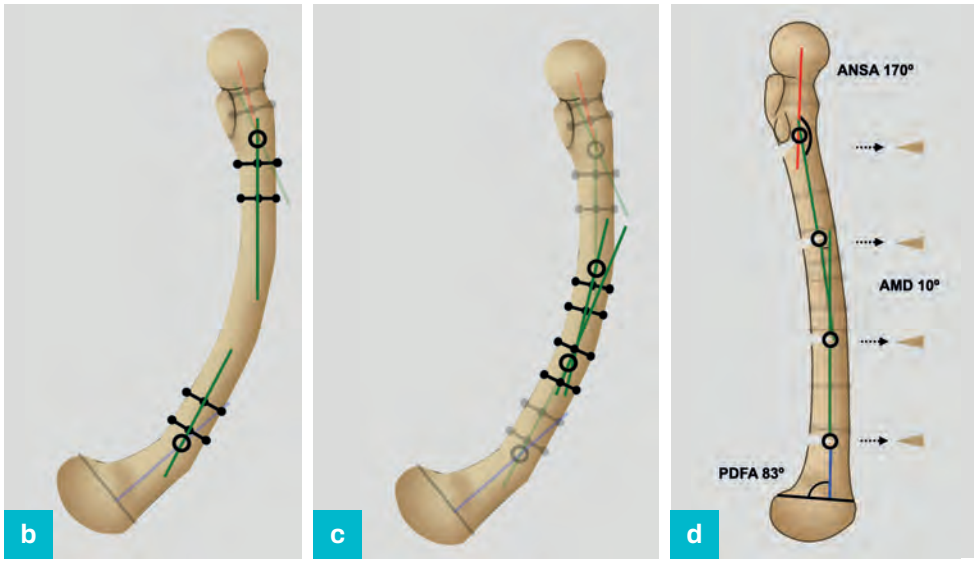

(b,c) Diaphyseal bisector lines constructed for each segment identify multiple apices. **(d)** Realignment of the axis with anatomical reconstruction of the diaphysis.

Constructing additional bisector lines for each diaphyseal segment identifies multiple apices (Figure 8.26b,c).

Osteotomy at each apex results in realignment of the axis, in addition to anatomical reconstruction of the diaphysis (Figure 8.26d). This is important in clinical practice, particularly if intramedullary fixation is planned.

A more straightforward solution involves initially constructing the proximal and distal axis lines (Figure 8.27a).

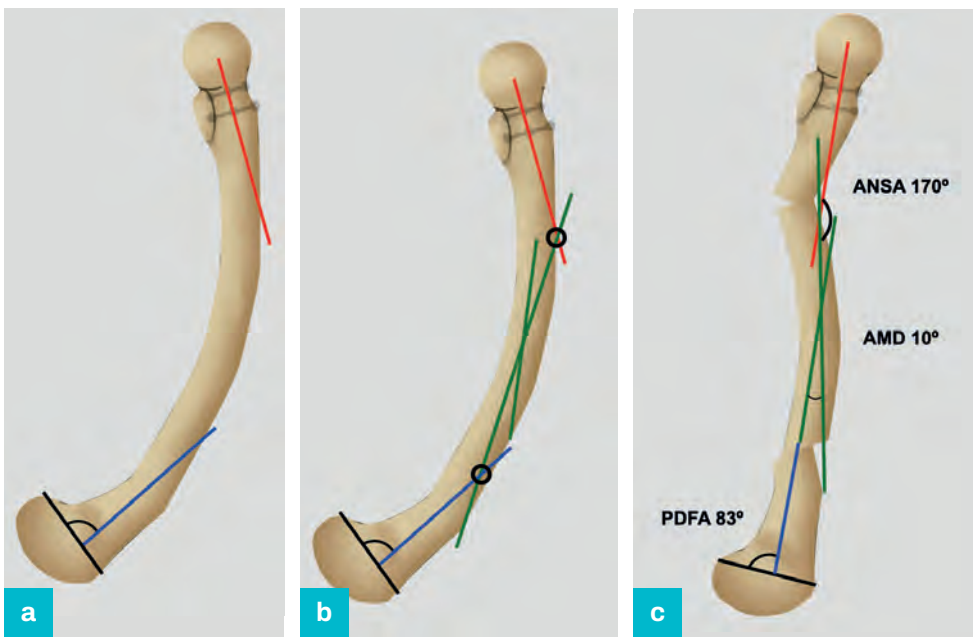

Figure 8.27
(a) Proximal and distal axis lines. **(b)** Mid-diaphyseal lines, representing the normal AMD. **(c)** Axis reconstruction with residual anatomical deformity.

A pair of mid-diaphyseal lines is added to accommodate the normal AMD, and the points of intersection with the proximal and distal axes are marked (Figure 8.27b).

Correction at these points will reconstruct the axis but produce anatomical abnormalities, which will limit implant options (Figure 8.27c).

Anticipating the consequences of a planned correction can be achieved by drawing the deformity with tracing paper or using a computer-based system designed for this purpose (see Chapter 2).

Combined diaphyseal and proximal peri-articular deformity

Comprehensive deformity analysis must be undertaken, even if one obvious deformity has been identified. In the example in Figure 8.28, the proximal joint orientation line is constructed and intersects with the proximal diaphyseal axis to form an abnormal ANSA (140°) (Figure 8.28a).

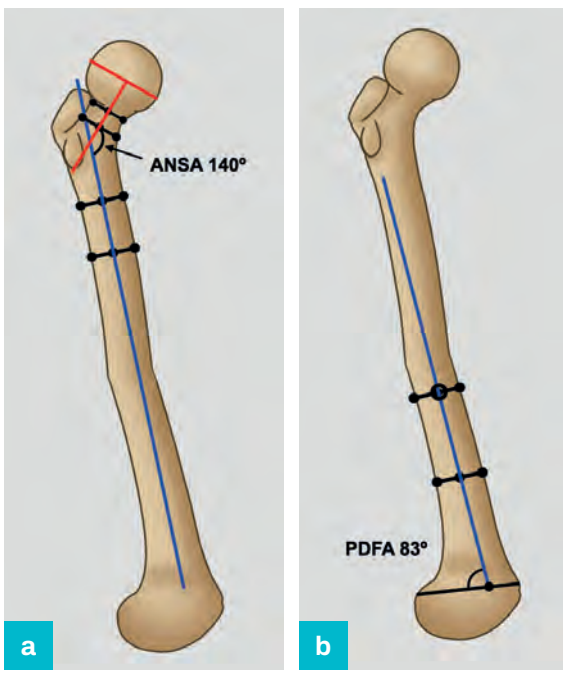

Figure 8.28
(a) Identification of abnormal ANSA.
(b) Identification of normal PDFA.

The distal modified mechanical axis is constructed and demonstrates a normal PDFA (83°) (Figure 8.28b).

The proximal and distal diaphyseal axes intersect with an AMD of 4°, indicating a 14° apex posterior mid-diaphyseal deformity (Figure 8.28c).

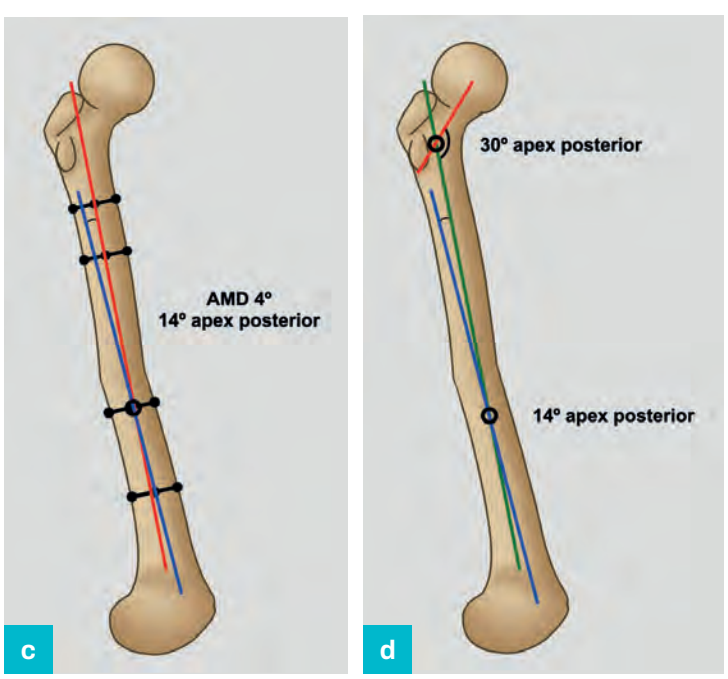

(c) Proximal and distal diaphyseal axes.
(d) 14° apex posterior mid-diaphyseal and 30° apex posterior proximal peri-articular deformity.

Complete analysis therefore identifies a 14° mid-diaphyseal apex posterior and 30° proximal apex posterior peri-articular deformity (Figure 8.28d).

Combined diaphyseal and distal peri-articular deformity

In the example in Figure 8.29, the ANSA is normal (170°) (Figure 8.29a).

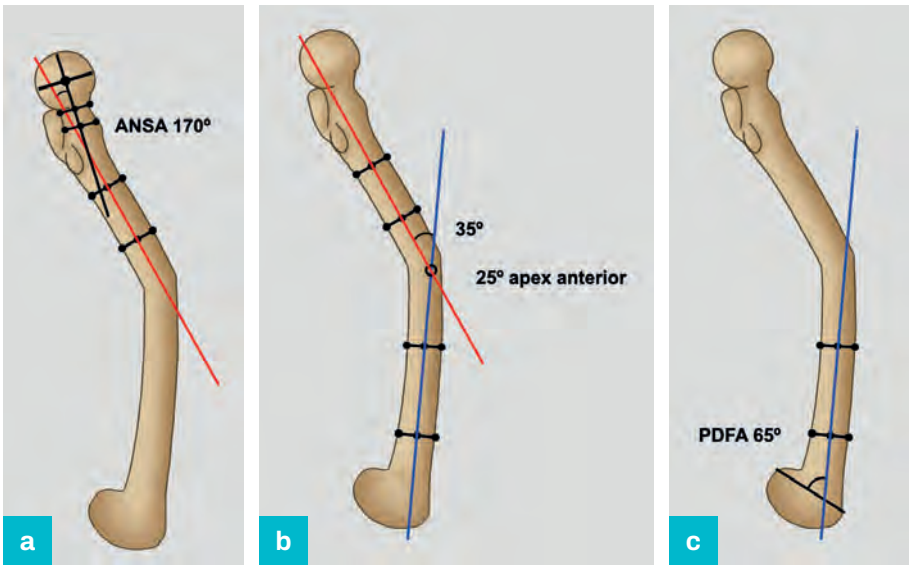

Figure 8.29
(a) Identification of normal ANSA.
(b) Proximal and distal axes.
(c) Abnormal PDFA indicates distal peri-articular deformity.
(d) Normal distal axis drawn in from the joint orientation line.
(e) 25° apex anterior mid-diaphyseal and 20° apex anterior distal peri-articular deformity.

The proximal and distal axes, represented by the mid-diaphyseal lines, intersect at 35°. The normal femur has 10° apex anterior configuration, therefore this indicates a 25° apex anterior mid-diaphyseal deformity (Figure 8.29b).

The PDFA is abnormal (65°), indicating distal peri-articular deformity (Figure 8.29c).

A distal axis is drawn from the joint orientation line using a population normal value of 83° (Figure 8.29d).

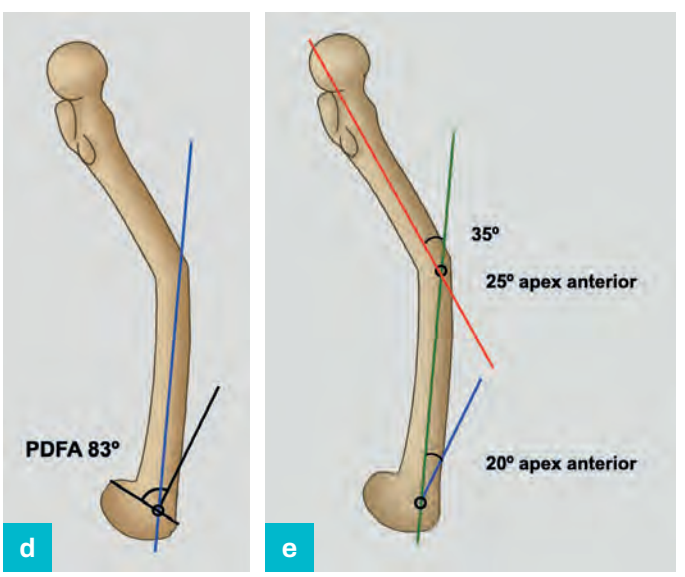

This indicates a 20° apex anterior distal peri-articular deformity at the level of the joint orientation line (Figure 8.29e).

KEYPOINTS

- The difference between the anatomical and mechanical axes
- The anatomical to mechanical axis angle
- Mechanical axis planning and reconstruction using joint orientation lines
- Anatomical axis planning using diaphyseal bisector and joint orientation lines
- Lateral axis planning using diaphyseal bisector lines, modified mechanical axis and joint orientation lines
- The relevance of the lateral mid-diaphyseal angle

CHAPTER

9

The tibia

Paul Harwood and Simon Britten

Introduction

This chapter will describe methods used to define the location and magnitude of frontal and lateral plane deformity in the tibia. Detailed initial assessment of the whole limb is a requirement and ensures that contributory deformities are identified. The approach is similar to femoral deformity analysis (see Chapter 8) but the mechanical and anatomical axes are virtually coincident in the tibia. There are subtle differences that introduce inaccuracies reconstructing the anatomical axis in the presence of peri-articular deformity and mechanical axis planning is recommended.

Frontal plane evaluation

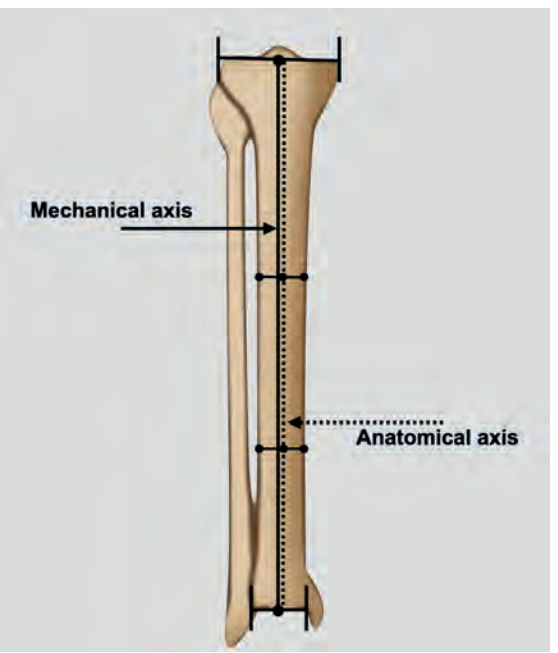

Figure 9.1
Tibial anatomical and mechanical axes.

The tibial mechanical axis runs slightly lateral and parallel to the anatomical axis but can be considered identical for measurement of joint orientation angles, in contrast to the femur where there is a clinically important divergence (Figure 9.1).

Use of the anatomical axis is more straightforward and is appropriate for obvious diaphyseal deformity but is less accurate than the mechanical axis, particularly if the segment is short. The accuracy associated with locating the joint centre and therefore the position of the mechanical axis, although subtle, provides an advantage in peri-articular deformity planning (Figure 9.2).

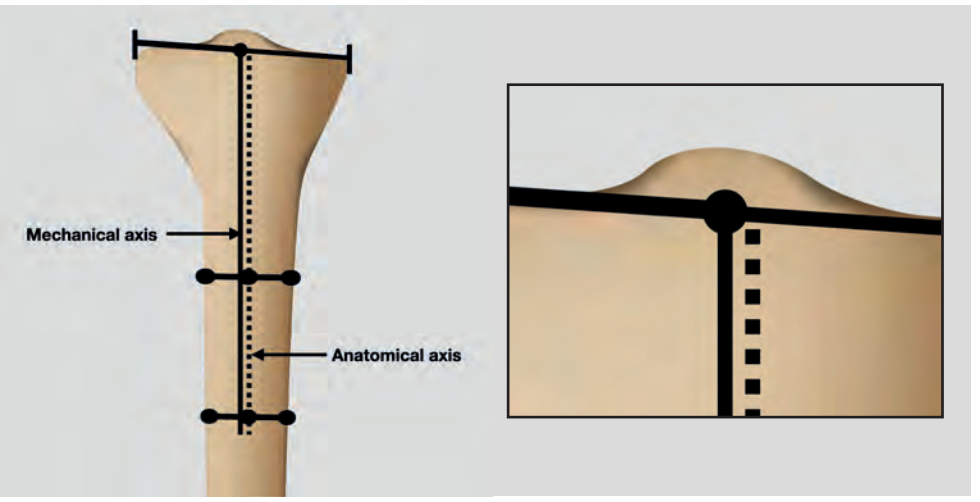

Figure 9.2
Intersection of the mechanical and anatomical axes.

Mechanical axis planning

Tibial mechanical axis planning in the frontal plane initially involves construction of a line between the knee and ankle joint centres and measurement of the medial proximal tibial angle (MPTA) and lateral distal tibial angle (LDTA). Abnormality of either angle indicates a tibial deformity and requires separate assessment of the proximal and distal segments.

Proximal mechanical axis reconstruction

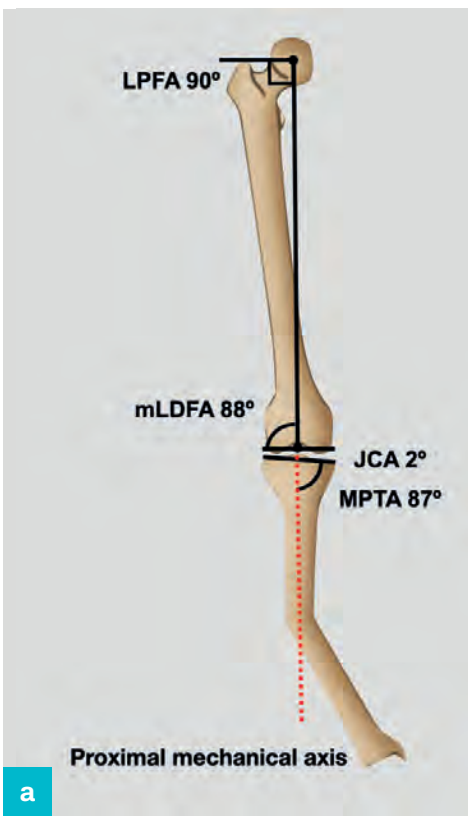

Figure 9.3
Identification of the proximal segment tibial mechanical axis: **(a)** by extending the mechanical axis of the normal femur;

The mechanical axis of the femur and tibia are normally collinear and pass through the knee joint centre. The femoral mechanical axis can therefore be extended distally to reconstruct the proximal tibial mechanical axis, provided there is no femoral or knee joint abnormality. This requires initial confirmation that the mechanical lateral distal femoral angle (mLDFA) and joint line convergence angle (JLCA) are normal and there is no joint subluxation (Figure 9.3a).

(b) using the MPTA;
(c) using the mid-diaphyseal line.

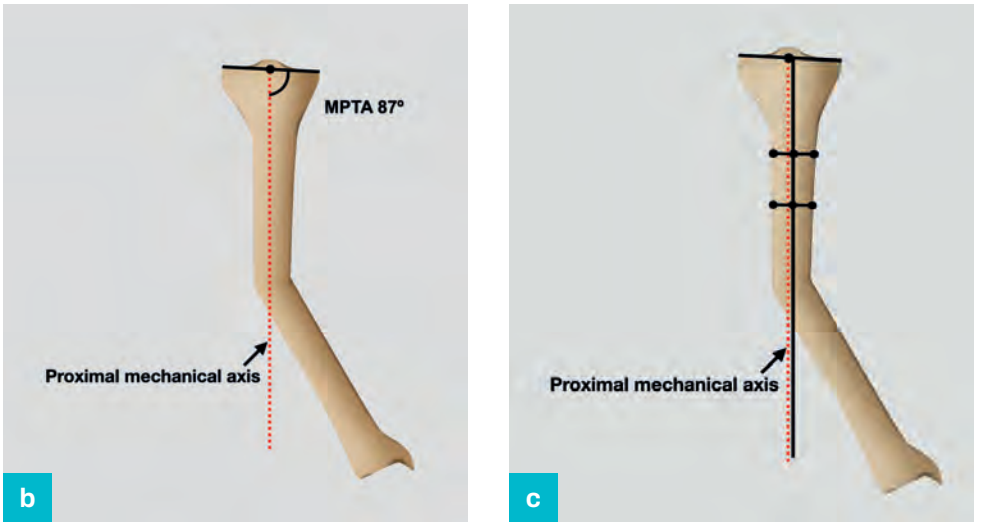

If the femur is abnormal, the opposite MPTA can be used to construct the proximal mechanical axis. If this is abnormal, the population normal of 87° is used as an alternative (Figure 9.3b).

The mechanical axis can also be represented by a line from the mid-point of the proximal tibial joint line, parallel to the proximal mid-diaphyseal line (Figure 9.3c).

Distal mechanical axis reconstruction

The mechanical axis of the distal tibia is also reconstructed to confirm normal anatomy or identify deformity. This is represented by a line from the mid-point of the tibial plafond, parallel to the distal mid-diaphyseal line (Figure 9.4a).

Figure 9.4
Identification of the distal segment mechanical axis:
(a) using a line from the mid-point of the tibial plafond, parallel to the distal mid-diaphyseal line;
(b) using the LDTA.

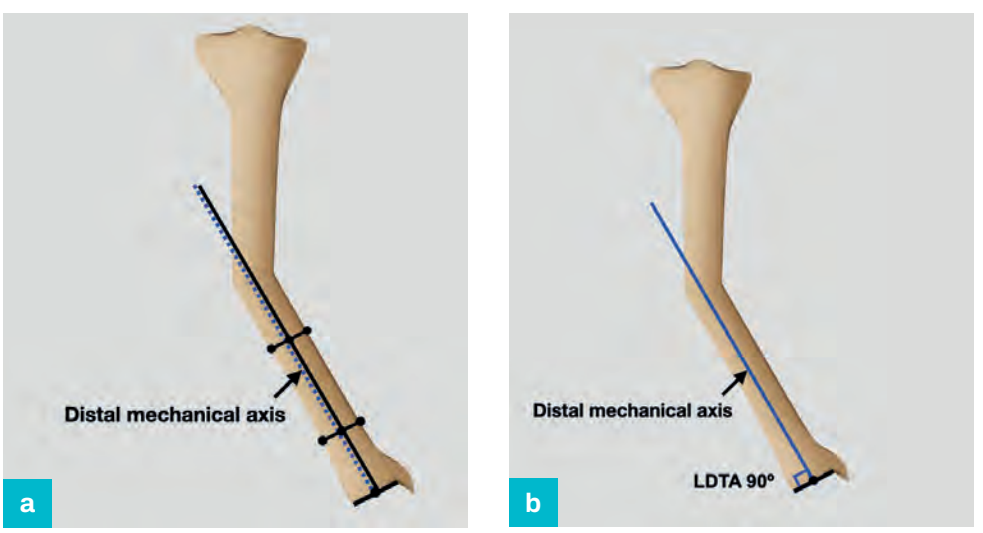

If the distal segment is short, the opposite LDTA can be used to construct the distal mechanical axis. If this is abnormal, the population normal of 90° is used as an alternative.

The intersection of the proximal and distal axis lines will identify the location and magnitude of a tibial deformity. This will depend on the nature of the deformity, illustrated by the following examples.

Proximal deformity

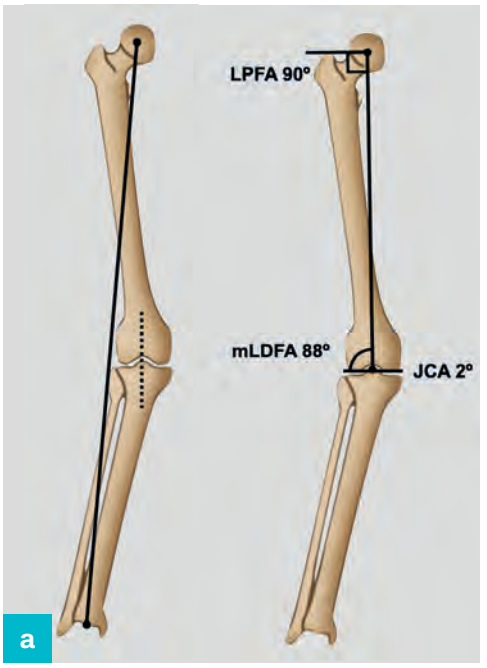

Initial analysis demonstrates an abnormal limb mechanical axis, normal femoral geometry and therefore identifies a deformity in the tibia (Figure 9.5a).

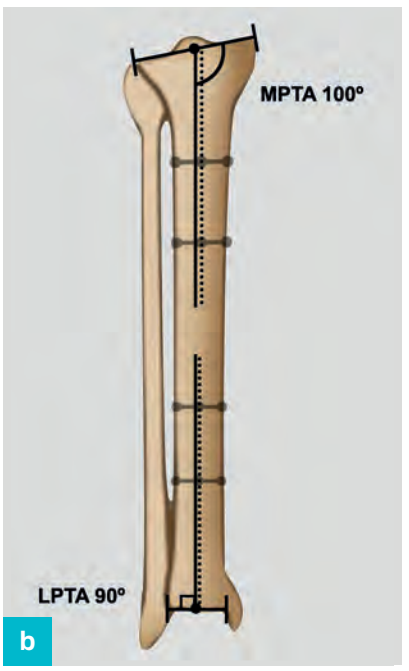

The proximal segment mechanical axis is reconstructed from the centre of the proximal tibial joint line, parallel to the mid-diaphyseal line and demonstrates that the MPTA (100°) is abnormal, identifying a proximal peri-articular deformity. The distal segment mechanical axis is reconstructed from the centre of the distal tibial joint line, parallel to the mid-diaphyseal line. The LDTA (90°) is normal and excludes distal deformity (Figure 9.5b).

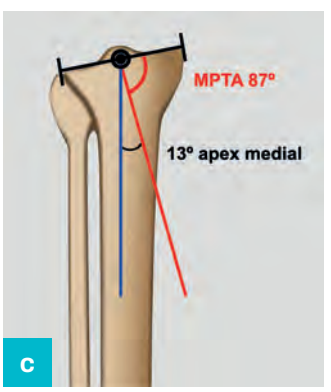

The normal proximal mechanical axis is reconstructed from the centre of the knee joint orientation line using the patient-specific MPTA. If the contralateral limb alignment is also abnormal, or radiology is unavailable, the population normal of 87° is used. The point of intersection of the proximal and distal axes localises a 13° apex medial peri-articular deformity (Figure 9.5c).

Figure 9.5
Proximal deformity: analysis.
(a) Identification of mechanical axis abnormality and normal femoral geometry.
(b) Reconstruction of the proximal and distal segment mechanical axis indicates proximal peri-articular deformity.
(c) 13° apex medial proximal peri-articular deformity.

Distal deformity

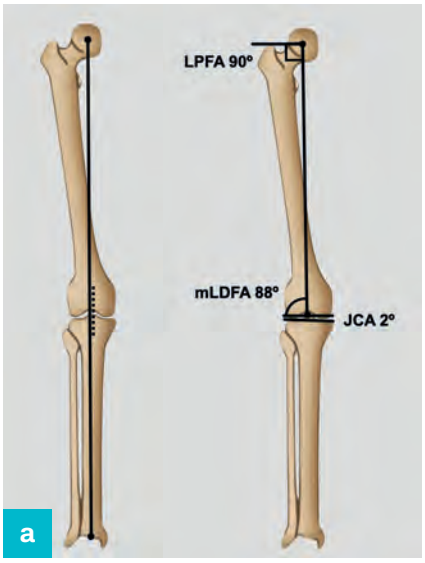

Initial analysis demonstrates a normal MAD with normal femoral geometry. Deformity cannot be excluded until analysis of both bones has been undertaken. In the example in Figure 9.6, distal tibial peri-articular deformity will not displace the limb axis and will be overlooked unless formal analysis is completed (Figure 9.6a).

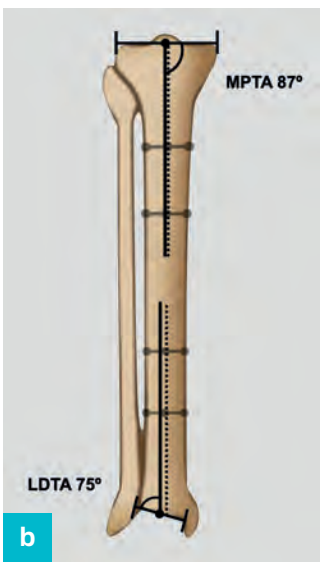

The distal segment mechanical axis is reconstructed from the centre of the distal tibial joint line, parallel to the mid-diaphyseal line, and demonstrates that the LDTA (75°) is abnormal, indicating distal peri-articular deformity. The proximal segment mechanical axis is reconstructed from the centre of the proximal tibial joint line, parallel to the mid-diaphyseal line. The MPTA (87°) is normal and excludes a proximal deformity (Figure 9.6b).

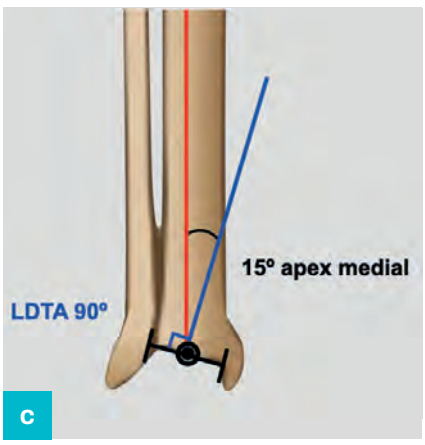

The normal distal segment mechanical axis is reconstructed from the centre of the ankle joint orientation line using the patient-specific LDTA. If the contralateral limb alignment is also abnormal, or radiology is unavailable, the population normal of 90° is used. The point of intersection of the proximal and distal axes identifies a 15° apex medial deformity. This corresponds with the visible deformity, making a translation or multi-apical deformity unlikely (Figure 9.6c).

Figure 9.6
Distal deformity: analysis.
(a) Identification of mechanical axis abnormality and normal femoral geometry.
(b) Reconstruction of the distal and proximal segment mechanical axis indicates distal peri-articular deformity.
(c) 15° apex medial distal peri-articular deformity.

Clinical example 9.1 Correction of a distal tibial apex medial (valgus) deformity using a ring fixator

a b c d

a Proximal (red) and distal (blue) axis lines define the apex at the level of deformity (left).

Simulated correction using a hinge on the bisector line to produce a distal opening wedge osteotomy (right).

b Intra-operative radiographs illustrate hinge placement.

c Post-operative radiographs before (left) and after (right) correction.

d Standing alignment radiographs demonstrate correction of the mechanical axis and ankle joint orientation.

Diaphyseal deformity

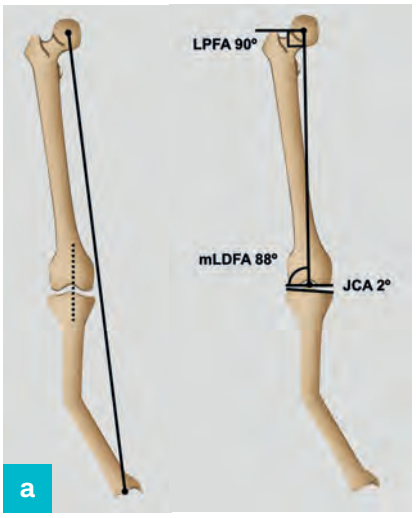

Initial analysis demonstrates an abnormal limb mechanical axis, normal femoral geometry and therefore identifies a deformity in the tibia (Figure 9.7a).

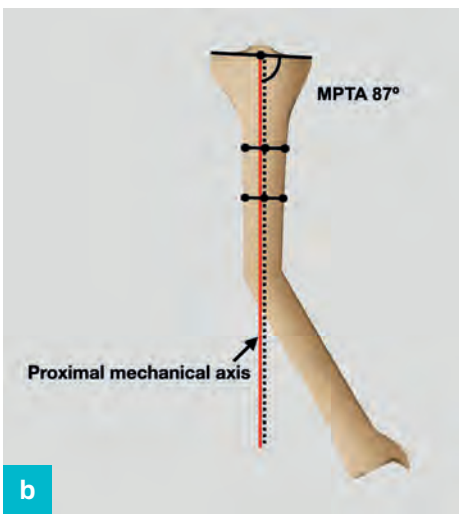

The proximal mechanical axis is reconstructed using a line parallel to the mid-diaphyseal line, drawn from the centre of the proximal tibial joint line. The MPTA is measured and, as this is normal, a peri-articular deformity is excluded (Figure 9.7b).

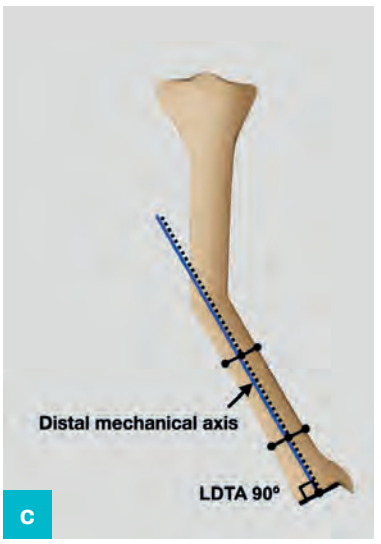

The distal mechanical axis is reconstructed using a line parallel to the mid-diaphyseal line, drawn from the centre of the distal tibial joint line. The LDTA is measured and, as this is normal, a peri-articular deformity is excluded (Figure 9.7c).

Figure 9.7
Diaphyseal deformity: analysis and correction.
(a) Identification of mechanical axis abnormality and normal femoral geometry.
(b,c) Identification of the proximal mechanical axis **(b)** and distal mechanical axis **(c)** excludes peri-articular deformity.
(d) Intersection of the proximal and distal axis lines identify a 30° apex lateral diaphyseal deformity.
(e) Deformity correction.

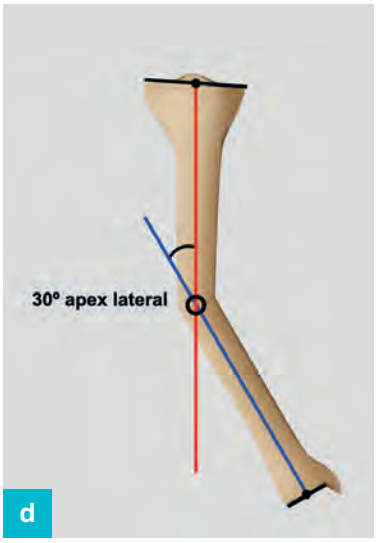

Figure 9.7
Diaphyseal deformity: analysis and correction.
(d) Intersection of the proximal and distal axis lines identify a 30° apex lateral diaphyseal deformity.
(e) Deformity correction.

The point of intersection of the proximal and distal mechanical axes in the example in Figure 9.7 demonstrates a 30° apex lateral diaphyseal deformity (Figure 9.7d).

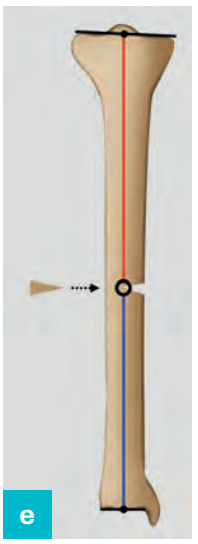

The point of intersection corresponds to the level of the obvious anatomical abnormality and correction at this point will realign the axis without introducing secondary deformity (Figure 9.7e).

Multi-apical deformity

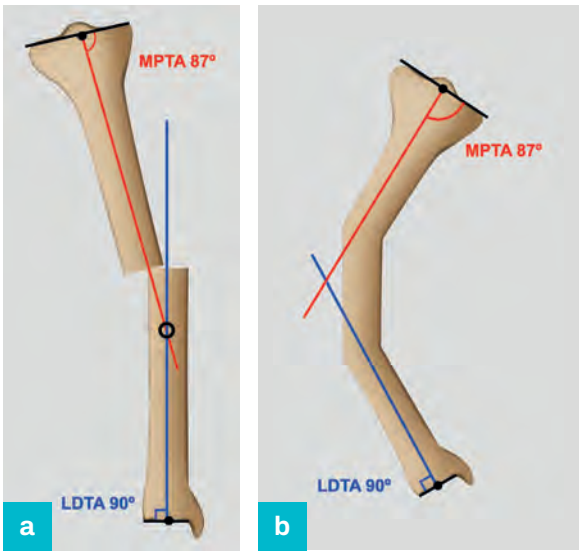

Figure 9.8 Axis intersection distant from the visible deformity suggests translation **(a)** or multi-level deformity **(b)**.

If the point of intersection of the proximal and distal axes is not at the level of obvious deformity (Figure 9.8a) or outside the tibial shaft (Figure 9.8b), an additional translation or multi-level deformity is likely.

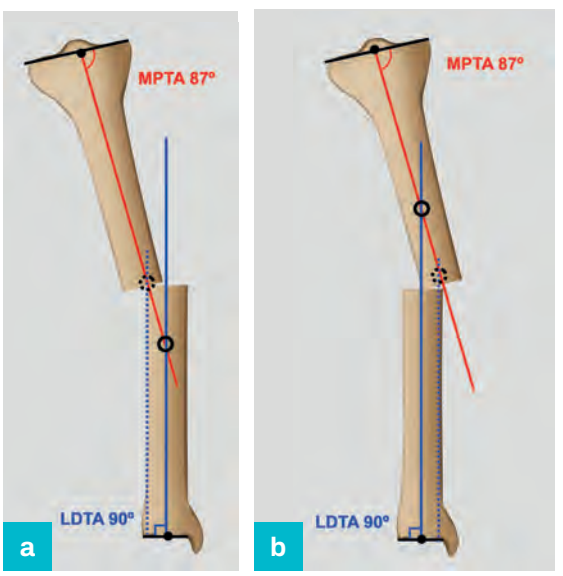

Figure 9.9 Lateral **(a)** or medial **(b)** translation of the distal axis line moves the point of intersection to the level of the deformity. An associated translational deformity is therefore likely.

If medialising or lateralising the distal axis line moves the point of intersection to the level of the obvious deformity, then an associated translation deformity is the most likely cause (Figure 9.9a,b).

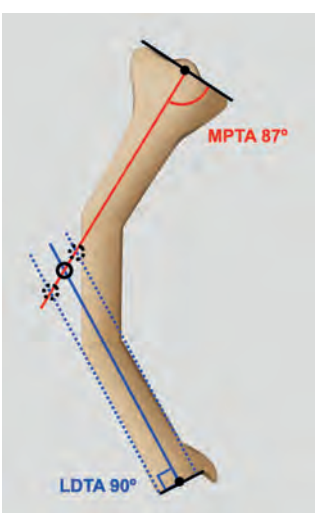

Figure 9.10 Medialising or lateralising the distal axis does not move the axis intersection to the level of the visible deformity and multi-apical deformity is therefore likely.

If the point at which the proximal and distal axes cross lies outside the bone or translating the axis line does not result in intersection at an obvious deformity, it is likely that a multi-level deformity is present (Figure 9.10).

The axis can be corrected at any point on the transverse bisector line, but this may introduce diaphyseal deformity, which will limit options for internal fixation and produce an unattractive correction (Figure 9.11).

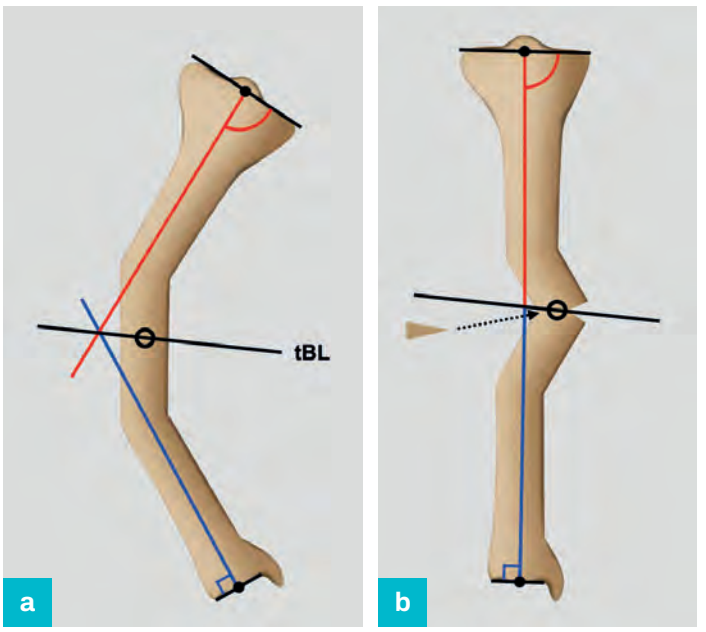

Figure 9.11 (a,b) Axis correction with diaphyseal abnormality.

Addition of a second diaphyseal mechanical axis line will identify both deformities, with axis correction possible at each level. Note that the mid-diaphyseal mechanical axis is drawn 2 mm lateral to the mid-diaphyseal anatomical axis, defined by the diaphyseal bisector lines (Figure 9.12).

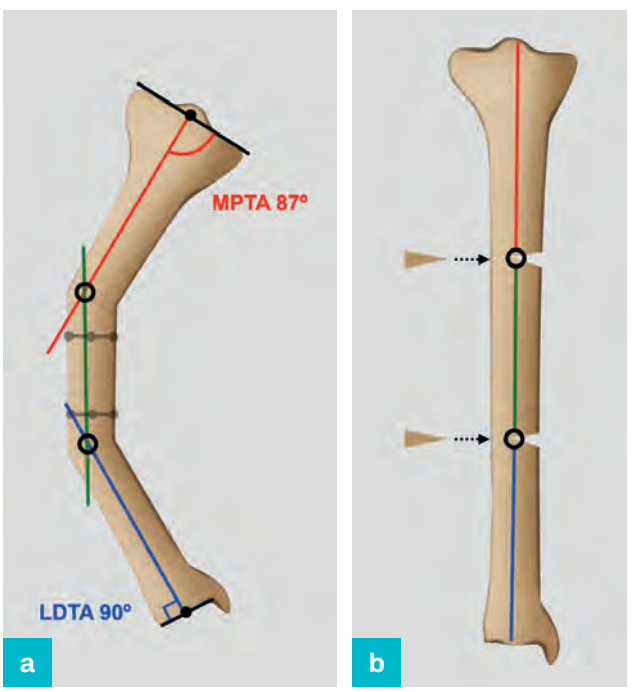

Figure 9.12 (a,b) Deformity resolved to two apices, producing axis realignment and anatomical correction.

In the example in Figure 9.13, the apex is distant from the site of obvious malalignment and suggests either translation or deformity at an additional level (Figure 9.13a). Correction with a single osteotomy at the point of intersection will result in realignment of the axis. This may produce unacceptable translation at an osteotomy site, articular malorientation or, in this case, diaphyseal malalignment (Figure 9.13b).

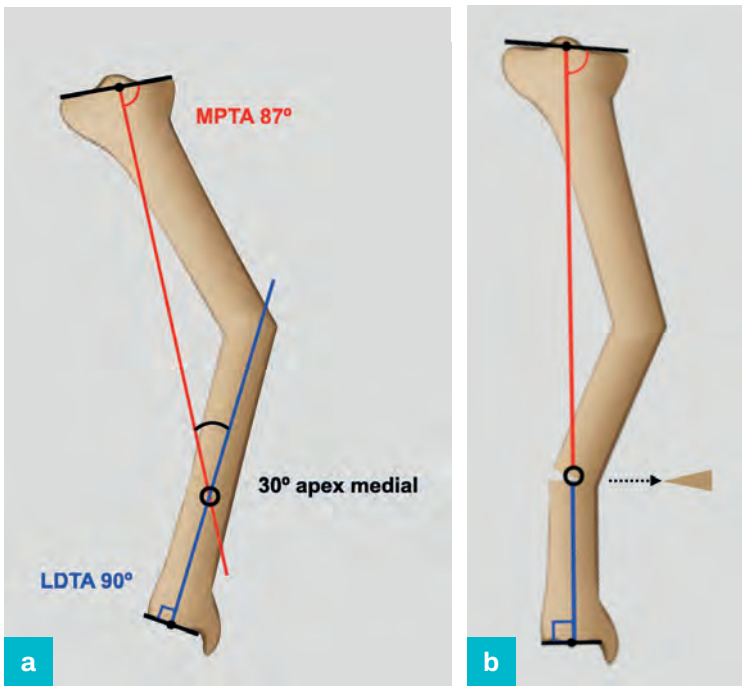

Figure 9.13 (a,b)
Axis correction with residual diaphyseal deformity.

Identification of an apex and correction with an osteotomy at each level results in normal diaphyseal alignment (Figure 9.14a,b).

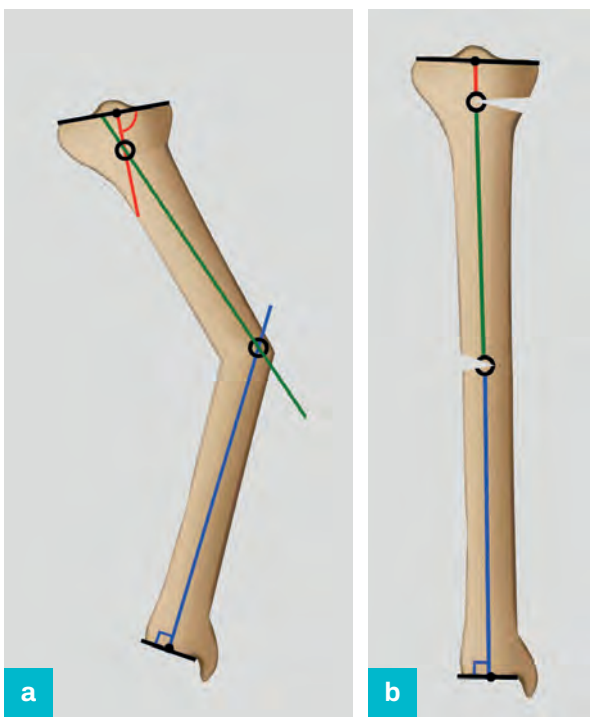

Figure 9.14 (a,b)
Correction at each apex with anatomical realignment.

The choice of approach is a matter of clinical judgement and depends on the position and magnitude of the deformities and the planned method of fixation. An osteotomy performed away from the point of axis intersection may be preferable to avoid abnormal bone or soft tissues or to involve metaphyseal bone, where healing is more predictable. The point at which correction is performed and the location of physical hinges will influence the geometry of correction. The position of a hinge may or may not be at the level of deformity or site of an osteotomy. It is important to understand this relationship as it determines the geometry of correction. It is described under the heading 'Osteotomy geometry' in Chapter 4.

Clinical example 9.2 Correction of a tibial diaphyseal deformity

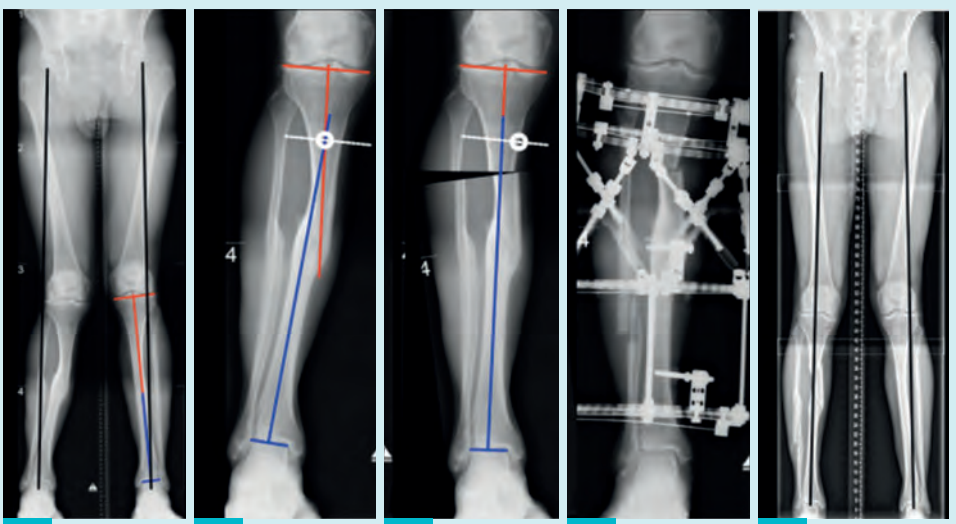

a Mechanical axis demonstrates constitutional valgus on the left with increased MAD on the right.

b Proximal and distal axis lines, the point of axis intersection and the bisector line.

c Effect of planned correction with an external hinge placed on the medial aspect of the bisector line to produce axis correction with an opening wedge.

d Hexapod correction.

e Standing alignment radiographs demonstrating correction of the mechanical axis.

Clinical example 9.3 Computer-aided planning of a predominantly frontal plane deformity below a total knee replacement

a Proximal and distal axis lines.

b Software assisted of correction allows planning of fixation.

c Standing alignment images prior to correction.

d Standing alignment images showing correction of the mechanical axis.

Anatomical axis planning

Anatomical planning will underestimate subtle peri-articular malalignment if the segment is short and is less accurate than mechanical axis planning. In the following examples (Figures 9.15–9.22), the initial assessment has been performed and demonstrates an axis abnormality with normal femoral geometry, localising deformity to the tibia, and will not be illustrated separately. If construction of the anatomical axis lines does not identify an obvious deformity, but joint orientation angles are abnormal, then a proximal or distal deformity is present.

Proximal deformity

Figure 9.15
Proximal deformity: analysis.
(a) Identification of abnormal MPTA and normal LDTA.

The MPTA is formed at the intersection of the proximal tibial joint orientation line and anatomical axis of the proximal diaphysis, represented by the proximal mid-diaphyseal line. In the example in Figure 9.15, the MPTA (73°) is abnormal, demonstrating proximal peri-articular deformity (Figure 9.15a).

The LDTA is formed at the intersection of the distal tibial joint orientation line and anatomical axis of the distal diaphysis, represented by the distal mid-diaphyseal line. Here, the LDTA (90°) is normal and excludes a distal deformity (Figure 9.15a).

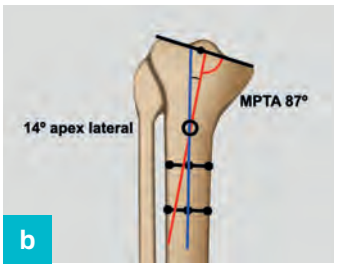

Figure 9.15
Proximal deformity: analysis.
(b) 14° apex lateral deformity.

The normal proximal anatomical axis is reconstructed using contralateral measurements, referenced to the knee joint orientation line at the normal point of intersection, 2 mm medial to the joint centre. If these are unavailable, the population normal of 87° is used. The acute angle formed by the diaphyseal and reconstructed proximal segmental anatomic axes identifies a 14° apex lateral deformity (Figure 9.15b).

Distal deformity

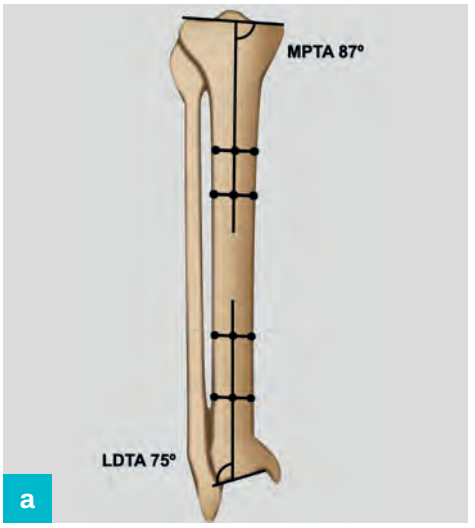

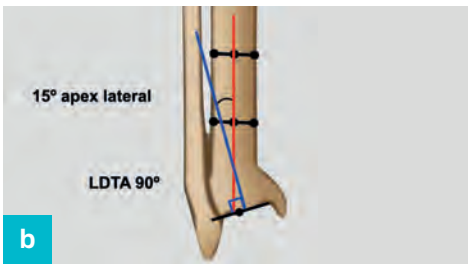

Figure 9.16
Distal deformity: analysis.
(a) Identification of abnormal LDTA and normal MPTA.
(b) 15° apex lateral deformity.

The joint orientation angles are constructed as described in previous paragraphs. In the example in Figure 9.16, the LDTA (75°) is abnormal, demonstrating distal peri-articular deformity. The MPTA (87°) is normal and excludes a proximal deformity (Figure 9.16a).

The normal distal anatomical axis is reconstructed using contralateral measurements, referenced to the ankle joint orientation line at the normal point of intersection, 2 mm medial to the joint centre. If these are unavailable, the population normal of 90° is used. In this example, the acute angle formed by the diaphyseal and reconstructed distal mechanical axes identifies a 15° apex lateral deformity (Figure 9.16b).

Diaphyseal deformity

The proximal joint orientation line and adjacent anatomical axis are constructed (Figure 9.17a).

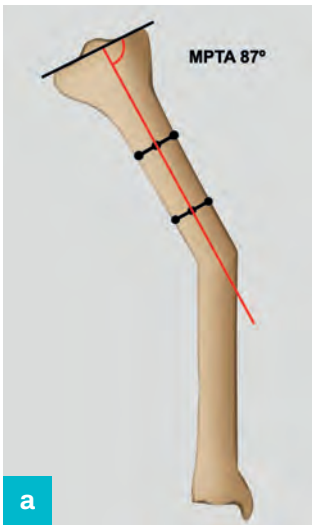

Figure 9.17
Diaphyseal deformity: analysis and correction.
(a) Proximal joint orientation line and anatomical axis.

(b) 30° apex medial single-level diaphyseal deformity.
(c) Deformity correction.

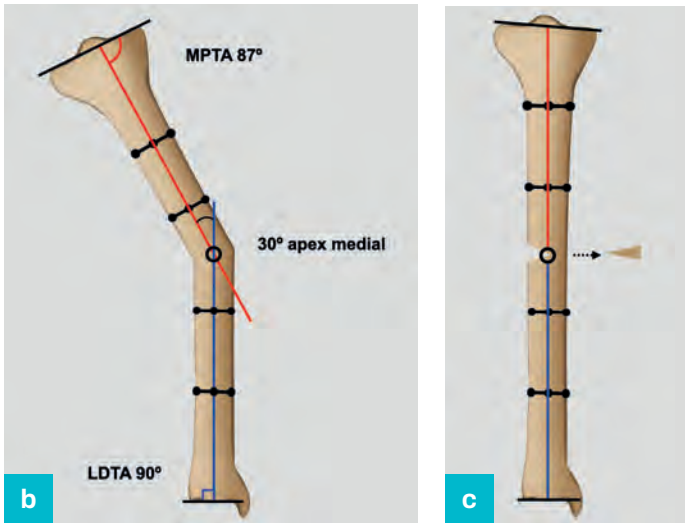

The distal joint orientation line and adjacent anatomical axis are constructed. The joint orientation angles are normal and the point of intersection of the proximal and distal anatomical axes corresponds to the visible level of an apex lateral diaphyseal deformity, in this example of 30° (Figure 9.17b).

The point of intersection corresponds to the level of the obvious anatomical abnormality and correction at this point will realign the axis without introducing secondary deformity (Figure 9.17c).

Multi-apical deformity

Resolution of multi-apical deformity involves reconstruction of an anatomical axis for each segment. The examples in Figures 9.18a–c and 9.19a–c demonstrate initial confirmation of normal joint orientation and subsequent evaluation of two- and three-level diaphyseal deformity.

Two-level deformity (Figure 9.18)

Figure 9.18
Two-level deformity: analysis and correction.
(a) Confirmation of normal joint orientation, with axis intersection distant from the visible deformity.
(b) An additional mid-diaphyseal line identifies the location of the individual deformities.
(c) Correction at the intersections of the axes.

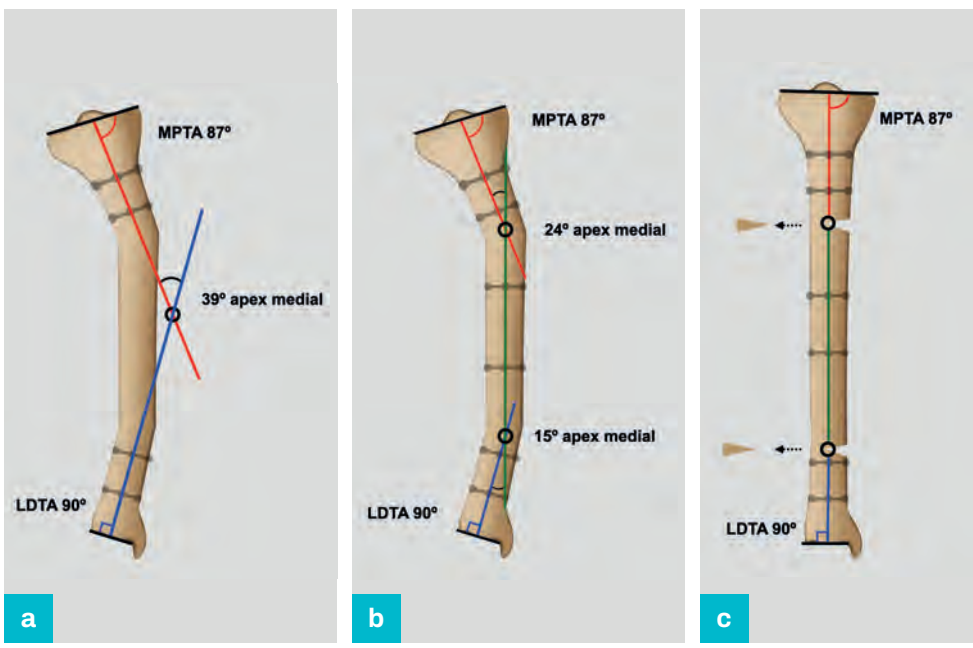

Three-level deformity (Figure 9.19)

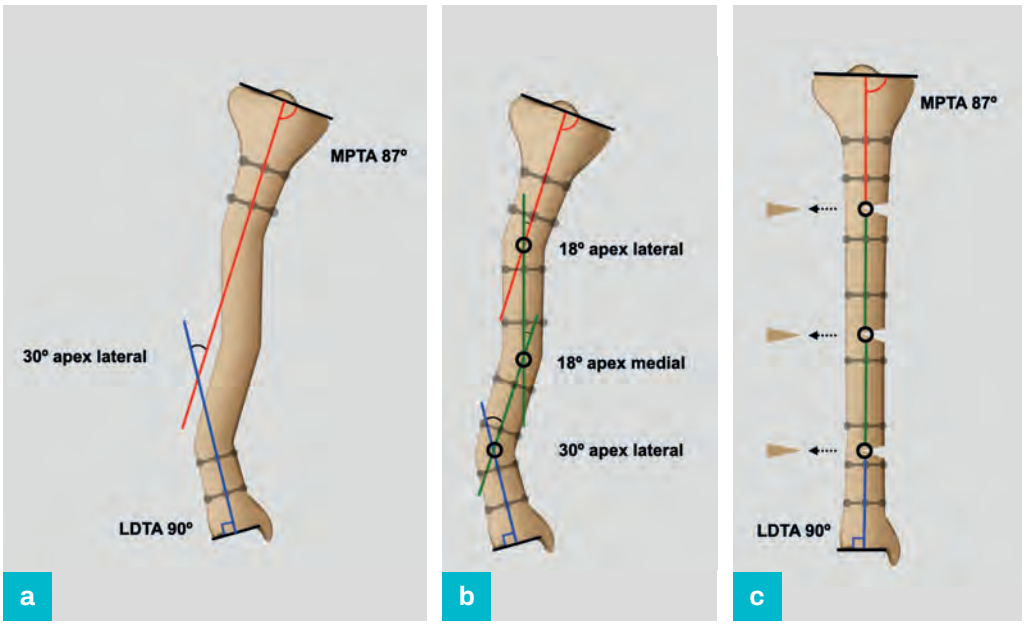

Figure 9.19
Three-level deformity: analysis and correction.
(a) Confirmation of normal joint orientation, with axis intersection distant from the visible deformity.
(b) Two additional mid-diaphyseal lines identify the locations of the individual deformities.
(c) Correction at the intersections of the axes.

Bowing

Figure 9.20
Multi-apical tibial deformity in Paget's disease.

'Bowing' describes a multi-apical deformity distributed throughout the diaphysis which occurs in conditions including congenital tibial pseudarthrosis (Figure 9.20), bone fragility (e.g. osteogenesis imperfecta), skeletal dysplasia (e.g. achondroplasia) and metabolic bone disease (e.g. X-linked rickets).

In the example in Figure 9.21, correction involves resolution of the axis in addition to anatomical reconstruction of the diaphysis. This initially involves reconstruction of the proximal and distal joint orientation angles (Figure 9.21a).

Construction of additional bisector lines for each diaphyseal segment identifies multiple apices (Figure 9.21b).

Osteotomy at each apex results in realignment of the axis, in addition to anatomical reconstruction of the diaphysis (Figure 9.21c). This is important in clinical practice, particularly if intramedullary fixation is planned (Figure 9.21c).

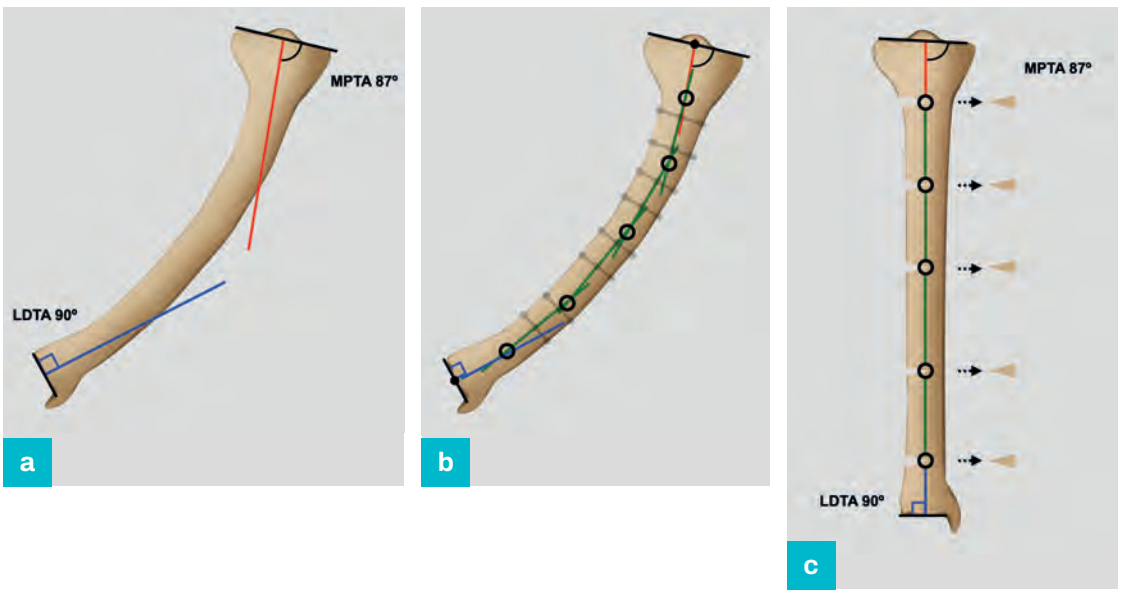

Figure 9.21
(a) Reconstruction of proximal and distal joint orientation angles.
(b) Diaphyseal bisector lines constructed for each segment identify multiple apices.
(c) Realignment of the axis with anatomical reconstruction of the diaphysis.

A more straightforward solution involves initially constructing the proximal and distal axis lines (Figure 9.22a).

A further line is added and the point of intersection with the proximal and distal axis is marked. The position of this line is variable and can be placed to accommodate the clinical circumstances, particularly the planned fixation (Figure 9.22b).

Correction at these points will reconstruct the axis but produce anatomical abnormalities, which will limit implant options (Figure 9.22c).

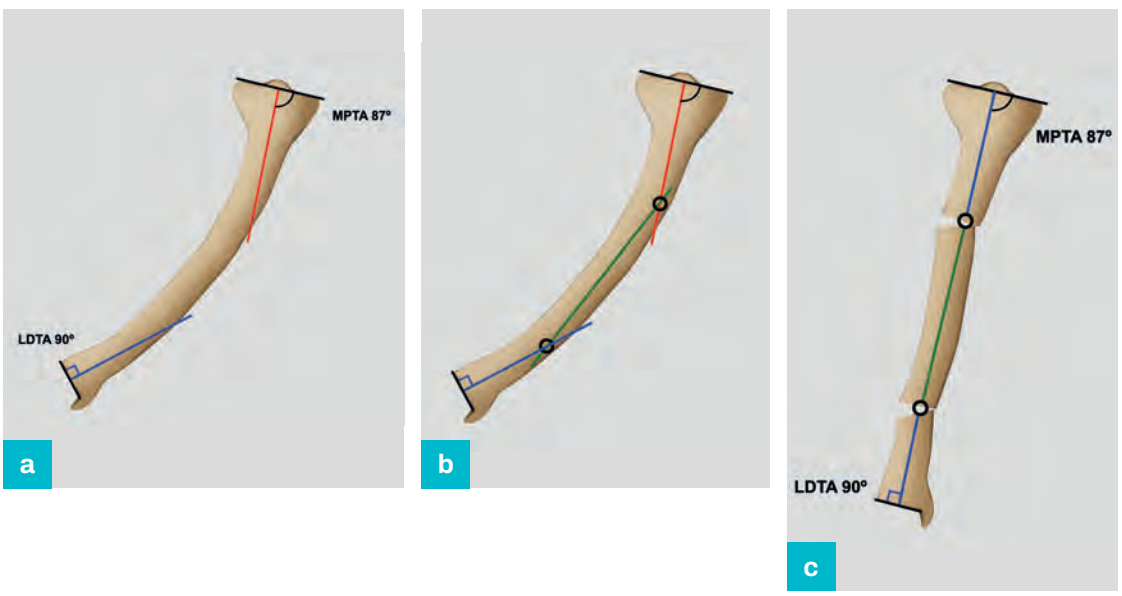

Figure 9.22
(a) Proximal and distal axis lines.
(b) Additional axis line.
(c) Axis reconstruction with residual anatomical deformity.

Lateral plane evaluation

The lateral anatomical and mechanical axes are coincident and either can be used for analysis of the tibia.

Proximal deformity

Initial analysis demonstrates an abnormal lateral limb mechanical axis and normal femoral geometry and therefore identifies a deformity in the tibia (Figure 9.23a).

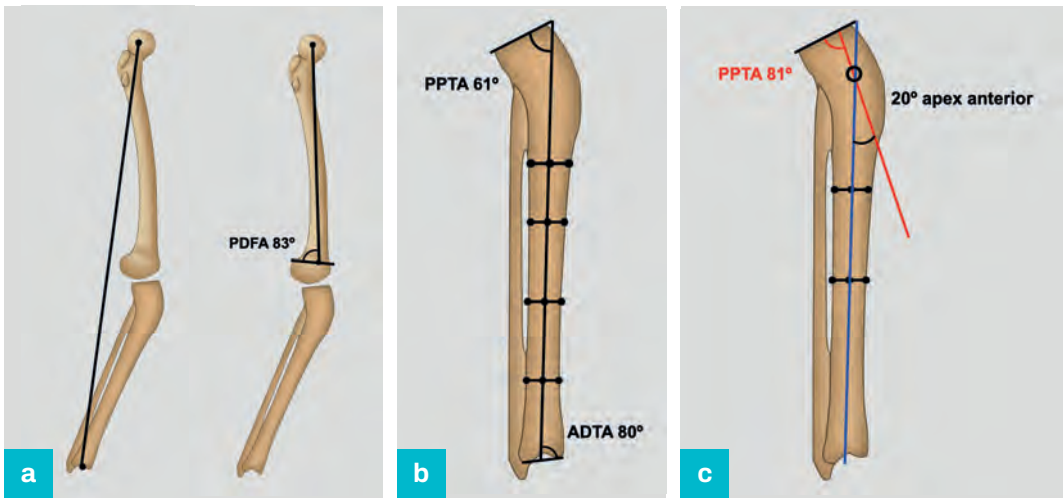

Figure 9.23
Proximal deformity: analysis.
(a) Identification of mechanical axis abnormality and normal femoral geometry.
(b) Identification of abnormal PPTA and normal ADTA.
(c) 20° apex anterior deformity.

The joint orientation lines and lateral axis are constructed. In this example, the PPTA is abnormal (61°), demonstrating proximal peri-articular deformity. The ADTA (80°) is normal and excludes a distal deformity (Figure 9.23b).

The proximal axis is reconstructed using contralateral measurements, referenced to the knee joint orientation line at the normal point of intersection, 1/5 from the anterior cortex, using patient-specific angles. If these are unavailable due to bilateral deformity or lack of appropriate radiology, the population normal of 81° is used. Here, this identifies a 20° apex anterior deformity (Figure 9.23c).

Distal deformity

Initial analysis demonstrates a normal MAD with normal femoral geometry. Deformity cannot be excluded until analysis of both bones has been undertaken. In the example in Figure 9.24, distal tibial peri-articular deformity will not displace the limb axis and will be overlooked unless formal analysis is completed (Figure 9.24a).

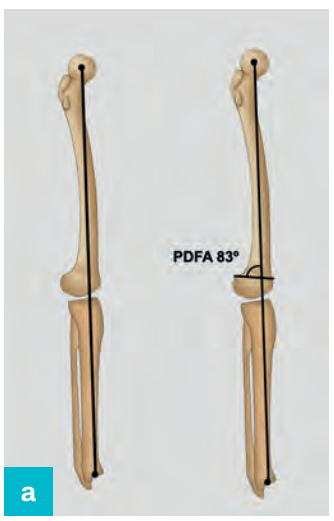

Figure 9.24
Distal deformity: analysis.
(a) Identification of normal limb axis and femoral geometry.

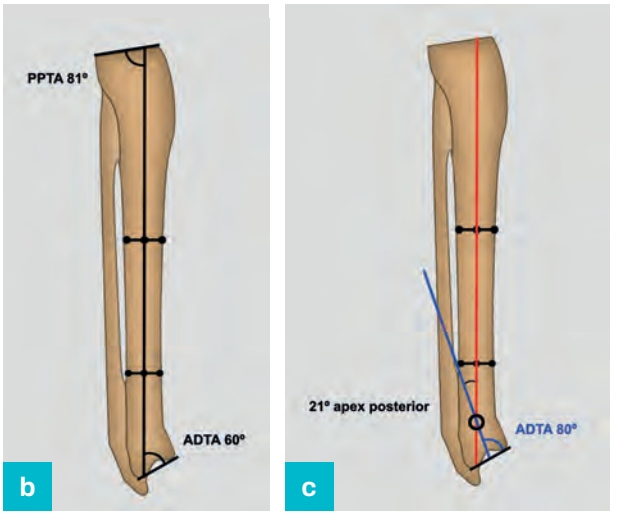

Figure 9.24
Distal deformity: analysis.
(b) Identification of abnormal ADTA and normal PPTA.
(c) 21° apex posterior deformity.

The joint orientation lines and lateral axis are constructed. In this example, the ADTA is abnormal (60°), demonstrating distal peri-articular deformity. The PPTA (81°) is normal and excludes a proximal deformity (Figure 9.24b).

The distal axis is reconstructed using contralateral measurements, referenced to the ankle joint orientation line at the normal point of intersection at the mid-point, using patient-specific angles. If these are unavailable due to bilateral deformity or lack of appropriate radiology, the population normal of 80° is used. The measurements in this example demonstrate a 21° apex posterior deformity (Figure 9.24c).

Diaphyseal deformity

Initial analysis demonstrates an abnormal limb mechanical axis and normal femoral geometry and therefore identifies a deformity in the tibia (Figure 9.25a).

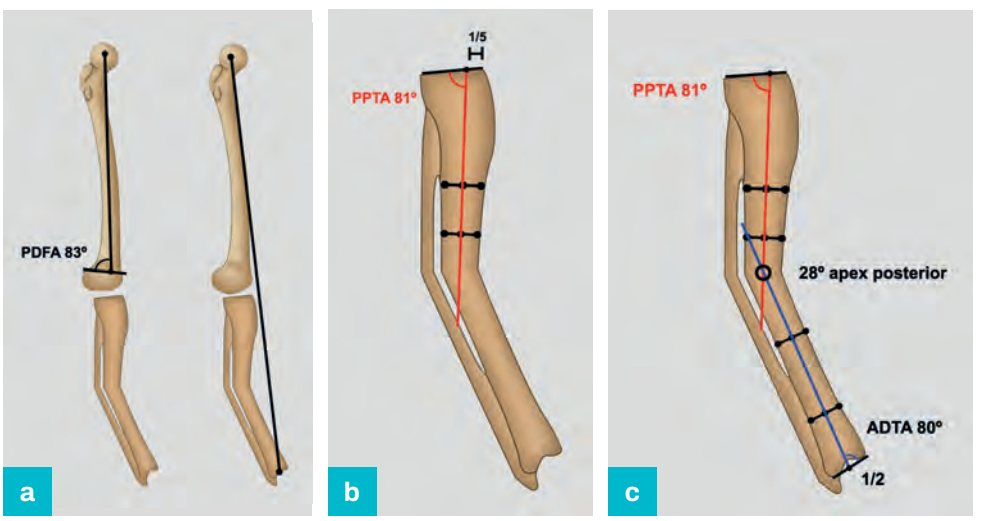

Figure 9.25
Diaphyseal deformity: analysis.
(a) Identification of an abnormal mechanical axis and normal femoral geometry.
(b) Identification of normal PPTA.
(c) 28° apex posterior deformity.

The proximal axis and joint orientation lines are constructed. The PPTA is normal, therefore excluding proximal deformity (Figure 9.25b). The distal axis and joint orientation lines are constructed. The ADTA is normal (80°), excluding distal deformity, and axes intersect at the site of visible deformity. In this example, this demonstrates a 28° apex poterior deformity (Figure 9.25c).

In subsequent examples, the initial assessment has been performed and demonstrates an axis abnormality with normal femoral geometry, localising deformity to the tibia, and will not be illustrated separately.

Bowing

'Bowing' in the lateral plane also describes multi-apical deformity, distributed throughout the diaphysis, which occurs in congenital tibial pseudarthrosis, bone fragility disorders, skeletal dysplasia and metabolic bone disease.

In the example in Figure 9.26, correction involves resolution of the axis in addition to anatomical reconstruction of the tibial diaphysis. This initially involves reconstruction of the proximal and distal joint orientation angles (Figure 9.26a).

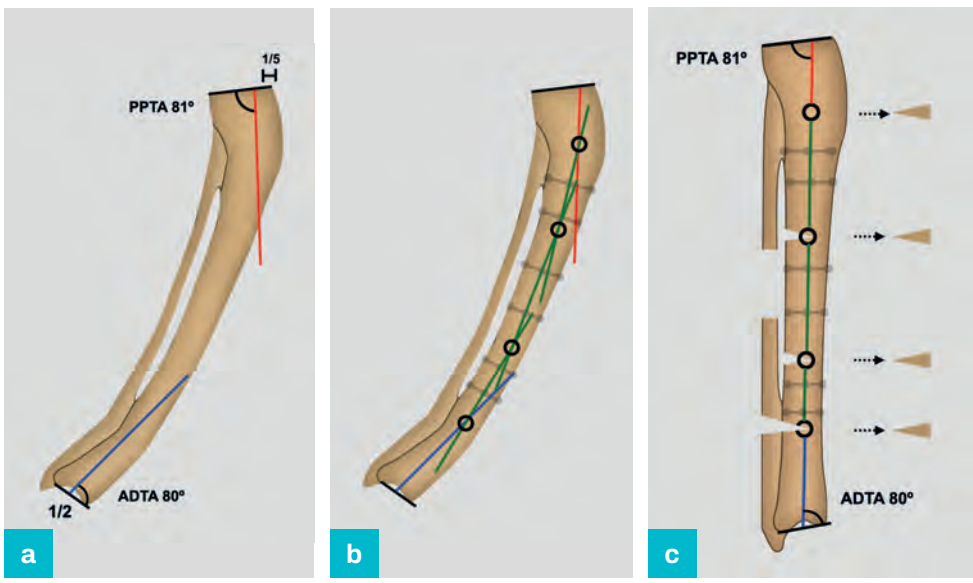

Figure 9.26
(a) Reconstruction of the proximal and distal joint orientation angles. **(b)** Diaphyseal bisector lines constructed for each segment identify multiple apices. **(c)** Realignment of the axis with anatomical reconstruction of the diaphysis.

Construction of additional bisector lines for each diaphyseal segment identifies multiple apices (Figure 9.26b).

Osteotomy at each apex results in realignment of the axis, in addition to anatomical reconstruction of the diaphysis (Figure 9.26c). This is important in clinical practice, particularly if intramedullary fixation is planned.

A more straightforward solution involves initially constructing the proximal and distal axis lines (Figure 9.27a).

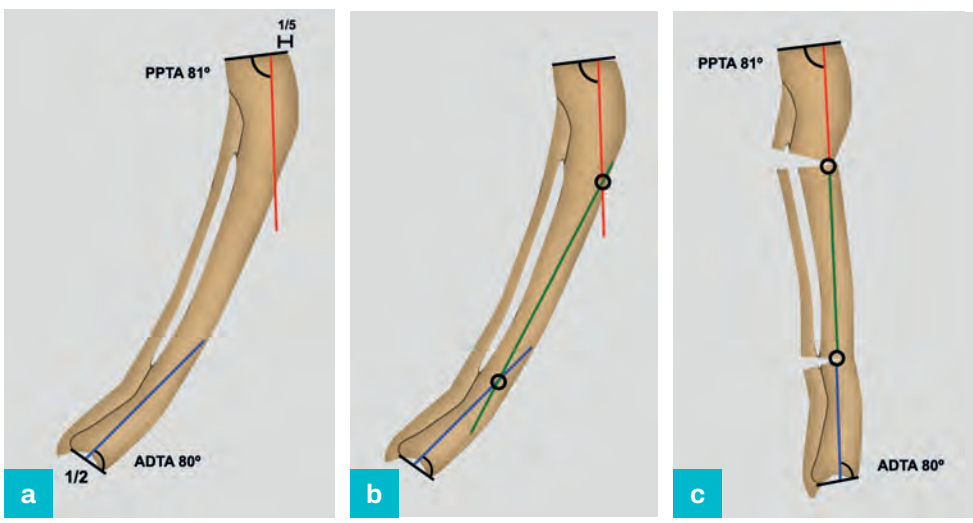

Figure 9.27
(a) Proximal and distal axis lines. **(b)** Mid-diaphyseal line, representing normal AMD. **(c)** Axis reconstruction with residual anatomical deformity.

Construction of the mid-diaphyseal line identifies two apices (Figure 9.27b).

Correction at these points will reconstruct the axis but produce anatomical abnormalities, which will limit implant options (Figure 9.27c).

Combined tibial diaphyseal and proximal peri-articular deformity

The distal mid-diaphyseal line demonstrates a normal ADTA and excludes a distal peri-articular deformity (Figure 9.28a).

The proximal mid-diaphyseal line intersects at the site of obvious diaphyseal deformity (in this example, 21° apex posterior) and also demonstrates an abnormal PPTA (41°), indicating additional proximal deformity (Figure 9.28b).

A proximal segment axis line is drawn from the anterior 1/5 of the knee joint orientation line at a population normal angle of 81°. This intersects with the proximal mid-diaphyseal line, indicating, in this case, a 40° apex anterior peri-articular deformity (Figure 9.28c).

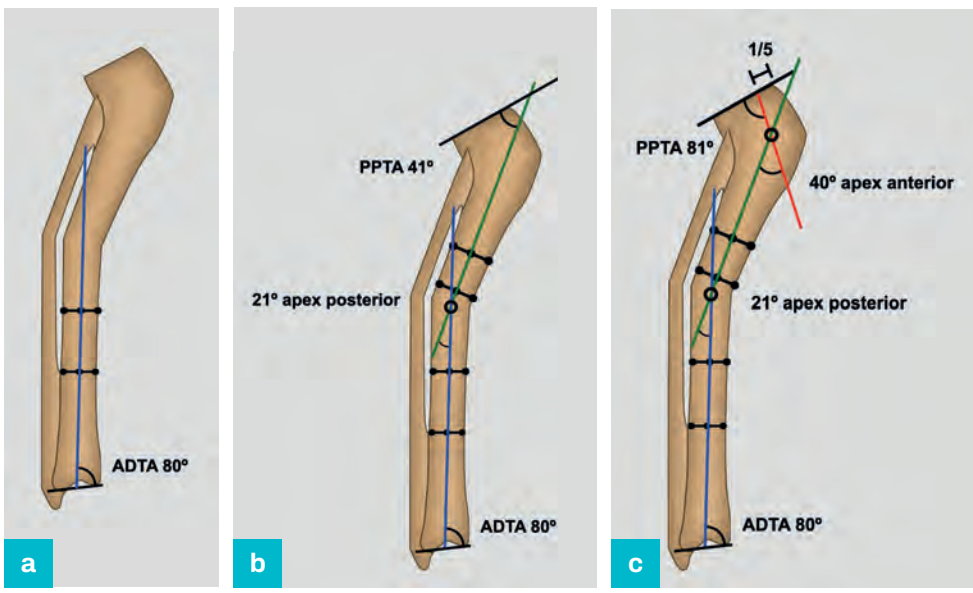

Figure 9.28 Combined tibial diaphyseal and distal peri-articular deformity: analysis. **(a)** Identification of normal PPTA. **(b)** Identification of abnormal ADTA. **(c)** 21° apex anterior diaphyseal and 25° apex posterior distal peri-articular deformity.

Clinical example 9.4 External fixator correction of tibial diaphyseal apex anterior deformity

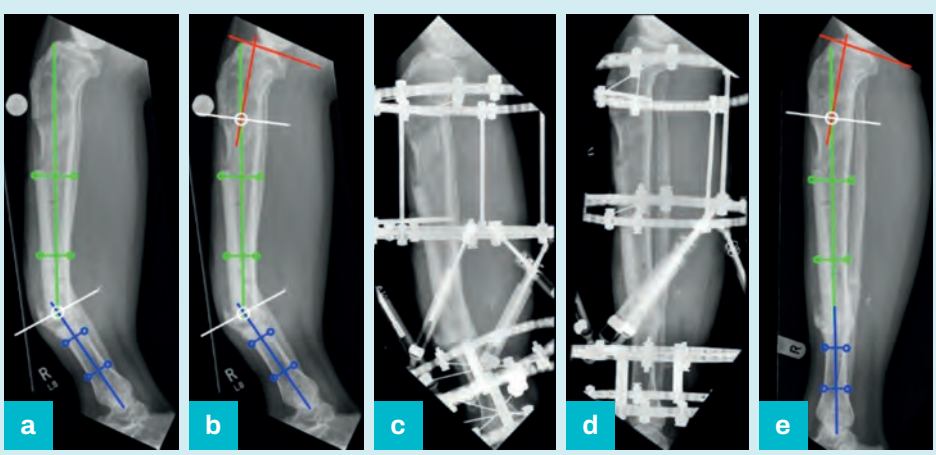

a Intercalary (green) and distal (blue) axis lines intersect at the visible deformity. The proximal axis line intersects the knee in an abnormal position indicating additional deformity.

b A proximal peri-articular (red) axis line based on the PPTA confirms deformity centred on the regenerate bone from previous correction.

c A hexapod fixator has been used to correct the distal deformity, ignoring the peri-articular deformity with planned distal over correction.

d The position following correction.

e Restoration of sagittal plane axis following correction. The proximal deformity has been ignored as it was not associated with loss of knee extension.

Combined tibial diaphyseal and distal peri-articular deformity

The proximal mid-diaphyseal line demonstrates a normal PPTA and excludes a proximal deformity (Figure 9.29a).

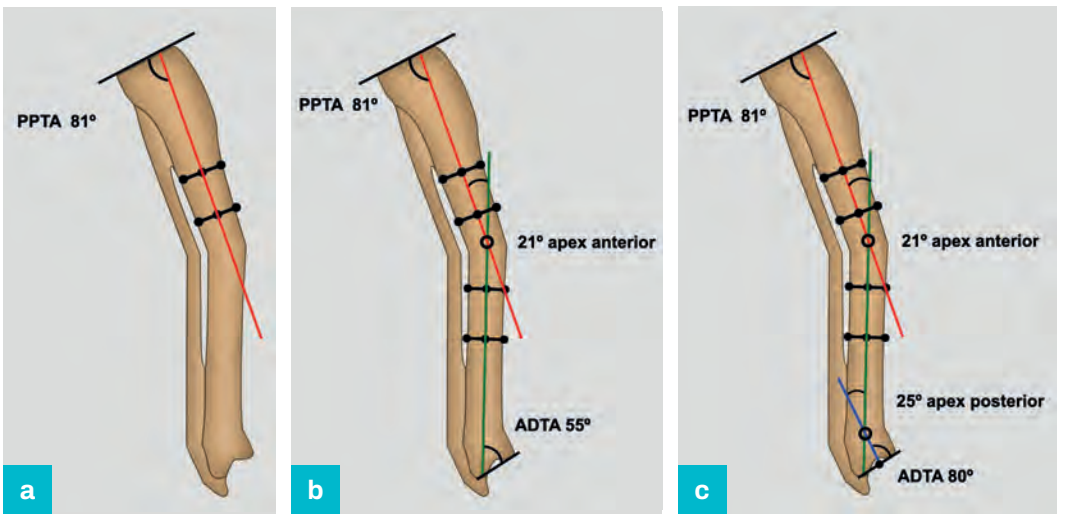

Figure 9.29
(a) Identification of normal ADTA.
(b) 21° apex posterior diaphyseal deformity with abnormal PPTA.
(c) 21° apex posterior diaphyseal and 40° apex anterior proximal peri-articular deformity.

In this example, the distal mid-diaphyseal line intersects at the site of obvious deformity, indicating a 21° apex anterior diaphyseal deformity, and also demonstrates an abnormal ADTA (in this example, 55°), indicating additional distal deformity (Figure 9.29b).

A distal segment axis line is drawn from the middle of the ankle joint line at a population normal angle of 80°. This intersects the distal mid-diaphyseal line, indicating a 25° apex posterior deformity (Figure 9.29c).

KEYPOINTS

- Assess tibial deformity systematically as part of a whole limb analysis
- Frontal plane analysis is undertaken using proximal and distal segment axes constructed by mechanical or anatomical methods
- Lateral plane analysis is undertaken using proximal and distal segment axes constructed by anatomical or modified mechanical axes
- The intersection of proximal and distal axes identifies the location and magnitude of deformity
- Check joint orientation angles to identify periarticular deformity. Consider that translation or multi-apical deformity may be present
- Construct a transverse bisector line and consider the effect of hinge position, deformity apex and osteotomy position on correction

CHAPTER

10

The foot and ankle

Gavin De Kiewiet and Om Lahoti

Introduction

The foot and ankle are complex anatomical structures, which provide a stable, flexible platform capable of adapting to a range of terrains and extremes of functional demand. Maintenance or restoration of function is a primary concern and comfortable shoe fitting is also an important consideration. Foot and ankle deformities are often multi-factorial with multiple apices and a structured approach to deformity analysis is essential. This requires an understanding of a patient's perception of their situation and involves a detailed clinical history, thorough clinical examination of the entire lower limb and radiographic examination with specialist views. A single solution does not suit every patient and this comprehensive approach assists in identifying the deformities and formulating a treatment strategy that is specific to an individual patient.

Clinical assessment of primary and compensatory foot deformities

The evolution of foot and ankle deformity in the frontal, lateral and axial planes is predictable and is a consequence of the degrees of freedom of the involved joints (Table 10.1). Frontal and lateral plane deformity is usually clinically obvious, while abnormalities of the mid- and forefoot that occur in the axial plane are better appreciated on a weight-bearing radiograph.

Table 10.1 Foot and ankle deformity

Joint level	Plane of deformity		
	Frontal	Lateral	Axial
Ankle/ Supramalleolar	Apex lateral (varus) Apex medial (valgus)	Apex anterior (recurvatum) Apex posterior (procurvatum)	Internal (tibial) rotation External (tibial) rotation
Hindfoot	Apex lateral (varus) Apex medial (valgus)	Apex anterior (equinus) Apex posterior (calcaneus)	Inversion Eversion
Mid/forefoot	Apex lateral (adducted) Apex medial (abducted)	Apex dorsal (cavus) Apex plantar (planus / rocker bottom)	Supination Pronation

Treatment goals

A surgical approach involves improving the biomechanics of weight-bearing and load transfer, correcting the plane and range of joint movement and maximising tendon function in the corrected position. The aim is to achieve these goals with minimal disruption of the soft tissues, to eradicate pain and to produce a plantigrade foot. Patient aspirations often include the ability to wear off-the-shelf shoes, perform occupational and domestic tasks and participate in recreational and sporting activities without pain. Specific additional goals should also be identified and agreed by patient and surgeon prior to treatment but it must be recognised by both that it is not always possible to achieve all the objectives.

Compensatory deformities

Flexible or fixed compensatory deformities develop in a predictable sequence to produce a functional, plantigrade foot. Incomplete compensation is frequently painful and results in loss of function. This may not originate at the site of primary deformity and, for example, a distal tibial apex lateral (varus) deformity that exceeds the normal range of subtalar joint eversion may result in subtalar rather than ankle pain. To discriminate between fixed and flexible components, the compensating joint is placed at the end of the available range and compared to the site of deformity. If the maximum range of subtalar inversion is at least equal in magnitude to a distal tibial deformity, the compensatory deformity is not fixed and a similar approach can be used to evaluate apex medial (valgus), apex anterior (procurvatum) and apex posterior (recurvatum) deformities of the lower tibia. It is also important to note that, if distal tibial deformity exceeds the range of subtalar joint movement, compensatory forefoot pronation and supination may also develop.

The degree and magnitude of the compensatory deformity depends on the available range and direction of movement in the compensating joint and the chronicity of the primary condition. This is not always proportionate to the primary deformity because compensation is often in a different plane and at a distance from the apex of the deformity. This is analogous to correction of long bone, angular deformity with obligatory translation when an osteotomy and apex of correction are not coincident. Fixed compensatory deformities must be included in planning to ensure that surgical correction of the primary deformity produces a plantigrade foot.

Deformity assessment

The individual characteristics of a clinical deformity are defined by a set of variables in six axes, highlighting the segment(s) of interest. Planning is patient-specific and consists of a defined sequence of steps using standardised radiographs. A marker pencil and tracing paper or more sophisticated software including Traumacad™, TL-Hexray™ and Bone Ninja™ are useful for radiological planning, education and patient information. Specialist imaging with magnetic resonance (MR), computed tomography (CT) and isotope bone scans can add important information, and pedobarographs and instrumented gait analysis are used in selected cases.

Frontal plane evaluation

Long leg alignment and calcaneal axial views of both legs, with comparison to the unaffected side, are essential for accurate deformity analysis. The tibial component of ankle deformity has been described in Chapter 9.

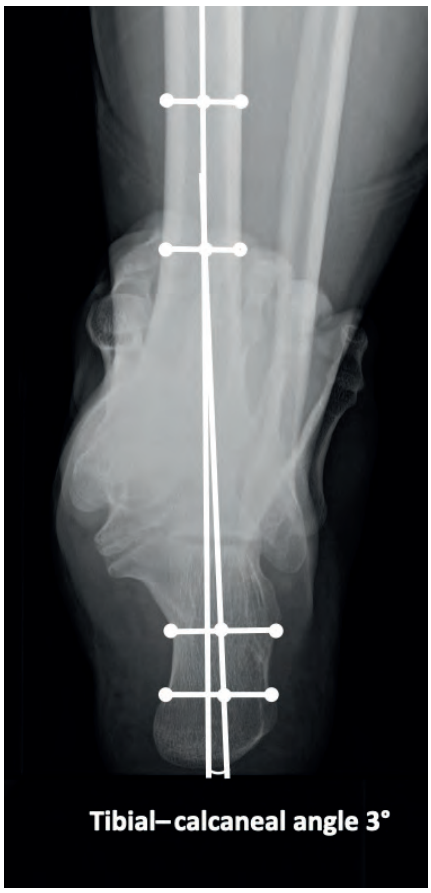

Figure 10.1 Tibial–calcaneal angle.

The long leg calcaneal axial view is used to determine the mid-diaphyseal line of the tibia and bisector line of the calcaneum and these lines intersect to form the tibial–calcaneal angle. A normal hindfoot is defined by an axis of 0–5° apex lateral (valgus) (Figure 10.1) and any degree of apex lateral (varus) is abnormal. An example of apex medial (valgus) deformity is shown in Figure 10.2.

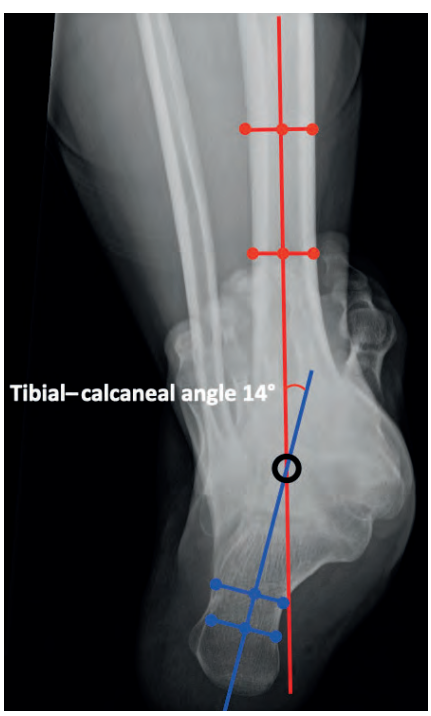

Figure 10.2 Increased tibial–calcaneal angle and tibial–calcaneal distance in a 30-year-old with fixed hind foot valgus, stiff subtalar joint and lateral impingement pain.

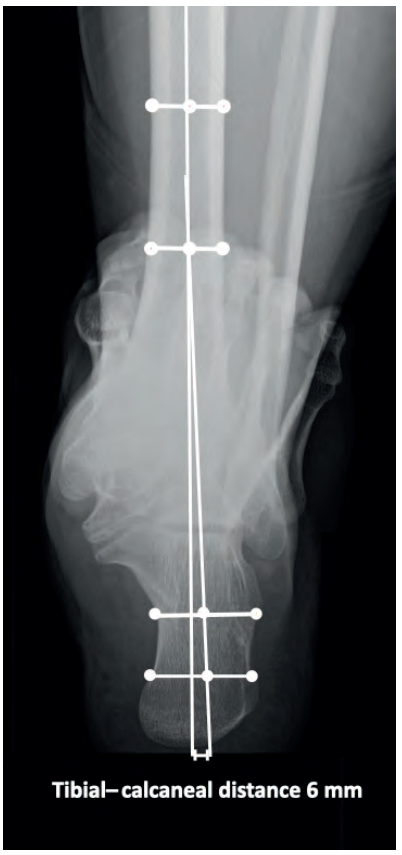

Figure 10.3
Tibial–calcaneal distance.

The tibial–calcaneal distance is represented by the distance between these lines. The calcaneal line is located lateral to the mid-tibial line with a normal range of 6–14 mm and population normal of 10 mm (Figure 10.3).

Lateral plane evaluation

A lateral weight-bearing radiograph from the proximal tibia to the foot is the baseline image for assessment of lateral plane foot deformity. The tibial component of ankle deformity has also been described in Chapter 9. If the tibia is normal, a radiograph from the mid-tibia is an acceptable alternative. If weight-bearing is not possible, then a simulated view should be obtained, with the foot supported against a block.

The lateral axis of the foot is represented by a line perpendicular to the sole of the foot that passes through the lateral process of the talus (Figure 10.4).

Figure 10.4
Lateral axis.

Figure 10.5
Lateral process of the talus.

The talus is a truncated cone or frustum, which appears as a wedge when viewed from above, with a broader anterior border. The rotational axis of the ankle joint is oblique and runs from the tip of the medial malleolus to the tip of lateral malleolus. This passes through the lateral process of the talus and is in neither the frontal nor the lateral plane. The lateral process is easily identifiable on a lateral radiograph and is normally ±3 mm anterior to the mid-diaphyseal axis of tibia (Figure 10.5). This is a convenient landmark that can be used to align simple hinges with a circular external fixator and to place a virtual hinge with a hexapod fixator.

Plantigrade angle

The plantigrade angle is formed by extending the mid-diaphysial line of the tibia to a line parallel to the sole of the foot (the plantigrade line) (Figure 10.6) and this measures the overall equinus deformity (Figure 10.7). The normal range for the plantigrade angle is 85–91° and the population normal is 88°).

Figure 10.6
Plantigrade angle.

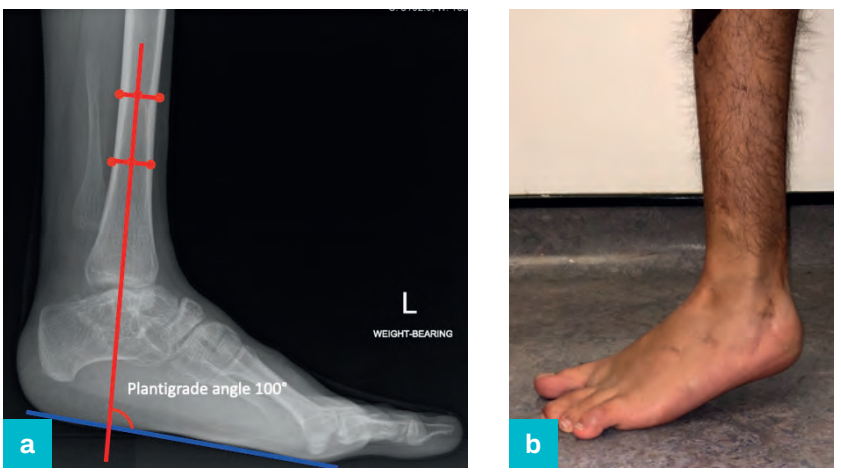

Figure 10.7
(a,b) Measurement of equinus.

Foot-to-floor angle

Figure 10.8
Foot-to-floor angle.

The angle between the plantar aspect of the foot and the flat horizontal plane with the radiograph obtained in maximum dorsiflexion is termed the foot-to-floor angle and is also a measurement of equinus deformity (Figure 10.8).

Foot deformity

Lateral plane evaluation

Calcaneal inclination angle

The line connecting the most inferior point of the calcaneal tuberosity (x in Figure 10.9) to the most inferior point of the 5th metatarsal head (z in Figure 10.9) is termed the plane of support (PS). The line drawn along the plantar aspect of the calcaneum, connecting the most inferior point of the tuberosity to the most distal and inferior point of the calcaneocuboid joint (y in Figure 10.9), is termed the calcaneal inclination line (Figure 10.9). The calcaneal inclination angle (CIA) is formed at the point of intersection of these lines.

Figure 10.9
Calcaneal inclination angle.

Figure 10.10
Calcaneus deformity.

The normal range for the CIA is 13–23° and the population normal is 18°. This angle differentiates between calcaneus (Figure 10.10) (>23°) and equinus (<13°) deformity.

Figure 10.11
Pronated foot – note plantar flexion of 1st Metatarsal.

Hindfoot deformity can also alter this relationship and a thorough clinical examination is an important component of the overall evaluation. Hindfoot varus with compensatory forefoot pronation results in plantar flexion of the 1st metatarsal and creates a high arch (Figure 10.11).

Figure 10.12
Supinated foot resulting in lowering of the arch.

Hind foot valgus results in decreased calcaneal pitch, with compensatory supination of forefoot and lowering of the arch (Figure 10.12).

Lateral angle (lateral Meary's angle)

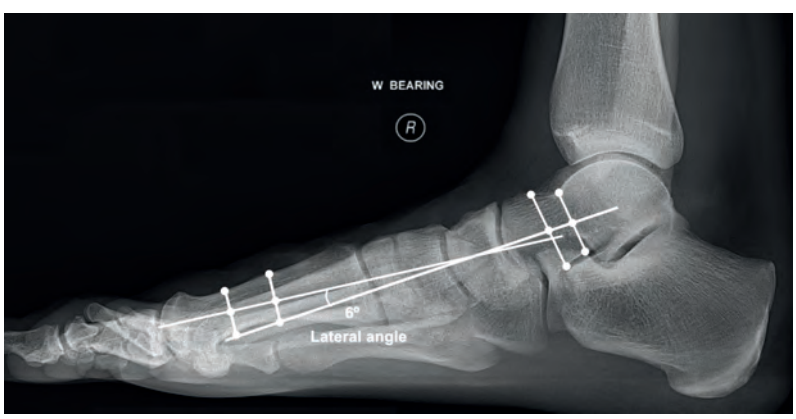

Figure 10.13
Lateral angle.

The talar neck bisector line is identified and extended distally. The mid-diaphyseal line of the 1st metatarsal is identified and extended proximally. The lines intersect to form the lateral angle.

The normal range for the lateral angle is 2–10° and the population normal is 6° (Figure 10.13).

Figure 10.14
(a,b) Cavus foot.

Pes cavus is indicated by an apex dorsal lateral angle >4° (Figure 10.14) and pes planus by an apex plantar lateral angle >4° (Figure 10.15).

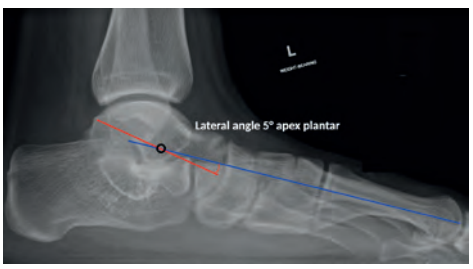

Figure 10.15
Flatfoot.

Metatarsal declination angle

The angle between the mid-diaphyseal line of the 1st metatarsal and the plantigrade line is termed the metatarsal declination angle. This is a measure of midfoot equinus, which is common in foot deformities that are a consequence of neurological abnormalities.

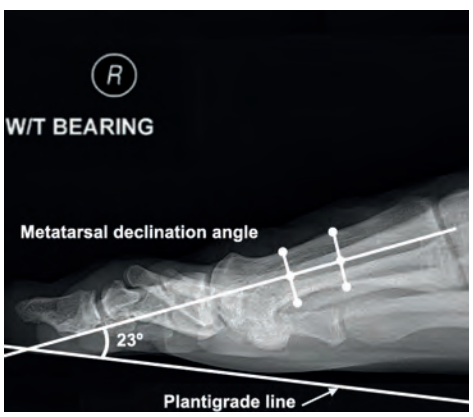

Figure 10.16
Metatarsal declination angle.

The normal range for the metatarsal declination angle is 20–26° and the population normal is 23° (Figure 10.16).

Transverse plane evaluation

Transverse plane deformities are typically seen in severe pes planus, congenital talipes equino-varus and hallux valgus. Weight-bearing antero-posterior (AP) radiographs with an exposure chosen to image the entire talus and calcaneus of both feet are essential for analysis.

AP talar–1st metatarsal angle (AP Meary's angle)

This requires a properly positioned AP view of the foot that includes the talus and calcaneum. The talar neck bisector line is identified and extended distally. The mid-diaphyseal line of the 1st metatarsal is identified and extended proximally to cross the centre line of the talus. The lines intersect to form the AP talar–1st metatarsal angle (Figure 10.17a,b).

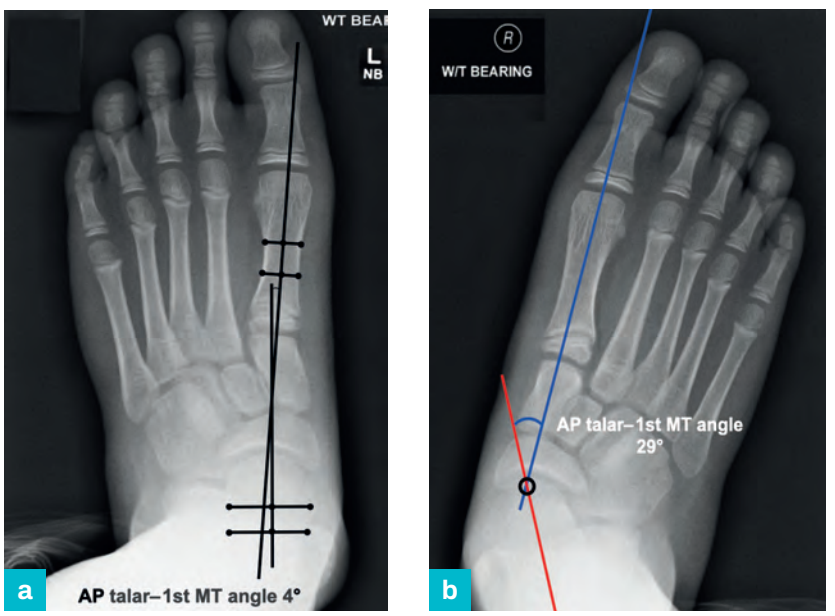

Figure 10.17 AP talar–1st metatarsal angle. **(a)** Normal. **(b)** Abnormal. Severe flatfoot. Note the apex is at the talonavicular joint.

The normal range for the AP talar–1st metatarsal angle is 3–11° and the population normal is 7°. This angle differentiates between forefoot abduction (>11°) (Figure 10.18) and adduction (<3°) deformity.

Figure 10.18 **(a,b)** Abnormal AP talar–1st metatarsal angle. Diabetic neuroarthropathy.

AP talo-calcaneal angle (Kite angle)

Figure 10.19
AP talo-calcaneal angle (dotted line indicates lateral border of calcaneum).

The talar head and neck bisector line is identified. A second line is drawn through the centre of the calcaneum. This line is often difficult to identify and an alternative is to draw a line along the lateral border of the calcaneum. The intersection of these lines is termed the AP talo-calcaneal angle (Figure 10.19).

The normal range for the AP talo-calcaneal angle is 15–30° and the population normal is 21°. This angle defines the relationship between the calcaneum and talus and differentiates between hindfoot varus (<15°) and valgus (>30°).

Talo-navicular coverage angle

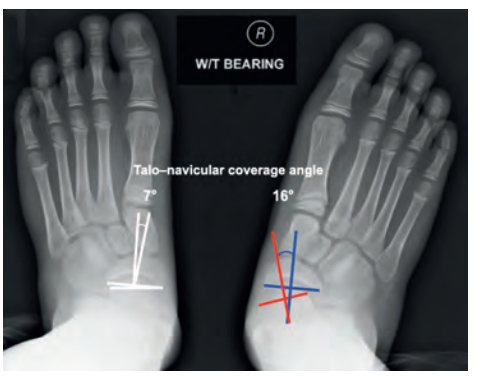

Figure 10.20
Talo-navicular coverage angle.

The line joining the medial and lateral edges of the articular surface of the head of the talus is drawn. The line joining the medial and lateral edges of the proximal articular surface of the navicular is drawn. These two lines intersect to form the talo-navicular coverage angle (Figure 10.20). This angle represents the relationship between the hindfoot and midfoot and an angle of >7° indicates lateral subluxation of the talo-navicular joint. Hindfoot valgus in pes planus may be associated with midfoot abduction, resulting in subluxation of the talo-navicular joint, uncovering the talar head.

Mechanical axis of the foot

The centre of the hindfoot is defined by the mid-point of a line joining the medial edge of the talonavicular joint (x in Figure 10.21) to the lateral edge of calcaneo-cuboid joint (y in Figure 10.21). The mechanical axis of the foot is represented by a line from the mid-diaphysis of the 2nd metatarsal to the centre of the hindfoot.

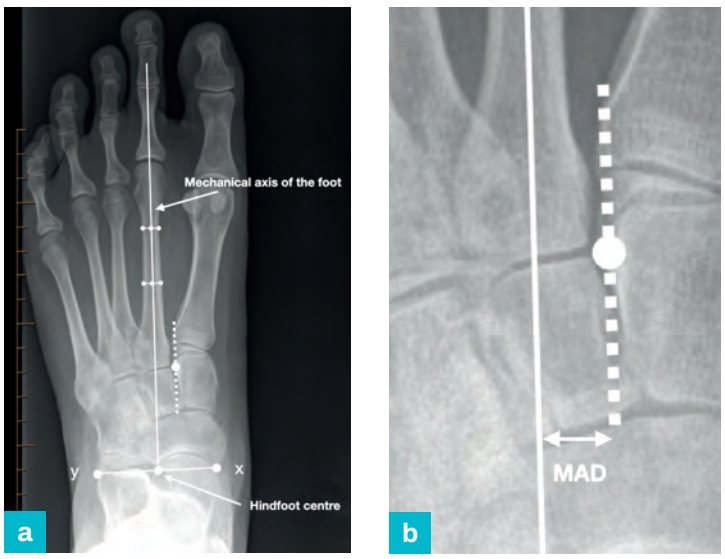

Figure 10.21 **(a,b)** Mechanical axis of the foot.

The normal range for the mechanical axis of the foot is 2–6 mm lateral from the medial most border of the 2nd metatarsal–intermediate cuneiform joint and the population normal is 4 mm. This is a measurement of transverse plane forefoot deformity.

Metatarsus adductus angle

Figure 10.22 Metatarsus adductus angle.

Figure 10.22 shows the calculation of the metatarsus adductus angle (MAA). A line that connects the most medial point of the 1st metatarsal base at the metatarso-cuneiform joint and the medial extent of the talo-navicular joint is drawn (1). A second line (2) that joins the lateral extent of the calcaneo-cuboid joint and the 4th metatarso-cuboid joint is drawn. A third line (3) that connects the mid-points of these two lines across the midfoot is drawn and this represents the bisector line of the midfoot. The mid-point of this line is marked and a perpendicular (4) is extended distally from this point. The mid-diaphyseal line of the 2nd metatarsal (5) is identified. The intersection of lines 4 and 5 is termed the MAA.

The normal range for the MAA is 6–16° and the population normal is 11°. This angle defines the normal relationship between the mid- and forefoot.

Surgical planning

Deformity correction should be prefaced by clearly stated goals that are determined by clinical and radiological assessment and understood by the patient, care-givers and medical practitioners. Factors that influence the treatment plan are the type and magnitude of primary and compensatory deformities, the condition of the soft tissues and the neurological status of foot and ankle. The presence of active or indolent infection, previous surgical procedures, co-morbidities and social circumstances are also relevant and will influence management decisions.

Gradual correction by soft-tissue stretching is often achievable in patients under 8 years of age. Soft-tissue surgery followed by splinting is generally confined to mild to moderate uni-planar deformities. Combined soft-tissue and bony procedures may be necessary in older patients and multi-apical deformity commonly requires correction at more than one level.

Triple arthrodesis is frequently used for acute correction of multi-planar hind- and midfoot deformity. There are a number of technical considerations that make this a demanding technique. It produces a rigid, short foot due to peri-articular wedge excision and this may increase the risk of osteoarthritis in the adjacent joints that are not fused. Avascular necrosis of the talus is a rare but devastating complication and, as there is no opportunity for adjustment following surgery, incomplete or over-correction is a frequent complication. It is, however, a useful procedure for feet in which deformities are associated with arthritic joints and fusion is necessary for symptomatic relief.

External fixator correction

An alternative approach is to correct deformity with distraction through an osteotomy using an external fixator. This can be performed in the presence of a compromised soft-tissue envelope due to previous surgery, active infection or poor bone quality in diabetic neuroarthropathy. Osteotomies can be performed at or close to the apex of deformity and distracted without bone resection. This joint-preserving approach is advantageous as the foot retains length and some flexibility. Correction can continue until satisfactory alignment is achieved in addition to simultaneous tibial lengthening if required.

While it is possible to use a uni-planar device to correct some deformities, circular external fixators are considerably more versatile and can be configured to correct complex deformity of the foot and ankle. The technique is demanding as accurate hinge placement is necessary and correction is often staged and may require frequent adjustment of the fixator.

The introduction of programmable hexapod fixators has simplified some aspects of correction because virtual hinge placement requires fewer components and less physical space, even in complex correction.

Irrespective of the fixator type, a common strategy is to consider the components of the foot and ankle separately as tibia, hind-, mid- and forefoot, rather than the anatomical approach that is conventional for long bone correction. An equinus deformity can be considered as a proximal component (tibia) and distal component (combined talus, calcaneus, mid- and forefoot). This is equivalent to a long bone deformity with an anterior apex at the ankle and a fixator that independently stabilises the tibia and foot can be constructed to correct the deformity.

Clinical example 10.1 External fixator correction of ankle equinus

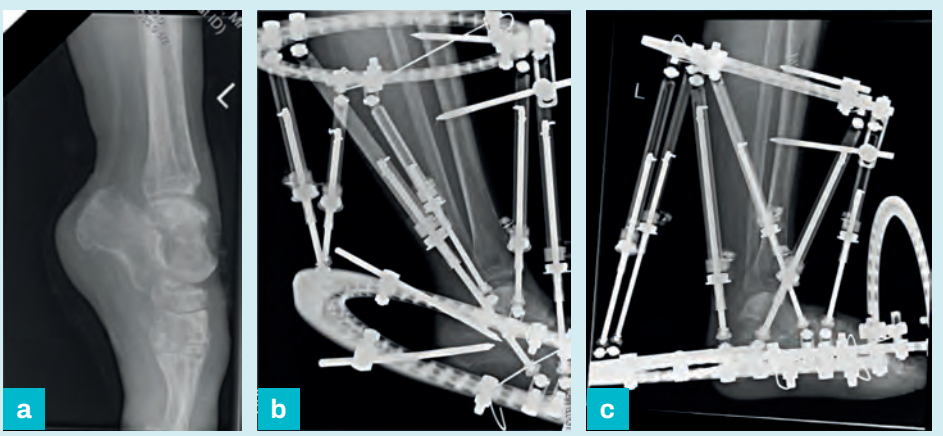

a Significant equinus following an ischaemic injury.

b Joint distraction.

c Complete correction without subluxation of ankle.

Pre-operative education and post-operative surveillance are fundamentally important. Patients should be reviewed frequently after fixator application to assess correction and identify secondary deformities including toe flexion deformity or tendo Achilles contracture, if the fixator does not include the ankle. Formal and patient-directed physiotherapy is essential to prevent contracture of the knee and ankle and early weight-bearing should be encouraged. Additional procedures may be required after fixator removal, particularly in neurologically driven deformity where tendon transfer or strategic joint fusion should be considered.

KEYPOINTS

- Clinical assessment of primary and compensatory foot deformities
- Formulate achievable treatment goals
- Compensatory deformity
- Frontal plane deformity evaluation
- Lateral plane deformity evaluation
- Radiological assessment with normal angles and relationships
- Surgical planning, including external fixator correction and post-operative management

Index

The aim of this book is to simplify the concepts necessary to plan complex limb deformity correction, irrespective of surgical discipline or method of stabilisation. It should be as relevant to reconstruction of simple fracture malunion as to complex congenital abnormality correction.

This has been written for a global audience and the interested, but inexperienced, reader should be able to work sequentially through each section. It introduces increasingly complex concepts in a logical order, and at the conclusion, readers should be confident in planning the correction of complex long-bone deformity.

The book has been produced free of charge in a PDF format and is accessible on any handheld mobile device irrespective of location.

We encourage you to register your copy so that the impact can be quantified, and updates can be distributed without any unnecessary delays associated with formal revision.

Please acknowledge possession by downloading a PDF version from: https://www.deformitycorrection.co.uk

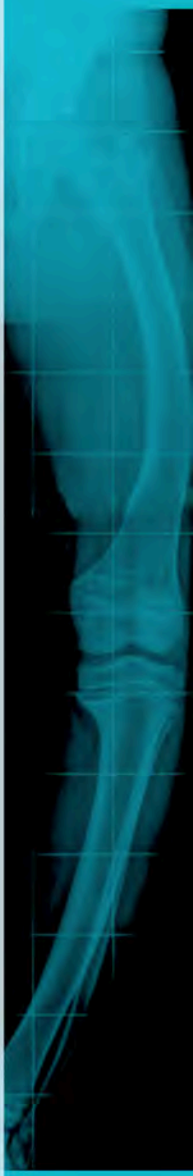

ISBN 978-1-7395873-0-7

DEFORMITY CORRECTION

NAUGHTON PUBLISHING